University of Southampton
Faculty of Engineering and the Environment
Water and Environmental Engineering Group
Bioenergy and Organic Resources Research Group

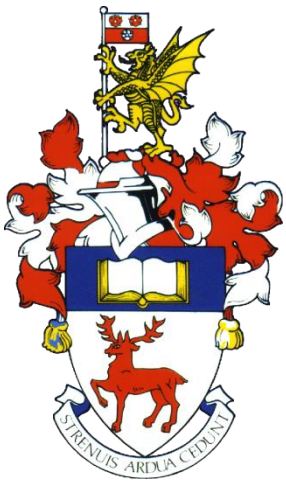

Submerged Anaerobic Membrane Bioreactor for Wastewater Treatment: Effect of Mean Cell Residence Time on Membrane Flux, Mixed Liquor Characteristics and Overall Reactor Performance

by

Santiago Pacheco Ruiz

Thesis submitted for the degree of Doctor of Philosophy

September – 2016

Supervisors: Dr Sonia Heaven and Professor Charles J. Banks

UNIVERSITY OF SOUTHAMPTON

ABSTRACT

FACULTY OF ENGINEERING AND THE ENVIRONMENT
Water and Environmental Engineering Group

Doctor of Philosophy

SUBMERGED ANAEROBIC MEMBRANE BIOREACTOR FOR WASTEWATER TREATMENT: EFFECT OF MEAN CELL RESIDENCE TIME ON MEMBRANE FLUX, MIXED LIQUOR CHARACTERISTICS AND OVERALL REACTOR PERFORMANCE

Santiago Pacheco-Ruiz

Mean cell residence time (MCRT) is a major operational parameter in all biological treatment systems because of its relationship to growth rate and thus to metabolic activity. Due to their mode of operation, submerged anaerobic membrane bioreactors (SAnMBR) offer a homogenous system in which MCRT can be simply controlled through volumetric wastage. Although a number of studies using SAnMBR have been reported, however, little information is available regarding the effect of MCRT on operational performance, mixed liquor characteristics and the influence of these on membrane performance. In this research an innovative SAnMBR using gravity-induced transmembrane pressure to maintain flux was developed and tested for first time. This configuration was then used to evaluate the impact of MCRT on membrane flux, mixed liquor characteristics and overall performance of SAnMBR treating low-to-intermediate strength wastewater.

Long-term experimental periods of more than 240 days allowed steady-state conditions under different MCRTs, in which the mixed liquor suspended solids (MLSS) adjusted to the applied load, making possible to assess the influence of this growth and metabolism-dependent kinetic parameter. The SAnMBRs were monitored for membrane flux, overall process efficiency and mixed liquor characteristics when operating at 36 ^{o}C and 20 ^{o}C. The results of this work showed that at both operational temperatures, the MCRT has a significant effect on the mixed liquor characteristics, particularly on the filterability which was higher at short MCRTs. This resulted in improved membrane flux at relatively short MCRT, although no advantages were observed if the MCRT was further reduced. Higher specific methane production was observed at longer MCRT, most probably due to a higher fraction of carbon incorporated into biomass as a result of higher microbial growth rates. Overall, the results of this research showed that the MCRT has a considerable effect on the mixed liquor characteristics and thus on the membrane fouling and overall reactor performance. It is clear that there is a trade-off to be made between enhanced membrane performance, specific methane production and sludge yield when considering the most suitable operational MCRT. Further studies are required to identify the optimum MCRT for a wider range of wastewater and other operational parameters and to fully understand the causes of these effects.

TABLE OF CONTENTS

ABSTRACT III
TABLE OF CONTENTS V
LIST OF FIGURES XI
LIST OF TABLES XVII
DECLARATION OF AUTHORSHIP XIX
ACKNOWLEDGEMENTS XXI
DEFINITIONS AND ABBREVIATIONS XXIII

1. INTRODUCTION 1
2. LITERATURE REVIEW 3
2.1. Wastewater treatment 3
2.1.1. Use of synthetic wastewater for research 5
2.2. Anaerobic wastewater treatment 6
2.3. Anaerobic membrane bioreactors 10
2.3.1. Membrane separation process 12
2.3.1.1. Membrane fouling 13
2.3.1.2. Membrane configuration 16
2.3.1.3. Membrane materials 18
2.3.1.4. Membrane module type 19
2.3.2. Hydrodynamic conditions 21
2.3.2.1. Membrane flux 21
2.3.2.2. Transmembrane pressure and permeation modes 21
2.3.3. Operational conditions 23
2.3.3.1. Temperature 23
2.3.3.2. Mean cell residence time (MCRT) 24
2.3.3.3. Organic loading rate 26
2.3.3.4. Hydraulic retention time (HRT) 26
2.3.4. Mixed liquor characteristics 27
2.3.4.1. Solids concentration, viscosity and filterability 27
2.3.4.2. Soluble microbial products and extracellular polymeric substances 29

2.3.5. Dissolved methane in the effluent 30
2.3.6. Conclusions from the literature review 31
2.4. Research aim and objectives 32
3. MATERIALS AND METHODS 33
3.1. Materials 33
3.1.1. General 33
3.1.2. Synthetic Wastewater 33
3.1.3. Trace elements supplementation 34
3.1.4. Inoculum 35
3.1.5. Submerged Anaerobic Membrane Bioreactors (SAnMBR) 35
3.1.5.1. Membranes 36
3.1.5.2. Preliminary tests 37
3.1.5.3. Final reactor design and construction 38
3.1.5.4. General SAnMBRs experimental set-up 40
3.2. Methods 42
3.2.1. Feed, mixed liquor and permeate analysis 42
3.2.1.1. Chemical Oxygen Demand (COD) 42
3.2.1.2. Total and suspended solids 44
3.2.1.3. pH 45
3.2.1.4. Capillary Suction Time (CST) 46
3.2.1.5. Frozen Image Centrifugation (FIC) 46
3.2.1.6. Extracellular Polymeric Substances (EPS) 47
3.2.1.7. Elemental composition analysis 49
3.2.1.8. Biochemical Oxygen Demand (BOD) 49
3.2.1.9. Total Kjeldahl Nitrogen (TKN) 50
3.2.1.10. Microscopic examination 51
3.2.2. Gas analysis 51
3.2.2.1. Gas composition 51
3.2.2.2. Gas volume 52
3.2.2.3. Dissolved gas 54
3.3. Operational parameters 58
3.3.1. Membrane flux 58
3.3.2. Transmembrane pressure 59
3.3.3. Hydraulic retention time 59

3.3.4. Mean cell residence time 60
3.3.5. Organic loading rate 61
3.3.6. COD removal rate 62
3.3.7. Biogas and methane production 62
3.3.7.1. Biogas volumetric production 62
3.3.7.2. Specific methane production 63
3.3.8. Observed biomass yield 63
3.3.9. COD balance 64
3.4. Laboratory practice 66
3.5. Statistical analysis 67
3.6. Research methodology 67
4. RESULTS – DEVELOPMENT AND TESTING OF A FULLY GRAVITATIONAL SANMBR 69
4.1. Method summary 69
4.2. Results and discussion – Development and testing of fully gravitational SAnMBR experiment at 36 ^{o}C 72
4.2.1. Operational performance 72
4.2.1.1. Membrane flux response and observed changes in MLSS, HRT, OLR_V, biogas production and COD removal rates 72
4.2.1.2. pH 76
4.2.1.3. Biogas composition 76
4.2.1.4. Specific methane production 77
4.2.2. Membrane performance and fouling phenomena 79
4.2.2.1. Factors influencing membrane flux 82
4.3. Conclusions 88
5. RESULTS – EFFECT OF MCRT ON SANMBR OPERATING AT 36 ^{O}C 91
5.1. Method summary 91
5.2. Results and discussion – MCRT effect experiment at 36 ^{o}C 94
5.2.1. Operational performance 94
5.2.1.1. Start-up 94
5.2.1.2. Membrane flux response to MCRT: observed changes in MLSS, HRT and OLR_V 98
5.2.1.3. COD removal rates and COD balance 100
5.2.1.4. Biogas composition 100
5.2.1.5. Specific methane production 100
5.2.1.6. pH and operational temperature 106

5.2.2. Membrane performance and fouling phenomena 106
5.2.3. Mixed liquor characteristics 107
5.2.3.1. Capillarity Suction Time (CST) 107
5.2.3.2. Microbial growth and kinetics 111
5.3. Conclusions 112
6. RESULTS – EFFECT OF MCRT ON SANMBR OPERATING AT 20 ^{o}C 115
6.1. Method summary 115
6.2. Results and discussion – MCRT effect experiment at 20 ^{o}C 116
6.2.1. Operational performance 116
6.2.1.1. Start-up 122
6.2.1.2. Membrane flux and TMP response to MCRT: observed changes in MLSS, HRT and OLR_V 125
6.2.1.3. COD removal rates and COD balance 128
6.2.1.4. Biogas composition 131
6.2.1.5. Specific methane production 131
6.2.1.6. pH and operational temperature 136
6.2.2. Membrane performance and fouling phenomena 137
6.2.3. Mixed liquor characteristics 138
6.2.3.1. Capillarity suction time (CST) 138
6.2.3.2. Frozen image centrifugation (FIC) 141
6.2.3.3. Extracellular Polymeric Substances (EPS) 141
6.2.3.4. Microscopic examination 146
6.2.3.5. Microbial growth and kinetics 146
6.3. Conclusions 148
7. DISCUSSION 151
7.1. Comparative analysis of the effect of MCRT on SAnMBRs performance at 36 ^{o}C and 20 ^{o}C 151
7.1.1. Membrane flux 151
7.1.2. Capillary suction time 152
7.1.3. Specific methane production 152
7.1.4. Gas composition 154
7.1.5. MLSS 155
7.1.6. COD removal rates 155
7.1.7. Observed biomass yield 156

7.1.8. Mixed liquor characteristics 157
7.2. Advantages and disadvantages of the gravitational configuration for the study of SAnMBRs and its potential for scalability 159
8. CONCLUSIONS AND FUTURE WORK 163
8.1. Conclusions 163
8.2. Future Work 168
REFERENCES 171
APPENDIX A. – LITERATURE REVIEW ON RELEVANT SANMBRS TREATING LOW-TO-INTERMEDIATE STRENGTH WASTEWATER - EXPERIMENTAL SET-UP AND OPERATIONAL PARAMETERS 180
APPENDIX B. – CONSIDERATIONS FOR OPERATION AND PERFORMANCE EVALUATION 183
APPENDIX C. – TMP EQUATION VALIDATION 189

LIST OF FIGURES

Fig. 2.1. Simplified diagram of main reactions in the anaerobic digestion process (van Lier et al., 2008): Steps carried out by (1) Hydrolytic and fermentative bacteria, (2) Acetogenic bacteria, (3) Homo-acetogenic or acetate oxidising bacteria, (4) Hydrogenotrophic methanogens, (5) Acetoclastic methanogens 7

Fig. 2.2. Membrane separation process schematic diagram (Judd and Judd, 2011). 12

Fig. 2.3. Membrane size-exclusion spectrum (WEF, 2012). 13

Fig. 2.4. Schematic representation of main membrane fouling mechanisms: (a) cake fouling, (b) pore blocking. (WEF, 2012) 15

Fig. 2.5. Schematic of common AnMBR configurations: (a) External, (b)(i) Submerged, (b)(ii) Submerged in external chamber (Adapted from Liao et al., 2006) 17

Fig. 2.6. Examples of membrane module types: (a) flat sheet; (b) hollow fibre;(c) tubular 20

Fig. 2.7. Effect of temperature on growth rate of methanogens (Lettinga et al., 2001). 24

Fig. 3.1. Schematic of initial SAnMBR design: membrane directly immersed in reactor with gaslift loop configuration for membrane fouling scouring and mixed liquor 36

Fig. 3.2. Prototype experimental tests: (a) experimental set-up for the preliminary tests with water, (b) experimental set-up for the preliminary test with digestate from Millbrook WWTP: effluent head-difference device, fermentation gas-lock, flux recording balance, flat sheet membrane, influent constant-head device, SAnMBR. 37

Fig. 3.3. Schematic diagram – Detailed design of the SAnMBRs used in all the experiments presented in this work 38

Fig. 3.4. Schematic diagram – SAnMBRs arrangement: (a) one reactor, (b) two reactors 39

Fig. 3.5. SAnMBR internal view: (a) temperature control coil, (b) back gas-lift baffle, (c) membrane, (d) front gas-lift baffle (e) complete inner structure 40

Fig. 3.6. Experimental set-up employed for the main studies in this work: Development and testing of a fully gravitational SAnMBR at 36 ^{o}C, (b) MCRT effect experiment at 36 ^{o}C, (c) MCRT effect experiment at 20 ^{o}C. 42

Fig. 3.7. (a) CST apparatus (Triton Electronics Ltd, UK), (b) Schematic of CST apparatus (APHA et al., 2012) 47

Fig. 3.8. (a) FIC apparatus, (b) schematic diagram of FIC apparatus 47

Fig. 3.9. Flowchart for EPS extraction procedure 48

Fig. 3.10.Diagram for gas volume measurement by weight-type water displacement gasometer (Walker et al., 2009) 52

Fig. 3.11. Calculated values of Henry's constant for solubility of O_2, N_2, CH_4 and CO_2 at different temperatures (L atm. mol^{-1}) 55

Fig. 3.12. Henry's constant for solubility for experimental determination of dissolved CH_4 and CO_2 (Pa) (Perry and Green, 1999) 58
Fig. 3.13. Diagram showing pressure in the gravitational SAnMBR configuration developed in this work 60
Fig. 3.14. Components in the COD balance in an anaerobic reactor (van Lier et al., 2008) 64
Fig. 3.15.SAnMBR considered COD inputs and outputs 65
Fig. 4.1. Experimental set-up schematic diagram – Development and testing of a fully gravitational SAnMBR: biogas collection bags, biogas recirculation pumps, constant head device, effluent collection containers, effluent head-difference device, fermentation gas-lock, flux recording balance, SAnMBR, stirred feed storage tank, and thermo-circulator 70
Fig. 4.2. Experimental set-up schematic picture – Development and testing of a fully gravitational SAnMBR: biogas collection bags, biogas recirculation pumps, constant head device, effluent collection containers, effluent head-difference device, fermentation gas-lock, flux recording balance, SAnMBR, stirred feed storage tank, and thermo-circulator 71
Fig. 4.3. Operational performance during experimental period – Development and testing of fully gravitational SAnMBR experiment at 36 ^oC: (a) Daily average membrane flux, (b) MLSS concentration, (c) TMP, (d) OLR_v, (e) biogas production and (f) COD removal rate. 74
Fig. 4.4 pH during experimental period – Development and testing of fully gravitational SAnMBR experiment at 36 ^oC 76
Fig. 4.5. Biogas composition during experimental period – Development and testing of fully gravitational SAnMBR experiment at 36 ^oC. 76
Fig. 4.6. Specific methane production during experimental period – Development and testing of fully gravitational SAnMBR experiment at 36 ^oC: (a) SMP, (b) SMP_{added} and (c) SMP_{MLSS} 78
Fig. 4.7. Real time membrane flux from EP-2 to EP-4 – Development and testing of fully gravitational SAnMBR experiment at 36 ^oC. 80
Fig. 4.8. (a) Effect of temperature variations on membrane flux, EP-2 (day 58-68), (b) Effect of failure of biogas recirculation pump on membrane flux, EP-4 (days 76-80) – Development and testing of fully gravitational SAnMBR experiment at 36 ^oC 84
Fig. 4.9. Membrane fouling at the end of experimental run before and after rinsing with running tap water and gentle manual wiping – Development and testing of fully gravitational SAnMBR experiment at 36 ^oC: (i) membrane front – before rinse, (ii) membrane back – before rinse, (iii) membrane front – after rinse, (iv) membrane back – after rinse 85
Fig. 4.10 (a) Effect of valve restriction on membrane flux, EP-3 (days 68-71), (b) Effect of biogas accumulation inside the cartridge on membrane flux – Development and testing of fully gravitational SAnMBR experiment at 36 ^oC. 86
Fig. 4.11. Example of a biogas bubble in the permeate line – Development and testing of fully gravitational SAnMBR experiment at 36 ^oC 87
Fig. 5.1. Experimental set-up schematic diagram – MCRT effect experiment at 36 ^oC: biogas collection bags, biogas recirculation pumps, constant head device, effluent collection containers, effluent head-

difference device, fermentation gas-lock, flux recording balance, SAnMBRs, stirred feed storage tank, and thermo-circulator 92
Fig. 5.2. Experimental set-up schematic picture – MCRT effect experiment at 36 ^{o}C: biogas collection bags, biogas recirculation pumps, constant head device, effluent collection containers, effluent head-difference device, fermentation gas-lock, flux recording balance, SAnMBRs, stirred feed storage tank, and thermo-circulator 93
Fig. 5.3. Operational performance during experimental period – MCRT effect experiment at 36 oC: (a) MCRT, (b) Daily average membrane flux, (c) TMP (d) MLSS concentration, (e) COD removal rate 95
Fig. 5.4 Start-up performance – MCRT effect experiment at 36 ^{o}C: (a) Feed temperature, (b) biogas composition in Reactor A and B 97
Fig. 5.5. COD balances during experimental period – MCRT effect experiment at 36 ^{o}C 101
Fig. 5.6. Biogas composition during experimental period – MCRT effect experiment at 36 ^{o}C 102
Fig. 5.7. Specific methane production during experimental period – MCRT effect experiment at 36 ^{o}C: (a) SMP, (b) SMP_{added} and (c) SMP_{MLSS} 103
Fig. 5.8. Fraction of SMP corresponding to the CH_4 dissolved in the effluent during experimental period – MCRT effect experiment at 36 ^{o}C 105
Fig. 5.9. pH during experimental period – MCRT effect experiment at 36 ^{o}C 106
Fig. 5.10 Operational temperature of SAnMBRs during experimental period – MCRT effect experiment at 36 ^{o}C 106
Fig. 5.11 Membrane fouling at the end of experimental run before and after rinsing with running tap water and gentle manual wiping – MCRT effect experiment at 36 ^{o}C: (i) membrane front – before rinse, (ii) membrane back – before rinse, (iii) membrane front – after rinse, (iv) membrane back – after rinse. 109
Fig. 5.12. Mixed liquor filterability during experimental period – MCRT effect experiment at 36 ^{o}C: (a) CST; (b) CST_{MLSS} 110
Fig. 5.13. Observed biomass yield during experimental period – MCRT effect experiment at 36 ^{o}C 111
Fig. 5.14. Observed biomass growth COD fraction during experimental period – MCRT effect experiment at 36 ^{o}C 112
Fig. 6.1. Experimental set-up schematic diagram – MCRT effect experiment at 20 ^{o}C: biogas collection bags, biogas recirculation pumps, constant head device, effluent collection containers, effluent head-difference device, fermentation gas-lock, flux recording balance, SAnMBRs, stirred feed storage tank, and thermo-circulator 117
Fig. 6.2. Experimental set-up schematic picture – MCRT effect experiment at 20 ^{o}C: biogas collection bags, biogas recirculation pumps, constant head device, effluent collection containers, effluent head-difference device, fermentation gas-lock, flux recording balance, SAnMBRs, stirred feed storage tank, and thermo-circulator 118
Fig. 6.3. Operational performance during experimental period – MCRT effect experiment at 20 ^{o}C: (a) MCRT, (b) Daily average membrane flux, (c) TMP (d) MLSS concentration, (e) COD removal rate 119

Fig. 6.4. Start-up performance from day 0 to 60 – MCRT effect experiment at 20 ^{o}C: (a) daily average membrane flux, (b) TMP, (c) MLSS, (d) COD removal, (e) feed COD, (f) HRT, (g) OLR_v, (h) pH, and (i) biogas production..... 123

Fig. 6.5. Feed COD target COD concentration during experimental period– MCRT effect experiment at 20 ^{o}C..... 125

Fig. 6.6 COD removal rates during experimental period – MCRT effect experiment at 20 oC (expanded from Fig. 6.3)..... 129

Fig. 6.7. COD balances during experimental period – MCRT effect experiment at 20 ^{o}C..... 130

Fig. 6.8. Biogas composition during experimental period – MCRT effect experiment at 20 ^{o}C..... 132

Fig. 6.9. Specific methane production during experimental period – MCRT effect experiment at 20 ^{o}C: (a) SMP, (b) SMP_{added} and (c) SMP_{MLSS}..... 133

Fig. 6.10. Fraction of SMP corresponding to the CH4 dissolved in the effluent during experimental period – MCRT effect experiment at 20 ^{o}C..... 135

Fig. 6.11. pH during experimental period – MCRT effect experiment at 20 ^{o}C 136

Fig. 6.12. Operational temperature of SAnMBRs during experimental period – MCRT effect experiment at 20 ^{o}C..... 136

Fig. 6.13. Membrane fouling at the end of experimental run before and after rinsing with running tap water and gentle manual wiping – MCRT effect experiment at 20 ^{o}C: (i) membrane front – before rinse, (ii) membrane back – before rinse, (iii) membrane front – after rinse, (iv) membrane back – after rinse 139

Fig. 6.14. Mixed liquor filterability during experimental period – MCRT effect experiment at 20 ^{o}C: (a) CST; (b) CST_{MLSS}..... 140

Fig. 6.15. Mixed liquor centrifugation during experimental period – MCRT effect experiment at 20 ^{o}C: FIC test..... 142

Fig. 6.16. Schematic picture of centrifuged mixed liquor (Reactor B, day 204) during FIC test; showing of no separation, 3 phase separation and 2 phase separation – MCRT effect experiment at 20 ^{o}C..... 143

Fig. 6.17. EPS concentration during experimental period – MCRT effect experiment at 20 ^{o}C: (a) Bound EPS protein, (b) Bound EPS carbohydrates, (c) Soluble EPS protein, and (d) Soluble EPS carbohydrates. 144

Fig. 6.18. Microscopic examination (10x) of mixed liquor on day 112: (a) Reactor A; (b) Reactor B; (c) Reactor C; (d) Reactor D. 146

Fig. 6.19. Observed biomass yield..... 147

Fig. 6.20. Observed biomass growth COD fraction during experimental period – MCRT effect experiment at 20 ^{o}C. 148

Fig. 7.1. Variation in CST with MCRT in experiments with AnMBR operating temperatures of 20 and 36 ^{o}C. 153

Fig. 7.2. Variation in SMP with MCRT in experiments with AnMBR operating temperatures of 20 and 36 ^{o}C. 153

Fig. 7.3. Average gas composition during experiments with variable MCRT at at 36 ^{o}C and 20 ^{o}C..... 154

Fig. 7.4. Variation in MLSS with MCRT in experiments with AnMBR operating temperatures of 20 and 36 ^{o}C 155
Fig. 7.6. Variation in average observed biomass yield with MCRT in experiments with AnMBR operating temperatures of 20 and 36 ^{o}C. 156
Fig. 7.7. Mixed liquor settleability through time – MCRT effect experiment at 36 ^{o}C: sample taken on day 245, where Reactor A was operated at 15 days MCRT, and Reactor B at 96 days MCRT. 157
Fig. 7.8. Mixed liquor settleability through time – MCRT effect experiment at 36 ^{o}C: sample taken on day 209, where Reactor A was operated at 20 days MCRT, Reactor B at 45 days MCRT, Reactor C at 30 days MCRT, and Reactor D at 30 days MCRT. 158

Appendix B - Fig. 1. COD reduction due to degradation and adherence on walls and lines at 20^{o}C 183
Appendix B - Fig. 2. Dissolved CH_4 contribution to COD in test: effluent samples from MCRT effect experiment at 20 ^{o}C (Chapter 6) of operational day 211. 184
Appendix B - Fig. 3. Air measured in biogas produced compared to the theoretical air entering the system dissolved in the feed at the saturation concentration – MCRT effect experiment at 36 ^{o}C (Chapter 5)... 185
Appendix B - Fig. 4. Dissolved CH_4 in the effluent – MCRT effect experiment at 36 ^{o}C (Chapter 5)..... 187
Appendix B - Fig. 5. Dissolved CH_4 in the effluent – MCRT effect experiment at 20 ^{o}C (Chapter 6)..... 187

Appendix C - Fig. 1. MBR gravitational Bernoulli diagram 189

LIST OF TABLES

Table 2.1. Typical sewage composition with and without industrial contribution 4
Table 2.2. Typical biogas composition (Seadi et al., 2008) 8
Table 2.3. Advantages and disadvantages of high-rate anaerobic sewage treatment systems over aerobic processes 9
Table 3.1. Synthetic wastewater composition 34
Table 3.2. Synthetic wastewater characterisation and elemental analysis 34
Table 3.3.Trace Elements concentration in stock solution 35
Table 3.4. SAnMBRs detailed design values 39
Table 3.5. FICODOX-plus and Ferroin Indicator composition 43
Table 3.6. Sample volume related to expected BOD range 50
Table 3.7. Gas constants (C) for the temperature correction of Henry's constant for solubility of O_2, N_2, CH_4 and CO_2 55
Table 4.1 Start-up and experimental phases – Development and testing of fully gravitational SAnMBR experiment at 36 ^oC 71
Table 4.2. Experimental results summary table – Development and testing of fully gravitational SAnMBR experiment at 36 ^oC: Daily average membrane flux, TMP feed COD, effluent COD, COD removal, OLR_v, HRT, biogas production, CH_4 in biogas, SMP, pH, MLSS and MCRT 73
Table 5.1. Start-up and experimental phases – MCRT effect experiment at 36 ^oC 91
Table 5.2. Experimental results summary table – MCRT effect experiment at 36 ^oC: MCRT, TMP, daily average membrane flux, OLR_v, HRT, feed COD, effluent COD, COD removal rate, CH_4 in biogas, SMP, MLSS, MLVSS, CST and pH. 96
Table 5.3. SMP values reported in studies evaluating the effect of MCRT and HRT on SAnMBRs treating low-strength wastewater 105
Table 6.1. Start-up and experimental phases – MCRT effect experiment at 20^{o}C 116
Table 6.2. Experimental results summary table – MCRT effect experiment at 20 ^oC: MCRT, TMP, daily average membrane flux, OLR_v, HRT, feed COD, effluent COD, COD removal rate 120
Table 6.3. Experimental results summary table – MCRT effect experiment at 20 ^oC: MCRT, CH_4 in biogas, SMP, MLSS, MLVSS, CST and pH. 121
Table 7.1. Advantages and disadvantages of the SAnMBRs in a gravitational configuration 160

Appendix A - Table 1. Literature compilation of relevant SAnMBRs treating low-to-intermediate strength wastewater - experimental set-up and operational parameters 180

DECLARATION OF AUTHORSHIP

I, Santiago Pacheco-Ruiz
Declare that the thesis entitled

"SUBMERGED ANAEROBIC MEMBRANE BIOREACTOR FOR WASTEWATER TREATMENT: EFFECT OF MEAN CELL RESIDENCE TIME ON MEMBRANE FLUX, MIXED LIQUOR CHARACTERISTICS AND OVERALL REACTOR PERFORMANCE"

and the work presented in the thesis are both my own, and have been generated by me as the result of my own original research. I confirm that:

- this work was done wholly or mainly while in candidature for a research degree at this University;
- where any part of this thesis has previously been submitted for a degree or any other qualification at this University or any other institution, this has been clearly stated;
- where I have consulted the published work of others, this is always clearly attributed;
- where I have quoted from the work of others, the source is always given. With the exception of such quotations, this thesis is entirely my own work;
- I have acknowledged all main sources of help;
- where the thesis is based on work done by myself jointly with others, I have made clear exactly what was done by others and what I have contributed myself;
- parts of this work have been published as:
  - Santiago Pacheco-Ruiz, Sonia Heaven & Charles J. Banks (2015): Development and testing of a fully gravitational submerged anaerobic membrane bioreactor for wastewater treatment, Environmental Technology, 36, 2328–2339. DOI:10.1080/09593330.2015.1026847
  - Santiago Pacheco-Ruiz, Sonia Heaven & Charles J. Banks (2016): Effect of mean cell residence time on transmembrane flux and overall performance of a submerged anaerobic membrane bioreactor, Environmental Technology, Online version. DOI:10.1080/09593330.2016.1225127.
- parts of this work are in the process of being published as:
  - Santiago Pacheco-Ruiz, Sonia Heaven & Charles J. Banks (Under Preparation): Kinetic control of submerged anaerobic membrane bioreactors operating at 20 ^{o}C and its influence on membrane flux, mixed liquor characteristics and overall reactor performance.

- parts of this work have been presented in the following conferences
  - Aquaenviro - Innovations in Wastewater Treatment conference (22/03/2016) – Oral Presentation
  - BBSRC-Anaerobic Digestion Network - Specialised Workshop: Anaerobic Membrane Bioreactors for Wastewater Treatment and Energy Recovery (14/01/2016) – Chair and Organiser. (Work presented by Professor Charles Banks).
  - 14th World Congress on Anaerobic Digestion (17/11/2015) – Oral and Poster presentation
  - BBSRC AD-Net. Early Career Researcher Conference (30/06/2015) – Oral Presentation
  - Aquaenviro - Short Retention Time Anaerobic Digestion Processes for Industrial Wastewater Treatment conference (11/12/2014) – Oral Presentation
  - EU-China Workshop on Resource Recovery from Biomass and Green Technology in Waste/Wastewater Treatment (09/11/2014) – Poster Presentation (Work presented by Professor Charles Banks.)

Signed: ……..

Date: 19 of September of 2016

ACKNOWLEDGEMENTS

I would like to express my deepest gratitude towards my supervisors Dr Sonia Heaven and Professor Charles Banks for their absolute support, constant encouragement and constructive and insightful advice. Special thanks to: my examiners Professor Jaeho Bae and Dr Yue Zhang for their valuable advice and useful feedback; to all the colleagues of the Bioenergy and Organic Resources Research Group for their friendship and delightful collaboration; to Dr Andrew Salter, Dr Dominic Mann and Pilar Pascual for their technical help and advice in the laboratory; to Angie Bywater and Dr Louise Bayfield from the BBSRC AD-Network for all their support; and to Paola Marticorena for her assistance in the measurement of proteins and carbohydrates from the EPS extracted samples.

The Mexican National Council on Science and Technology (CONACYT), the Faculty of Engineering and the Environment at the University of Southampton, the EU FP7 ALL-GAS project 268208, the ERA-Net / BBSRC AmbiGAS project (BEN6-12-19, BB/L000024/1), and the BBSRC NIBB Anaerobic Digestion Network are gratefully acknowledged for funding and supporting this research.

Finally I would like to thank all my beloved family, particular to my wife and love of my life Sofia for being with me at every step of this long adventure; to my mother Ana Maria, for showing me the path since I was born and for being the best example I could have had; to my brother Rodrigo for being my best friend, colleague and advisor; and last but not least, to my fluffy friend Torkoll for making me smile even in the most difficult days.

DEFINITIONS AND ABBREVIATIONS

AeMBR	Aerobic Membrane Bioreactor
AnMBR	Anaerobic Membrane Bioreactor
COD	Chemical Oxygen Demand
CST	Capillary Suction Time
CSTR	Continuously Stirred Tank Reactor
EP	Experimental Phase
EPS	Extracellular Polymeric Substances
FS	Flat Sheet
GC	Gas Chromatography
HF	Hollow fibre
HRT	Hydraulic Retention Time
MBR	Membrane bioreactor
MCRT	Mean Cell Residence Time
MLSS	Mixed Liquor Suspended Solids
MLVSS	Mixed Liquor Volatile Suspended Solids
OLR	Organic Loading Rate
OLR_v	Volumetric organic loading rate
SAnMBR	Submerged Anaerobic Membrane Bioreactor
SMP	Specific Methane Production
SRT	Solids Retention Time
STP	Standard Pressure and Temperature
TE	Trace Elements
TKN	Total Kjeldahl Nitrogen
TMP	Transmembrane pressure
TS	Total Solids
UASB	Up-flow Anaerobic Sludge Blanket
VFA	Volatile Fatty Acid
VS	Volatile Solids

1. INTRODUCTION

Wastewater treatment is an essential process to protect human health by reducing transmission of excreta-related diseases (Mara, 2003), as well as to mitigate the environmental impact of waste production from human activities (Muga and Mihelcic, 2008, Water-UK, 2011). Current domestic wastewater treatment processes, however, are energy-consuming, produce large quantities of waste, and fail to recover the potential resources available in wastewater (Smith *et al.*, 2012). This leads to a dilemma between the benefits of increased water quality standards, and the financial and environmental costs of the necessary treatment processes to achieve them (Muga and Mihelcic, 2008). Hence the growing need, not only in the developing world but also in industrialized countries, to develop sustainable treatment technologies that reduce the overall process impact by minimising investment costs and energy consumption, optimising the treatment efficiency, and recovering resources in the form of water, materials and energy (Smith et al., 2012, Seghezzo *et al.*, 1998, Muga and Mihelcic, 2008).

This approach towards a sustainable water management has driven the application of innovations in anaerobic biotechnology for wastewater treatment, as they allow energy recovery through the conversion of organic matter to energy in form of biogas (Smith et al., 2012). Sustainable anaerobic treatment of sewage is particularly challenging due to its relatively low strength and production at high flow rates per capita (Smith et al., 2012), which results in: (1) difficulty in retaining slow-growth anaerobic microorganisms with short hydraulic retention times (Lin *et al.*, 2013); and (2) a low energy recovery during the anaerobic treatment that compromises the net energy balance of the process and thus the economic and environmental viability (Gomec, 2010, Lew *et al.*, 2004).

High rate anaerobic reactors aim to tackle these issues as they allow biomass retention either by formation of granular sludge or by attachment to a fixed or mobile support material (Liao *et al.*, 2006). Among the high-rate anaerobic reactors, the anaerobic

membrane bioreactor (AnMBR) provides a complete solid-liquid separation by using a membrane, as well as high quality effluents, small footprints and potential positive net energy balances (Lin et al., 2013). The AnMBR has the potential to be the next major step in the development of anaerobic wastewater treatment technology as it is able to generate a high-quality effluent during operation at reasonable hydraulic retention times (HRT) and at low temperatures, while producing methane-rich biogas and a fraction of the sludge compared to aerobic treatment (Smith *et al.*, 2014).

Although the advantages of AnMBR systems have been well demonstrated in the literature (Lin et al., 2013), there are still considerable technical challenges to be overcome before full-scale application of the technology becomes widespread. These include recovery of dissolved methane from the effluent, and reduction of membrane fouling and/or the high energy consumption of membrane cleaning systems (Smith et al., 2012, Stuckey, 2012, Smith et al., 2014). Of these, membrane fouling still represents the main limitation on AnMBR, as it reduces the flux by decreasing the overall membrane permeability (Navaratna and Jegatheesan, 2011). Alternative methods for assessment of AnMBR membrane performance may contribute to finding operational regimes that establish the best balance between fouling, membrane flux, cleaning frequency and other operational parameters (Judd *et al.*, 2008). Future AnMBR research should, therefore, focus on the relationship between operational parameters, treatment performance and membrane fouling, which is complex and poorly defined in the literature (Smith et al., 2012).

This thesis presents a literature review of the state of the art of AnMBRs, followed by a programme of experimental work designed to address some of the gaps in current knowledge with aims and objectives identified at the end of the literature review.

2. LITERATURE REVIEW

2.1. Wastewater treatment

Wastewater can be simply defined as waste liquid or water-borne waste produced by human activities (Metcalf and Eddy, 2004). Untreated wastewater causes major damage to the environment and to human health, and it should therefore be treated in order to reduce the transmission of excreta-related diseases and to minimise water pollution and any consequent damage to the environment (Mara, 2003). Wastewater can be classified according to its source, which in turn will determine its characteristics and appropriate treatment processes. When wastewater originates from homes and businesses it is usually known as sewage or as municipal wastewater. This typically contains pollutants such as: faecal and vegetable matter, grease and scum, detergents, rags and sediment. On the other hand, wastewater from an industrial process is known as industrial effluent or wastewater and may include toxic chemicals and metals, strong organic wastes, radioactive materials, large amounts of sediment, acidic/caustic wastes and may be at a high temperature (SWQB, 2007). Wastewaters with a high concentration of organic matter are said to be 'stronger' (Mara, 2003). Municipal sewage is the most abundant type of wastewater, and is characterized by low organic strength and high particulate organic matter content. This falls into the category of low-strength waste streams (Ozgun et al., 2013), as the concentration of the organic matter may be far lower than in industrial wastewaters; which in turn are referred as high-strength wastewaters. There is no single agreed classification system for wastewater strength, however, and categories depend to an extent on the source of the wastewater. A medium-high strength municipal sewage may fall within the range of low strength industrial wastewaters: the latter can be as low as 270-1200 mg COD L^{-1} for sugar cane and dairy industries but can also be above 100,000 mg COD L^{-1} for distillery and paper industries (Rajeshwari et. al, 2000). Since this study aims to address wastewaters within a range of 500-1,000 mg COD L^{-1} (regardless of their origin) from this point onwards they will be referred to as low-to-intermediate strength wastewaters.

Whilst industrial wastewater composition can be stable as it is usually governed by a fixed processes, the characteristics of municipal sewage are subject to a number of changing factors, such as: water availability, climatic conditions, economic status and social customs. These may vary from one location to another and over hourly, daily and seasonal timescales (Henze and Comeau, 2011, Ali, 2014). For this reason, it is difficult to provide a precise characterization of municipal sewage. Table 2.1 summarises a typical composition for municipal sewage, with and without minor industrial contributions. Another important characteristic of municipal wastewater is the temperature, which depending on the geographical location and time of year can range between 3-27 ^{o}C in United States and could even reach up to 35 ^{o}C in some places of Africa and the Middle East (Metcalf and Eddy, 2004).

Table 2.1. Typical sewage composition with and without industrial contribution

Constituent		**Concentration (mg L^{-1})**					
		No industrial contribution[a]			**With industrial contribution[b]**		
		High	**Med.**	**Low**	**High**	**Med.**	**Low**
Solids	Total	1,200	720	350			
	Dissolved, total	850	500	250			
	Fixed	525	300	145			
	Volatile	325	200	105			
Suspended solids	Total	350	220	100	600	400	250
	Fixed	75	55	20			
	Volatile	275	165	80	480	320	200
	Settleable	20	10	5			
Chemical Oxygen Demand (COD)		1,000	500	250	1,200	750	500
Biochemical oxygen demand (BOD_5)		400	220	110	560	350	230
Total organic carbon (TOC)		290	160	80			
Nitrogen		85	40	20	100	60	30
Organic		35	15	8			
Free ammonia		50	25	12	75	45	20
Phosphorus		15	8	4	25	15	16
Organic		5	3	1			
Inorganic		10	5	3			
Chlorides		100	50	30			
Alkalinity (as CaCO3)		200	100	50			
Grease		150	100	50			

Sources: a (Metcalf and Eddy, 2004) ; b (Henze and Comeau, 2011)

Current sewage treatment processes are energy-consuming, produce large quantities of waste, and fail to recover some of the resources potentially available in wastewater. For this reason, there is growing interest in sustainable water management, and sewage treatment practices are being revaluated to reduce energy demands and environmental impacts while enhancing recovery of resources in the form of water, materials, and energy. Sustainable treatment of municipal sewage is particularly challenging due to its relatively low strength and large volumes. As a result, this approach towards sustainable development is driving the application of innovations in anaerobic biotechnology for sewage treatment, as they allow energy recovery through the conversion of organic matter to methane-rich biogas (Smith et al., 2012). Treatment of municipal sewage by anaerobic systems is still considered a challenge, however, due to the high fraction of particulate organic material, moderate biodegradability and low strength (Ozgun et al., 2013).

2.1.1. Use of synthetic wastewater for research

As discussed above, the composition of municipal sewage is constantly changing due to several factors. This makes very difficult to conduct controlled experiments and simulations for the study and development of treatment processes using real sewage. For that reason, synthetic wastewaters are commonly used in research as this allows production of a material with repeatable and reproducible characteristics which is easy to prepare, safe to store and handle, cheap, and avoids the risk of exposure to pathogens present in real sewage (Ali, 2014). The use of a synthetic substrate also allows experimental runs to be carried out over long durations without changes in the properties of the influent feed. This eliminates the substrate variability that can make interpretation of results difficult; and is thus considered justifiable at an early stage in this type of research (Visvanathan and Abeynayaka, 2012, Lin et al., 2013), as it gives a greater degree of control where a specific aspect of operation is under investigation.

2.2. Anaerobic wastewater treatment

Anaerobic digestion is a process in which different groups of microorganisms break down biodegradable material in the absence of air. These microorganisms gain energy from biochemical reactions that allow their growth and establishment in these oxygen-limited environments (Rittmann and McCarty, 2001, Speece, 1996). From a process perspective, anaerobic digestion can be considered to consist of four stages as outlined in Fig. 2.1 and explained below (van Lier *et al.*, 2008):

- *Hydrolysis* – a relatively slow process (compared to other anaerobic digestion stages) where hydrolytic organisms secrete extracellular enzymes that breakdown complex molecules into smaller and simpler soluble organics which can then pass through the cell wall and membranes of fermentative bacteria
- *Acidogenesis (fermentation)* - the small molecules formed during the hydrolysis step are taken out of solution by the fermentative and acid-producing bacteria and, in absence of oxygen, converted predominantly to acid products.
- *Acetogenesis* - intermediate acid production stage where digestion products, such as longer chain volatile fatty acids (VFA), are converted by acetogenic bacteria into acetate, hydrogen and carbon dioxide, as well as new cell material
- *Methanogenesis* - in this stage methanogenic archaea, also known as methanogens, convert acetate, hydrogen plus carbonate and methanol into methane, carbon dioxide and new cell material

Anaerobic digestion is a robust and well-established technology (Appels *et al.*, 2011), widely used since the time of the first engineered wastewater treatment plants to reduce the environmental impact of several concentrated pollution streams (Foresti *et al.*, 2006, Collet *et al.*, 2011). Currently, it is one of the most important processes used in wastewater treatment as it combines pollution control/reduction and energy production (Lin et al., 2013). The energy product is biogas which is rich in methane, a flexible energy source for fuel and power applications. Furthermore, anaerobic processes produce mineralized nutrients in the form of ammonia and orthophosphate enabling direct agricultural use of the effluent for ferti-irrigation (Ozgun et al., 2013).

While aerobic processes have been widely used to treat organic wastewater due to their high treatment efficiency, they have a high sludge production and high energy consumption due to the requirement for oxygen supply; these items represent the two main costs associated with aerobic wastewater treatment (Seghezzo et al., 1998). On the other hand, in anaerobic treatment processes, no oxygen supply is needed and sludge production is 3-20 times smaller than in aerobic methods, hence the costs and energy requirements are dramatically reduced (Seghezzo et al., 1998). Furthermore, anaerobic treatment systems are capable of producing biogas (containing methane (CH_4) and carbon dioxide (CO_2) as its major components, see Table 2.2) as a by-product of the treatment process, and thus representing not only a sustainable method for treating wastewater, but also a renewable energy source (Mahmoud *et al.*, 2004, Aiyuk *et al.*, 2006).

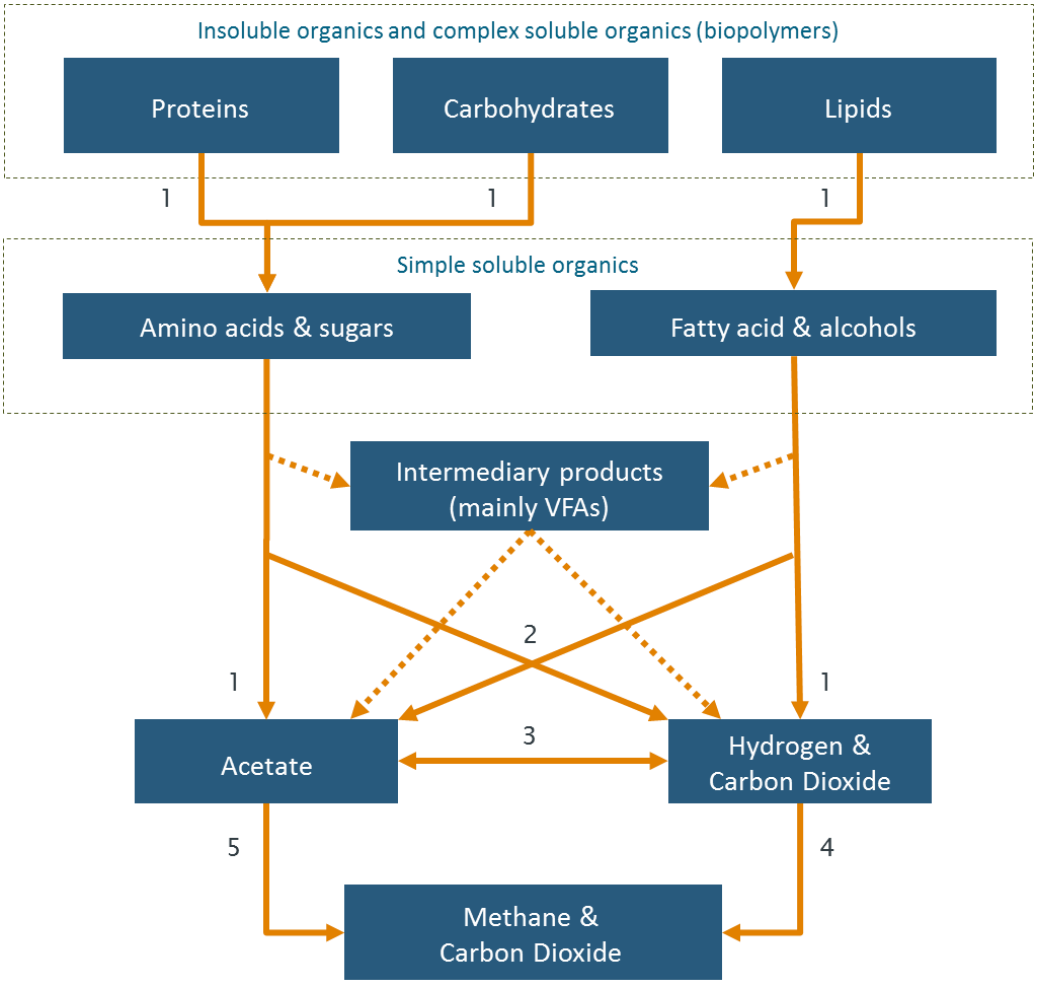

Fig. 2.1. Simplified diagram of main reactions in the anaerobic digestion process (van Lier et al., 2008): Steps carried out by (1) Hydrolytic and fermentative bacteria, (2) Acetogenic bacteria, (3) Homo-acetogenic or acetate oxidising bacteria, (4) Hydrogenotrophic methanogens, (5) Acetoclastic methanogens

Table 2.2. Typical biogas composition (Seadi et al., 2008)

Compound	Chemical symbol	Content (%)
Methane	CH_4	55 – 75
Carbon dioxide	CO_2	25 – 45
Water in form of vapour	H_20_g	2 (20 ^oC) – 7 (40 ^oC)
Oxygen	O_2	< 2
Nitrogen	N_2	< 2
Ammonia	NH_3	< 1
Hydrogen	H_2	< 1
Hydrogen sulphides	H_2S	< 1

On the basis of the concept of resource (energy) recovery and utilization, anaerobic processes have been increasingly recognized as the core method of an advanced technology for environmental protection and resource preservation (Seghezzo et al., 1998, Chan *et al.*, 2009). Direct treatment of sewage by anaerobic processes is undoubtedly an attractive and appropriate alternative, especially for developing countries, due to the low initial investment and easy maintenance in comparison with conventional aerobic processes (Gomec, 2010). Anaerobic treatment processes, however, have mainly been applied to wastewaters containing high strength soluble substrates (Lin et al., 2013). This is mainly because:

- Energy recovery from low strength wastewater per unit volume treated tends to be low. This means that additional energy inputs may be required to operate the system, compromising the net energy balance and thus the economic and environmental viability of the process (Lew et al., 2004, Gomec, 2010).
- There are problems in retaining slow-growth anaerobic microorganisms at the short hydraulic retention times associated with low-strength wastewater treatment (Lin et al., 2013).

Despite the substrate strength, anaerobic micro-organisms grow very slowly due to their low energy yields per gram of substrate. This, together with the relatively poor

settling properties of the biomass in conventional anaerobic systems, results in low biomass retention. An efficient reactor design, therefore, requires decoupling of the hydraulic retention time (HRT) from the solids retention time (SRT) to avoid washout of slow-growth anaerobic microorganisms from the reactor such as methanogens (Ozgun et al., 2013, Stuckey, 2012, Lin et al., 2013). This has led to the development of commercial high-rate anaerobic reactors, which are feasible because they allow biomass retention either by formation of granular sludge or attachment to a fixed or mobile support material, successfully decoupling the SRT from the HRT (Liao et al., 2006). The main advantages and disadvantages of high-rate anaerobic sewage treatment systems over aerobic processes are shown in Table 2.3.

Table 2.3. Advantages and disadvantages of high-rate anaerobic sewage treatment systems over aerobic processes

Advantages	Disadvantages
• Substantial savings in operational costs as no energy is required for aeration	• The extent of organic matter removal is less than in activated sludge processes, requiring in most cases adequate post-treatment to meet the effluent requirements or reuse criteria
• Potential reductions in investment cost considering that primary clarification, the bioreactor, secondary clarification and the sludge digester are combined into one tank	• The produced CH_4 is partially dissolved in the effluent (depending on the influent COD concentration and the applicable hydraulic flow).
• The produced CH_4 is of interest for energy recovery or electricity production	• So far no measures are applied in full-scale plants to prevent CH_4 escaping to the atmosphere
• The process is robust and can handle periodic high hydraulic and organic loading rates	• The collected CH_4 is often not utilized for energy generation and in some cases not even flared (contribution to greenhouse gas emissions)
• The system is compact with HRTs of 6–9 h, and is therefore suitable for applications in urban areas, minimizing conveyance costs	• There is little experience with full-scale application especially at moderate to low temperatures
• Small-scale applications may allow decentralized treatment, making sewage treatment less dependent on the extent of sewage networks	• Reduced gases, like H_2S, that are dissolved in the effluent may escape causing odour problems
• The sludge production is low, well stabilized and easily dewatered; consequently reducing post treatment costs	• High influent sulphate concentrations may limit the applicability of sewage treatment
• Valuable nutrients (N and P) are conserved which give the treated wastewater a high potential for crop ferti-irrigation	

Source: Adapted from Chernicharo *et al.* (2015)

Currently most high rate anaerobic processes use biofilm support media or granulated sludge to obtain a high biomass concentration. Membrane separation could represent an alternative which may have other advantages such as high-quality effluent and may be particularly attractive when biofilm or granulation are not easily achievable (Spagni *et al.*, 2010) and for low-strength wastewater with high particulates (Lin et al., 2013).

2.3. Anaerobic membrane bioreactors

Among high rate anaerobic reactors, the anaerobic membrane bioreactor (AnMBR) is capable of providing complete retention of biomass by using a membrane, avoiding the washout of slow-growth anaerobic microorganisms from the reactor. The AnMBR process can be defined as a biological treatment process operated without oxygen and using a membrane to provide complete solid-liquid separation (Visvanathan and Abeynayaka, 2012, Lin et al., 2013). The design evolved from aerobic membrane bioreactors (AeMBR) which, although more common, have obvious drawbacks such as high solids production and energy use (Stuckey, 2012). In contrast, AnMBRs potentially transform energy-consuming wastewater treatment processes into bioprocesses with neutral or even positive energy balances (Yeo and Lee, 2013), while generating an effluent quality comparable to aerobic treatment (Smith et al., 2012).

AnMBRs were first introduced in the 1980s but remain less studied than AeMBR (Lin et al., 2013). After three decades of development, AnMBR systems seem to be emerging as a promising technology for municipal wastewater treatment as they have the potential to generate a high-quality effluent during operation at reasonable HRTs, while producing methane-rich biogas and a fraction of the sludge compared to aerobic treatment (Smith et al., 2014). Furthermore, since pathogens can be retained by the membrane unit and macronutrients are not removed by anaerobic bioprocesses, permeates of AnMBRs are certainly of interest for agricultural use (Ozgun et al., 2013). On the other hand, AnMBRs can operate at HRTs similar to their aerobic counterparts, and research over recent years has shown they can successfully adapt to low temperatures (Ho and Sung, 2009, Huang *et al.*, 2011, Huang *et al.*, 2013) resulting in potential net energy production.

Energy use has now become an environmental indicator of resource utilization and performance of the wastewater treatment processes (Muga and Mihelcic, 2008). The relatively high energy consumption of membrane bioreactor (MBR) technology compared to conventional treatment systems is, therefore, a major drawback for their environmental and economic feasibility (WEF, 2012). In AnMBRs fouling control contributes significantly to overall energy demand and operational costs, as does the potential energy loss from dissolved methane in the effluent (Smith et al., 2014). So far there are very few studies on the energy requirements of MBRs and even fewer for anaerobic systems. A recent modelled calculation estimated that depending on the configuration the energy demand in AnMBRs can range between 0.03 to 16.5 kWh m^{-3} (Martin *et al.*, 2011), a wide range.

On the other hand, low sewage temperatures in temperate and cold climates have been considered a barrier for mesophilic anaerobic treatment because the energy requirements associated with heating large quantities of wastewater to the operating temperature can significantly exceed the energy recovery potential. Although the mesophilic anaerobic treatment of municipal wastewater could still be achievable in locations where its temperature can reach up to 35 ^{o}C (Section 2.1), low-temperature (<20 ^{o}C) operation seems the only economically feasible option for locations with colder climates (Smith et al., 2012). At low temperatures, however, the rate of biomass growth is considerably reduced, requiring longer MCRT at relatively low HRT as well as the avoidance of any possible microorganism washout (Smith et al., 2012, Ozgun et al., 2013). Hence the interest in implementing AnMBRs for low-to-intermediate strength wastewater treatment at ambient temperature. While the optimization of AnMBR systems generally focus on either the biological process or on the membrane separation, few authors, have studied the interaction between both processes and the impact of key operational parameters (Ozgun et al., 2013). Furthermore, little work has been done so far on AnMBRs for low-strength wastewater treatment, where most of the studies have focused on proof of concept and membrane fouling (Smith et al., 2012). Recent reviews on AnMBRs (Stuckey, 2012, Smith et al., 2012, Visvanathan and Abeynayaka, 2012) suggest that future research should focus particularly on developments to:

- reduce energy demand and increase the efficiency of membrane cleaning mechanisms
- understand the link between operational parameters, treatment performance and membrane fouling
- improve the management, handling and recovery of dissolved methane
- understand the changes and/or necessary modifications for successful operation at low-temperature

2.3.1. Membrane separation process

A membrane as applied to water and wastewater treatment is simply a material that allows some physical or chemical components to pass more readily through it than others (Fig. 2.2). It is thus perm-selective, since it is more permeable to those constituents passing through it (permeate) than those which are rejected by it (retentate); where the degree of selectivity depends on the membrane pore size (Judd and Judd, 2011).

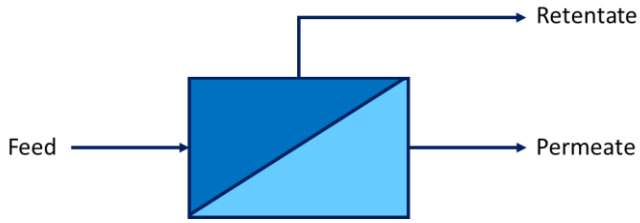

Fig. 2.2. Membrane separation process schematic diagram (Judd and Judd, 2011).

Membranes can be defined according to the type of separation process they are used for, which then provides an indication of the pore size. The four key membrane separation processes in which water forms the permeate product are reverse osmosis (RO), nanofiltration (NF), ultrafiltration (UF) and microfiltration (MF) (Fig. 2.3). While the coarsest membrane is associated with MF being able to reject particulate matter, the most selective membrane is associated with RO as it can reject singly charged ions, such as sodium and chloride, with a diameter of less than 1 nm thus indicating that the pores in an RO membrane are very small. (Judd and Judd, 2011). UF and MF are the main membrane separation processes integrated in membrane bioreactor (MBR) systems (WEF, 2012).

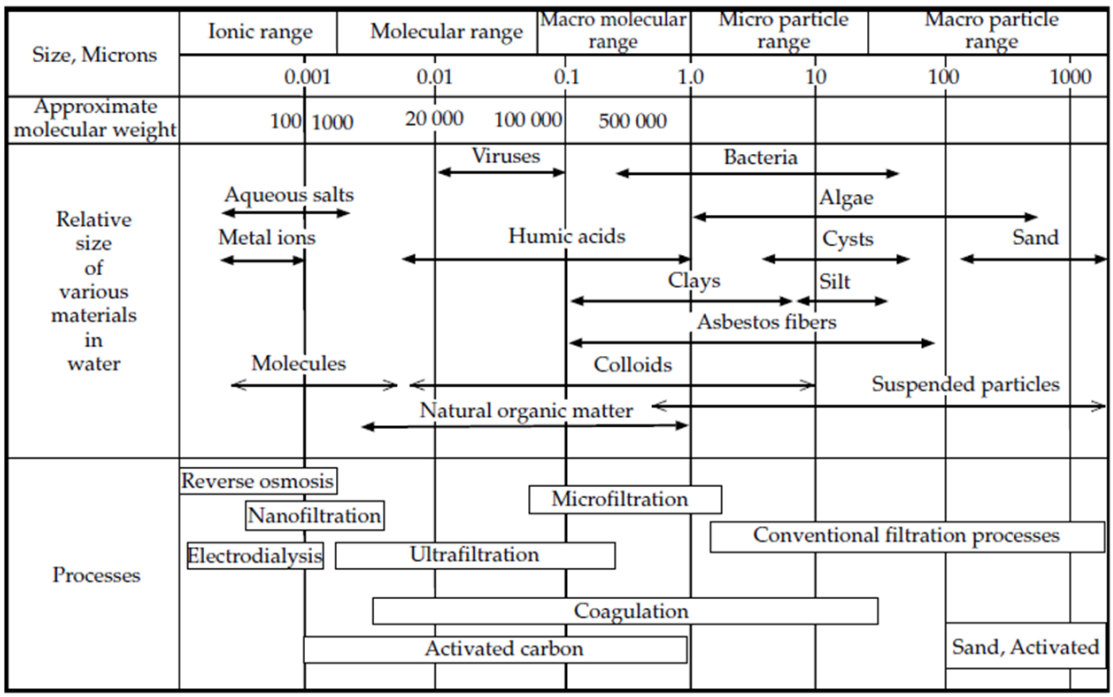

Fig. 2.3. Membrane size-exclusion spectrum (WEF, 2012).

Rejection of contaminants represents a fundamental constraint on all membrane processes as these tend to accumulate at the membrane surface, producing various phenomena which lead to a reduction in the flow of liquid through the membrane (i.e. the flux) at a given transmembrane pressure (TMP), or conversely an increase in the TMP for a given flux (reducing the permeability, which is the ratio of flux to TMP). These phenomena are collectively referred to as fouling. Given that membrane fouling represents the main limitation on membrane process operation, it is unsurprising that the majority of membrane material and process research and development conducted is dedicated to its characterization and amelioration (Judd and Judd, 2011).

2.3.1.1. Membrane fouling

Membrane fouling is considered an inevitable phenomenon of all membrane processes (Ng *et al.*, 2006). Its control represents the most intensive energy demand associated with AnMBR treatment, and reducing this demand is therefore central to maximising the net potential energy recovery (Smith et al., 2012). The inability to adequately control or reduce fouling results in substantially higher costs due to the need for periodic chemical cleaning or membrane replacement to sustain daily operation, and a possible inability to treat the design flux (WEF, 2012, Ng et al., 2006).

Membrane fouling is an extremely complex phenomenon, caused by a combination of components in the reactor such as the soluble organics, inorganic precipitates and colloidal particles from the feed and cell lysis (Stuckey, 2012). It occurs when these materials deposit and accumulate internally in the membrane pores and externally on the membrane surface, which reduces flux, increases TMP, and potentially necessitates chemical cleaning or membrane replacement (Smith et al., 2012, WEF, 2012). The nature and degree of fouling are strongly influenced by four main factors (Rosenberger *et al.*, 2006, Stuckey, 2012, Navaratna and Jegatheesan, 2011):

- Membrane characteristics
- Hydrodynamic conditions – flux, TMP and cross flow velocity
- Operational conditions – temperature, SRT, HRT and inflow characteristics
- Mixed liquor characteristics – mixed liquor suspended solids and volatile suspended solids, viscosity and substances attached to the microorganisms or in the liquid phase

These factors are discussed in sections 2.3.1.2 to 2.3.3.4 below.

The design of membrane reactors is driven by the balance between hydrodynamic and operational conditions, fouling control and cleaning frequency, and energy demand (Judd et al., 2008). Therefore, a fuller understanding of the membrane fouling phenomena could lead to more practical solutions through prevention and minimisation and may suggest more efficient mechanisms for membrane cleaning (Le-Clech et al., 2006). Membrane fouling can be characterised based on the applicable treatment and cleaning mechanisms (WEF, 2012):

- *Physically reversible*. Caused by loosely attached foulants that can be removed using some form of physical cleaning or treatment, such as: backwashing with permeate, relaxation breaks, membrane surface scouring by gas bubbles in a liquid (Siembida *et al.*, 2010).
- *Chemically reversible*. Caused by foulants that are more strongly attached to the membrane surface or inside pores and are more difficult to remove, requiring chemical cleaning.
- *Irreversible* – Permanent; cannot be cleaned by physical or chemical means.

Membrane fouling can also be classified by its mechanism of occurrence (WEF, 2012):

- *Cake fouling*. Caused by the physical accumulation of colloidal and suspended material above the membrane surface (Fig. 2.4a). This material is larger in size than the membrane pores and forms a cake layer at the surface, which offers an additional resistance for filtration, and is physically reversible.
- *Pore blocking*. Caused by the precipitation of colloids, solutes, microbial cells and inorganic compounds inside the membrane pores (Fig. 2.4b). In general this type of fouling is chemically reversible; however, in some cases it may be irreversible for certain types of inorganic fouling.

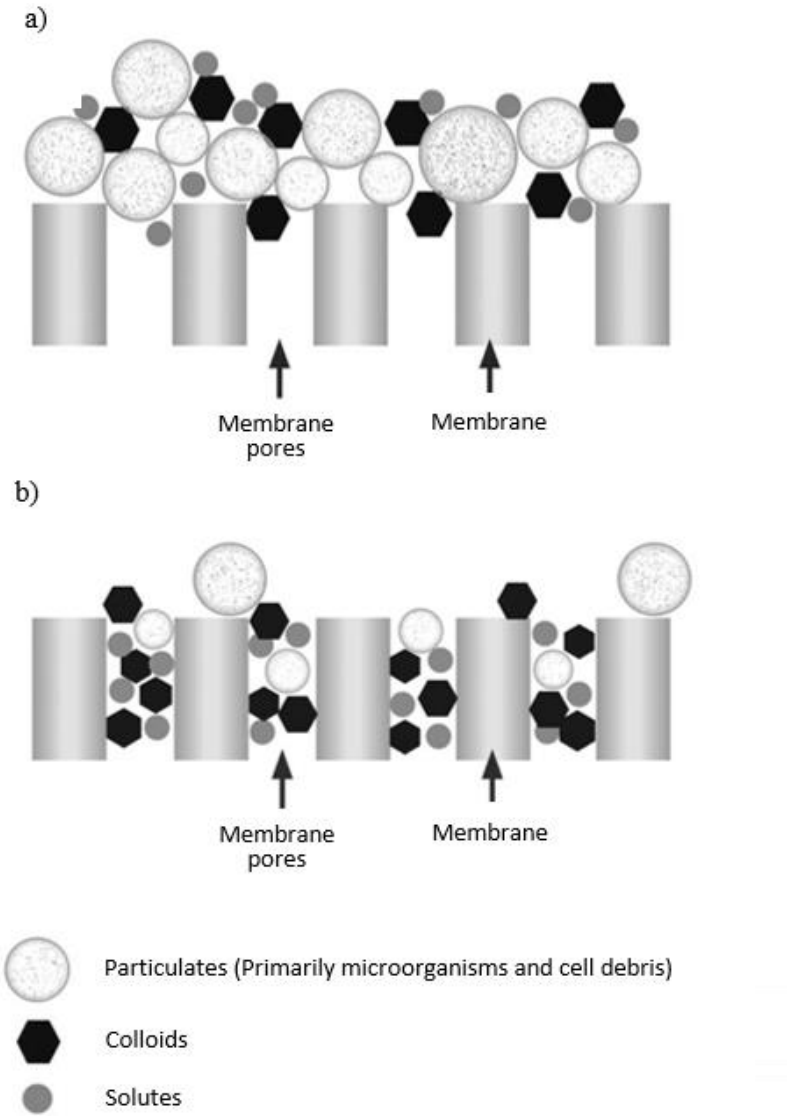

Fig. 2.4. Schematic representation of main membrane fouling mechanisms: (a) cake fouling, (b) pore blocking. (WEF, 2012)

2.3.1.2. Membrane configuration

In AnMBR two configurations are employed: external (side-stream) and submerged (immersed) (Fig. 2.5). In the first, the main membrane is housed in a vessel separate from the main reactor and the digester liquor is circulated through it as a side-stream; in the second, the membrane is submerged in the main reactor itself and the mixed liquor circulates around it. While the external configuration can achieve high fluxes due to the relative ease of maintenance and cleaning, its major reported limitations when compared to submerged configuration are: higher energy requirement; mixing and shear caused by the pumping system can lead to a reduction in particle sizes; and the release of soluble organics can lead to high volatile fatty acid concentrations that may inhibit methanogenesis (Stuckey, 2012). The advantages of a submerged membrane configuration are that it has a lower energy demand per unit volume of wastewater treated, and the biomass in the reactor is subjected to lower shear. The major disadvantage is that the membrane is less accessible for cleaning, and in situ methods such as gas scouring need to be employed (Stuckey, 2012). The success of submerged aerobic MBRs (AeMBR) in the early 2000s, however, highly encouraged the investigation of submerged AnMBRs (SAnMBRs) for wastewater treatment with a significant increase in studies since 2010s aiming to improve energy efficiency, extend the application scope and solve technical problems such as membrane fouling (Lin et al., 2013). Although SAnMBRs are expected to be superior in economic terms to external membrane systems when operated at a large scale, there is as yet insufficient evidence to confirm this (Stuckey, 2012), and hence the need of further research on them.

This work focuses on the application of submerged anaerobic membrane bioreactors (Fig. 2.5a) due to the relatively low energy consumption compared to the external configuration, as well as the potential suitability for municipal sewage treatment and their applicability in research. The outcome of this work, however, can be useful in the study of both configurations with the appropriate interpretation.

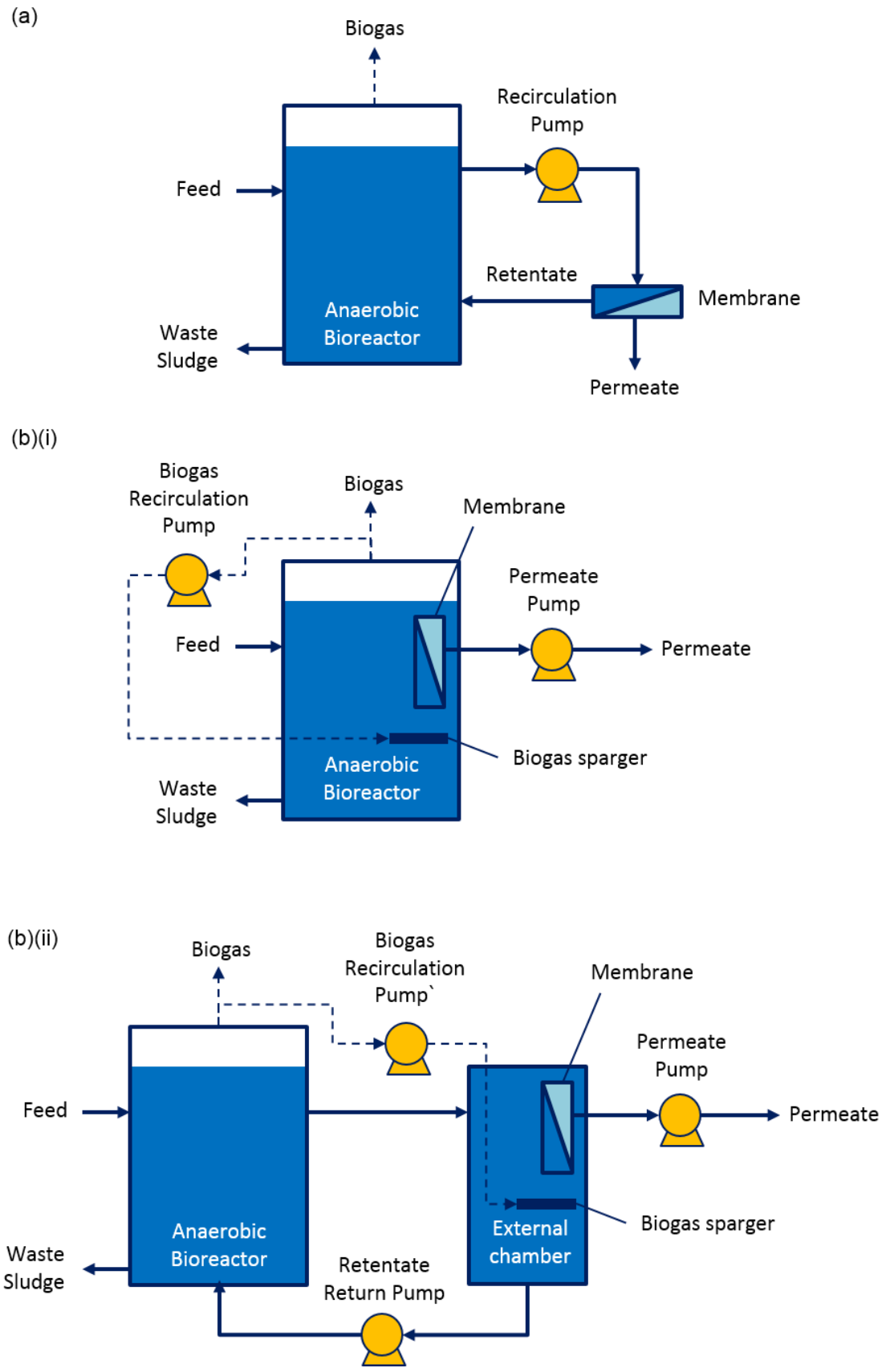

Fig. 2.5. Schematic of common AnMBR configurations: (a) External, (b)(i) Submerged, (b)(ii) Submerged in external chamber (Adapted from Liao et al., 2006)

2.3.1.3. Membrane materials

There are mainly two different types of membrane material, polymeric and ceramic. A number of different polymeric and ceramic materials are used to form membranes, which generally comprise a thin surface layer which provides the required perm-selectivity on top of a more open, thicker porous support which provides mechanical stability. Membranes are usually fabricated both to have a high surface porosity and narrow pore size distribution to provide as high a throughput and selectivity as possible. The membrane must also be mechanically strong, provide some resistance to thermal and chemical attacks (extremes of temperature, pH and/or oxidant concentrations that normally arise when the membrane is chemically cleaned), and should ideally offer some resistance to fouling.

Materials of commercial UF and MF membranes can range from fully hydrophilic polymers such as cellulose acetate, to fully hydrophobic polymers such as polypropylene (PP), polyethylene (PE) and fluoropolymers such as polytetrafluoroethylene (PTFE). Between the two extremes, there is the polysulfone (PS)/polyethersulfone (PES) family, polyacrylonitrile (PAN) and polyvinylidene difluoride (PVDF). Whilst the earliest commercial products in the water and wastewater field were based on PS, CA and PP, the MBR market is now supplied with products mainly based on PES, PVDF or on derivatives of PE. Whilst in principle a membrane can be formed from a very wide range of polymeric materials, to be cost effective for large-scale applications a membrane polymer needs to be made from a commodity product. The PS/PES family and PVDF are now emerging as the dominant polymers of choice for the water industry, but with PP, PE, PAN and, more recently, PTFE also being available. Both of the two main polymer families have favourable properties depending on their application to MBRs. For example PS/PES copolymers can provide a hydrophilic membrane, a narrow pore size distribution of UF rating and excellent all round chemical tolerance. On the other hand PVDF provides excellent strength and flexibility, with very high chlorine tolerance, and can be formed into a UF or fine MF membrane (Judd and Judd, 2011).

2.3.1.4. Membrane module type

Membranes can be categorised by module type as (Fig. 2.6): flat sheet, hollow fibre or tubular (Judd and Judd, 2011). While hollow fibre membranes are popular for submerged configurations due to their high packing densities and cost effectiveness, flat sheet modules are of special interest due to their good stability, and the ease of cleaning and replacement of defective membranes, which also makes them suitable for research purposes (Lin et al., 2013). Although this study centres in flat sheet membranes modules in SAnMBRs, the outcome with the correct interpretation can be compared to research and data of SAnMBRs using other membranes module types. The term 'membrane' is therefore used to refer to this particular module type from now onwards (Fig. 2.6a), unless otherwise stated.

Fig. 2.6. Examples of membrane module types: (a) flat sheet[1]; (b) hollow fibre[2];(c) tubular[3]

[1] Kubota http://nett21.gec.jp/water/data/water_18-8.html
[2] GE- ZeeWeed http://www.ecomagination.com/portfolio/zeeweed-membrane-technology
[3] Spintek and Liqtech http://spintek.com/tubular-membrane-systems/ and http://www.liqtech.com

2.3.2. Hydrodynamic conditions

2.3.2.1. Membrane flux

Membrane flux is considered the main parameter for evaluation of the performance and determination of the economic feasibility of membrane bioreactors, as it defines the required membrane area for a given flow as well as the hydraulic treatment capacity (Liao et al., 2006). The concept of critical flux has been used to describe the relationship between flux and the fouling rate in controlled steady-state environments, and has been defined in the literature as 'the flux rate above which above which rapid fouling and reduction of permeability will occur' (WEF, 2012). This concept can be problematic in practical applications, however, as membrane bioreactors are rarely operated under steady-state conditions and thus fouling rate is a highly variable parameter. A more appropriate concept is the sustainable flux, defined as 'the flux at which a modest degree of fouling occurs that can be handled by the MBR's fouling control mechanisms, providing an acceptable compromise between capital and operation and maintenance costs for MBRs' (WEF, 2012). When membrane bioreactors are operated beyond the sustainable flux, the fouling rate exceeds the capability of the control mechanisms to remove foulants and consequently the membrane permeability decreases at a rate that cannot be sustained operationally. Sustainable flux is site-specific and is a function of inflow composition, membrane characteristics, mixed liquor characteristics and operational conditions, as well as the fouling cleaning methods and frequency (WEF, 2012). Whilst the sustainable membrane flux in most submerged aerobic MBR studies has ranged between 4–85 L m^{-2} $hour^{-1}$, the reported range for SAnMBRs appears to be typically below 15 L m^{-2} $hour^{-1}$ thus representing a bottleneck for its full-scale application (Lin et al., 2013). In line with this, most relevant studies of SAnMBR working on low-strength wastewater (synthetic or real) have reported membrane fluxes below 20 L m^{-2} $hour^{-1}$ (Appendix A - Table 1).

2.3.2.2. Transmembrane pressure and permeation modes

Transmembrane pressure (TMP) refers to the pressure differential across the membrane or the driving force required to achieve a given flux, measured by the

difference in feed pressure and permeate pressure after adjustment for losses from the discharge to the pressure gauge. Membrane flux in the submerged configuration is driven by either gravity head or a vacuum pumping system on the permeate side. In either case, it is difficult to measure feed-side and permeate side pressure and estimates or averages are required (WEF, 2012). While the TMP operating range is membrane-product specific and generally ranges from 3 to 21 kPa for flat-sheet membranes (WEF, 2012), Appendix A - Table 1 shows that the TMPs reported in most relevant SAnMBR studies working on low-to-intermediate strength wastewater (synthetic or real) are below 50 kPa.

In submerged systems the most common method of operation is to draw permeate through the membrane by using a pump to reduce the pressure in the membrane lumen. As the membrane pores block, this pressure must be increased to maintain a constant flow. In this case membrane performance can be evaluated by measuring the increase or decrease in the transmembrane pressure (TMP) under a constant flux rate. It is also possible, however, to operate a MBR by gravity permeation, as has been demonstrated in aerobic systems (Ueda and Horan, 1999, Ueda and Hata, 1999, Zheng and Liu, 2006, Meng *et al.*, 2008). This relies on a head differential between the inlet and the outlet to the next downstream process. Using this method it is possible to generate a pressure similar to that applied in pumped systems (Judd and Judd, 2011). Operation of an AnMBR by gravity could reduce the parasitic energy requirement for reactor operation (Zheng and Liu, 2006, Ueda and Hata, 1999), although in practice this pumping component may be small compared to the energy required for membrane cleaning e.g. by bubble scouring. Martin et al. (2011) estimated that the pumping energy requirement can represent up to 5% of the total energy consumption in pumped SAnMBRs.

Operating the reactor in this way with a fixed head differential gives a constant TMP, but the flux may be variable, as this changes in response to changes in membrane permeability due to fouling (WEF, 2012). It is possible, however, that a steady state condition could be reached at which there is a constant flux at a constant gravitationally-induced TMP. What is not known is whether the flux rates under these

conditions would be comparable to those in pumped systems. The concept of operating in gravitational mode at a constant TMP also provides an alternative method for assessing membrane performance as a result of fouling. In this case the rate of change of flux provides a measure of the rate of fouling to the point where a steady state is achieved and thus gives us a tool to see response of flux and fouling to changes in operating conditions. According to Judd et al. (2008) alternative methods for assessment of AnMBR membrane performance may contribute to finding operational regimes that establish the best balance between fouling membrane flux, cleaning frequency and other operational parameters Although gravitational operation of SAnMBR has been suggested by Hong (2012), no work appears to have been carried out to date to test or further develop this concept.

2.3.3. Operational conditions

Temperature, mean cell residence time, organic loading rate and hydraulic retention time are the key parameters in AnMBR operation as they have strong influence on the microbial ecology (Stuckey, 2012). This contributes to different treatment performance and mixed liquor characteristics, inevitably affecting the development of membrane fouling AnMBRs (Huang et al., 2011).

2.3.3.1. Temperature

It is well known that temperature has an effect on the efficiency of treatment processes for several reasons: these include the temperature dependence of biochemical reaction rates, effects on gas solubility, and on settling characteristics due to changes in liquid viscosity (Ozgun et al., 2013). The rate of all chemical reactions is influenced by temperature, and since microbial growth involves a series of chemical reactions, their rate of growth is also greatly influenced by temperature. Although higher treatment rates are associated with higher growth rates this may require energy inputs that could counter the benefits accomplished at higher operational temperatures (Rittmann and McCarty, 2001). As shown in Fig. 2.7, microorganisms can be classified into 'temperature classes' on the basis of the optimum temperature, in which the species are able to grow and metabolize (Lettinga *et al.*, 2001). Anaerobic

treatment processes are normally operated near the optimum of 35°C for mesophilic organisms, or at 55 to 60 °C for thermophillic operation, but not at 45°C, which is suboptimal for either group (Rittmann and McCarty, 2001). According to a recent review by Skouteris *et al.* (2012) most of the AnMBRs studies have been operated either at around 35 ^{o}C in the mesophilic range or at around 55 ^{o}C in the thermophillic range. While benefits associated to higher operational temperatures (i.e. thermophillic) would be helpful for AnMBR performance, such as higher reaction rates and higher membrane fluxes due to lower mixed liquor viscosities, successful operation of these systems at ambient temperatures is still considered a crucial step to improve the applicability of AnMBRs for municipal wastewater treatment (Stuckey, 2012).

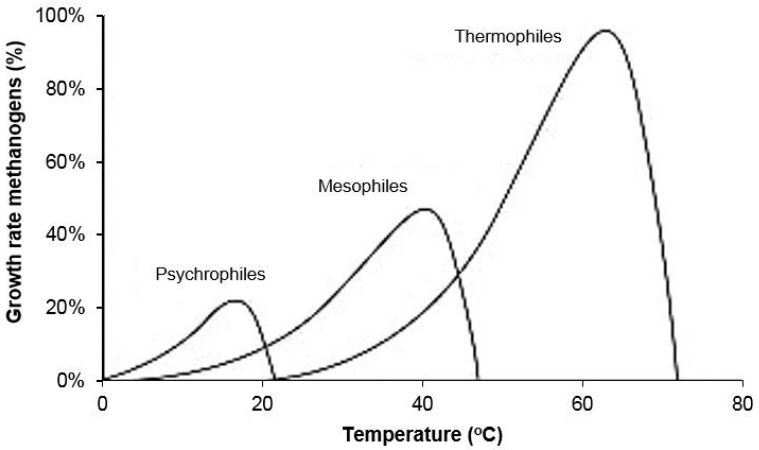

Fig. 2.7. Effect of temperature on growth rate of methanogens (Lettinga et al., 2001).

As summarised in Appendix A - Table 1, most SAnMBR studies reported, working on low-strength wastewater (synthetic or real), have mainly been operated between 30-35 ^{o}C, with just a couple near 20 ^{o}C or below it. Although recent work has shown that successful wastewater treatment and biogas production can be achieved in AnMBR at operational temperatures as low as 15^{o}C (Smith et al., 2013), there is still little information available about any temperatures other than mesophilic (Stuckey, 2012).

2.3.3.2. Mean cell residence time (MCRT)

Biomass retention in AnMBRs allows decoupling of the SRT from the HRT and thus providing a means of controlling the mean cell residence time (MCRT) of the system

(Smith et al., 2012). The MCRT is an important parameter as through it the growth rate of the system and its metabolic activity and energy conversion efficiency can be controlled (Spellman, 2003). Control of MCRT through proportional biomass wastage is the simplest way to exert kinetic control over a biological wastewater treatment system, as well as over the physical characteristics of the biomass (Rittmann and McCarty, 2001). In the case of AnMBR both membrane fouling and reactor performance are likely to be directly affected by MCRT as the mixed liquor characteristics and biomass concentration both depend upon this parameter (Ng et al., 2006, Huang et al., 2013), which also controls the microbial growth rate and metabolic activity (Tan *et al.*, 2008). The production of extracellular polymeric (EPS) materials and soluble microbial products, which are known to influence membrane fouling, has also been shown to be related to MCRT and HRT (Stuckey, 2012, WEF, 2012) and may be particularly important where the membrane is directly submerged in the mixed liquor (Ng et al., 2006).

MCRT reported in AnMBR studies treating low-to-intermediate strength wastewater have ranged between 25 and 335 days (Appendix A - Table 1). Long MCRTs are essential to maintain the slow growing anaerobic microbial populations in the treatment systems, especially at low operational temperatures (Smith et al., 2012) and will result in a minimal production of a non-biodegradable sludge (Stuckey, 2012). At present the strategy appears to be to operate MBRs at long MCRT, since research on aerobic systems has shown that decreasing the MCRT tends to increase the concentration of soluble microbial products and EPS, both of which may have a greater effect on membrane fouling than the concentration of mixed liquor suspended solids (MLSS) alone (Stuckey, 2012, Jinsong *et al.*, 2006, Ng et al., 2006).

The evidence in the case of AnMBR is much less clear, however. In work using a flat sheet SAnMBR to treat low strength synthetic wastewater, Huang et al. (2011) found that a long MCRT resulted in higher fouling; yet a more recent paper by the same authors showed more fouling at very short MCRT when treating domestic wastewater in the same reactor type (Huang et al., 2013). While the relationship between operational parameters, treatment performance and membrane fouling is recognised

as being complex and poorly defined (Smith et al., 2012), there are very few other studies have looked at the effect of MCRT on AnMBRs, and even less centred on the treatment low-to-intermediate strength wastewater. It is therefore clear that the impacts of MCRT on AnMBR performance and the relationship between this and membrane fouling are still far from being fully understood.

2.3.3.3. Organic loading rate

Although volumetric organic loading rates (OLR_V) between 0.3 to 12.5 g COD $L^{-1}day^{-1}$ have been reported in AnMBRs treating low-to-intermediate strength wastewater (Ozgun et al., 2013), these are generally lower than 3 g COD L^{-1} day (Lin et al., 2013). As it can be seen in Appendix A - Table 1, this range also applies specifically for the submerged configuration where the studies on SAnMBR for low-strength wastewater treatment reported OLR_V between 0.5-13 g COD $L^{-1}day^{-1}$, with the vast majority always below 2.2 g COD $L^{-1}day^{-1}$.

2.3.3.4. Hydraulic retention time (HRT)

HRT is major parameter in wastewater treatment processes due to its strong influence on capital costs, where its main significance in microbial terms is (i) the fact that with the same strength of wastewater a change in HRT would represent a change in OLR and (ii) the potential for washout and for selecting in favour of faster or slower-growing organisms. In the context of AnMBR for sewage treatment, a short HRT is necessary to treat the large volumes of dilute wastewater in order to minimise the reactor size and therefore the overall footprint of operation (Smith et al., 2012, Ozgun et al., 2013). There is an optimum HRT for each case in order to provide both efficient biological removal and membrane performance, determined by many factors such as system hydraulics, wastewater characteristics and mixed liquor properties (Ozgun et al., 2013). So far studies on SAnMBR treating low strength wastewater (synthetic or real) have reported HRTs within a range of 3-48 hours (Appendix A - Table 1). While the lowest range of HRTs for AnMBR treating a wide range of wastewater found in summaries of the literature was 8–12 hours (Stuckey, 2012), for low-to-intermediate strength wastewater it is generally longer than 8 hours. Although these compare favourably with conventional anaerobic systems treating sewage, they are still well

above typical values for AeMBRs which usually operate at HRTs of 4-8 hours (Lin et al., 2013).

2.3.4. Mixed liquor characteristics

Mixed liquor characteristics, bacterial flora, and nutritional requirements, are mainly dependent on the type and operational conditions of bioreactors (Ozgun et al., 2013). The characteristics of mixed liquor in AnMBR most frequently reported in the literature are the solids concentration, viscosity filterability and the concentration of soluble microbial products and extracellular polymeric substances.

2.3.4.1. Solids concentration, viscosity and filterability

Mixed Liquor Suspended Solids (MLSS) concentration is a key operational parameter for membrane bioreactor technology, as it has a direct impact on characteristics such as viscosity and thus filterability and consequently on membrane fouling. The possibility of using high MLSS concentrations to reduce footprint is stated as one of the big advantages of membrane bioreactor technology (Lousada-Ferreira et al., 2010). However, according to Lousada-Ferreira et al. (2010), the influence of MLSS on fouling is not fully understood as literature reports are inconsistent and sometimes contradictory. For example, on one hand some authors report an increase on fouling with increasing MLSS concentrations, although it is not clear which parameter determines the resulting flux. On the other hand, there are other authors that report no effect of solids on the transmembrane pressure or permeate quality and others a decrease in transmembrane pressure for samples with higher MLSS concentrations. For example, Lin *et al.* (2011) reported a relative stability in the permeate COD regardless of fluctuations of the influent COD and MLSS concentration (6.4-9.3 g L^{-1}) when operating a lab-scale AnMBRs with municipal wastewater treatment. A possible explanation for these contradictions could be that the effect of MLSS concentration on membrane fouling varies according to the applied MLSS range (Lousada-Ferreira et al., 2010). Le-Clech et al. (2006) state that the lack of a clear correlation between MLSS concentration in AeMBRs and any other foulant characteristics indicates that the MLSS concentration alone is a poor indicator of biomass fouling propensity. There might,

however, be a critical MLSS concentration above which AeMBR sludge filterability improves due to the retention of fouling particles in the mixed liquor (Lousada-Ferreira, 2011).

Mixed liquor filterability can also provide information about the sludge fouling propensity and as such, is often referred to as the quality of the sludge (Lousada-Ferreira, 2011). According to Ozgun et al. (2013) AnMBRs are generally operated at higher biomass concentrations than aerobic MBRs, affecting rheology and thus reactor hydraulics and pumping. This higher MLSS concentration in AnMBRs results in a more rapid and dense cake layer build up in comparison to AeMBRs, requiring frequent physical cleaning, intermittent operation (alternation of operation with short cleaning intervals), and likely sub-critical flux operation, in order to sustain the flux.

Mixed liquor viscosity is closely related to its concentration, and has been cited as a main foulant parameter in membrane systems (Le-Clech et al., 2006). Viscosity tends to increase as the MLSS concentration increases and therefore will cause a shift from turbulent to laminar flow conditions along the membrane component of the system (Bérubé *et al.*, 2006). There is a critical MLSS concentration, however, below which the viscosity remains low and increases slowly with the concentration. Above this critical value, the mixed liquor viscosity increases exponentially with the solids concentration. Similar observations have been reported with the capillary suction time (CST), another parameter closely related to viscosity (Le-Clech et al., 2006).

Most studies so far on the mixed liquor characteristics in membrane bioreactors have been carried out for AeMBR. Although it is expected that certain fundamental principles derived from submerged AeMBR are similar in SAnMBR (Huang et al., 2011), further work is needed to understand the effect of mixed liquor characteristics on the degree of membrane fouling and the overall performance of AnMBRs.

2.3.4.2. Soluble microbial products and extracellular polymeric substances

While it is clear that optimal operation of membrane bioreactors relies on the successful control of membrane fouling, so far there is no universally agreed constituent in the mixed liquor to which fouling can be primarily attributed (Judd, 2008). It is well known, however, that membrane fouling is affected by the formation of soluble microbial products and extracellular polymeric substances (EPS or EPS) (Aquino *et al.*, 2006, Menniti and Morgenroth, 2010, WEF, 2012). These terms both refer to a variety of macromolecules such as polysaccharides, proteins, nucleic acids, phospholipids and other polymeric compounds that are produced by active secretion, shedding of cell surface material or cell lysis and are significant in the formation of flocs and biofilms (WEF, 2012). Soluble microbial products have been defined as the pool of organic compounds that are released into solution from substrate metabolism and biomass decay. On the other hand, EPS represents a mixture of polymers secreted by cells, produced from cell lysis and hydrolysis, which often constitute around 20% of the total soluble microbial material (Kunacheva and Stuckey, 2014). EPS are the most important single microbial product group within soluble microbial products, which function is to provide adhesion of microbial cells in bioflocs and biofilms, to form a barrier to protect the cell against harmful toxicants in wastewater, and to accumulate nutrients by adsorption (Kunacheva and Stuckey, 2014). Both soluble microbial products and EPS decrease the permeate flux by decreasing the effective size of membrane pores and increasing frictional resistance to permeate flow (Gao *et al.*, 2010). The identification of soluble microbial products, however, is quite challenging as they are mixtures of a variety of unknown compounds that do not belong to a specific well-defined group (Kunacheva and Stuckey, 2014). The concentration of EPS and soluble microbial products in the mixed liquor has been found to influence various mixed liquor properties such as: floc size distribution, dewaterability, settleability and compressibility, non-settleable solids fraction, cake filtration properties such as CST and filtration resistance, hydrophobicity, viscosity, and surface charge (Janus and Ulanicki, 2010, WEF, 2012).

Research has shown some correlations between production of fouling components such as EPS and soluble microbial products, and operating conditions such as MCRT and HRT (Stuckey, 2012, WEF, 2012). It should therefore theoretically be possible to operate an AnMBR by adjusting HRT or MCRT in such a way to minimise or control membrane fouling and avoid unexpected membrane flux deterioration (Stuckey, 2012, Huang et al., 2011); particularly when the membrane is directly submerged in the bioreactor as the mixed liquor characteristics will have a major impact on the membrane performance (Ng et al., 2006). The role of EPS quantity and characteristics in fouling as a function of MCRT and other operational variables is not well understood in AnMBRs, however, and controlling MCRT is further complicated by its interrelatedness with treatment performance. Furthermore, the terms EPS and soluble microbial products are often loosely applied in the literature, and at times used interchangeably (Gao et al., 2010), which could potentially result in misinterpretation of their effects and relationships with the membrane performance. It is therefore clear that other simpler methods to evaluate the effect of operational parameters in mixed liquor characteristics and their effect on membrane fouling may have a use.

2.3.5. Dissolved methane in the effluent

Dissolution of methane in the effluent is a known issue in high-rate anaerobic reactors, as it is more difficult to capture than in the gaseous phase and can represent a significant loss in methane production and energy potential. A recent study to quantify the dissolved methane in up-flow anaerobic sludge bed reactors (UASB) treating municipal wastewater under different conditions showed that 36-41% of total methane generated leaves the reactor dissolved in the effluent (Souza *et al.*, 2011). In addition, methane may represents a source of fugitive greenhouse gas emissions if it is not recovered, with a global warming potential 25 times that of carbon dioxide (Yeo and Lee, 2013, Smith et al., 2014, Smith et al., 2012). According to Yeo and Lee (2013) dissolved methane seems to be inevitable in AnMBRs due to gas-liquid mass transfer limitations. Smith et al. (2012) state that methane oversaturation should be expected in AnMBR permeate as the TMP will force additional methane into solution; supersaturation could also be caused in part by methane generation in the biofilm,

given the substantial soluble COD removal that takes place there. For these reasons, although membrane fouling is the main operational constraint for both aerobic and anaerobic membrane bioreactors, dissolved methane in the effluent is one of the most challenging barriers to implementation of AnMBRs for sewage treatment (Smith et al., 2012). So far there is still limited information on the fate and control of dissolved methane in AnMBRs (Yeo and Lee, 2013), as only a few studies have addressed methane solubility in AnMBR and even fewer have quantified dissolved methane (Smith et al., 2012). Therefore, the identification of an appropriate technology and methods to recover and handle dissolved methane is still crucial to achieve energy-neutral and sustainable sewage treatment (Ozgun et al., 2013, Smith et al., 2012).

2.3.6. Conclusions from the literature review

Anaerobic digestion is considered to be a core technology in moving towards sustainable wastewater treatment, and the application of membrane bioreactors looks promising due to their complete biomass retention and high quality effluents. Their performance under anaerobic conditions is not completely understood, however, and still presents challenging barriers to full-scale application of which the two most significant are membrane fouling and dissolved methane in the effluent. These result in high energy consumption as well as potential energy losses, consequently reducing the economic viability of these systems. Although low temperature operation seems the only feasible option to achieve sustainable anaerobic sewage treatment, this raises further issues for AnMBRs as biomass growth rates are greatly reduced, methane dissolution in the effluent is higher and the fluid viscosity reduces resulting in lower membrane fluxes.

Current knowledge of the links between operational parameters, reactor performance and membrane fouling in AnMBRs is also limited, particularly when treating low-to intermediate strength wastewater, where a broader understanding could be vital to encouraging full-scale implementation. While most AnMBR studies to date focus on proof of concept and membrane fouling, other approaches to increase the full-scale applicability of AnMBRs for sewage treatment should be investigated such as the

optimisation of operational parameters to control membrane fouling and system simplification to reduce inherent energy consumption. Given the importance of solving the above identified issues, the following chapters in this work aim to investigate some of these points through experimental work and discussion of the results obtained.

2.4. Research aim and objectives

Based on the results of the literature review, the overall aim of this research was to better understand the impact of MCRT on membrane flux, mixed liquor characteristics and overall performance of submerged anaerobic membrane bioreactors (SAnMBR), when treating low-to-intermediate strength wastewater with high suspended solids at both 36 ^{o}C and 20 ^{o}C. To achieve this aim four major objectives were defined:

- Design, build and test a laboratory-scale prototype of a SAnMBR for sewage treatment in a fully gravitational configuration to evaluate membrane fouling phenomena by direct flux variations
- Investigate the effect of operational parameters on SAnMBR treating low-to-intermediate strength wastewater with high suspended solids; with particular focus on the effect that MCRT has on membrane flux, mixed liquor characteristics and overall reactor performance when working at operational temperatures of 36 ^{o}C and 20 ^{o}C.

3. MATERIALS AND METHODS

3.1. Materials

3.1.1. General

Except where otherwise stated all chemicals used were of laboratory grade and obtained from Fisher Scientific (Loughborough, UK). Analysis solutions and standards were prepared using ultra-pure deionised water obtained from a Barnstead Nanopure ultrapure water purification system (Thermo Scientific, UK).

3.1.2. Synthetic Wastewater

In this research it was decided to use a synthetic wastewater rather than real wastewater, based on the fact that that the strength and composition of real wastewater vary depending on a number of factors as discussed above in Section 2.1. Most recent studies on AnMBR use synthetic wastewater to test new concepts or study general aspects of membrane fouling due to its ease for process control. Its use in research is reasonable, considering that AnMBR, especially SAnMBR, is still a novel process for wastewater treatment, where membrane performance is a central research topic (Lin et al., 2013, Visvanathan and Abeynayaka, 2012).

The composition of the synthetic wastewater is shown in Table 3.1 and the characterisation and elemental analysis in Table 3.2. The substrate has been previously used to simulate unsettled sewage (Whalley, 2008, Ali, 2014, Idrus, 2013), and was formulated to have a high suspended solids concentration and a balanced nutrient composition in the form of carbohydrate, protein, fat and mineral salts. This synthetic wastewater was achieved by using a sterilised yeast culture giving a settleable cellular component similar in nature to that found in wastewater biosolids. Colloidal organic components are provided by common dairy and meat products. Other components include sugar as a readily utilisable soluble carbon source; urea as the final breakdown product present in urine; and mineral supplements. The mix has been described as a synthetic wastewater, as the COD/BOD ratio as well as the C:N ratio and ratio of solids components is based on typical values for sewage when used at a lower strength

(Henze and Comeau, 2011). Concentrated synthetic wastewater was prepared fresh every morning and diluted to give the required COD strength and solids content.

Table 3.1. Synthetic wastewater composition

Component	Quantity	Unit	Preparation
Yeast (block bakers form)	23.0	g L^{-1}	Dissolved in 0.23 l of tap water and autoclaved for 15 min.
Urea	2.14	g L^{-1}	Added directly
Full cream milk (UHT sterilised)	144	mL L^{-1}	Added directly
Sugar (granulated white)	11.5	g L^{-1}	Added directly
Blood (freeze dried)	5.75	g L^{-1}	homogenised with 0.2 l of water
Ammonia phosphate	3.4	g L^{-1}	added directly
Tap water	-	-	to make up to 1 litre

Table 3.2. Synthetic wastewater characterisation and elemental analysis

Characterisation			Elemental composition	
Constituent	**Value**	**Unit**	**Element**	**Content (%)**
COD	51.3 ± 0.9	g L^{-1}	Nitrogen	8.5 %
BOD_5	33.9 ± 2.4	g L^{-1}	Carbon	46.9 %
COD/BOD_5	1.52		Hydrogen	6.4 %
TS	42.5	g L^{-1}	Sulphur	0.3 %
VS	37.4	g L^{-1}	Oxygen	38.1 %
VS/TS	88%			
TKN	3.84 ± 0.1	g L^{-1}		

(±) One standard deviation

3.1.3. Trace elements supplementation

Feed trace elements supplementation was specific for each experiment, as stated in the method summary for each. The trace elements stock solution used was based on a formula developed by the Water and Environmental Engineering Research Group at the University of Southampton, and comprised two solutions; one composed of cations and the other of oxyanions (Table 3.3).

Table 3.3.Trace Elements concentration in stock solution

Solution	Trace element as	Compound used	Element concentration at working condition; after 1000 times dilution (mg L^{-1})	Compound concentration in stock solution (g L^{-1})
Cation	Aluminium (Al)	AlCl3· 6H2O	0.10	0.895
	Boron (B)	H3BO3	0.10	0.572
	Cobalt (Co)	CoCl2· 6H2O	1.00	4.038
	Copper (Cu)	CuCl2· 2H2O	0.10	0.268
	Iron (Fe)	FeCl2· 4H2O	10.00	35.597
	Manganese (Mn)	MnCl2· 4H2O	1.00	3.602
	Nickel (Ni)	NiCl2· 6H2O	1.00	4.050
	Zinc (Zn)	ZnCl2	1.00	2.084
Oxyanion	Molybdenum (Mo)	(NH4)6Mo7O24· 4H2O	0.10	0.184
	Molybdenum (Mo)	(NH4)6Mo7O24· 4H2O	0.10	0.184
	Tungsten (W)	Na2WO4· 2H2O	0.10	0.179

3.1.4. Inoculum

All the reactors in the experiments reported in this work were inoculated with digestate from a mesophilic digester treating municipal wastewater biosolids at Millbrook wastewater treatment plant (WWTP) in Southampton, UK operated by Southern Water Plc. Prior to inoculation, the digestate was passed through a 1 mm sieve and diluted with tap water to the desired solids concentration.

3.1.5. Submerged Anaerobic Membrane Bioreactors (SAnMBR)

As highlighted in Chapter 2, there is currently a wide range of designs for SAnMBRs, with differences that mainly reside in the membrane type and configuration, membrane cleaning mechanism, reactor geometry, and digestate mixing system. The SAnMBRs used in this research were engineered as directly immersed membrane bioreactors in a gaslift configuration (Fig. 3.1). This was induced by placing the flat sheet membrane cartridge between two vertical PVC baffles under which headspace biogas was recirculated through a sparger. This created an inner upcomer section containing the membrane where the bubble curtain acted as a membrane fouling

scouring mechanism, and two outer downcomer sections that ensured a completely mixed liquor.

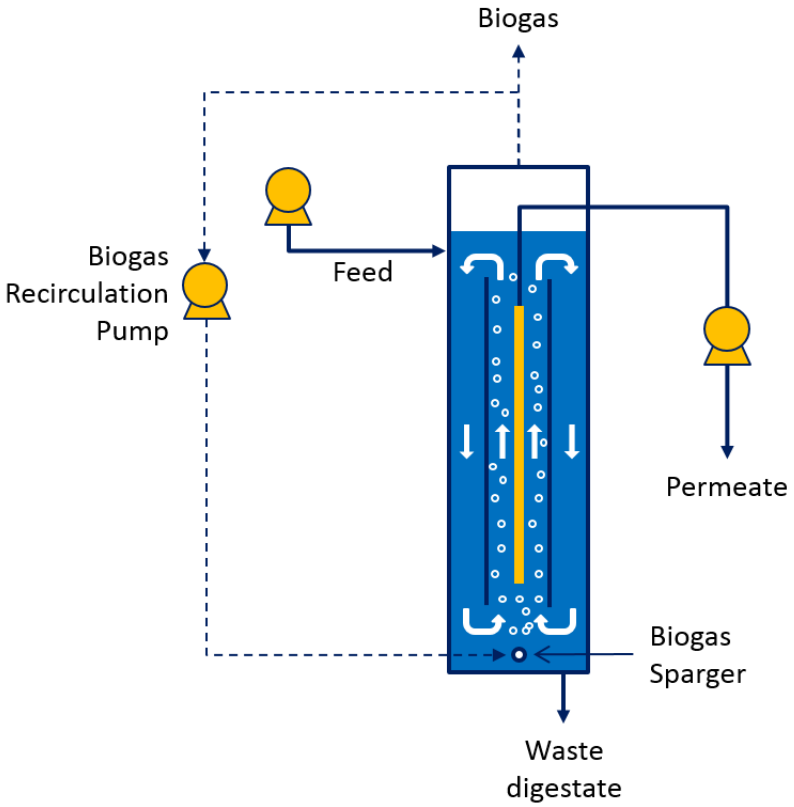

Fig. 3.1. Schematic of initial SAnMBR design: membrane directly immersed in reactor with gaslift loop configuration for membrane fouling scouring and mixed liquor

3.1.5.1. Membranes

The membranes employed throughout all the experiments in this work were Kubota flat sheet membrane type 203 of chlorinated polyethylene, with an effective surface area of 0.113 m^2 and a nominal pore size of 0.4 µm (Kubota Co., Japan). New membranes were always used at the start each experiment to avoid any bias when comparing the membrane flux between reactors, as it might not be possible completely to remove permanent fouling after a previous experiment. This ensured that all the reactors started each experiment with the same membrane conditions and thus allow an even baseline for membrane flux evaluation. New membranes flux were tested with tap water and a transmembrane pressure of 5 kPa (as recommended by

manufacturer), applied with a siphon head difference of 50 cm and resulting in an average membrane flux of 100 ± 7 L m^{-2} $hour^{-1}$.

3.1.5.2. Preliminary tests

A number of preliminary tests were performed to define the optimum design of the laboratory-scale SAnMBR, and to better understand the internal hydrodynamics of the gaslift loop configuration and the pressure balance in the system, as well as the coupling of input and output streams. These were carried out using a prototype-SAnMBR with a working volume of 11.40 L, made of PVC lateral and back panels, and a Perspex front pane to allow visual monitoring (Fig. 3.2). Flow through the prototype-SAnMBR was achieved by maintaining a head differential between the constant head device and a syphon outlet from the lumen of the membrane cartridge. Tests were initially performed with tap water to evaluate the system hydrodynamics and pressure balance and then with diluted digestate from Millbrook WWTP (Section 3.1.4).

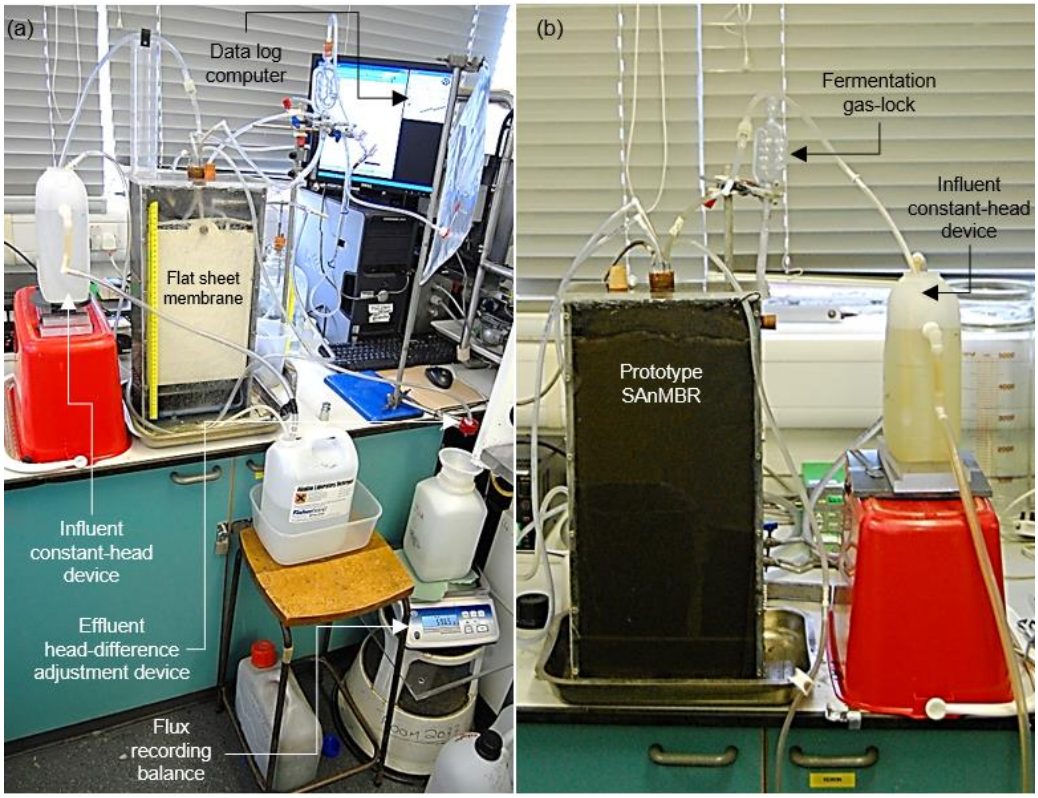

Fig. 3.2. Prototype experimental tests: (a) experimental set-up for the preliminary tests with water, (b) experimental set-up for the preliminary test with digestate from Millbrook WWTP: effluent head-difference device, fermentation gas-lock, flux recording balance, flat sheet membrane, influent constant-head device, SAnMBR.

3.1.5.3. Final reactor design and construction

The preliminary studies provided enough information to compare with relevant SAnMBRs systems in the literature (Appendix A - Table 1) and thus obtain the optimal design parameters to develop a SAnMBR that could fulfil the needs of this research. The final design of the SAnMBR is described below and shown in Fig. 3.3 and Table 3.4.

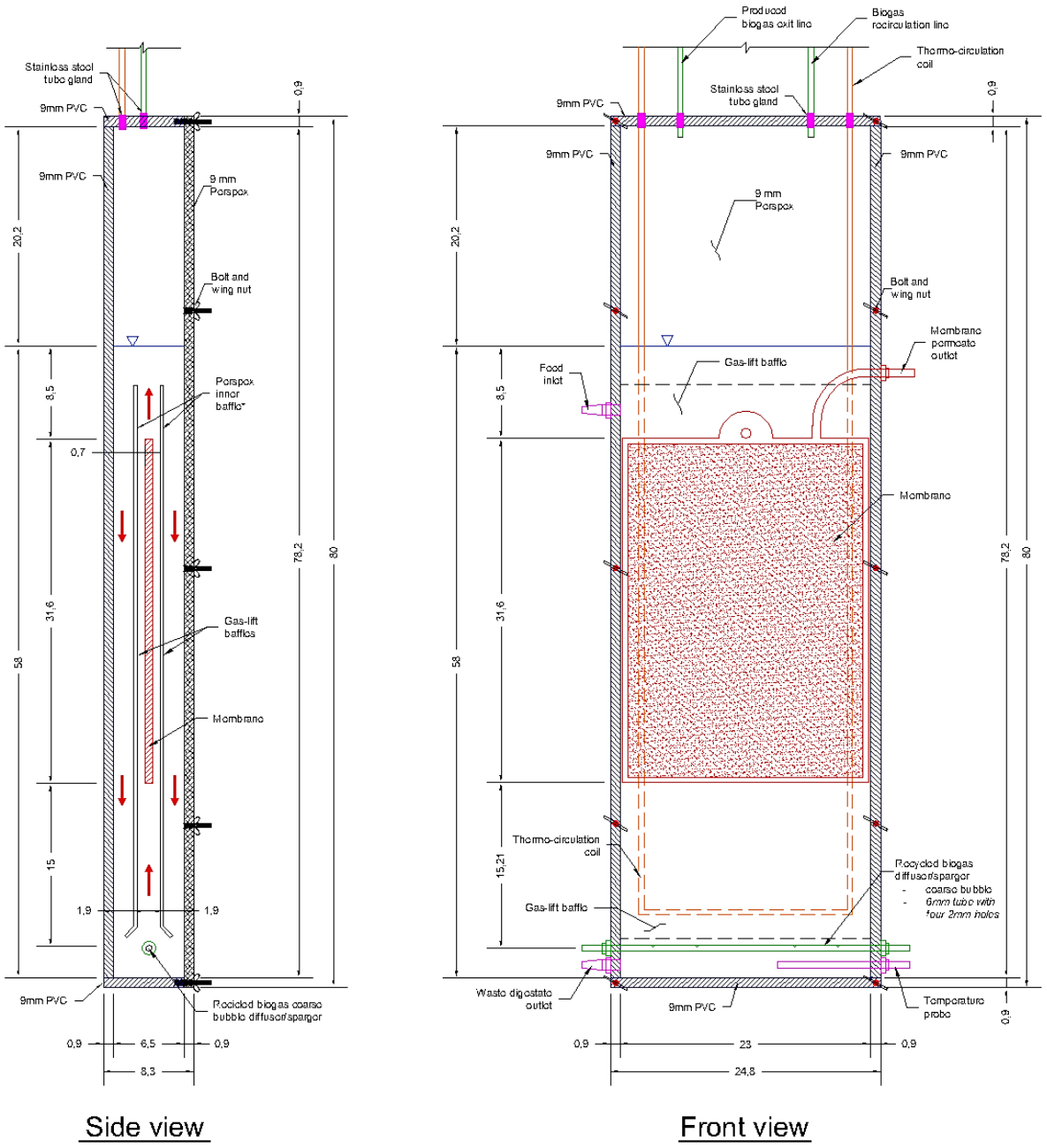

Fig. 3.3. Schematic diagram – Detailed design of the SAnMBRs used in all the experiments presented in this work

Table 3.4. SAnMBRs detailed design values

Reactor	Value	Units
Height	78.2	cm
Width	6.5	cm
Length	23	cm
Surface-Area	0.015	m^2
Reactor total volume	11.7	L
Reactor working volume*	9.57	L
Reactor head space volume*	2.12	L
Packing density	0.012	$m^2 L^{-1}$

**Calculated at 64 cm of water head*

The reactor arrangement and internal view once built are shown in Fig. 3.4 and Fig. 3.5, respectively. The SAnMBRs were constructed in 9 mm PVC with a Perspex front panel which allowed observation of the water level, solids deposition, and general functioning. The membrane was mounted between two vertical PVC baffles each 7 mm from the membrane surface. These formed the inner upcomer section and two outer downcomer sections as described above.

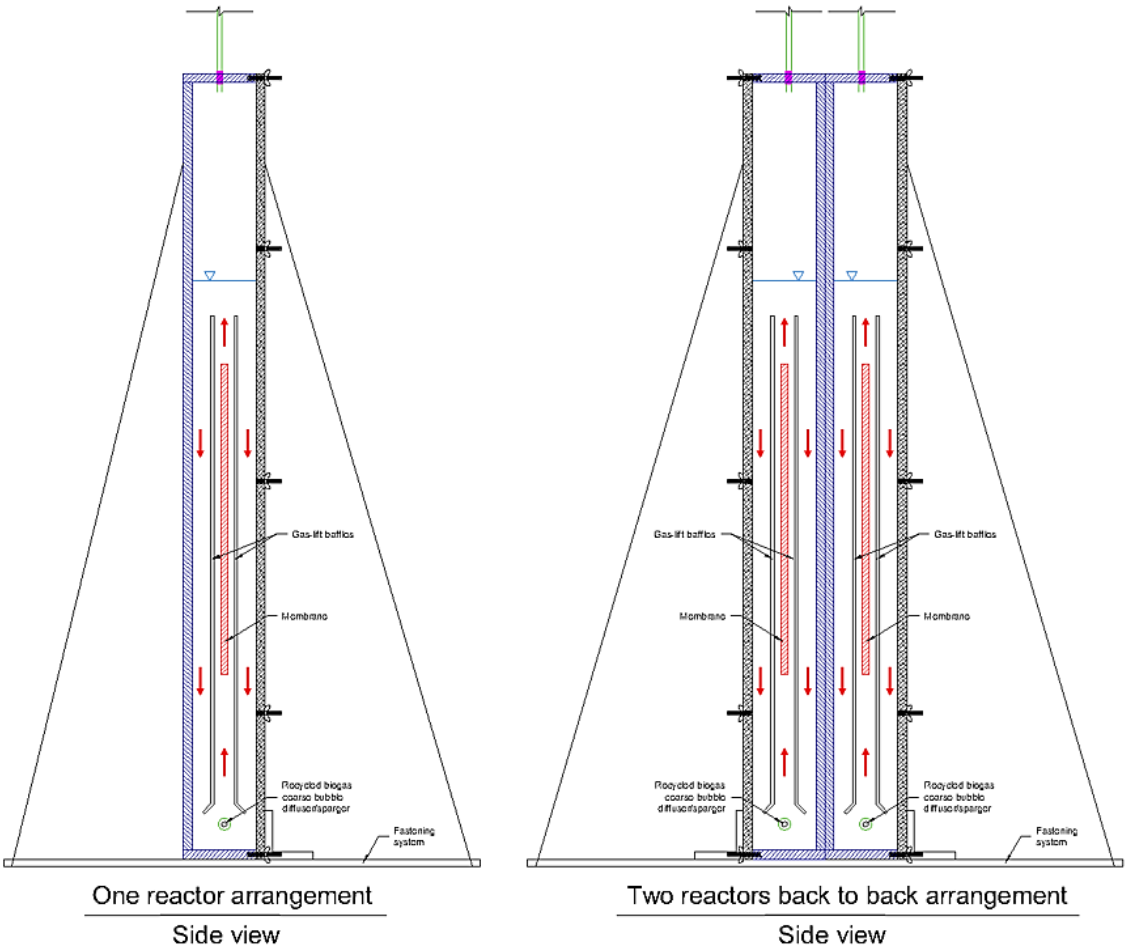

Fig. 3.4. Schematic diagram – SAnMBRs arrangement: (a) one reactor, (b) two reactors

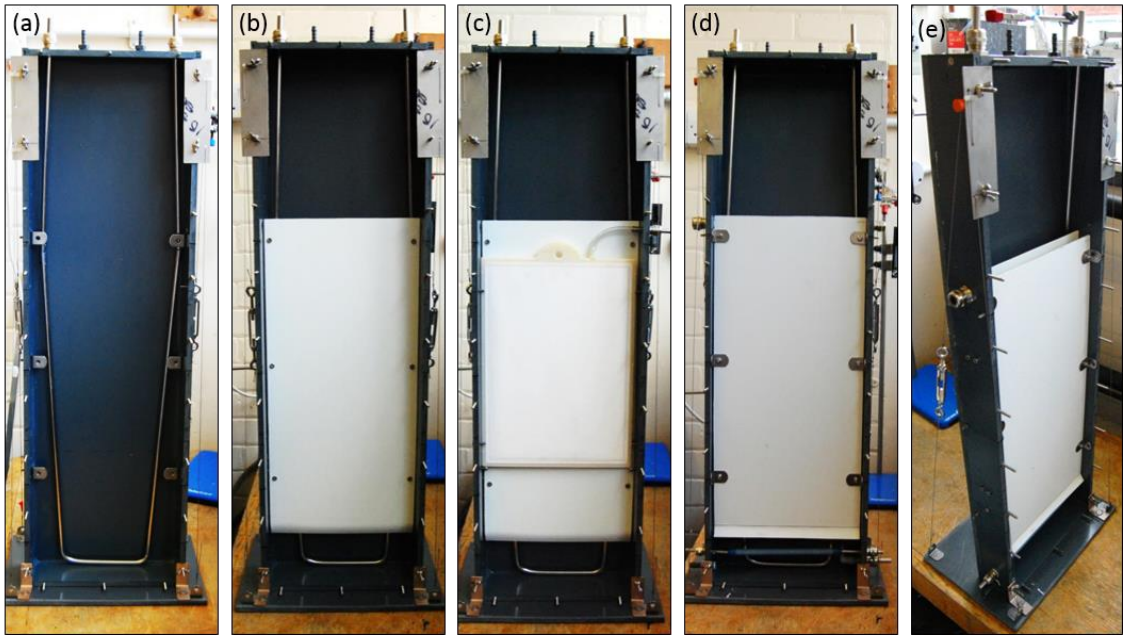

Fig. 3.5. SAnMBR internal view: (a) temperature control coil, (b) back gas-lift baffle, (c) membrane, (d) front gas-lift baffle (e) complete inner structure

3.1.5.4. General SAnMBRs experimental set-up

The membranes were cleaned by recirculating biogas through a 6 mm tubular stainless steel sparger with four 2 mm holes spaced evenly along its length. The sparger was mounted 15.5 cm from the base of the membrane, and a continuous bubble curtain was maintained using a 12 V DC diaphragm pump (AIRPO^{TM}, UK) to provide a gas flow rate of approximately 0.6 L min^{-1} L^{-1} reactor or 48.7 L min^{-1} m^{-2} membrane. The gas flow rate was initially set and periodically verified using a rotameter.

The liquid depth inside the reactor during the first experiment was kept at 61 ± 0.5 cm, giving a working volume of 9.1 litres. During the second and third experiment this was kept at 65 ± 0.5 cm, giving a working volume of 9.6 litres. The reactors were designed to have at least 20 cm of vertical headspace to avoid blockage of the biogas outlet in the event of foaming, and to allow determination of the appropriate liquid level from operation of the system. Feed entered the reactors through a siphon from a constant head device through which substrate was continuously circulated from a cooled feed storage tank (Grant FH15 and CC25, Germany) using a peristaltic pump (Cole-Parmer Master Flex L/S, UK), with any excess returned via an overflow. This gravitational feeding system automatically compensated for the volume of effluent passing through

the membrane, thus maintaining a constant level in the reactor. Flow through the reactors was achieved by maintaining a head differential between the constant head device and a syphon outlet from the lumen of the membrane cartridge.

The back pressure in the reactor headspace was maintained at approximately 0.3 kPa using a fermentation gas-lock through which the biogas produced escaped into a gas collection bag. Changes in liquid levels in the gas-lock also allowed a quick visual check on any pressure differences in the headspace that might occur due to leakage or blockage. Transmembrane pressure could be kept constant, in which case the membrane flux varied relative to the degree of fouling; alternatively the membrane flux could be adjusted by increasing or decreasing the head differential.

The flow through the reactors was measured by recording the weight of the collected permeate at 5-minute intervals, using laboratory scales with a capacity of 15 kg and a readability of 0.5 g) (PCE Instruments UK Ltd BDM 15, UK) for the first experiment and capacity of 32 kg and a readability of 1.0 g (Adam Equipment CBK 32, UK) for the second and third experiment. Flow volumes were calculated assuming a density of permeate and feed equal to that of water (1000 kg m^{-3}). The feed was stored in mechanically-stirred plastic storage tanks. Reactors and feed temperature was controlled by circulating water from a thermo-circulator (MGW Lauda thermo-star, Germany; Grant FH15V and FC15, Germany) through a stainless steel heating coil inside the reactors. Reactor and feed temperature is specified in each individual experiment. Heat loss from the reactors was reduced by attaching 10 cm high-performance insulation panels to the front and the back of the SAnMBR, which were removable to allow visual monitoring. Feed temperature, reactor temperature and room temperature were recorded continuously using solid-state IC temperature probes (Texas Instruments LM35DZ, USA) connected to a data logger (model U3-LV, Labjack, USA).

Fig. 3.6 shows the experimental set-up for the main studies in this work to illustrate the above described configuration. Detailed schematic diagrams and pictures of the set-up in each experiment are presented in the respective method summaries.

Fig. 3.6. Experimental set-up employed for the main studies in this work: Development and testing of a fully gravitational SAnMBR at 36 ^{o}C, (b) MCRT effect experiment at 36 ^{o}C, (c) MCRT effect experiment at 20 ^{o}C.

3.2. Methods

3.2.1. Feed, mixed liquor and permeate analysis

3.2.1.1. Chemical Oxygen Demand (COD)

COD was measured by the closed tube reflux method with titrometric determination of the end point (Environment-Agency, 2007). If the sample COD was more than 400 mg L^{-1} pre-dilution was carried out. 2 mL of sample (or 2 mL DI water for blanks) was placed into the reflux tubes followed by the addition of 3.8 mL of FICODOX-plus reagent (Fisher Scientific Ltd, UK), the composition of which is shown in Table 3.5. The tube was sealed with a PTFE screw cap and the mixture refluxed at 150 ^{o}C for 2 hours. After cooling, a few drops of ferroin indicator (Table 3.5) were added (Fisher Scientific Ltd, UK) and the mixture titrated with acidified (2% Sulphuric acid) 0.025M ferrous ammonium sulphate (FAS) solution.

The FAS was standardised with a 0.02083M potassium dichromate solution by adding 6.129 g $K_2Cr_2O_7$ (previously dried for 2 hrs at 104 ^{o}C) in about 500 ml of deionised water and make up to 1 litre. Dilutions of a standard solution containing 3.8 g l^{-1} of potassium hydrogen phthalate with a COD of 4 g COD L^{-1} were used as a standard to check calculated values of COD. COD values were calculated according to Equation 3.1

(Environment-Agency, 2007). The synthetic substrate employed has been widely studied in the research group (Ali, 2014, Idrus, 2013) and it has been observed that interference from chlorides at the working concentrations used is negligible and thus the addition of silver nitrate in the test is not essential.

Table 3.5. FICODOX-plus and Ferroin Indicator composition

Substance	Chemical	Concentration	Units
FICODOX-Plus	Potassium di-chromate	1.7	g L^{-1}
	Silver sulphate	8.1	g L^{-1}
	Sulphuric acid	81.1	%
Ferroin Indicator	1,10-phenantroline monohydrate	14.85	g L^{-1}
	Iron (II) sulphate heptahydrate	6.95	g L^{-1}

$$COD = \frac{(V_{blank} - V_{sample})(M)(8000)}{ml\ of\ sample}$$ Equation 3.1

Where:

COD = Chemical oxygen demand of sample (mg O_2 L^{-1})

V = volume of FAS used in the titration (mL)

M = molarity of FAS (0.025M)

8000 = milliequivalent weight of oxygen × 1000 mL/L.

The method used was designed to eliminate or minimise any dissolved gases (CH_4, H_2S) by taking the sample drop by drop from the effluent outlet and then allowing it to stand for 30-60 minutes in contact with the atmosphere, as described in Appendix B.I.b. The COD values are therefore assumed not to include any contribution from dissolved CH_4 or H_2S.

It has been observed in previous uses of the synthetic substrate that the COD concentration in a batch of feed may reduce over the day, due to solids adherence to

the walls of the stirred feed storage container walls as well as the occurrence of some microbial degradation. A controlled in situ test with the synthetic wastewater at 1 g COD L^{-1} indicated the rate of decline was approximately linear (see Appendix B.I.a). Therefore feed COD was measured on preparation and at the end of the feeding period and the average value used as the feed COD for all calculations.

3.2.1.2. Total and suspended solids

3.2.1.2.1. Total Solids (TS) and Volatile Solids (VS)

Total solids and volatile solids analysis were carried out based on Standard Method 2540 G (APHA *et al.*, 2012). After thorough agitation, approximately 60 g of mixed liquor sample was transferred into a weighed crucible by pipetting. Samples were weighed to an accuracy of 60 g (to ± 0.001 g) (Sartorius LC6215 balance, Sartorius AG, Gottingen Germany) and placed in an oven (LTE Scientific Ltd., Oldham UK / Heraeus Function Line series, UK) for drying overnight at 105 ± 1 ^{o}C. After drying the samples were transferred to a desiccator to cool for at least 40 minutes. Samples were then weighed again with the same balance for TS determination, and then transferred to a muffle furnace (Carbolite Furnace 201, Carbolite, UK) and heated to 550 ± 10 ^{o}C for two hours. After this ashing step, samples were again cooled in a desiccator for at least one hour before weighing a third time for VS determination. After all analyses, crucibles were washed with detergent, rinsed with deionised water, and stored in an oven until required for the next analysis. Crucibles were transferred from the oven to a desiccator for cooling to room temperature before each analysis. Total and volatile solids were calculated according to the following equations:

$$TS = \left(\frac{W_3 - W_1}{W_2 - W_1}\right) \qquad \text{Equation 3.2}$$

$$\mathrm{VS} = \left(\frac{W_3 - W_4}{W_2 - W_1}\right) \qquad \text{Equation 3.3}$$

Where:

TS = total solids (mg L^{-1})

VS = volatile solids (mg L^{-1})

W_1 = weight of crucible (g)

W_2 = weight of crucible (g) + weight of wet sample

W_3 = weight of crucible + weight of sample after drying at 105 ^{o}C (g)

W_4 = weight of crucible + weight of sample after igniting to 550 ^{o}C (g)

3.2.1.2.2. Total Suspended Solids (TSS) and Volatile Suspended Solids (VSS)

Total suspended solids and volatile suspended solids analysis were carried out based on Standard Method 2540 D and E (APHA et al., 2012). Total suspended solids (TSS) content was measured by passing a sample of known volume through a standard glass fibre filter paper (GF/C, Whatman, UK) of known dry weight (± 0.1 mg) and placed in an oven (LTE Scientific Ltd., Oldham UK / Heraeus Function Line series, UK) for drying overnight at 105 ± 1 ^{o}C. After drying the filter papers with sample were transferred to a desiccator to cool for at least 40 minutes. Samples were then weighed again with the same balance for TSS determination, and then transferred to a muffle furnace (Carbolite Furnace 201, Carbolite, UK) and heated to 550 ± 10 ^{o}C for two hours. After this ashing step, the filter papers with ashes were again cooled in a desiccator for at least one hour before weighing a third time to measure for VSS determination. TSS and VSS were calculated according to the following equations:

$$TSS = \frac{(W_2 - W_1)\,(1000)}{V_s} \qquad \text{Equation 3.4}$$

$$VSS = \frac{(W_2 - W_3)\,(1000)}{V_s} \qquad \text{Equation 3.5}$$

Where:

TSS = total suspended solids (mg L^{-1})

VSS = volatile suspended solids (mg L^{-1})

W_1 = weight of clean filter paper (mg)

W_2 = weight of filter paper + sample (mg)

W_3 = weight of filter paper + sample after igniting to 550 ^{o}C (g)

3.2.1.3. pH

pH was measured using a Jenway 3010 meter (Bibby Scientific Ltd, UK) with a combination glass electrode, calibrated in buffers at pH 4.0, 7.0 and 9.2. The pH meter was temperature compensated and had a sensitivity of ± 0.01 pH unit and accuracy of

0.01 ± 0.005 pH units. Buffer solution used for calibration was prepared from buffer tablets (Fisher Scientific, UK) prepared according to the supplier's instructions. During measurements, the sample was stirred to ensure homogeneity. The pH probe was rinsed with deionised water in between measurements and placed into a mild acid solution to avoid cross-contamination. pH of digestate samples was measured immediately after sampling to prevent changes due to the loss of dissolved CO_2.

3.2.1.4. Capillary Suction Time (CST)

The Capillary Suction Time (CST) test was carried out based on Standard Method 2710 G (APHA et al., 2012), using a Triton-WRPL type 130, a type 319 Multi CST apparatus and paper (Triton Electronics Ltd, UK) according to the manufacturer's instructions (Fig. 3.7). 4 mL of the mixed liquor sample was poured into the 18 mm diameter circular funnel which presses down onto a piece of CST filter paper placed on the lower perspex block of the apparatus. Two electrodes at fixed distances from the funnel detect the presence of water in the filter paper. The CST is defined as the time taken for the water to travel along a standard filter paper between two electrodes. The time interval depends on the resistance of the cake to giving up its water (Scholz, 2005). The rate at which water permeates through the filter paper varies depending on the condition of the substance and the filterability of the cake formed on the filter paper (Triton Electronics Ltd, UK).

3.2.1.5. Frozen Image Centrifugation (FIC)

The FIC test was carried out using a Triton WRC model I6I centrifuge (Triton Electronics Ltd, UK) with a maximum speed of 1070 rpm (Fig. 3.8). This test uses a stroboscopic techniques in which a ‘frozen image’ of the sample is generated which allows changes in the solid liquid interface to be observed and measured in real time. The mechanism operates by matching the frequency of the strobe light to the rotor speed of the centrifuge The centrifugation speed was fixed at 660 ± 10 rpm and observations were made every minute up to 8 minutes ; with the supernatant height recorded against time.

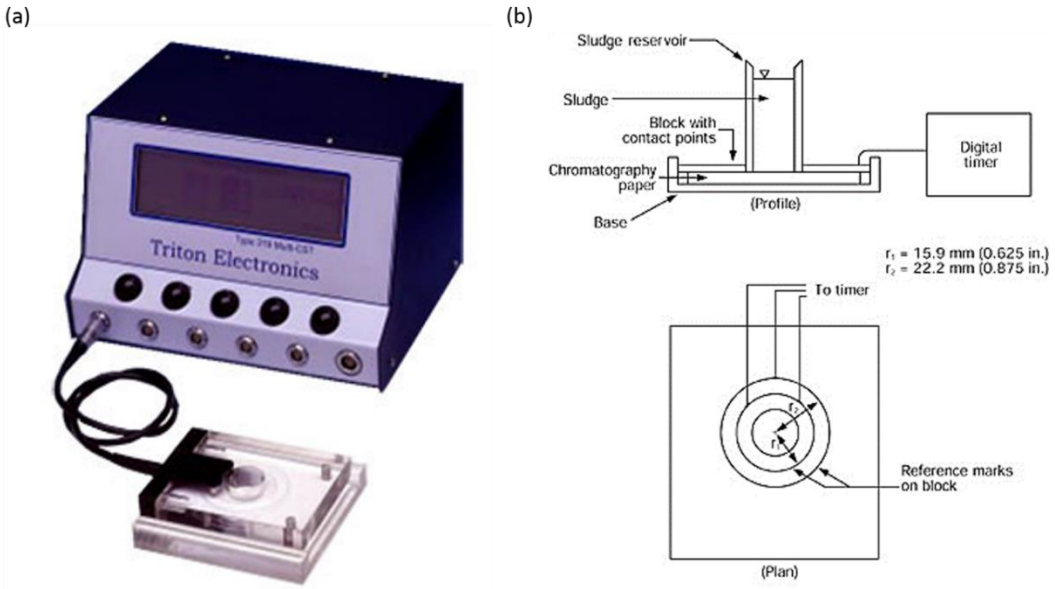

Fig. 3.7. (a) CST apparatus (Triton Electronics Ltd, UK), (b) Schematic of CST apparatus (APHA et al., 2012)

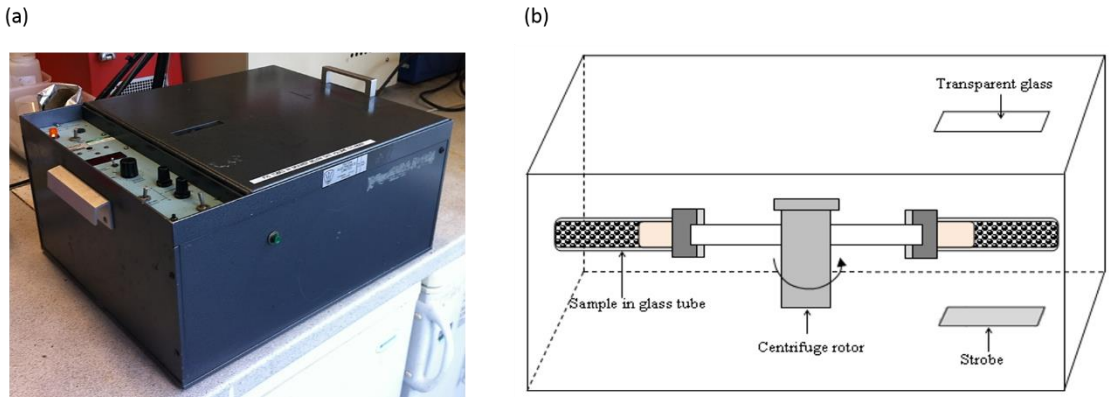

Fig. 3.8. (a) FIC apparatus, (b) schematic diagram of FIC apparatus

3.2.1.6. Extracellular Polymeric Substances (EPS)

Bound EPS were extracted following the formaldehyde plus NaOH procedure based on the methods proposed by Liu and Fang (2002). This method, however, was modified by dividing the extraction method as suggested by Domínguez et al. (2010) and Liang et al. (2010) to allow extraction of the soluble and the bound (lightly and tightly) EPS. The soluble EPS was obtained from the mixed liquor supernatant by centrifugation according to the method by Chabaliná *et al.* (2013). The complete procedure for the extraction of soluble, lightly and tightly bound EPS is summarised in Fig. 3.9. Samples

obtained by EPS extraction were immediately stored at -18 ^{o}C for future analysis to determine carbohydrates and protein. Carbohydrate and protein in the extracted EPS samples were measured by colorimetric methods. Carbohydrate was determined by a phenol-sulphuric acid method following Dubois *et al.* (1956), using glucose as a standard. Protein content was determined by the Lowry Folin-Ciocalteu modified method proposed by Frølund et al. (1995), using bovine serum albumin (BSA) as a standard.

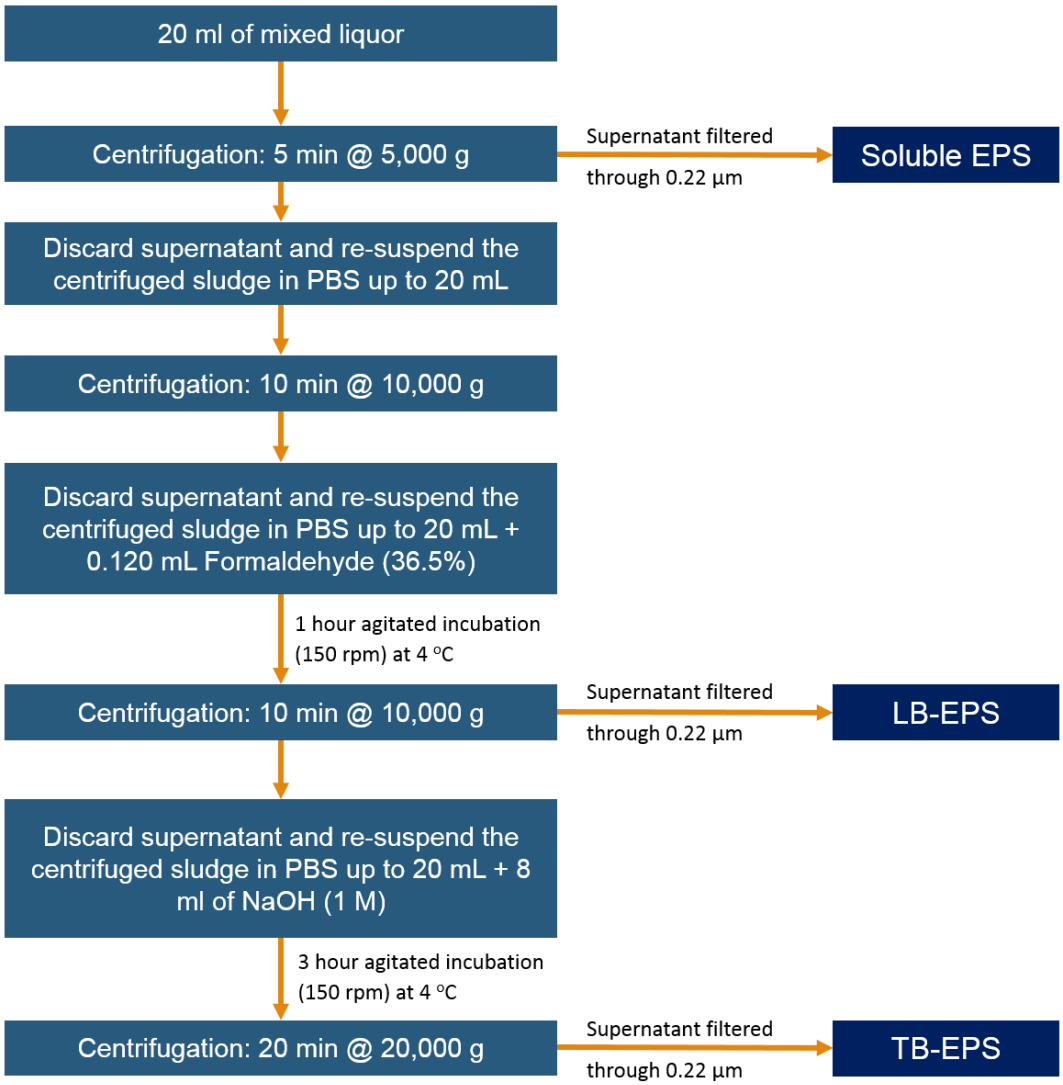

PBS - Phosphate buffer saline tablets (Oxoid, Dubecco A)
1 tablet per 100 ml of distilled water

Fig. 3.9. Flowchart for EPS extraction procedure

3.2.1.7. Elemental composition analysis

Carbon, hydrogen, nitrogen and sulphur contents of samples were determined using a FlashEA 1112 Elemental Analyser (Thermo Finnigan, Italy). Samples were air dried and milled to obtain a homogenous sample. Sub-samples of approximately 0.3-0.4 mg were weighed into standard tin disks using a five decimal place analytical scale (Radwig, XA110/X, Poland). These were placed in a combustion/reduction reactor held at 900°C then flash combusted in a gas flow temporarily enriched with oxygen resulting in a temperature greater than 1700 ^{o}C with the release of N_xO_x, CO_2, H_2O and SO_2 (depending on the composition of the sample). Vanadium pentoxide was added to aid in the release of sulphur. Birch leaf was used as a standard. The gas mixture was then analysed by GC. The working conditions of the elemental analyser were as described in the manufacturer's technical literature and method sheets.

3.2.1.8. Biochemical Oxygen Demand (BOD)

BOD was determined using the respirometric method in an OxiTop system (WTW, Germany). This system is comprised of manometric respirometers that relate oxygen uptake to the change in pressure caused by oxygen consumption while maintaining a constant volume (APHA et al., 2012). The BOD measuring range of the sample to be analysed is first estimated based on the COD/BOD ratio. The brown glass 0.510 L bottles are filled with the selected volume of homogenized sample according to the expected BOD range (Table 3.6), and the required amount of nitrification inhibitor is added.

A magnetic stirrer bar is inserted into the bottle and 2 sodium hydroxide pellets are placed in a rubber sleeve, which is then inserted onto the bottle. OxiTop measuring head (manometric head) is then tightly screwed on, with the rubber sleeve sealing the system. The measurement is started using the OxiTop controller (WTW OxiTop-OC-110, Germany). The bottles are then placed on a magnetic stirrer (WTW OxiTop-IS-12, Germany) inside an incubator for five days at 20 ^{o}C. The results are collected after five days using the OxiTop controller (WTW, 2000).

Table 3.6. Sample volume related to expected BOD range

Volume of sample (ml)	Expected BOD range (mg/l)	Nitrification inhibitor NTH 600 (drops)
432	0 - 40	9
365	0 - 80	7
250	0 - 200	5
164	0 - 400	3
97	0 - 800	2
43.5	0 - 2000	1
22.7	0 - 4000	1

Source: WTW, 2000

3.2.1.9. Total Kjeldahl Nitrogen (TKN)

Total Kjeldahl Nitrogen (TKN) analysis was carried out on duplicate samples alongside blanks and controls as follows: 3-5 g (weighed to ± 1 mg) of sample was placed in a glass digestion tube. Two Kjeltab Cu 3.5 catalyst tablets were added to facilitate acid digestion by lowering the activation energy of the reaction. 12 ml of low nitrogen concentrated H_2SO_4 was added carefully to each digestion tube and agitated gently to ensure that the entire sample was completely exposed to acid. The digestion tubes were then placed into a heating block with an exhaust system using either a Foss Tecator 1007 Digestion System 6 (Foss Analytical, Hoganas Sweden) or a Büchi K-435 Digestion Unit (Büchi, UK), for approximately two hours at 420 ± 5 ^{o}C until the solution colour became a clear blue-green. Once the reaction was completed the tubes were cooled to around 50 ^{o}C and 40 ml of DI water slowly added to the digestion tube to prevent later crystallisation on further cooling. Samples, blanks and standards were then distilled and titrated as for Total ammonia nitrogen based on Standard Method 4500-NH3 B and C (APHA et al., 2012). Blanks (50 ml DI water) and standards (containing 10 ml of 1000 mg l^{-1} NH_4Cl with 40 ml DI water) were also prepared in digestion tubes. 5 ml of 10 M sodium hydroxide (NaOH) was added to each digestion tube to raise the pH above 9.5 and the samples were distilled using either a Foss Tecator Kjeltec system 1002 distillation unit (Foss Tecator A-B, Hoganas, Sweden) or a Büchi K-350 Distillation Unit (Büchi, UK). Erlenmeyer flasks previously filled with 25 ml of boric acid as an indicator were used to collect the distillate and progress of the

distillation was indicated by a colour change from purple to green. The distillate was titrated manually with 0.25N H_2SO_4 using a digital titration system (Schott Titroline, Gerhardt UK Ltd) until an endpoint was reached as indicated by a colour change to purple at which point the volume of titrant added was recorded. Standards and blanks were distilled in the same way. The TKN concentration was then calculated using Equation 3.6.

$$TKN = \frac{(A - B)(14)(N)(1000)}{W_s} \qquad \text{Equation 3.6}$$

Where:

TKN = total Kjeldhal nitrogen (mg kg^{-1} wet weight)

A = volume of titrant used to titrate the sample (mL)

B = volume of titrant used to titrate the blank (mL)

N = normality of the H_2SO_4 titrant, or the theoretical normality multiplied by a correction factor for the specific batch of titrant

Ws = wet weight of sample (kg)

3.2.1.10. Microscopic examination

Microscopic examination of the mixed liquor was carried out with a Nikon Eclipse E200 microscope (Nikon, China), using a 10x/0.25 Nikon EPlan lens (Nikon, China). Images were taken with a 10 MP microscope camera TCA-10.0-N (TUCSEN Imaging Tec. Co. Ltd, China) with a 0.5x lens.

3.2.2. Gas analysis

3.2.2.1. Gas composition

Methane and carbon dioxide of the biogas produced were quantified using a Varian Star 3400 CX gas chromatograph (Varian Ltd, Oxford, UK). The GC was fitted with a Hayesep C column and used either argon or helium as the carrier gas at a flow of 50 mL min^{-1} with a thermal conductivity detector. The biogas composition was compared

with a standard gas (BOC, UK) containing 65 % CH_4 and 35% CO_2 (v/v) for calibration. A sample of 10 ml was taken from a Tedlar bag or directly from the reactor headspace with a syringe and was injected into a gas sampling loop.

3.2.2.2. Gas volume

Biogas was collected in gas-impermeable sampling bags. Volumes were measured using a weight-type water displacement gasometer Fig. 3.10. The measurement procedure was as follows: the initial height of solution in the gasometer (h_1) was recorded before the collected gas was introduced into the column through the top valve. After the bag was empty, the final height (h_2) and the weight of water (m) were recorded, as well as the temperature (T) and pressure (P) in the room.

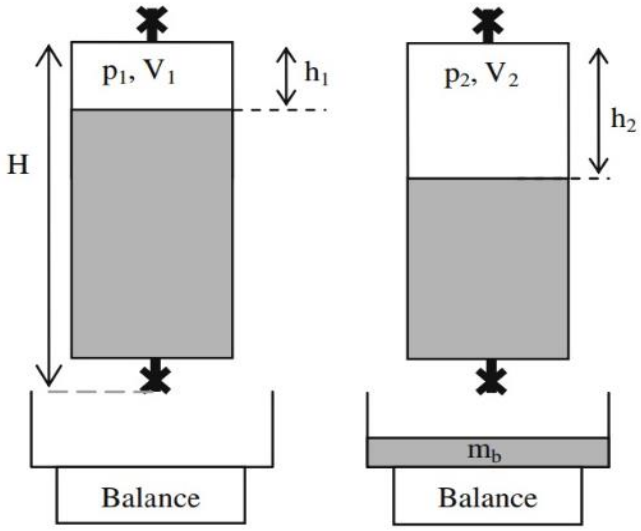

Fig. 3.10.Diagram for gas volume measurement by weight-type water displacement gasometer (Walker et al., 2009)

All gas volumes reported were corrected to standard temperature and pressure (STP) of 0^{o}C, 101.325 kPa as described by Walker et al. (2009), Gas volumes corrected for water vapour were calculated using Equation 3.7 while volumes not corrected for water vapour were calculated using Equation 3.8.

$$V_{stp} = \frac{T_{stp}A}{T_{atm}p_{stp}}\left[\left(\left(P_{atn} - p_{H_2O}(T_{atm}) + \rho_b g\left(H - h_1 - \frac{m_b}{A\rho_b}\right)\right)\left(h_1 + \frac{m_b}{A\rho_b}\right)\right) - \left(p_{atn} - p_{H_2O}(T_{atm}) + \rho_b g(H - h_1)\right)h_1\right]$$

Equation 3.7

$$V_{stp} = \frac{T_{stp}A}{T_{atm}p_{stp}}\left[\left(\left(P_{atn} + \rho_b g\left(H - h_1 - \frac{m_b}{A\rho_b}\right)\right)\left(h_1 + \frac{m_b}{A\rho_b}\right)\right) - \left(p_{atn} + \rho_b g(H - h_1)\right)h_1\right]$$

Equation 3.8

Where:

Output data:

V_{stp}= biogas volume at standard conditions (m^3)

Input data:

Mb = mass of barrier solution (kg)

Patm = atmospheric pressure (Pa)

T_{atm} = atmospheric temperature (K)

h_1 = distance of liquid surface to a standard level of the column where the measurements are taken from (m)

Constants:

P = standard pressure (Pa) = 101325 Pa

T_{stp} = standard temperature (K) = 273.15 K (0 °C)

ρ = density of barrier (kg m^{-3}) = 1000 kg m^{-3}

g = gravitational acceleration (m s^{-2}) = 9.81 m s^{-2}

H = total height of column (m) = 0.66 m

A = cross-sectional area of gasometer (m^2) = 0.0158 m

3.2.2.3. Dissolved gas

3.2.2.3.1. Estimation of saturation concentration of dissolved gases in water

The saturation concentration of gases dissolved in water was calculated with Equation 3.9, derived from Henry's Law.

$$C = \left(\frac{P}{K}\right) \frac{(w)}{\rho} \qquad \text{Equation 3.9}$$

Where:

C = dissolved gas saturation concentration (L of gas L^{-1} of water)

P = Partial fraction of gas (%)

p_{atm}= atmospheric pressure (atm)

w = gas molar weight (g mol^{-1})

K = Henry's Law constant (L atm mol^{-1})

ρ = gas density (g L^{-1})

Henry's Law constants were determined as function of temperature using Equation 3.10 (adapted from Sander, 1999), for which the initial data is shown in Table 3.7. Calculated Henry's law constants at different temperatures for O_2, N_2, CH_4 and CO_2 are summarised in Fig. 3.11.

$$K = K^{\theta} \exp\left((-C)\left(\frac{1}{T} - \frac{1}{T^{\theta}}\right)\right) \qquad \text{Equation 3.10}$$

K = Henry's Law constant at the desired temperature (L atm mol^{-1})

K^{θ} = Henry's Law constant at the standard temperature (L atm mol^{-1})

T^{θ} = 298.15 (K)

T = Operating temperature (K)

C = Gas constant (Sander, 1999)

Table 3.7. Gas constants (C) for the temperature correction of Henry's constant for solubility of O_2, N_2, CH_4 and CO_2

Gas	K at 25 °C[a] (L atm mol^{-1})	C[b] (K)
CH_4	714	1700
CO_2	29.4	2400
O_2	769	1700
N_2	1539	1300

Sources: (a)(Peace-software); (b) (Sander, 1999)

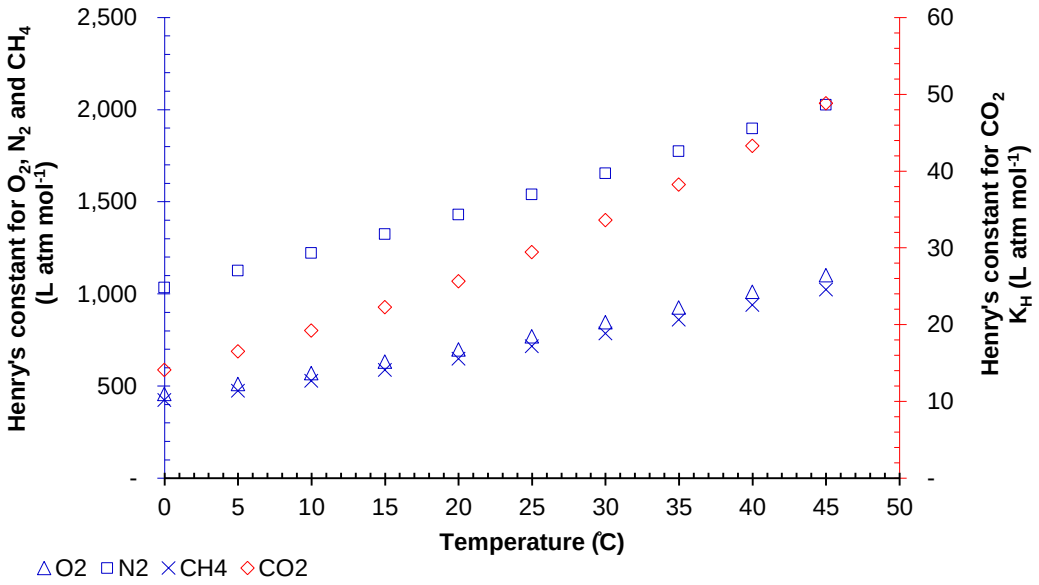

Fig. 3.11. Calculated values of Henry's constant for solubility of O_2, N_2, CH_4 and CO_2 at different temperatures (L atm. mol^{-1})

The saturation concentration of a mixture of gases dissolved in water, such as air or biogas, was calculated using Equation 3.11

$$C_M = \frac{\left(\frac{P_A}{k_{H\,A}}\,(p_{atm})(w_A)\right)}{\rho_A} + \frac{\left(\frac{P_B}{k_{H\,B}}\,(p_{atm})(w_B)\right)}{\rho_B} \qquad \text{Equation 3.11}$$

Where:

C_M = Mixed gas concentration dissolved in water

Other variables are the same as for Equation 3.9, where subscripts A and B represent the respective variables for two different gases.

Saturation concentration of dissolved methane was calculated with respective partial pressures of the measured gas composition.

3.2.2.3.2. Experimental determination of concentration of dissolved gases in water

Biogas dissolved in the effluent was determined experimentally following the method established by (Walsh and McaLaughlan, 1998) and adapted for this study's requirements.

The first part of this method consisted in obtaining the sample, which in this work was carried out by two methods. The first, used for the experiment reported in Chapter 5, consisted in completely filling a vial bottle with effluent then stoppering without leaving headspace. A 10-20% headspace is then created by injecting air with a syringe while concurrently removing the displaced water with a second syringe. The bottle is then mixed by thoroughly shaking the flask and then left at room temperature over 24 hours to allow the dissolved gas to equilibrate with the liquid and gaseous headspace. The weights of the empty serum bottle plus stopper, closed bottle filled with effluent and final weight of the bottle after headspace generation are recorded to allow effluent and gas volume calculation.

The second sampling method, used in the experiment reported in Chapter 0, was a modification of the first method where the vials were replaced for syringes with a valve. These allowed a more controlled collection of the effluent without contact to the atmosphere thus avoiding any escape of dissolved biogas during sampling. The headspace in this method was created by extracting the required amount of effluent from the full syringe and replacing that volume with air. The weight of the syringe and valve is recorded empty, filled with effluent and after creating the headspace to allow

effluent and gas volume calculation. Further details and comparisons between both sampling methods for the experimental determination of dissolved gases are shown in Appendix B.iii.

The result of either sampling method is then used to determine the concentration of methane and carbon dioxide in the headspace by collecting a vial/syringe headspace gas sample in equilibrium after 24 hours for immediate analysis by GC as in Section 3.2.2.1. The concentration of dissolved methane prior to the addition of the helium/air bubble is calculated based on the following equations derived (Walsh and McaLaughlan, 1998) from Henry's law and constants from Fig. 3.12:

$$n_L = \frac{(n_g \cdot R \cdot T)(n_S)}{V_g \cdot K} \qquad \text{Equation 3.12}$$

$$n_S = n_g + n_L \qquad \text{Equation 3.13}$$

$$C_{CH4} = \frac{n_s}{V_L} \qquad \text{Equation 3.14}$$

Where:

n_L = number of moles of gas in liquid phase (mol)

n_g = number of moles of gas in gas phase (mol); calculated with the total gas volume in the vial and the methane composition (% CH_4) measured in the desorbed biogas

n_S = number of moles of sample (mol)

R = ideal gas constant (8.3145 J K^{-1} mol^{-1})

T = temperature (K)

V_g = volume of gas created in the vial (m^3)

V_L = is the volume of liquid in the vial (m^3)

C_{CH4} = calculated methane concentration in the liquid before the desorption (mol L^{-1})

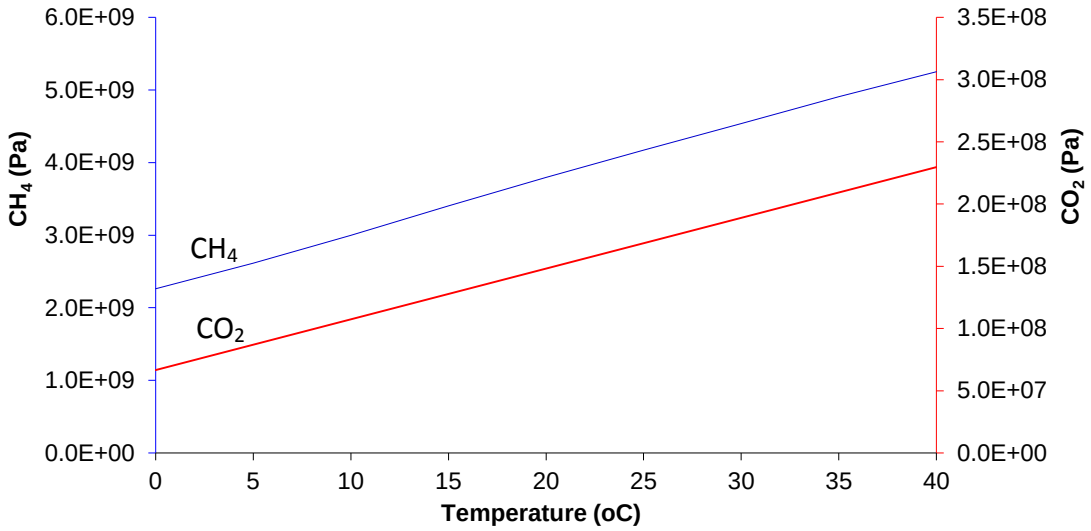

Fig. 3.12. Henry's constant for solubility for experimental determination of dissolved CH_4 and CO_2 (Pa) (Perry and Green, 1999)

3.3. Operational parameters

3.3.1. Membrane flux

Membrane performance was assessed by directly analysing the membrane flux (permeate flow rate) at a constant TMP. The reactor flow was calculated using Equation 3.15 and the membrane flux was determined with Equation 3.16.

$$Q = \frac{(w_{i+1} - w_i)}{(\rho)(t)} \left(\frac{60\,min}{hr}\right) \qquad \text{Equation 3.15}$$

Where:

Q = reactor flow[4] (L hour $^{-1}$)

w_i = permeate weight record in time lapse "i" (g)

ρ = liquid density (g L^{-1})

t = measurement time lapse (min) → 5 min

[4] The permeate flow was assumed equal to the inflow of the system, neglecting losses of water during the anaerobic digestion process. Therefore the reactor flow (Q) represents both inflow and outflow.

$$J = \frac{Q}{A_M}$$ Equation 3.16

Where:

J = membrane flux (L m^{-2} $hour^{-1}$)

A_M =membrane area (m^{-2})

3.3.2. Transmembrane pressure

The transmembrane pressure (TMP) was estimated as the pressure-head of mixed liquor over the membrane modules as defined for AeMBRs in gravitational systems by Ueda and Hata (1999) and verified with Bernoulli's equation (see Appendix C). The TMP was calculated using Equation 3.17, which takes into account the backpressure of the biogas produced inside the reactor (Fig. 3.13).

$$TMP = \left((H_{ML} - H_e) + (P_b)\right) g$$ Equation 3.17

Where:

TMP = transmembrane pressure (kPa)

H_{ML} = surface level of the mixed liquor inside the reactor (m)

H_e = level of the effluent outlet (m)

P_b = estimated gas-lock pressure-head (m)

9.81 = conversion factor - 1 m of $pressure\text{-}head_{water}$ = 9.81 kPa

3.3.3. Hydraulic retention time

The hydraulic retention time was determined using Equation 3.18.

$$HRT = \frac{V_R}{Q}$$ Equation 3.18

Where:

HRT =hydraulic retention time (hours)

V_R = reactor working volume (L)

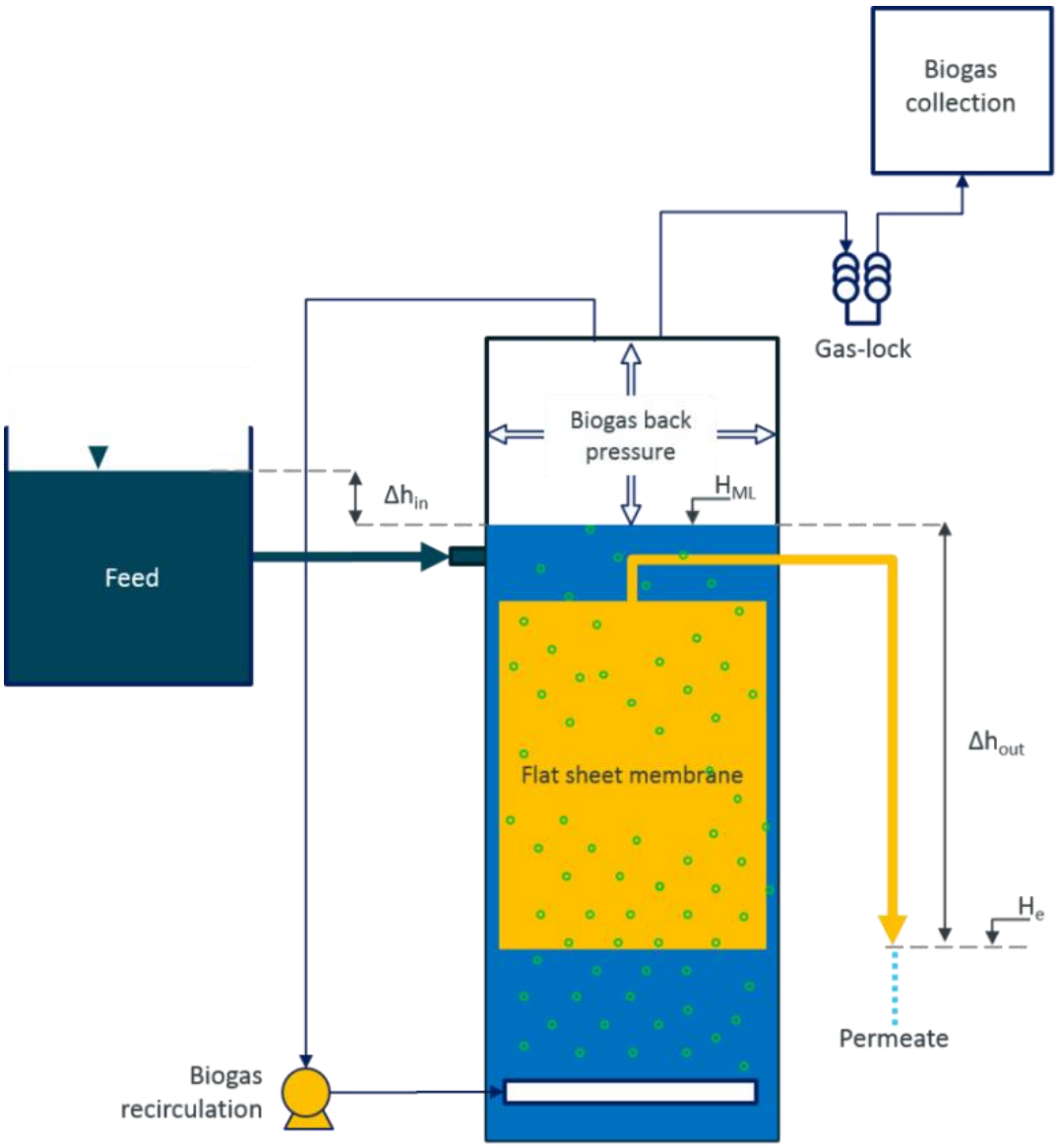

Fig. 3.13. Diagram showing pressure in the gravitational SAnMBR configuration developed in this work

3.3.4. Mean cell residence time

The MCRT was controlled through proportional biomass wastage and calculated using Equation 3.19.

$$MCRT = \frac{(V_R)(MLSS)}{Q(SS_e) + Q_w\,(SS_w)} \qquad \text{Equation 3.19}$$

Where:

MCRT = Mean cell residence time (day)

MLSS =Mixed liquor suspended solids (g L^{-1})

Q_w = Waste digestate flow (L day^{-1})

SS_E = Suspended solids in the effluent (g L^{-1})

SS_W = Suspended solids in waste digestate (g L^{-1})

Since the membrane removes all the suspended solids in the effluent and the gas-lift loop system is assumed to achieve complete mixing in the reactor, the suspended solids in the waste digestate was considered identical to the MLSS, and thus Equation 3.19 was simplified to Equation 3.20.

$$MCRT = \frac{V_R}{Q_w} \qquad \text{Equation 3.20}$$

3.3.5. Organic loading rate

The organic loading rate (OLR) was obtained using Equation 3.21.

$$OLR = (Q)\left(\frac{24\ hrs}{day}\right)(COD_f) \qquad \text{Equation 3.21}$$

Where:

OLR = organic loading rate (g COD day^{-1})

COD_f = COD in the feed (g COD L^{-1})

The volumetric organic loading rate (OLR_v) was obtained by using Equation 3.22.

$$OLR_v = \frac{OLR}{V_R} \qquad \text{Equation 3.22}$$

Where:

OLR_v = volumetric organic loading rate (g COD L^{-1} day^{-1})

3.3.6. COD removal rate

The COD daily removal and removal rate were calculated with Equation 3.23 and Equation 3.24, respectively.

$$COD_{removed} = OLR - \left((Q)\left(\frac{24\ hrs}{day}\right)(COD_e)\right) \quad \text{Equation 3.23}$$

$$\gamma = \frac{COD_{removed}}{OLR}\ (100) \quad \text{Equation 3.24}$$

Where:

$COD_{removed}$ = COD removed (g COD day^{-1})

COD_e = COD in the effluent (g COD L^{-1})

γ= COD removal rate (%)

3.3.7. Biogas and methane production

3.3.7.1. Biogas volumetric production

The biogas volumetric production was determined using Equation 3.25

$$B_{vol} = \frac{(Biogas\ V_{stp})(\tau)}{V_R} \quad \text{Equation 3.25}$$

Where:

B_{vol} = daily biogas production per litre of reactor (L L^{-1} day^{-1})

$Biogas\ V_{stp}$= measured biogas volume (L day^{-1}) from Equation 3.8[5]

τ = percentage of CH_4 plus CO_2 of the gas composition (%); not normalised

[5] The biogas quantification method used the gas volume Equation 3.8 without the correction factor for water vapour as when the measured volume of biogas is multiplied by the not normalised CO_2 and CH_4 fraction of the biogas composition the volume of other gases, including the dissolved air introduced through the influent and the water in form of vapour, is automatically taken into account.

3.3.7.2. Specific methane production

The specific methane production (SMP) per gram of COD removed was determined using Equation 3.26. The term SMP in this work will always refer to the SMP per gram of COD removed, unless noted.

$$SMP = \frac{(Biogas\ V_{stp})(CH_4\%)}{COD_{removed}} \qquad \text{Equation 3.26}$$

Where:

SMP = specific methane production per gram of COD removed (L CH_4 g^{-1} COD removed)

CH_4 % = methane fraction of τ (%)

SMP per gram of COD added (SMP_{added}) was determined using Equation 3.27.

$$SMP_{added} = \frac{(Biogas\ V_{stp})(CH_4\%)}{OLR} \qquad \text{Equation 3.27}$$

Where:

SMP_{added}= specific methane production per gram of COD added (L CH_4 g^{-1} COD added)

3.3.8. Observed biomass yield

The observed biomass yield was determined using Equation 3.28.

$$Y_{obs} = \frac{(MLVSS)(V_R)}{(MCRT)(COD_{removed})} \qquad \text{Equation 3.28}$$

Where:

Y_{obs} = observed or apparent biomass yield (g VSS g^{-1} COD)

$MLVSS$ = Mixed liquor suspended solids (g L^{-1})

It should be noted that values obtained from Equation 3.28 are only representative under steady state conditions as this calculation does not take into account the change in MLSS stored in the reactor.

3.3.9. COD balance

COD balance is a useful tool to operate and better understand an anaerobic system (van Lier et al., 2008). In contrast to aerobic systems, in anaerobic reactors there is no COD destruction but only a "rearrangement" of the COD. All the COD that enters an anaerobic system ends up either in the end product CH_4, incorporated as new cell mass, leaving the system in the effluent or removed sludge, or channelled to oxidised anions like SO_4^{2-} and NO_3^- reducing to gases such as H_2S which can be present in gaseous form or dissolved in the effluent (Fig. 3.14) (van Lier et al., 2008).

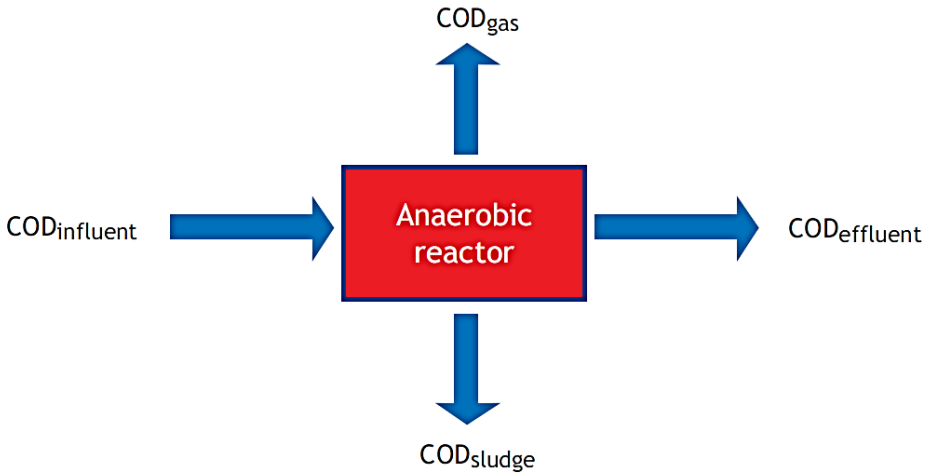

Fig. 3.14. Components in the COD balance in an anaerobic reactor (van Lier et al., 2008)

In the COD mass balances carried out in this study, the influent was the only pathway considered for COD input to the system (Fig. 3.15). The pathways for COD output were: the COD in the effluent, the COD as CH_4 produced, the COD as CH_4 dissolved in the effluent, and the COD utilised for biomass growth. The COD output fraction corresponding to H_2S was not considered in the COD balances of this study. Reported COD/VSS ratios vary between 1.2-1.6 g COD/g VSS (Parker *et al.*, 2008) with a reported

global measured value of 1.48 mg COD/ g VSS (Mara and Horan, 2008). The ratio employed in this work was experimentally determined, and ranged between 1.40-1.45 g COD g^{-1} MLSS. The COD balances in this study did not take into account changes in COD stored in biomass and therefore are for steady-state conditions.

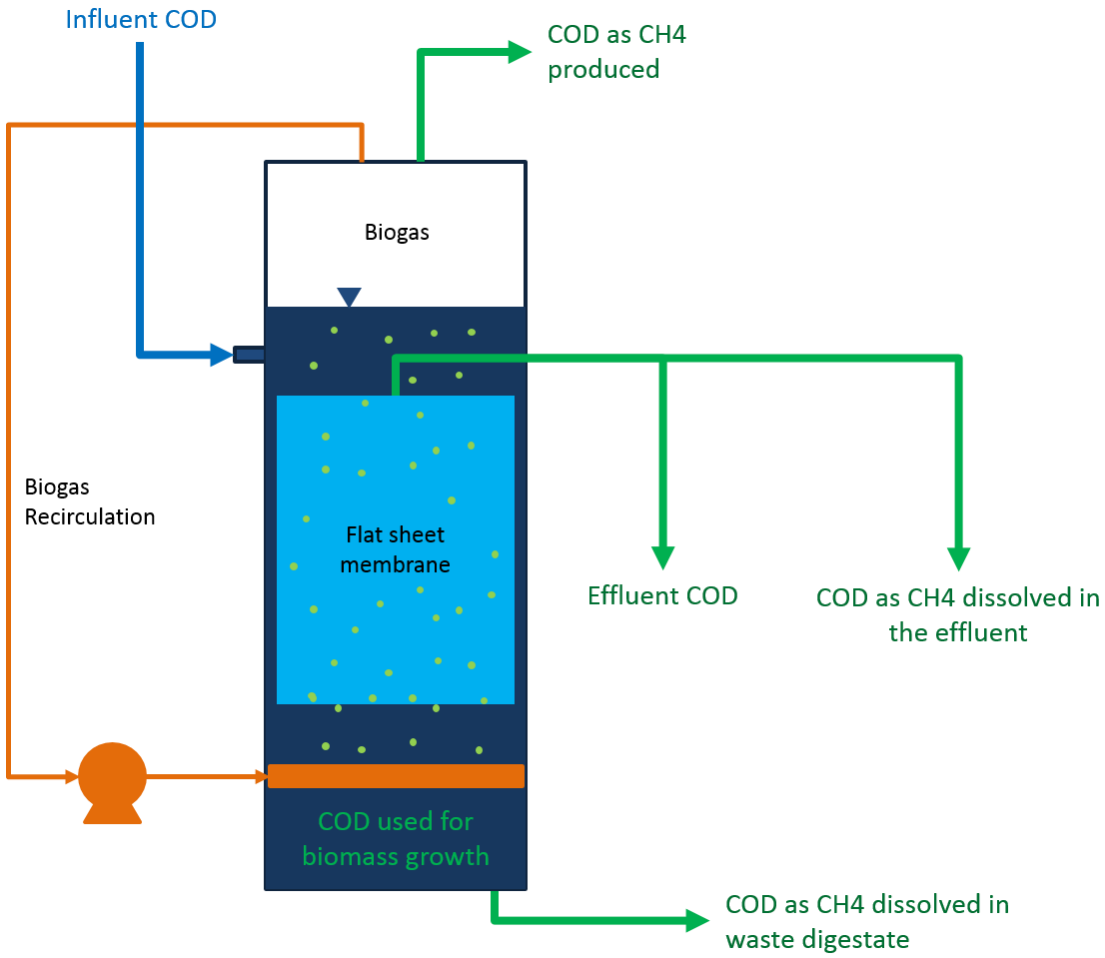

Fig. 3.15.SAnMBR considered COD inputs and outputs

All pathways were determined in g COD day^{-1}, using the following equations:

$$COD_{influent} = OLR \qquad \text{Equation 3.29}$$

$$COD_{effluent} = (Q)\left(\frac{24\ hrs}{day}\right)(COD_e) \qquad \text{Equation 3.30}$$

$$COD_{CH_4} = \frac{(Biogas\ V_{stp})(CH_4\%)}{(0.35)}$$ Equation 3.31

$$COD_{CH_4(D)} = \frac{(Q)\left(\frac{24\ hrs}{day}\right)}{\emptyset_{CH_4(T)}(0.35)}$$ Equation 3.32

$$COD_{Biomass} = \frac{Q_w\ (SS_W)}{\mu}$$ Equation 3.33

Where:

$COD_{influent}$ = COD entering the system through the influent (g COD day^{-1})

$COD_{effluent}$ = COD exiting the system through the effluent (g COD day^{-1})

COD_{CH_4} = COD as CH_4 produced (g COD day^{-1})

$COD_{CH_4(D)}$ = COD as CH_4 produced dissolved in the effluent (g COD day^{-1})

$COD_{Biomass}$ = COD as biomass produced (g COD day^{-1})

$\emptyset_{CH_4(T)}$ = Calculated dissolved CH_4 saturation concentration (L CH_4 L^{-1}) at temperature T (^oC) – see Section 3.2.2.3.1

μ = mixed liquor COD/VSS ratio

0.35 = theoretical CH_4 production at STP (L CH_4 g^{-1} COD)

3.4. Laboratory practice

All operations were carried out using good laboratory practice, and having first carried out the appropriate risk assessments and, where necessary, COSSH assessments. All equipment, laboratory apparatus, and analytical instruments were operated in accordance with the manufacturer's instructions unless noted. All glassware was washed using washing detergent followed by rinsing with tap water and deionised water. The glassware used for the acid digestion was soaked in a 10% nitric acid bath for a 24 hour period after which the glassware was rinsed with ultrapure water.

3.5. Statistical analysis

Regression analysis was employed to compare experimental values between two parameters. For experimental data reported in this work, particularly in the results tables, standard deviation (±) was employed to quantify the spread of experimental data values from the average during a stable performance or steady state period. For periods where no stable performance was achieved, the data was reported as a 'variable trend' (→) by presenting the initial, middle and final value during the specified period.

3.6. Research methodology

The work involved experimental studies at laboratory scale to investigate the performance of SAnMBR when treating low-to-intermediate strength synthetic wastewater with high solids content at 36 ^{o}C and 20 ^{o}C. The work is centred in:

- Development and testing of a fully gravitational SAnMBR to investigate rates of membrane flux under constant TMP for detailed study of the effect of operational parameters on membrane fouling and overall reactor performance.
- Study of the long-term effect of MCRT on membrane fouling, mixed liquor characteristics and overall performance of SAnMBRs operating at 36 ^{o}C.
- Study of the long-term effect of MCRT on membrane fouling, mixed liquor characteristics and overall performance of SAnMBRs operating at 20 ^{o}C.
- Comparative analysis on the effect of MCRT on SAnMBRs performance at 36 ^{o}C and 20 ^{o}C,
- Evaluation of the operation and performance of the proposed SAnMBR system, its potential problems, strengths and weaknesses, and its scale-up potential.

A summary of the methods used in each experiment is given in the respective results chapters.

4. RESULTS – DEVELOPMENT AND TESTING OF A FULLY GRAVITATIONAL SANMBR

Objective: To develop and test a fully gravitational SAnMBR for the treatment of low-to-intermediate synthetic wastewater at 36 ^{o}C in order to investigate rates of membrane flux under constant TMP and to establish achievable steady state flux rates in a model system.

This experiment was intended to assess the concept and to establish the likely steady-state flux rates that might be achieved, using a synthetic substrate that was formulated to have a relatively high concentration of suspended solids. The work used a flat plate membrane with gas scouring to maintain membrane permeability, and thus to provide reproducible comparative results over a range of induced TMP values.

4.1. Method summary

A gravity-operated SAnMBR was set up in order to test its principle of operation as an alternative to conventional pumped permeation of the membrane. The experimental set-up is shown in Fig. 4.1 and Fig. 4.2, and fully detailed in Section 3.1.5.

The reactor was operated at constant TMP and at mesophilic temperatures (36 ^{o}C) for a period of 115 and comprised a start-up period and four experimental phases (EP), as shown in Table 4.1. During this time process control was achieved by maintaining the OLR_V (based on COD) within defined limits, and by regulation of the reactor MLSS by controlled wastage. The reactor was fed with a nutrient-balanced synthetic wastewater with a high suspended solids concentration (Section 3.1.2). This was prepared fresh every morning and diluted to give the required COD strength and solids content, and thus obtain the desired OLR_V. The synthetic wastewater was stored at ambient temperature during the experiment.

Transmembrane pressure could be kept constant, in which case the membrane flux varied relative to the degree of fouling; alternatively the membrane flux could be

adjusted by increasing or decreasing the head differential. The reactor was inoculated with digestate from a mesophilic digester treating municipal wastewater biosolids (Section 3.1.4). This was diluted to 50% with tap water, and after filling of the reactor the headspace was purged with nitrogen. Membrane fouling, mixed liquor characteristics and overall reactor performance were assessed by monitoring the membrane flux at constant TMP, influent and effluent COD concentrations, MLSS, pH, volumetric biogas production, biogas composition and specific methane production (SMP, SMP_{added} and SMP_{MLSS}).

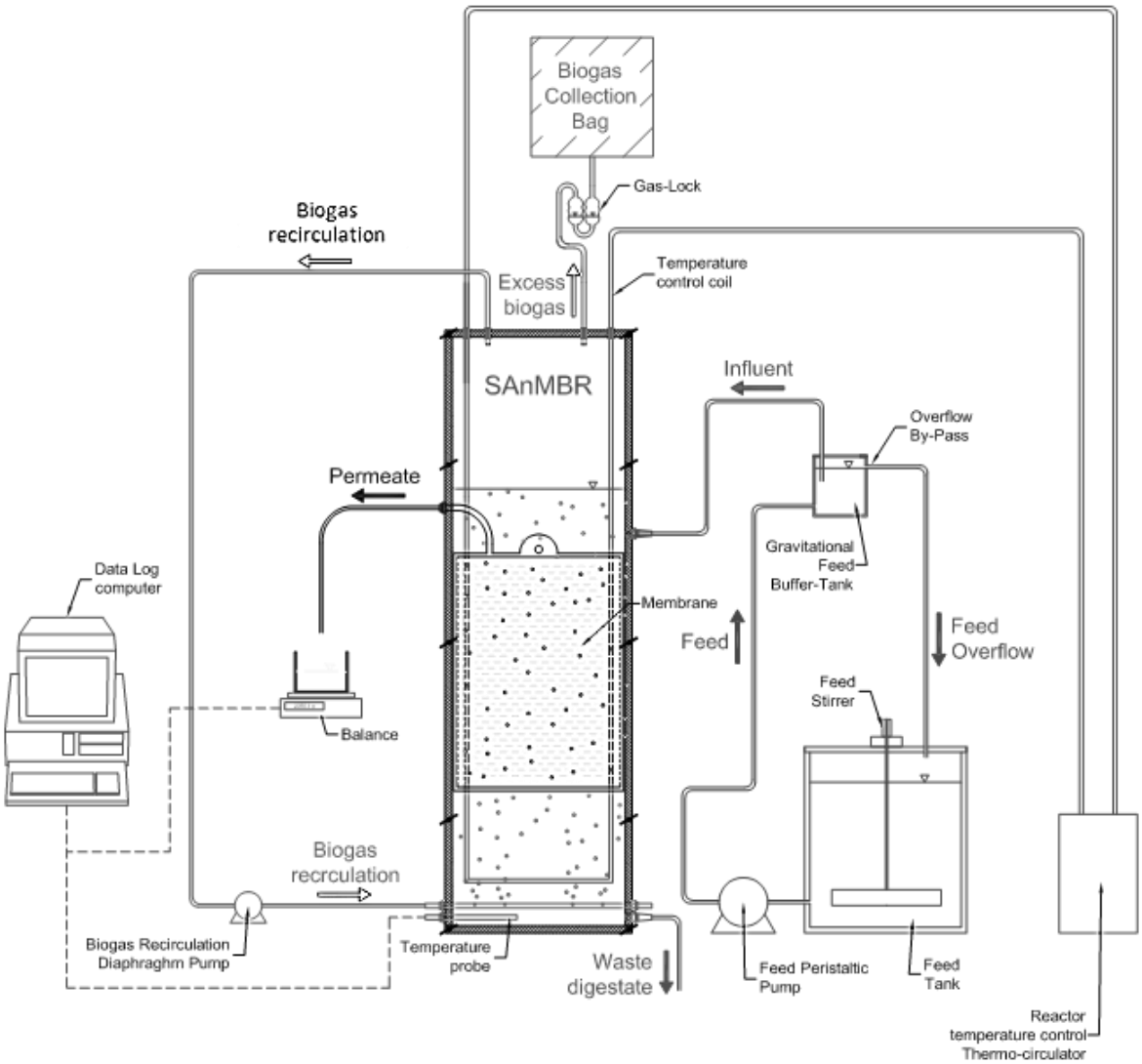

Fig. 4.1. Experimental set-up schematic diagram – Development and testing of a fully gravitational SAnMBR: biogas collection bags, biogas recirculation pumps, constant head device, effluent collection containers, effluent head-difference device, fermentation gas-lock, flux recording balance, SAnMBR, stirred feed storage tank, and thermo-circulator

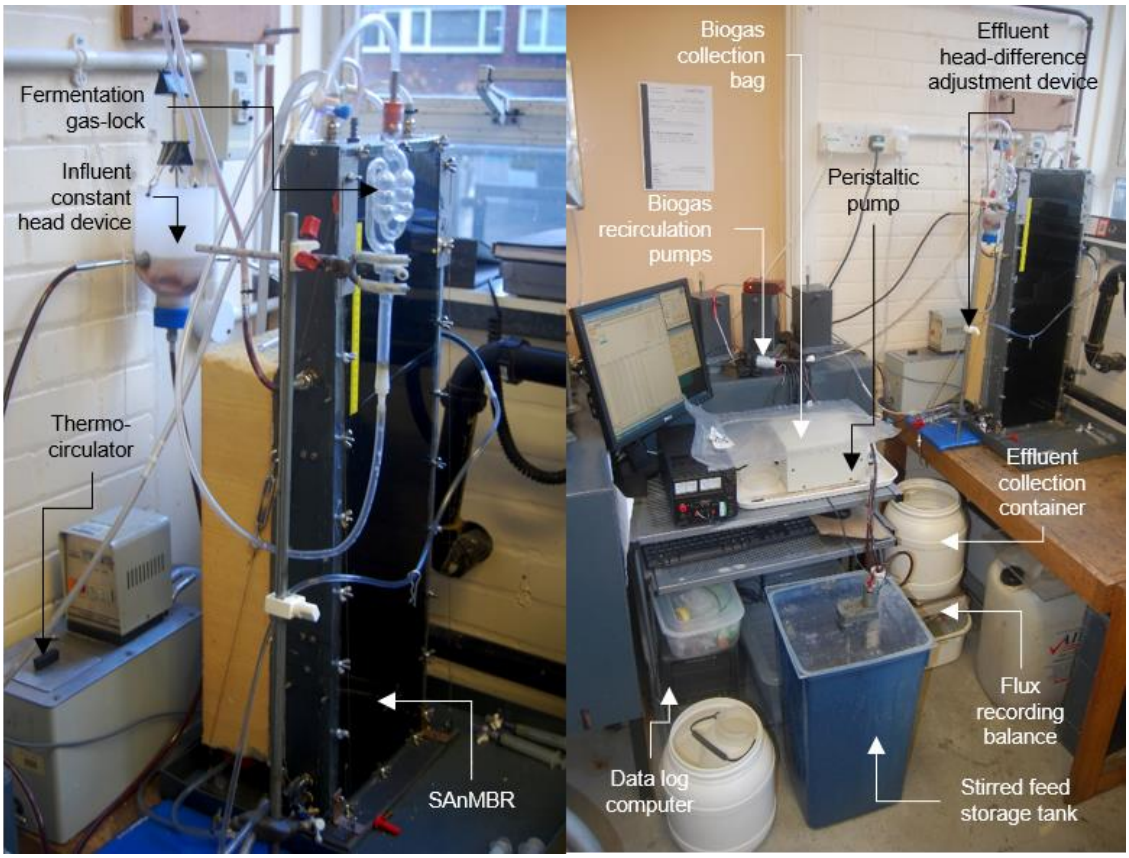

Fig. 4.2. Experimental set-up schematic picture – Development and testing of a fully gravitational SAnMBR: biogas collection bags, biogas recirculation pumps, constant head device, effluent collection containers, effluent head-difference device, fermentation gas-lock, flux recording balance, SAnMBR, stirred feed storage tank, and thermo-circulator

Table 4.1 Start-up and experimental phases – Development and testing of fully gravitational SAnMBR experiment at 36 ^{o}C

Phase	**Duration** (days)	**Objective**	**TMP** (kPa)
Start-up	10	Start-up experiment and stabilise system for the experimental phases	7.0
EP-1	43	First insight into fully gravitational SAnMBR operation and understanding of the system functioning	7.0
EP-2	15	Evaluate membrane performance at high TMP	7.0
EP-3	3	Evaluate performance with a flow restriction at high TMP	7.0
EP-4	44	Evaluate membrane performance at a low TMP and different OLR_V	2.3

4.2. Results and discussion – Development and testing of fully gravitational SAnMBR experiment at 36 °C

4.2.1. Operational performance

4.2.1.1. Membrane flux response and observed changes in MLSS, HRT, OLR_V, biogas production and COD removal rates

Average values for the main parameters measured or calculated for each of the experimental phases are summarised in Table 4.2. Details are shown in Fig. 4.3 and are discussed in the sections below.

Start-up. The system was operated at a constant TMP of 7.0 kPa. The daily average membrane flux dropped from 20.2 to 11.0 L m^{-2} $hour^{-1}$ over the first 8 days and then began to stabilise (Fig. 4.3). Mixed liquor was removed at a rate of 100 mL day^{-1} resulting in a fall in the reactor MLSS concentration from 21.7 g L^{-1} to around 15 g L^{-1} (Fig. 4.3).

EP-1. In this phase the MLSS concentration was maintained between 14 - 16 g L^{-1} and the TMP at 7.0 kPa. The daily average membrane flux gradually reduced from 11.3 to 6.7 L m^{-2} $hour^{-1}$ over the next 43 days (Fig. 4.3) due to membrane fouling. As a result of this the OLR_V decreased from 1.9 to 1.1 g COD L^{-1} day^{-1} and the HRT increased from 7 to 12 hours. COD removal was initially 75% and gradually increased to 96%. Biogas production was variable, with an initial drop in production followed by a recovery. From day 35, however, there was a gradual fall in production as the load to the reactor decreased due to the falling rate of flux.

EP-2. On day 53 a deliberate intervention was carried out in an attempt to reduce the flux to a lower and more sustainable value. This involved stopping feeding for 5 hours whilst still drawing permeate from the mixed liquor through the membrane. This gave a sharp but transient increase in the MLSS concentration which accelerated the membrane fouling. The result was observable by a reduction in flux from 6.7 to 5.8 L m^{-2} $hour^{-1}$ (Fig. 4.3), even though the TMP was maintained at 7.0 kPa. Initially it appeared that a steady state had been established, but flux again began to decline around day 60 reaching a value of 5.0 L m^{-2} $hour^{-1}$ by day 68.

Table 4.2. Experimental results summary table – Development and testing of fully gravitational SAnMBR experiment at 36 ^{o}C: Daily average membrane flux, TMP feed COD, effluent COD, COD removal, OLR_v, HRT, biogas production, CH_4 in biogas, SMP, pH, MLSS and MCRT

Parameter	**EP-1**	**EP-2**	**EP-3**	**EP-4** OLR_{V1}	**EP-4** OLR_{V2}	**EP-4** OLR_{V3}
Membrane flux (J)* ($L\ m^{-2}\ hour^{-1}$)	11.4 → 6.6	5.8 → 5.0	4.0 ± 0.36	2.2 ± 0.08	2.2 ± 0.03	2.2 ± 0.03
TMP (kPa)	7.0	7.0	7.0	2.3	2.3	2.3
OLR_V ($g\ COD\ L^{-1}$ reactor day^{-1})	1.9 → 1.1	0.9 → 0.8	0.7 ± 0.06	0.4 ± 0.01	0.7 ± 0.01	1.0 ± 0.01
HRT (hours)	7 → 12	14 → 16	20 ± 2.0	37 ± 1.3	37 ± 0.5	37 ± 0.5
Feed COD ($mg\ L^{-1}$)	551 ± 55	556 ± 44	583 ± 37	587 ± 24	1111 ± 38	1513 ± 45
Effluent COD ($mg\ L^{-1}$)	104 → 25	33 → 27	28 ± 1	23 ± 5	48 ± 7	49 ± 8
COD removal (%)	75% → 96%	95% ± 0%	95% ± 0%	96% ± 1%	96% ± 1%	97% ± 1%
Biogas production ($L\ L^{-1}$ reactor day^{-1})	0.66 → 0.33	0.35 → 0.26	0.24 ± 0.02	0.17 ± 0.01	0.27 ± 0.01	0.33 ± 0.02
CH_4 content in biogas** (%)	88 % ± 2	87 % ± 1	86%	85 % ± 1	82 % ± 1	81 ± 1 %
SMP ($L\ CH_4\ g^{-1}$ COD removed)	0.27 ± 0.03	0.28 ± 0.02	0.29 ± 0.04	0.46 → 0.32	0.29 ± 0.02	0.26 ± 0.01
pH	6.8 ± 0.06	6.8 ± 0.03	6.8 ± 0.01	6.8 ± 0.02	6.8 ± 0.06	7.0 ± 0.04
MLSS ($g\ L^{-1}$)	14.7 ± 0.6	14.5 ± 0.1	14.0 ± 0.2	12.8 → 14.2	12.5 ± 0.2	12.4 → 14.0
MCRT (days)	261	203	365	608	608	608

(→) Variable trend: initial → middle → final; (±) Stable performance: One standard deviation to show the spread of the data from the average value under stable performance; (*) Daily average; (**) Normalised to total biogas content in sample (i.e. neglecting fraction of other gases in the headspace)

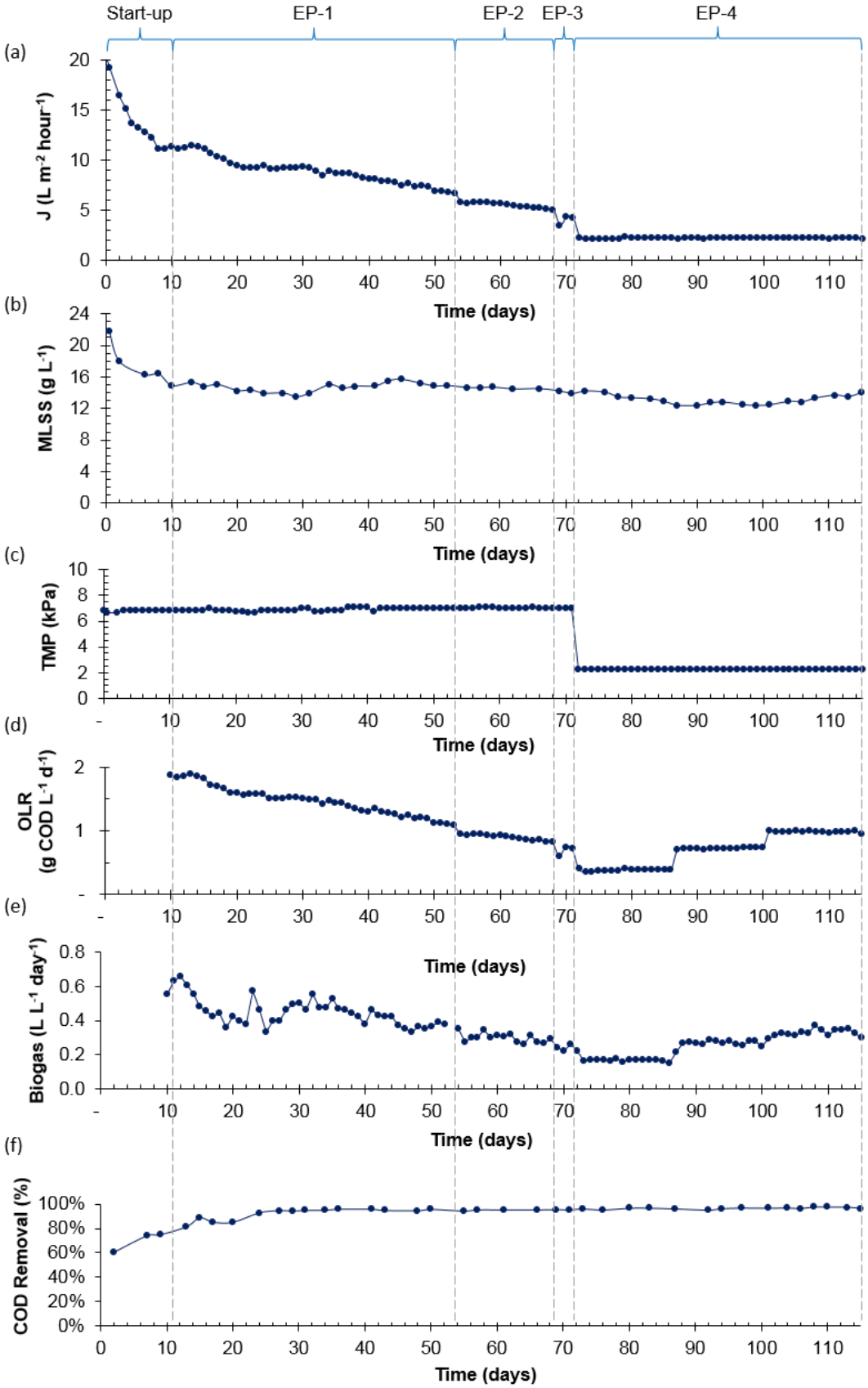

Fig. 4.3. Operational performance during experimental period – Development and testing of fully gravitational SAnMBR experiment at 36 ^{o}C: (a) Daily average membrane flux, (b) MLSS concentration, (c) TMP, (d) OLR_v, (e) biogas production and (f) COD removal rate.

This led to a reduction in OLR_V from 1.0 to 0.8 g COD L^{-1} day^{-1} and an increase in HRT from 14 to 16 hours with a further reduction in biogas production. To maintain the MLSS concentration at a more or less constant value between day 10 and 68, the amount of biomass removed from the system as a proportion of the total biomass present was equivalent to a calculated mean cell residence time of ~200 days.

EP-3. On day 68 a valve was installed in the permeate line in an attempt to provide control over the flux rate by decoupling it from membrane fouling: in effect the valve was meant to reduce the outlet permeate flow relative to the degree of valve closure. This intervention was not successful in giving control of the flux rate, and the reasons for this are discussed in Section 4.2.2.1. The valve was removed on day 71.

EP-4. The final intervention to establish a stable membrane flux involved a large reduction in TMP from 7.0 to 2.3 kPa. This resulted in an instant decrease in membrane flux from 4.2 L m^{-2} $hour^{-1}$ to 2.2 ± 0.08 L m^{-2} $hour^{-1}$ (Fig. 4.3), which then remained constant for the following 44 days until the end of the trial on day 115. The reduced flux gave a HRT of 37 hours corresponding to a rather low OLR_V of 0.4 g COD L^{-1} day^{-1}. During this phase no attempt was made to control the MLSS, and no wastage took place. As a consequence of the low OLR_V and extended HRT the MLSS fell to around 12 mg L^{-1}, and biogas production decreased to less than 0.17 ± 0.01 L L^{-1} day^{-1}. In hindsight, the severe reduction in TMP was far greater than needed to establish steady state flux conditions at the applied load. Rather than increasing the TMP again, the OLR_V on the system was raised by increasing the COD of the feed substrate, first to 0.75 g COD L^{-1} day^{-1} on day 86 and then to 1.0 g COD L^{-1} day^{-1} on day 100. The MLSS responded to these increases in load and the decline in concentration was reversed, albeit slowly. Biogas production increased stepwise with each increase in OLR_V. As no MLSS wastage took place during this phase the calculated MCRT increased, but would not have reached a steady state value within the time span of the trial. At the end of this phase the reactor was operating very stably with an OLR_V of 1.0 g COD L^{-1} day^{-1}, a membrane flux of 2 L m^{-2} $hour^{-1}$ at a TMP of 2.3 kPa, a COD removal of 97 % and a SMP typical of the range reported for SAnMBRs working at around this COD concentration (Hu and Stuckey, 2006, Huang et al., 2011, Lin et al., 2011).

4.2.1.2. pH

The pH remained relatively constant throughout the experimental phases (Fig. 4.4 and Table 4.2) as the feed was sufficiently buffered due to its relatively high nitrogen content. There was thus no need to add sodium bicarbonate ($NaHCO_3$) to prevent acidification, either manually or using an automatic doser, as has been done in other studies (Hu and Stuckey, 2006, Akram and Stuckey, 2008, Gao *et al.*, 2011, Zamalloa *et al.*, 2012).

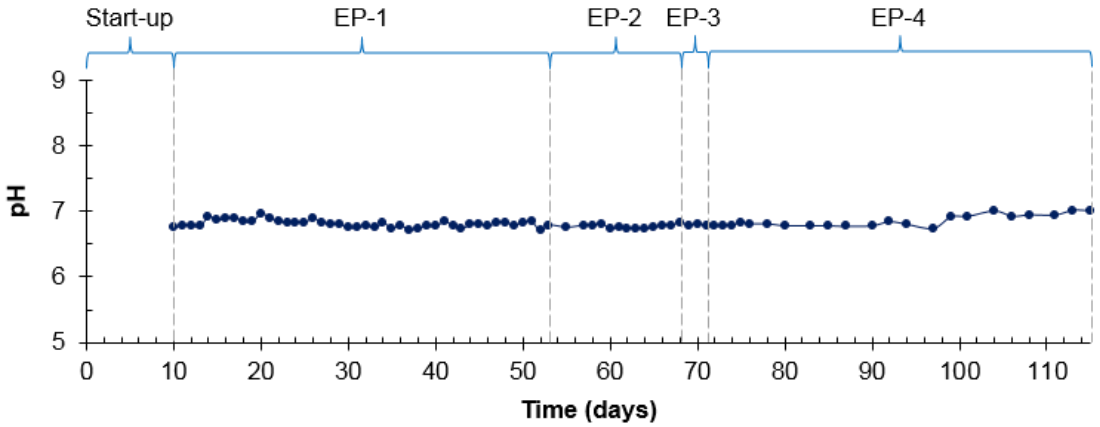

Fig. 4.4 pH during experimental period – Development and testing of fully gravitational SAnMBR experiment at 36 °C

4.2.1.3. Biogas composition

As shown in Fig. 4.5 and Table 4.2, the methane content of the biogas produced was always between 73-83%. This is in agreement with Lin et al. (2013) who noted that biogas produced in AnMBR generally contains between 70-90% CH_4.

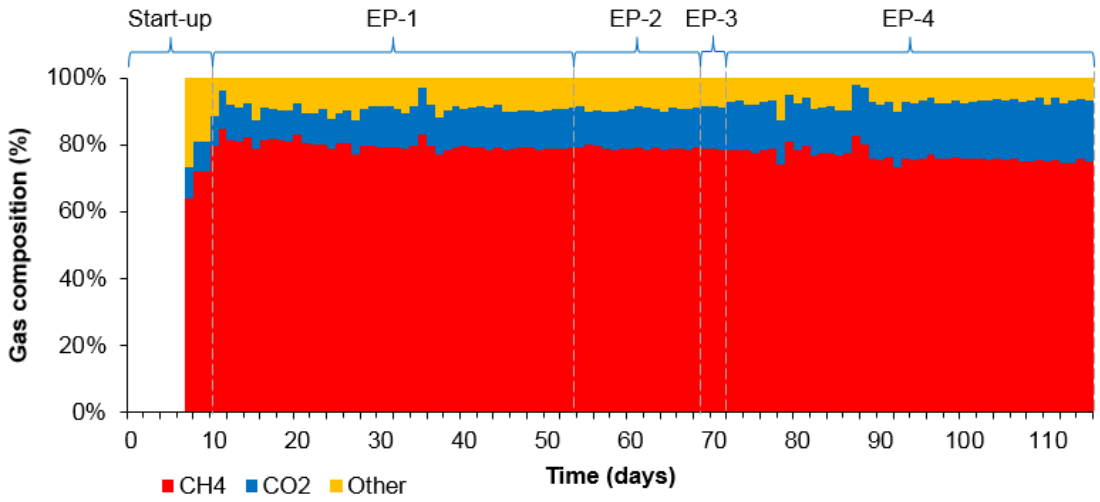

Fig. 4.5. Biogas composition during experimental period – Development and testing of fully gravitational SAnMBR experiment at 36 °C

4.2.1.4. Specific methane production

The SMP in EP-1 was initially unstable as a result of variable biogas production and COD removal rates, and ranged from 0.19-0.38 L CH_4 g^{-1} COD removed (Fig. 4.6a). From day 40 SMP stabilised at around 0.27 L CH_4 g^{-1} COD removed, indicating that the reactor was performing stably in terms of COD conversion. SMP remained stable during EP-2 and EP-3 at 0.28 ± 0.02 L CH_4 g^{-1} COD removed. During the first part of EP-4 the SMP increased to 0.46 L CH_4 g^{-1} COD removed, probably due to the natural reduction in MLSS concentration in response to near-starvation conditions and the internal release of COD through endogenous decay of the biomass. SMP then gradually decreased, stabilising at around 0.30 L CH_4 g^{-1} COD removed during operation at an OLR of 0.75 g COD L^{-1} day^{-1} and around 0.27 L CH_4 g^{-1} COD removed during operation at OLR 1.0 g COD L^{-1} day^{-1}. This is below the theoretical value of 0.35 m^3 CH_4 kg^{-1} COD removed.

COD removal rates during most of the experimental period were above 95%, and the SMP per g of COD added (SMP_{added}, Fig. 4.6b) was therefore almost identical to the SMP. SMP normalised to MLSS (SMP_{MLSS}) also showed similar trends to SMP.

The SMP in this experiment can be compared with that reported in a recent study (Ali, 2014) in which laboratory-scale UASB reactors were operated at 35 ^oC using the same synthetic wastewater and also at low-strength COD concentrations. The SMP reported for an OLR of 1 g COD L^{-1} day^{-1} and a HRT of 25 hours was of 0.31 L CH_4 g^{-1} COD removed while the SMP_{added} for a similar COD removal rate around 95% resulted of 0.30 L CH_4 g^{-1} COD added. This comparison shows a very similar performance between the SAnMBR and UASB reactors in comparable operational conditions. It should be noted, however, that the energy consumption of the UASB reactors would probably be much lower as there is no need for energy consumption related to membrane cleaning. This further emphasises the importance of research to reduce energy requirements in SAnMBRs to make them more competitive with proven technologies like UASB, particularly for the treatment of low strength wastewaters.

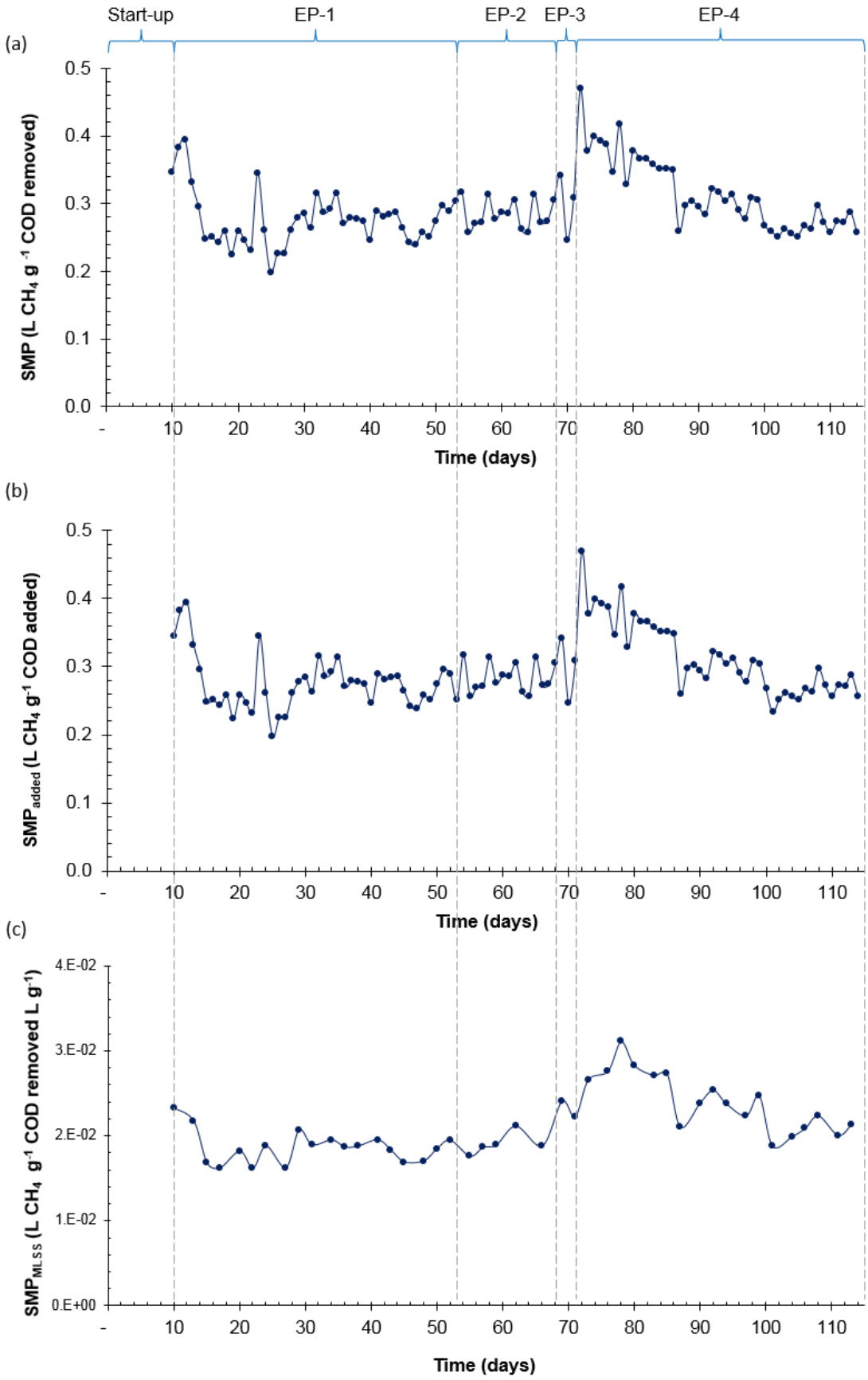

Fig. 4.6. Specific methane production during experimental period – Development and testing of fully gravitational SAnMBR experiment at 36 ^{o}C: (a) SMP, (b) SMP_{added} and (c) SMP_{MLSS}

4.2.2. Membrane performance and fouling phenomena

The critical membrane flux is defined as the permeate flux above which irreversible fouling appears. For an MBR operating in pumped permeation mode the TMP is increased as fouling occurs to maintain a constant flux. This flux is set below the critical value and is defined as the sustainable membrane flux for the fouling control mechanism in operation (WEF, 2012). When operating in a gravitational mode the same principles are applied, but in this case the TMP is controlled by the hydrostatic head applied across the membrane. The same definitions apply for critical and sustainable flux. For AeMBR in continuous operation a critical pressure head has also been defined: this is the minimum head that must be applied if irreversible membrane fouling is to be prevented (Zheng and Liu, 2005). In the experimental system a sustainable membrane flux of 2.2 L m^{-2} $hour^{-1}$ was maintained over a 44-day period (Fig. 4.7) with a hydrostatic pressure head of around 2.3 kPa. Further work is needed, however, to determine the influence of other factors on this parameter in addition to those associated with the membrane cleaning system.The experiment reported here is the first on the operation of a SAnMBR and thus the TMP values applied were selected without prior operating knowledge; likewise it was not known what sustainable flux could be achieved for this design of reactor and its gas scour membrane cleaning system. The operational changes between the four experimental phases were attempts to reach a sustainable flux condition within a limited experimental duration. If the original TMP of 7 kPa had been maintained it is likely that a sustainable flux would have been achieved, but its value cannot be calculated from the data available. Ideally a series of different TMPs would be tested until steady state 'sustainable flux' conditions were achieved, and an empirical relationship established: this however would still be dependent on other operating conditions. The effect of these on the system and on flux rates has not been extensively researched: in this experiment the impact of OLR_V was investigated in *EP-4*. The operational performance results as shown in Fig. 4.3 indicate that a constant flux could be maintained irrespective of the organic load applied, but the sustainability of this constant flux was not fully tested.

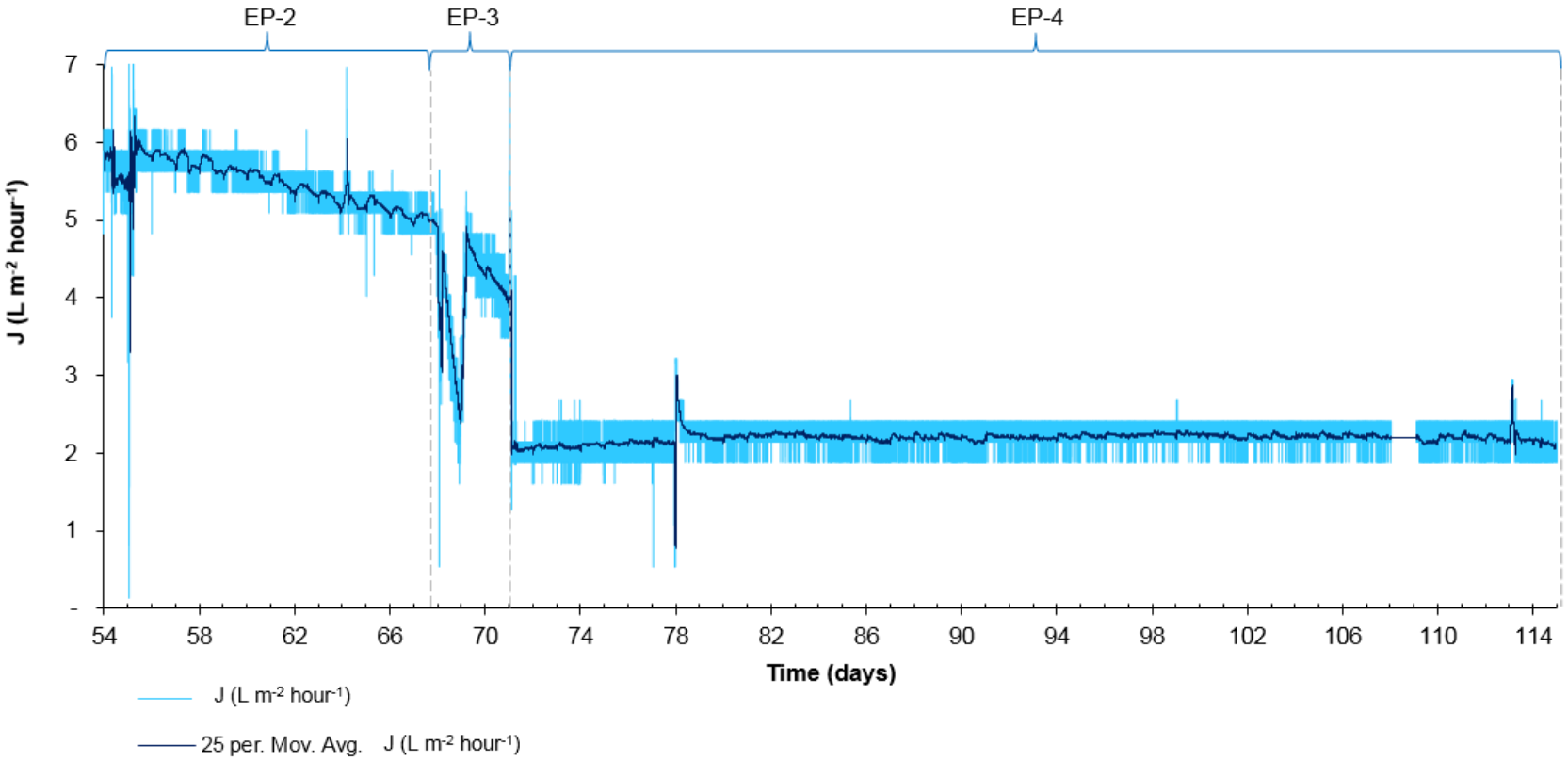

Fig. 4.7. Real time membrane flux from EP-2 to EP-4 – Development and testing of fully gravitational SAnMBR experiment at 36 ^{o}C

The MLSS concentration increased as a result of the increased OLR_V, but only minimally, indicating that the system had sufficient metabolic capacity to be able to degrade the additional COD load. As the system was operated without biomass wastage the food-to-mass ratio remained constant, and further increases in COD load would be expected to lead to a proportional increase in MLSS. The system is further complicated by the effect of endogenous decay, with long operating periods potentially required for the establishment of stable conditions due to the very high MCRT (calculated as 600 days for EP-4).

The MCRT controls the biomass growth rate and in many biological systems this is known to influence the production of extracellular polymeric (EPS) materials, which in turn may affect membrane fouling (Stuckey, 2012). This experiment did not investigate this or other microbiologically mediated factors that may contribute towards membrane fouling. The importance of these and of the parameters controlling them has been noted by several authors (Stuckey, 2012, Huang et al., 2011, Jinsong et al., 2006, Ng et al., 2006), and should be studied in future work.

Within the literature there is a wide variety of reported data for SAnMBRs, all of which have used pumping to maintain a constant flux, so direct comparison with other gravity permeation systems is not possible. The long-term constant flux of 2.2 L m^{-2} $hour^{-1}$ is, however, comparable to a constant flux of 1.25 L m^{-2} $hour^{-1}$ reported by Hu and Stuckey (2006) at a TMP of 2.5 kPa. For higher operational fluxes of 10 and 15 L m^{-2} $hour^{-1}$, they obtained TMPs of 29 and 40 kPa, respectively; many times higher than the maximum TMP of 7.0 kPa employed in this experiment. Furthermore, the MLSS in their study was three times lower (4.1 ± 0.3 g L^{-1}) than the range for sustainable flux during this experiment (12.3 – 14.2 g L^{-1}). Similarly, Huang et al. (2011) reported TMP up to 30 kPa when operating SAnMBRs at different MCRT and membrane fluxes between 5 and 8 L m^{-2} $hour^{-1}$.

In principle the flux induced by a gravitational system should be the same as that for a pumped system when the TMP values are the same and all other conditions are equal. The limitation in a gravitational system is the maximum TMP value that can be induced, and this is dependent on the hydrostatic pressure head which is determined by the engineering design. For example some full-scale Kubota AeMBR use vertically-stacked membrane cassettes to create additional hydrostatic head; this of course is only energetically more favourable where additional head is available in the system upstream of the reactor.

While absolute values of flux are dependent on the membrane cleaning system, the nature of the wastewater substrate, and the characteristics of the biomass, the current results suggest that a gravitational system could be an alternative to pumped systems if additional head is available and measures are developed to incorporate this into the design, as they have been for AeMBRs. Until steady state conditions are established in the system, the influent flow and load will decline as these are regulated by the achievable membrane flux. Once a constant flux is achieved, however, the system becomes self-regulating, avoiding the need to couple permeate pump flow to influent flow: a gravitational system could thus be simpler to operate than a pumped system.

4.2.2.1. Factors influencing membrane flux

A continuous detailed log of membrane flux was achieved by recording effluent weight every minute. This showed (Fig. 4.7) a variation in flux throughout the day with observable oscillations that could be as a result of small environmental changes. The effect of temperature is shown in Fig. 4.8a where it can be seen that there is a small increase in reactor temperature at the beginning of each day as a result of replenishing the feedstock; with the associated lag in cooling, and also an increase in laboratory ambient temperature during the day. The 25-point moving average for flux mirrors this change in temperature. Temperature is known to affect the viscosity of the substrate, and may also affect the headspace partial pressure and therefore the hydrostatic pressure head on the membrane.

Previous research on gravity permeation AeMBRs has shown that temperature has a significant effect on the flux in long-term operation (Zheng and Liu, 2005). On the other hand, the synthetic substrate is also subject to some degradation in the feed storage tank during the day, at a rate dependent on the ambient temperature. Fig. 4.7 shows in more detail how the membrane flux increased at the beginning the day, when the synthetic wastewater has been recently prepared and the room temperature typically starts to rise. It is therefore clear that changes over time in substrate properties and other parameters must be taken into account when membrane performance is evaluated to avoid misinterpretation of fouling phenomena and membrane flux. It is worth noting that this is also an example of how the developed gravitational system used allows detailed observation of very small changes in membrane flux and system behaviour over both short and long timescales.

The effectiveness of biogas scouring in membrane cleaning can be seen in Fig. 4.8b when the biogas recirculation diaphragm pump failed on day 78. This resulted in an immediate and severe flux reduction. Once the pump was replaced there was a rapid increase in membrane flux to a value which was initially higher than that prior to failure, then rapidly returned to the constant flux previously achieved. The membrane fouling as a result of this failure was therefore not deeply embedded, and did not result in critical flux conditions.

The general condition of the membrane was assessed visually at the end of the experiment. Fig. 4.9 shows the membrane before and after rinsing with running water: it can be seen that severe fouling occurred only at the centre of the membrane sheet, and was the same on both sides of the membrane cartridge. It is clear that the gas scouring could be improved by better bubble distribution, and this in turn would change the constant flux rate achievable.

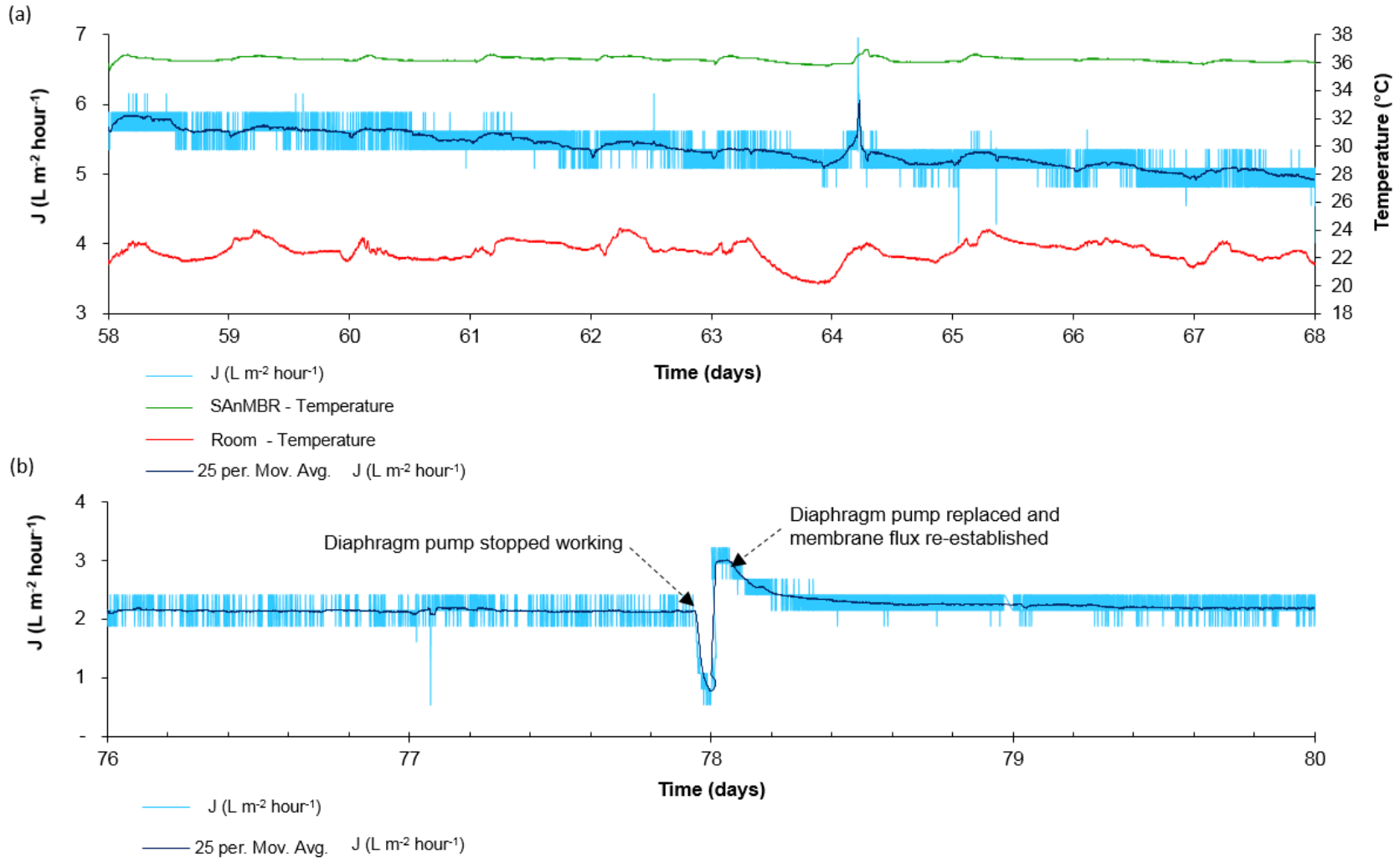

Fig. 4.8. (a) Effect of temperature variations on membrane flux, EP-2 (day 58-68), (b) Effect of failure of biogas recirculation pump on membrane flux, EP-4 (days 76-80) – Development and testing of fully gravitational SAnMBR experiment at 36 ^{o}C

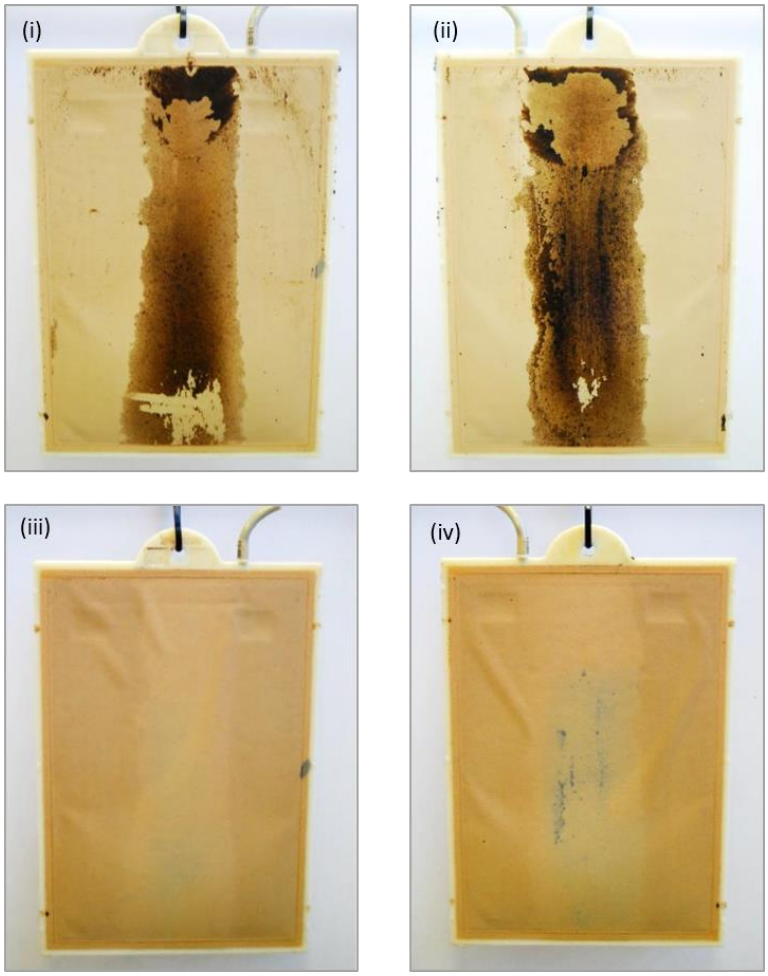

Fig. 4.9. Membrane fouling at the end of experimental run before and after rinsing with running tap water and gentle manual wiping – Development and testing of fully gravitational SAnMBR experiment at 36 ^{o}C: (i) membrane front – before rinse, (ii) membrane back – before rinse, (iii) membrane front – after rinse, (iv) membrane back – after rinse

Restricting the flow of effluent from the lumen by inserting an in-line valve failed to provide control over the membrane flux as desired, but it did show an interesting result (Fig. 4.10a). It was anticipated that closing the valve would give a lower and stable permeate flow due to a reduction in TMP caused by a local head loss in the outlet rather than due to membrane fouling. What was observed was a continuous fall in permeate flow, the rate of which depended on the degree of valve closure, and which did not stabilise over periods of a day or more. When the valve was opened the permeate flow returned to its previous value, indicating that the restriction had not increased the degree of membrane fouling. The loss of flux was attributed to the accumulation of dissolved biogas inside the membrane, as whenever the valve was re-opened a considerable amount of biogas was released through the permeate line.

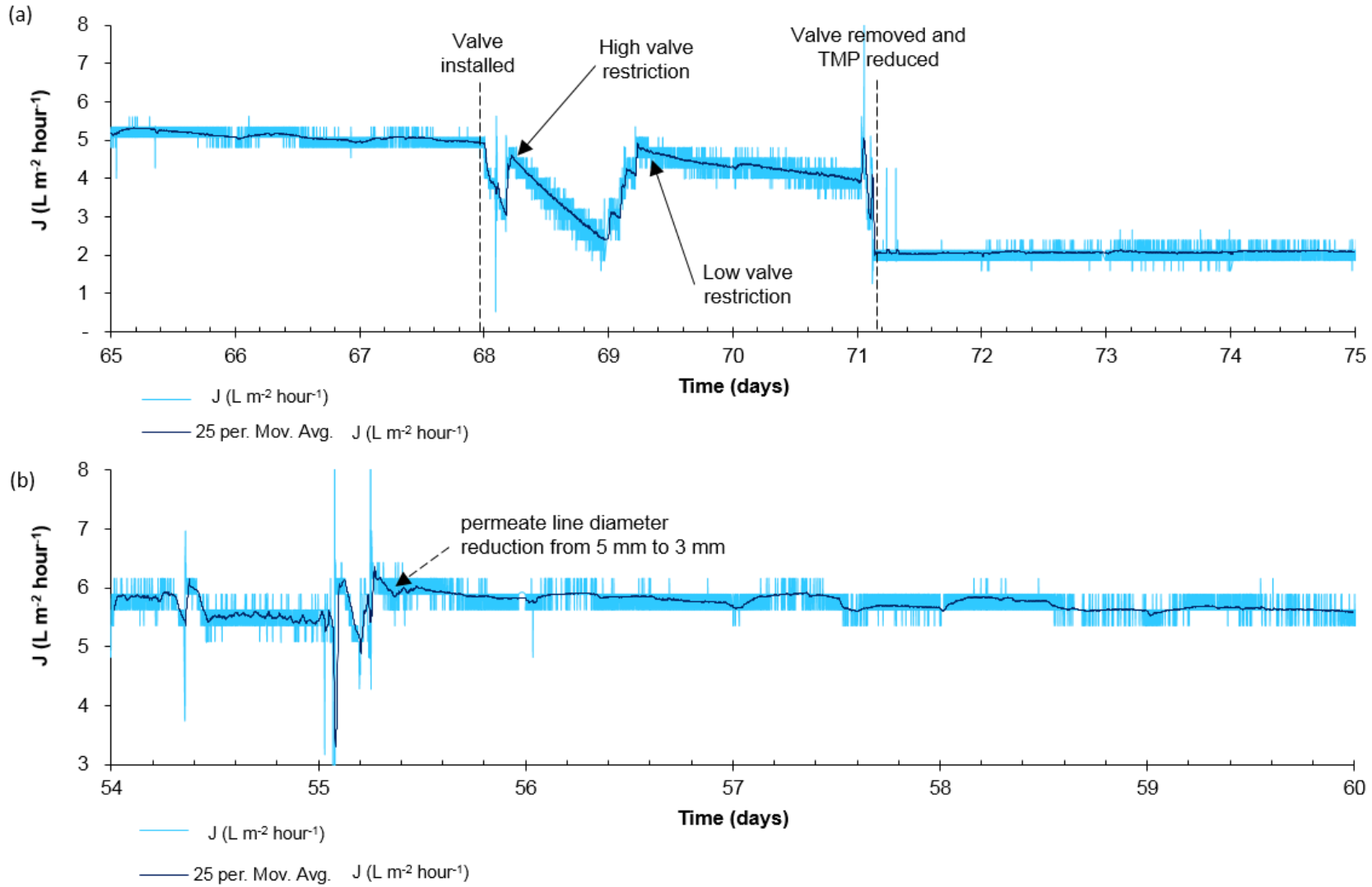

Fig. 4.10 (a) Effect of valve restriction on membrane flux, EP-3 (days 68-71), (b) Effect of biogas accumulation inside the cartridge on membrane flux – Development and testing of fully gravitational SAnMBR experiment at 36 ^{o}C

Throughout the trial occasional gas bubbles could be seen in the membrane permeate line (Fig. 4.11), most probably caused when dissolved biogas enters the membrane cartridge and desorbs inside changing into the gaseous phase. During start-up and EP-1 the membrane flux was high enough to carry these bubbles out of the lumen with the effluent stream. As the flux decreased there was an increasing tendency for biogas to accumulate inside the cartridge, interfering with the siphon effect of the permeate line and drastically reducing the flow over short periods, until the volume accumulated was sufficient to eject it from the system; at which point the flux returned to the previous value and biogas accumulation started again. This effect can be seen in Fig. 4.10b as a series of peaks and troughs in the membrane flux. The solution to the problem was to reduce the effluent permeate line diameter from 5 mm to 3 mm: this increased the velocity of flow which effectively dragged the bubbles out with the permeate. It is possible, however, that understanding how the dissolved biogas desorbs inside the membrane cartridge may eventually lead to practical methods for effective recovery.

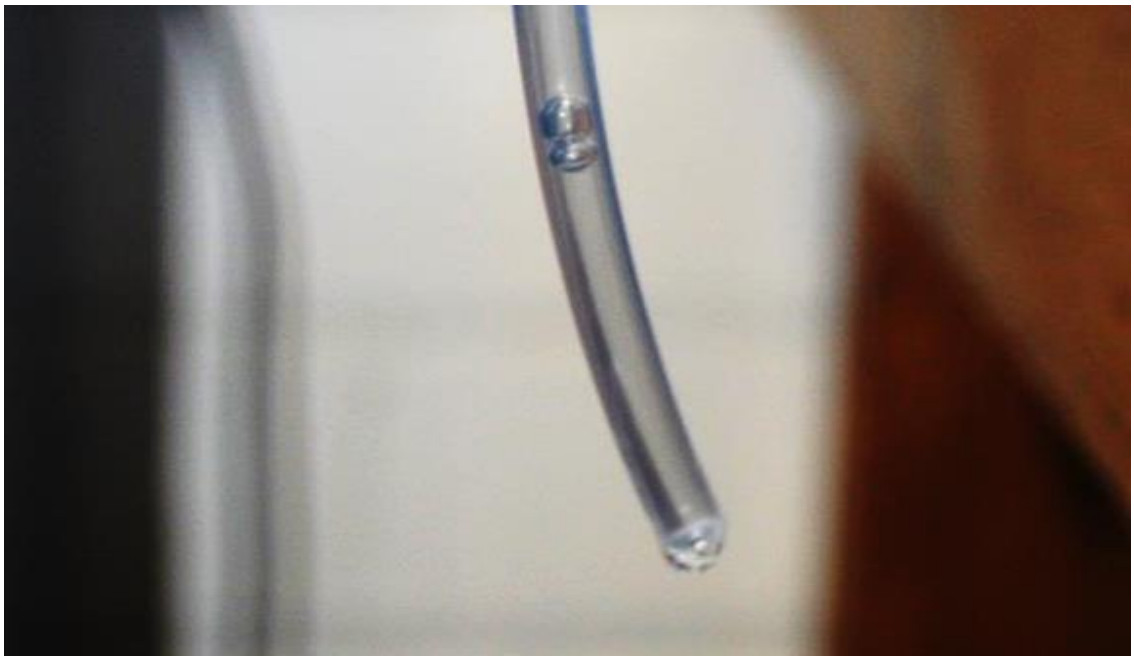

Fig. 4.11. Example of a biogas bubble in the permeate line – Development and testing of fully gravitational SAnMBR experiment at 36 ^{o}C

The problem of gas liquid phase separation in the lumen highlights one of the issues associated with dissolved methane in the effluent, and also to localised biogas generation on and within the membrane itself, as discussed by Smith et al. (2012).

Within the context of research and operational control, if the biogas dissolved in the effluent is not considered, the measurements of biogas and thus of SMP will result lower.

As noted in the literature review, dissolved methane can represent a significant loss in methane production and energy potential, as well as a source of fugitive greenhouse emissions (Yeo and Lee, 2013, Smith et al., 2014). While this is also a problem in the operation of a gravitational SAnMBR, this reactor configuration could possibly be engineered to recover dissolved methane as a proportion returns to the gaseous state before leaving the system. More research is therefore required to improve the understanding of the gas bubble phenomenon and exploit any advantages it might offer. Dissolved gases were not measured in this experiment, but the slightly acidic pH of the effluent (Table 4.2) and the low percentage concentration in the biogas suggests a high proportion of the CO_2 was dissolved.

4.3. Conclusions

Although not tested to its full extent, the principle of using a gravitational SAnMBR was established and a constant flux of 2.2 L m^{-2} $hour^{-1}$ was achieved and was maintained over a period of 44 days at a hydrostatic pressure head of 2.3 kPa. The experimental procedure adopted to establish the system could be used to estimate the rate of long-term fouling, and this technique could have future applications in evaluating fouling rates under different head conditions. The experimental system was also sensitive enough to show small transient changes in membrane flux and could thus be a valuable tool to study the effect of phenomena such as temperature change or changes in mixed liquor characteristics on membrane fouling. In practical operational terms the gravitational system may be simpler to operate than pumped permeation, as once a sustainable flux is achieved the inlet and outlet flows are self-compensating. The major disadvantage was the dissolution of biogas in the membrane lumen, but this could also potentially be turned to advantage if the effluent-entrained biogas could be captured rather than escaping: this is more easily facilitated if it has come out of solution rather than remaining dissolved. The reactor acclimated well to the substrate

used, although the initial choice of influent COD concentration was, with hindsight, too low for the constant flux finally achieved. The results showed that a much greater loading could be applied whilst maintaining operational performance, as indicated by specific methane yield, COD removal, and volumetric biogas production.

To bring the gravitational SAnMBR to a practical reality a greater understanding is required of the operational factors likely to change the mixed liquor characteristics, especially where these impact on membrane fouling. This developed gravitational configuration proved to be useful in studying this as it can accurately quantify very small changes in membrane flux whist operating at a constant TMP. This configuration was, therefore, employed in the main experiments of the rest of this research to assess the impacts of MCRT on membrane flux as a direct indicator of membrane fouling, mixed liquor characteristics and overall reactor performance, presented in Sections 5.1 and 5.2.

5. RESULTS – EFFECT OF MCRT ON SANMBR OPERATING AT 36 ^{O}C

Objective: Assess the long-term effect of MCRT on membrane flux, mixed liquor characteristics and overall performance of SAnMBRs treating low-to-intermediate synthetic wastewater at 36 ^{o}C.

5.1. Method summary

Two fully gravitational SAnMBRs designated A and B were operated at 36 ^{o}C for 245 days, including a start-up period and four experimental phases (EP). The TMP was maintained at 2.2 kPa throughout the four EP, and the MCRT in one reactor was progressively reduced as shown in Table 5.1, while the membrane flux varied relative to the degree of fouling. The experimental set-up of this trial is shown in Fig. 5.1 and Fig. 5.2.

Table 5.1. Start-up and experimental phases – MCRT effect experiment at 36 ^{o}C

Phase	**Duration** (days)	**Objective**	**Reactor**	**TMP** (kPa)	**MCRT** (days)
Start-up	25	Acclimate the digestate to the reactor and substrate, and pre-foul the membrane for the TMP reduction	A	6.0	96
			B	6.0	96
EP-1	25	Couple both reactors to establish a common baseline for the next stages	A	2.2	96
			B	2.2	96
EP-2	95	Evaluation of MCRT effect on membrane and reactor performance, mixed liquor characteristics and microbial growth	A	2.2	40
			B	2.2	96
EP-3	55	As above	A	2.2	25
			B	2.2	96
EP-4	45	As above	A	2.2	15
			B	2.2	96

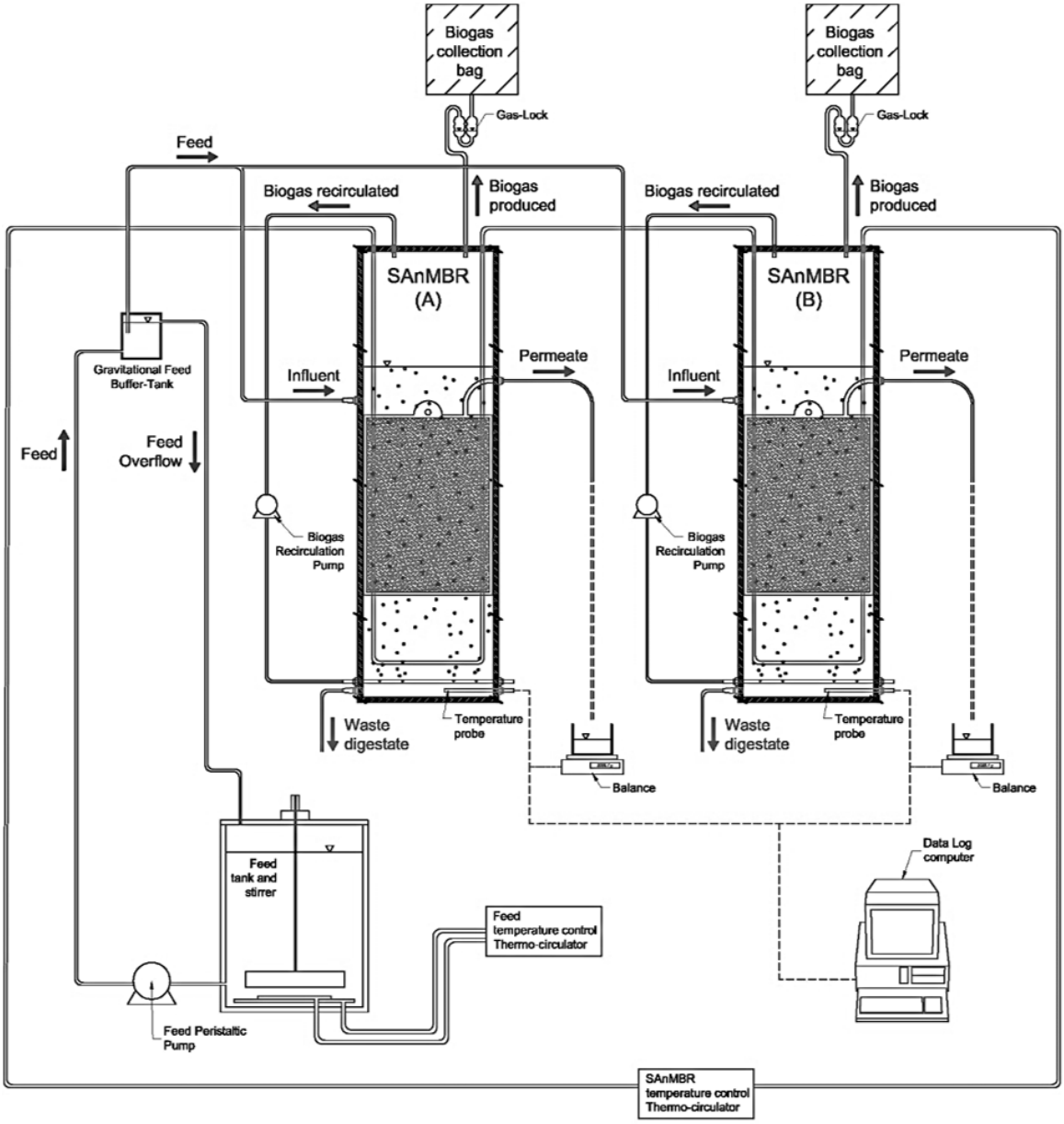

Fig. 5.1. Experimental set-up schematic diagram – MCRT effect experiment at 36 ^{o}C: biogas collection bags, biogas recirculation pumps, constant head device, effluent collection containers, effluent head-difference device, fermentation gas-lock, flux recording balance, SAnMBRs, stirred feed storage tank, and thermo-circulator

The biochemical characteristics and stability of the reactors were assessed based on biogas production, biogas composition, COD conversion, specific methane production, pH, MLSS and MLVSS. The reported SMP, SMP_{added} and SMP_{MLSS} values include the methane dissolved in the effluent as well as that produced in the headspace. This is to improve comparability between the reactors, since if the two reactors have different membrane fluxes the fraction of methane produced leaving the system dissolved in the effluent will be different.

Fig. 5.2. Experimental set-up schematic picture – MCRT effect experiment at 36 ^{o}C: biogas collection bags, biogas recirculation pumps, constant head device, effluent collection containers, effluent head-difference device, fermentation gas-lock, flux recording balance, SAnMBRs, stirred feed storage tank, and thermo-circulator

The dissolved methane in the effluent was estimated using Henry's Law as described in Section 3.2.2.3.1, with the saturation concentration at 36 ^{o}C taken as 22.9 mL CH_4 L^{-1}. This value was checked by experimental measurement, as described in Section 3.2.2.3.2. Measurements of observed biomass yield at each MCRT were made along with physical characterisation of each mixed liquor using CST tests. The study also constructed COD mass balances (Section 3.3.9) taking into account carbon converted into new biomass and that as dissolved methane in the effluent. Both reactors were inoculated with digestate from Millbrook WWTP (Section 3.1.4). This was diluted to 50% with tap water, and after filling of the reactor the headspace was purged with nitrogen. The reactors were fed with synthetic wastewater (Section 3.1.2), prepared fresh each day and diluted to an average COD concentration of 890 mg L^{-1} during the main experimental period. At the beginning of the experimental run the synthetic wastewater feed was stored at 10 ^{o}C but on day 11 the storage temperature was modified to 20 ^{o}C, as explained below.

5.2. Results and discussion – MCRT effect experiment at 36 ^{o}C

5.2.1. Operational performance

The performance of the two reactors over the 245-day experimental period is shown in Fig. 5.3, and summary results are given in Table 5.2. Key parameters are discussed below in relation to operational changes in each of the four experimental phases.

5.2.1.1. Start-up

Both reactors were started with a TMP of 6.0 kPa and daily biomass wastage aimed to give an MCRT of 96 days. The membrane flux in both Reactor A and B was initially very high at 17.5 and 19.2 L m^{-2} $hour^{-1}$ respectively, but decreased and converged throughout the start-up period resulting in fluxes of 11.0 and 11.3 L m^{-2} $hour^{-1}$ at the end of start-up (Fig. 5.3). Because of the high initial flux, a more dilute feed was used during start-up with an average COD of 427 ± 27 mg COD L^{-1}. As a consequence of the declining flux the initial OLR_V dropped from 2.10 and 2.31 g COD L^{-1} day^{-1} to 1.35 and 1.38 g COD L^{-1} day^{-1} in Reactor A and B respectively, and the initial HRT increased from 5.0 and 4.5 hours to 7.7 and 7.6 hours. The initial MLSS of 17.3 g L^{-1} showed some variation, but by the end fall to 16.2 g L^{-1} in Reactor A and 16.9 g L^{-1} in Reactor B.

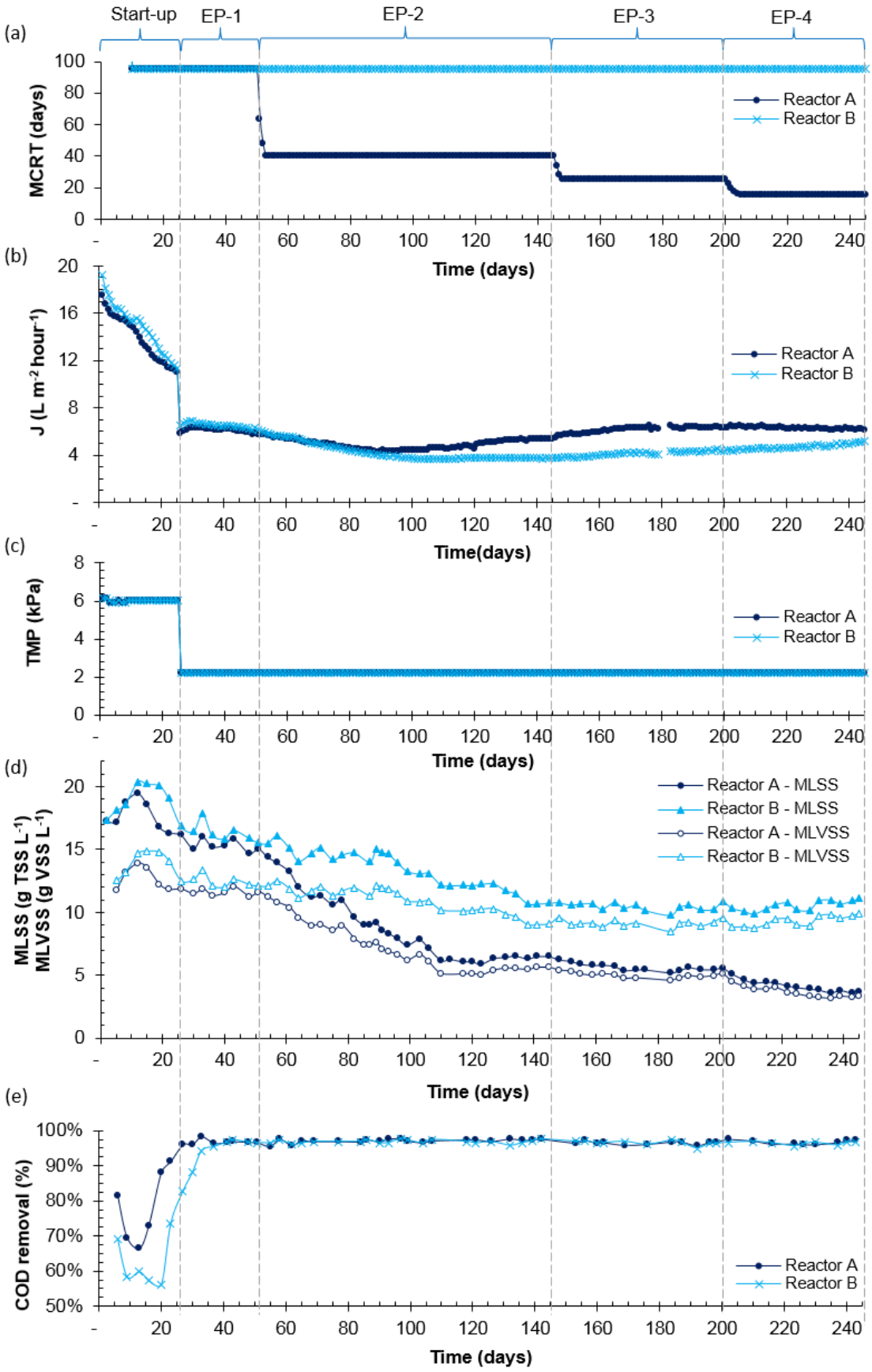

Fig. 5.3. Operational performance during experimental period – MCRT effect experiment at 36 oC: (a) MCRT, (b) Daily average membrane flux, (c) TMP (d) MLSS concentration, (e) COD removal rate

Table 5.2. Experimental results summary table – MCRT effect experiment at 36 ^{o}C: MCRT, TMP, daily average membrane flux, OLR_v, HRT, feed COD, effluent COD, COD removal rate, CH_4 in biogas, SMP, MLSS, MLVSS, CST and pH.

Parameter	Reactor A				Reactor B			
	EP-1	**EP-2**	**EP-3**	**EP-4**	**EP-1**	**EP-2**	**EP-3**	**EP-4**
MCRT (days)	96	40	25	15	96	96	96	96
TMP (kPa)	2.2	2.2	2.2	2.2	2.2	2.2	2.2	2.2
Membrane flux (J)* ($L\ m^{-2}\ hour^{-1}$)	6.2 ± 0.2	5.8 → 4.3 → 5.4	5.5 → 6.3	6.3 ± 0.1	6.5 ± 0.2	6.1 → 3.7	3.8 → 4.3	4.4 → 5.1
OLR_v ($g\ COD\ L^{-1}\ day^{-1}$)	1.56 ± 0.03	1.43 → 1.07 → 1.34	1.58 ± 0.07	1.67 ± 0.02	1.67 ± 0.18	1.51 → 0.90 → 0.93	1.05 ± 0.05	1.15 → 1.33
HRT (hours)	14.0 ± 0.4	14.8 → 20.0 → 15.9	13.9 ± 0.5	13.6 ± 0.2	13.1 ± 0.4	14.0 → 23.5 → 22.8	22.6 → 19.6	19.3→ 16.6
Feed COD ($mg\ L^{-1}$)	901 ± 19	872 ± 33	898 ± 20	911 ± 19	901 ± 19	872 ± 33	898 ± 20	911 ± 19
Effluent COD ($mg\ L^{-1}$)	29 ± 6	25 ± 5	31 ± 4	31 ± 5	107 → 31	28 ± 5	32 ± 5	33 ± 3
COD removal rate (%)	97% ± 1%	97% ± 1%	97% ± 1%	97% ± 1%	83% → 97%	97% ± 1%	96% ± 1%	96% ± 1%
CH_4 in biogas** (%)	84% ± 1%	84% ± 1%	85% ± 1%	85% ± 1%	84% ± 1%	84% ± 1%	84% ± 1%	84% ± 1%
SMP*** ($L\ CH_4\ g^{-1}$ COD removed)	0.30 ± 0.02	0.32 ± 0.01	0.27 ± 0.02	0.27 ± 0.01	0.30 ± 0.01	0.33 ± 0.03	0.30 ± 0.02	0.29 ± 0.01
MLSS ($g\ L^{-1}$)	16.2 → 14.7	15.1 → 6.2 → 6.5	5.5 ± 0.1	5.6 → 3.6 → 3.7	16.9 → 17.9 → 15.9	15.6 → 10.8	10.5 ± 0.3	10.9 → 11.2
MLVSS ($g\ L^{-1}$)	11.8 → 11.3	11.6 → 5.6	5.0 ± 0.3	5.1 → 3.3 → 3.4	12.5 → 13.3 → 12.2	12.1 → 9.1	9.1 ± 0.3	9.5 → 9.9
CST (seconds)	509 → 761	768 → 798 → 338	312 → 34	33 → 23	555 → 745	778 → 1211 → 952	1012 → 824	810 → 760
pH	6.9 ± 0.1	6.9 ± 0.1	7.0 ± 0.1	6.9 ± 0.0	6.9 ± 0.1	6.9 ± 0.1	6.9 ± 0.1	6.9 ± 0.1

(→) Variable trend: initial → middle → final; (±) Stable performance: One standard deviation to show the spread of the data from the average value under stable performance); (*) Daily average; (**) Normalised to total biogas content in sample (i.e. neglecting air introduced dissolved through feed); (***) Takes into account the methane dissolved in the effluent

The first measurement of COD removal rate made on day 6 showed 82% removal in Reactor A and 69% in Reactor B, although these values were not reflected in biogas production which was low in both reactors. The reactor headspaces were found to contain a high proportion of nitrogen; this was attributed to equilibration of dissolved atmospheric gases in the influent, which was maintained at 10 ^{o}C and continuously 'aerated' through the constant head feed system before being fed into the reactors at a high dilution rate (Fig. 5.4). The feeding set-up may thus have led to some respiratory oxidation of COD, and the presence of residual oxygen may possibly have hindered the start-up. Keeping the test substrate at low temperatures reduces the rate of degradation and thus improves control of an experiment; however, the lower the temperature the greater the input of air dissolved in the influent. To overcome this problem the feed temperature was raised to 20 ºC on day 11 to reduce atmospheric gas solubility, at the expense of slightly greater COD degradation during the daily feeding period. From this time onward a significant increase in biogas production was observed, with no more than 10% (v/v) atmospheric gases present in the headspace. Coupled with the slightly longer HRT, this resulted in COD removal rates of 96% in Reactor A and 83% in Reactor B. Given the direct effect of temperature on the dissolution of gases in liquids, it is very important to consider the effect that the feed temperature has on the system particularly during the start-up process.

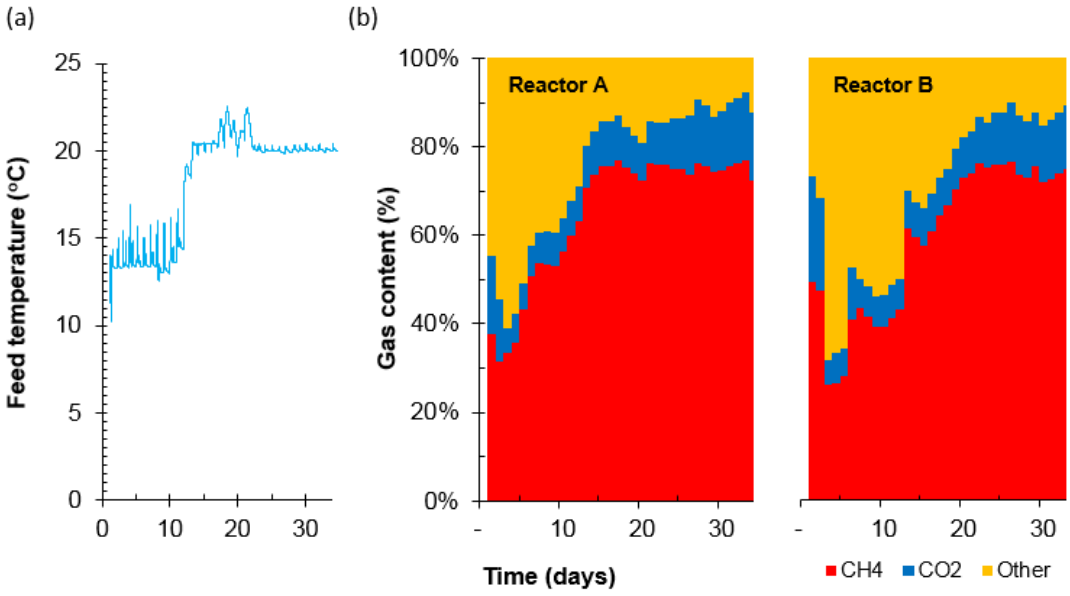

Fig. 5.4 Start-up performance – MCRT effect experiment at 36 ^{o}C: (a) Feed temperature, (b) biogas composition in Reactor A and B

5.2.1.2. Membrane flux response to MCRT: observed changes in MLSS, HRT and OLR_V

EP-1. The TMP was deliberately reduced from 6.0 to 2.2 kPa at the beginning of this phase to establish a more consistent flow regime by stabilising the membrane flux around a target value of 6 L m^{-2} $hour^{-1}$ (Fig. 5.3). This was successful: the flux in both reactors stabilised almost immediately at around 6.1 and 6.6 L m^{-2} $hour^{-1}$ and at the end of this phase had only dropped to 5.8 L m^{-2} $hour^{-1}$ and 6.1 L m^{-2} $hour^{-1}$ for Reactors A and B, respectively. The overall effect was an almost constant OLR_V of 1.56 ± 0.03 g COD L^{-1} day^{-1} for Reactor A and 1.67 ± 0.18 g COD L^{-1} day^{-1} for Reactor B, with correspondingly stable HRT of 14.0 and 13.1 hours. Operation of both reactors at an MCRT of 96 days continued and by the end of this phase the MLSS concentration had fallen to 15.1 and 15.6 g L^{-1} in Reactor A and B respectively.

EP-2. Both reactors were kept at a TMP of 2.2 kPa. MCRT in Reactor A was reduced to 40 days while Reactor B remained at 96 days. Despite the difference in MCRT both reactors maintained a similar membrane flux during the first 30 days of this phase (Fig. 5.3), although a gradual decline was seen in both, resulting in fluxes around day 90 of 4.5 and 4.2 L m^{-2} $hour^{-1}$ in Reactors A and B respectively. After this the flux rates diverged, with Reactor B falling further and then maintaining an almost constant flux of 3.7 ± 0.1 L m^{-2} $hour^{-1}$, whilst the flux in Reactor A gradually increased to 5.4 L m^{-2} $hour^{-1}$ around day 130 and remained at this value until the end of EP-2. The changes in flux resulted first in an increase in HRT in both reactors, then a reduction in Reactor A to 15.9 hours and a further increase to 22.8 hours in Reactor B. As a result the OLR_V in Reactor A initially fell to 1.07 g COD L^{-1} day^{-1} and then rose to 1.34 g COD L^{-1} day^{-1} by the end of EP-2; while in Reactor B OLR_V fell from 1.51 and stabilised at around 0.93 g COD L^{-1} day^{-1}. MLSS concentrations also reflected changes in MCRT and OLR_V, with Reactor A stabilising at around 6.3 ± 0.2 g L^{-1}, while the fall in MLSS in Reactor B, which was maintained at a constant MCRT, simply reflected the decreasing organic load applied.

EP-3. A TMP of 2.2 kPa was maintained in both reactors. MCRT in Reactor A was reduced to 25 days and in Reactor B remained at 96 days. This resulted in an initial

increase of the membrane flux in Reactor A from 5.5 L m^{-2} $hour^{-1}$ (day 145) to 6.3 L m^{-2} $hour^{-1}$ (day 169), after which it remained constant at 6.3 ± 0.1 L m^{-2} $hour^{-1}$. The flux in Reactor B showed a slight increase during this phase, with a final value of 4.3 L m^{-2} $hour^{-1}$ (Fig. 5.3). Changes in HRT and OLR_V corresponded to the changes in flux, while any expected increase in MLSS in response to the increased load in Reactor A was counteracted by the shorter MCRT which results in higher microbial activity. As a consequence the MLSS in Reactor A decreased to 5.5 ± 0.1 g L^{-1} while in Reactor B it remained at 10.5 ± 0.3 g L^{-1}.

Technical difficulties on days 180-2 resulted in feed lines blocking and disruption to feeding. This resulted in some loss of membrane flux over this period, but the flux returned to its previous value when the problem was resolved and the lines cleaned. Due to the long duration of the experiment a mixture of trace elements was added to the feed for a period of three days (day 170-172), at a rate 0.1 mL of each solution described in Section 3.1.2 per liter of diluted synthetic wastewater. No notable change was observed in the overall performance, suggesting that the limiting trace elements were still available in the mixed liquor despite the overall turnaround of biomass at the MCRTs being evaluated.

EP-4. Both reactors remained at a TMP of 2.2 kPa. MCRT was reduced to 15 days in Reactor A and maintained at 96 days in Reactor B. Reactor A showed no further increase in membrane flux, which remained constant around 6.3 ± 0.1 L m^{-2} $hour^{-1}$ (Fig. 5.3). Further improvements in the membrane flux in Reactor B were observed, giving a final flux of 5.1 L m^{-2} $hour^{-1}$ over the last three days of operation. Apart for the flux-related changes to OLR_V and HRT, which were as expected, the MLSS concentration in Reactor A reduced to 3.7 ± 0.1 g L^{-1} during the last 10 days of the experimental run. MLSS in Reactor B increased slightly to 11.2 g L^{-1} reflecting the increased load applied as a result of the slightly higher flux.

5.2.1.3. COD removal rates and COD balance

As can be seen in Fig. 5.3 and Table 5.2, the COD removal rate remained at 96-97% in both reactors throughout EP-1 to EP-4, with the COD balance showing a substantial proportion of this being converted to methane (Fig. 5.5). This result indicates that under the loading and hydraulic conditions applied MCRT does not have any effect on COD removal rates in mesophilic operation. This suggests that similar metabolic activity can be maintained at a MLSS of 3.7 g L^{-1} at a MCRT of 15 days as at a MLSS of 11.2 g L^{-1} at the longer MCRT of 96 days.

The COD balances closed to around 93-94% during the greater part of the experimental phases. Gaps in the balances could be attributed to unaccounted-for biogas leaving the reactors in gaseous form through the permeate as observed in section 4.2.2.1, and to the unaccounted-for fraction corresponding to gaseous and dissolved H_2S. The discrepancy of a higher COD output than the input at the beginning of phase 1 and 2 probably reflects to endogenous decay of the high MLSS inoculum used. This extra methane production from an endogenous source rather than exogenously supplied substrate might be one of the reasons for higher SMP at longer MCRT. Spikes observed in the COD balance after a change of MCRT at the start of a new experimental phase, which then disappear once the reactor responds to the new operational conditions, could also be due to the calculation method as the change in COD stored within the reactor during unsteady state periods is not taken into account.

5.2.1.4. Biogas composition

Apart from during the start-up period discussed above, biogas composition was stable throughout the four experimental phases with 76% CH_4, 14% CO_2 and 10% atmospheric nitrogen (Fig. 5.6).

5.2.1.5. Specific methane production

SMP expressed as L CH_4 g^{-1} COD removed followed a very similar pattern in both reactors despite the considerable differences in MCRT and biomass concentration (Fig. 5.7a and Table 5.2). There was, however, a difference in the SMP value, which tended

to decrease slightly at shorter MCRTs, reaching its lowest value of 0.27 L CH_4 g^{-1} COD removed in Reactor A during EP-3 and 4; whilst during the corresponding period in Reactor B the value remained around 0.3 L CH_4 g^{-1} COD removed.

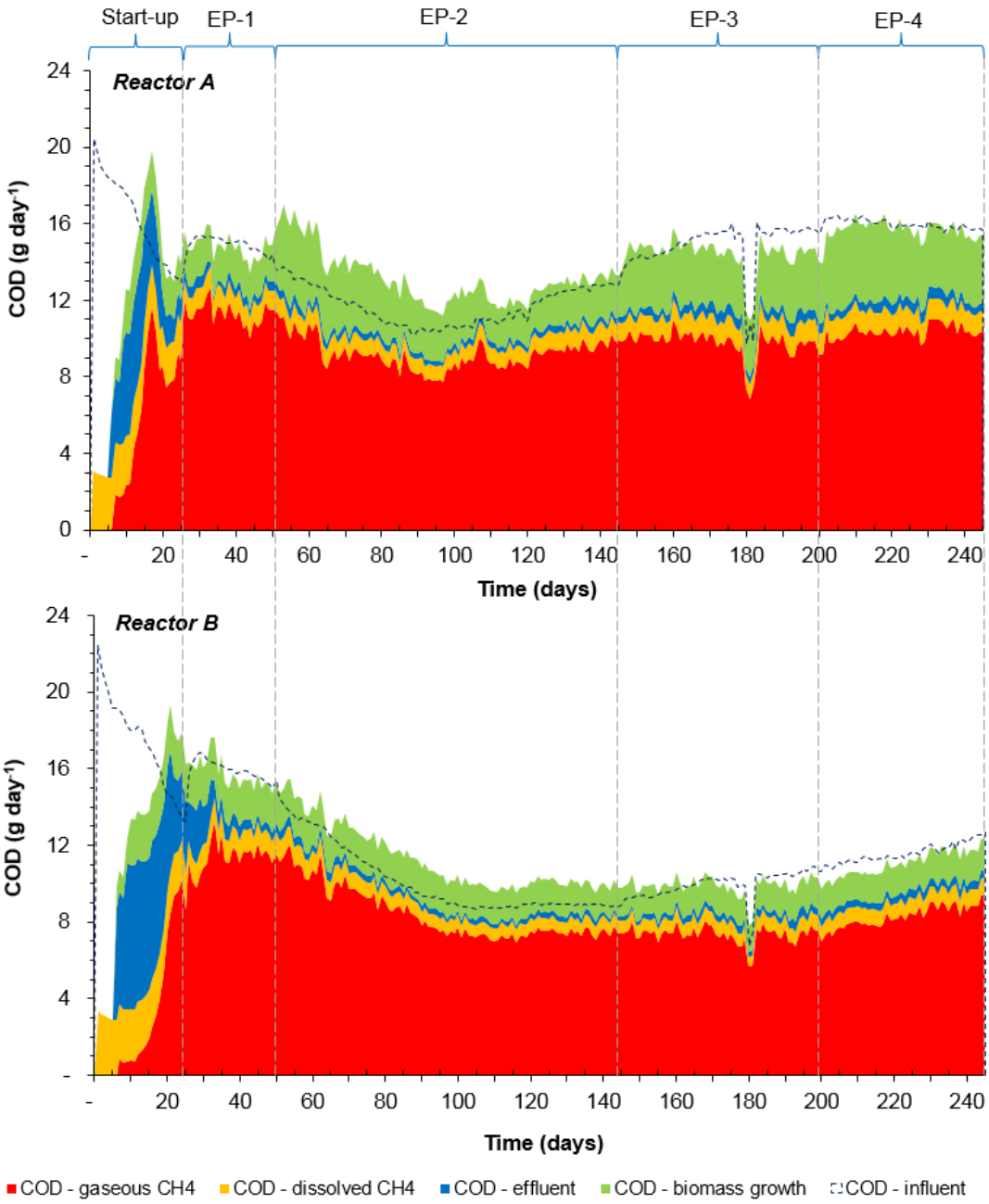

Fig. 5.5. COD balances during experimental period – MCRT effect experiment at 36 °C

The SMP may be lower under short MCRT operation as more carbon is lost from the system through biomass growth and subsequent wastage, and is therefore not available for reduction to methane (see below). The importance of biomass turnover in

interpreting SMP is further highlighted by the COD balance (Fig. 5.5) which shows that the COD output was higher than the input during phase 1 and 2: this discrepancy is probably due to endogenous decay of the high MLSS inoculum used. This extra methane production from an endogenous source rather than exogenously supplied substrate might account for the higher SMP recorded in the early phases of operation (Fig. 5.7a).

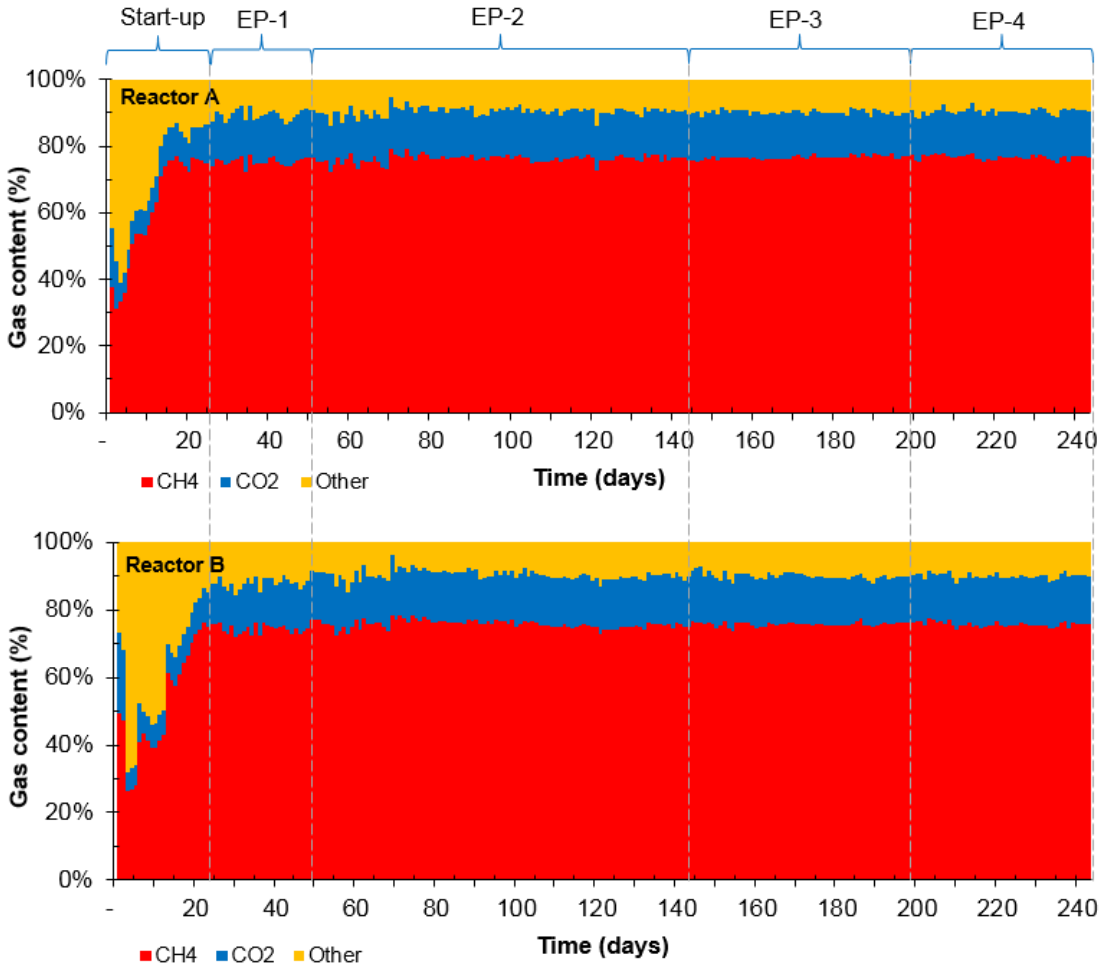

Fig. 5.6. Biogas composition during experimental period – MCRT effect experiment at 36 ^{o}C

The SMP_{added} during this experiment was nearly identical to the SMP, as the COD removal rate in both reactors was almost identical and above 96% (Fig. 5.7b). The Fig. 5.7c shows, however, that SMP_{MLSS} increased with reducing MCRT, clearly indicating a higher metabolic activity which is consistent with kinetic theory (Rittmann and McCarty, 2001).

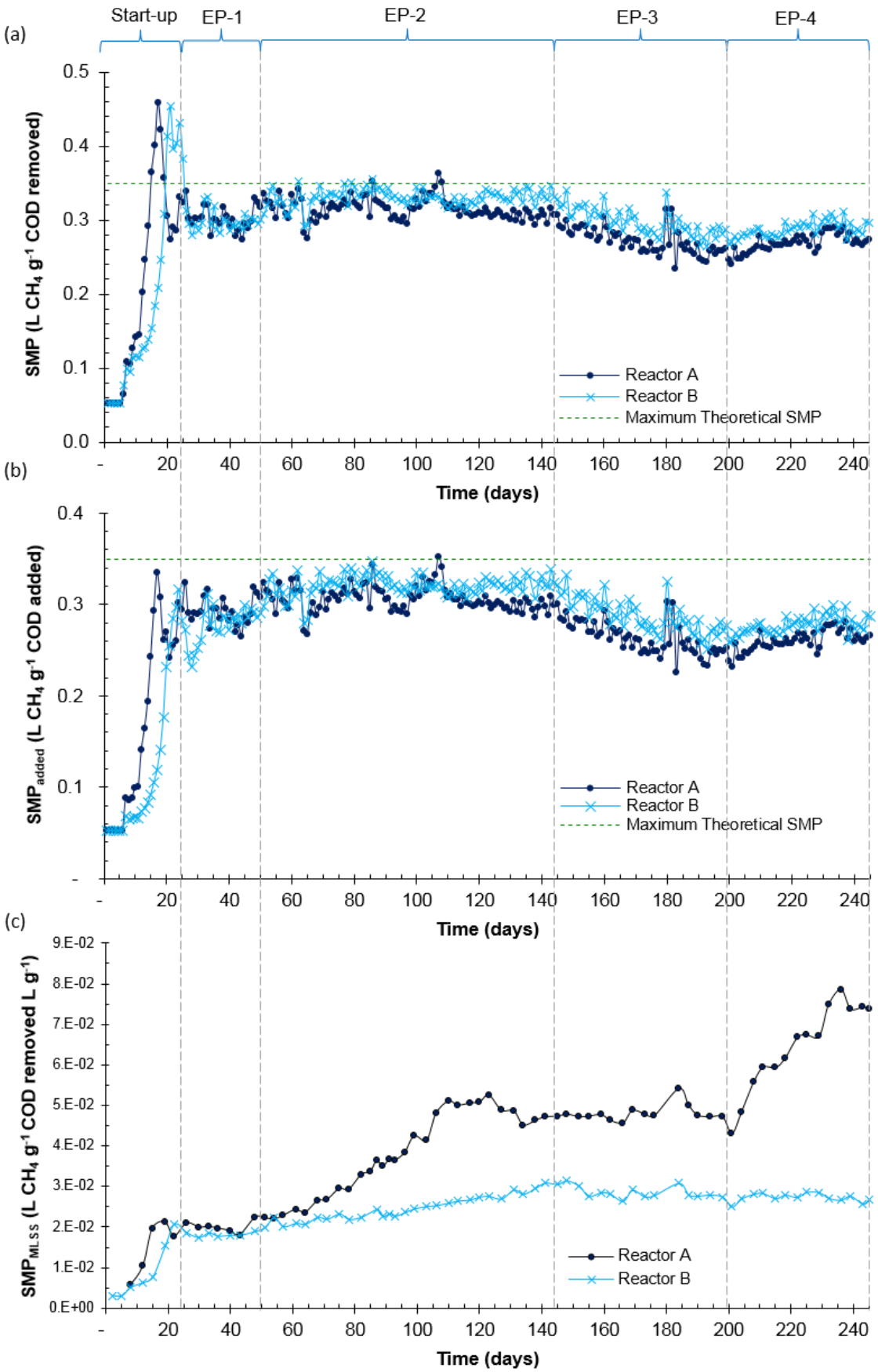

Fig. 5.7. Specific methane production during experimental period – MCRT effect experiment at 36 ^{o}C: (a) SMP, (b) SMP_{added} and (c) SMP_{MLSS}

The SMP_{MLSS} in Reactor A during EP-2 was initially 0.022 L CH_4 g^{-1} COD removed L g^{-1}, but by the end of the phase had reached 0.048 L CH_4 g^{-1} COD removed L g^{-1} while running at an MCRT of 45 day. This value remained fairly steady during EP-3 at 25 days MCRT. During EP-4 however, the SMP_{MLSS} in Reactor A increased to 0.074 L CH_4 g^{-1} COD removed L g^{-1} after the MCRT was further reduced to 15 days. In contrast, the SMP_{MLSS} in Reactor B started EP-2 at 0. L CH_4 g^{-1} COD removed L g^{-1} and gradually increased to 0.028 L CH_4 g^{-1} COD removed L g^{-1}, where it remained stable during EP-3 and EP-4 having been operated at 96 days MCRT throughout.

Huang et al. (2011) also reported that SMP increased with increasing MCRT when treating low-strength synthetic wastewater in SAnMBRs at a temperature between 25-30 ^{o}C, giving average values of 0.13, 0.20 and 0.22 L CH_4 g^{-1} $COD_{removed}$ at 30, 60 and infinite days MCRT, respectively (Table 5.3). Their explanation for this phenomenon was that the longer MCRT would benefit methanogenesis and lead to more biogas generation; this, however, does not account for almost identical COD conversion efficiencies that observed in the current work. SMP calculated from the data presented in a later study by Huang et al. (2013) shows increasing SMP of 0.04, 0.09, 0.09 L CH_4 g^{-1} COD removed at 30, 60 and 90 days MCRT, respectively when fed at an OLR_V of 1.02 g COD L^{-1} day^{-1} (Table 5.3). These SMP values are 3-8 times lower than those in Huang et al. (2011), where synthetic wastewater was used rather than domestic wastewater.

Whilst the SMP values reported in this experiment are generally higher than those reported by Huang et al. (2011) and Huang et al. (2013), it is worth restating that the SMP reported in this experiment includes the theoretical methane loss in the effluent to enhance comparability between reactors. Nonetheless, however, the trend of lower SMP at shorter MCRTs is still consistent between their studies and the outcome of this experiment. Although Huang et al. (2011) did not report normalised SMP_{MLSS}, this parameter can also be calculated from their data. If this is done, the values (Table 5.3) appear to those found here, and suggest that the methane productivity per unit of biomass is higher at long MCRTs and hence low growth rates.

Table 5.3. SMP values reported in studies evaluating the effect of MCRT and HRT on SAnMBRs treating low-strength wastewater

		SMP (L CH4 g^{-1} COD removed)			SMP_{MLSS} (L CH_4 g^{-1} COD removed L g^{-1})			
MCRT (Days)		30	60	∞	30	60	∞	
HRT (hours)	12	0.14	0.17	0.21	0.025*	0.030*	0.032*	Huang et al. (2011)
	10	0.12	0.18	0.22	0.018*	0.020*	0.024*	
	8	0.14	0.24	0.25	0.019*	0.028*	0.024*	
MCRT (Days)		30	60	90	30	60	90	
HRT (hours)	10	0.04*	0.09*	0.09*	0.004*	0.007*	0.007*	Huang et al. (2013)

**Calculated from reported data*

As shown in Fig. 5.8 the fraction of SMP dissolved in the effluent during the experimental phases represented ranged between 8-13%, depending on the membrane flux and COD removal rate; and was generally higher at higher values of membrane flux. Apart from the importance of quantifying the fraction of SMP dissolved in the effluent, this result also shows that if dissolved CH_4 is not taken into account, the apparent SMP for the reactor with the higher membrane flux would have been reduced by up to 5%.

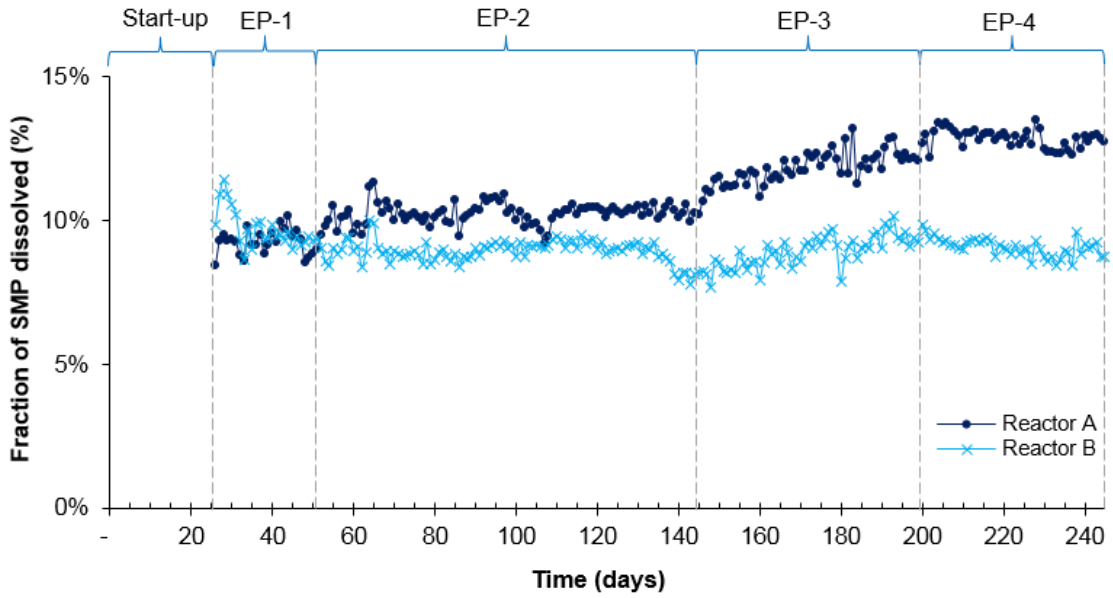

Fig. 5.8. Fraction of SMP corresponding to the CH_4 dissolved in the effluent during experimental period – MCRT effect experiment at 36 ^{o}C

5.2.1.6. pH and operational temperature

The pH remained relatively constant throughout the experimental phases (Fig. 5.9 and Table 5.2). As in the previous experiment addition of $NaHCO_3$ to prevent acidification was not required due to sufficient buffering capacity in the synthetic wastewater.

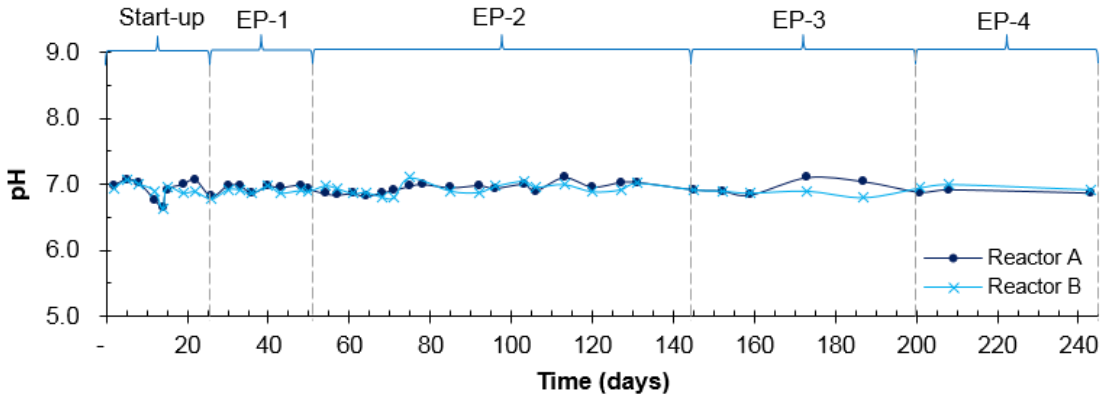

Fig. 5.9. pH during experimental period – MCRT effect experiment at 36 ^{o}C

The operational temperature of both reactors remained relatively constant throughout the experimental phases at 36.0 oC ± 0.5 (Fig. 5.10).

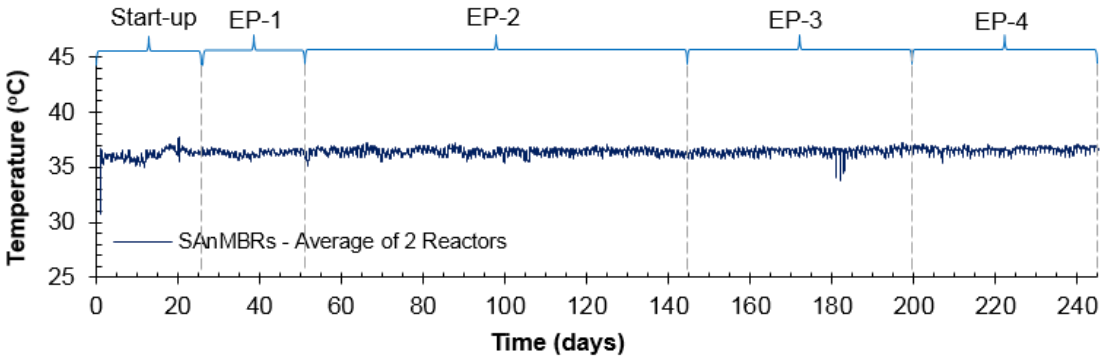

Fig. 5.10 Operational temperature of SAnMBRs during experimental period – MCRT effect experiment at 36 ^{o}C

5.2.2. Membrane performance and fouling phenomena

Throughout the four experimental phases both reactors maintained a sustainable membrane flux as defined by WEF (2012) at a constant TMP, although the value for of this was different at each MCRT, as shown in Fig. 5.3 and reported above. It is clear that MCRT can affect membrane fouling, and that this is not necessarily just as a function of the MLSS concentration. Earlier research has suggest that membrane fouling may result from constituents such as EPS and soluble microbial products, the production of which is related to growth and hence MCRT (Stuckey, 2012). The

relationship between these factors is still unclear, however, and studies in AeMBRs (Jinsong et al., 2006) and anoxic/anaerobic membrane bioreactors (Ahmed *et al.*, 2007) have shown more fouling at shorter MCRTs; whilst in the current SAnMBR study fouling appears worse at longer MCRTs. This result is in agreement with one of the studies by Huang et al. (2011) in which performance decreased with increasing MCRT: this was attributed to higher production of soluble microbial products inducing more pore blocking in the membrane and enhanced surface biofilm/biocake development. Later work by Huang et al. (2013) showed biofouling increased at both long and short MCRTs, with maximum flux rates being achieved at 60 days and an equal COD removal rate of around 85% at all the tested MCRTs. The SMP values calculated from their data (Table 5.3) are extremely low, however, and it is perhaps questionable whether the performance of their SAnMBRs when treating real wastewater is sufficient for realistic evaluation of other parameters such as the influence of the MCRT on the membrane fouling and biomass characteristics. It is evident that more studies to investigate the effect of MCRT on membrane fouling and overall performance in AnMBR are needed, as these so far are scarce; while none of the existing research has previously evaluated this parameter using a gravitationally-mediated constant TMP with continuous measurement of flux rate as reported here.

Physical examination of the membrane cassettes (Fig. 5.11) showed that the shorter MCRTs in Reactor A resulted in lower biocake formation on the membrane surface, when compared to Reactor B. The possibility that this could be due to differences in the performance of the membrane scouring system was discarded, as both reactors performed equally well when operated a the same conditions during start-up and EP-1.

5.2.3. Mixed liquor characteristics

5.2.3.1. Capillarity Suction Time (CST)

The CST is a standard, quick and reliable method to evaluate the filterability of sludge with the result defined in units of time (Sawalha and Scholz, 2007) and a parameter closely related to viscosity (Le-Clech et al., 2006) and thus a good indicator of the mixed liquor physical characteristics, and its relationship with operational parameters

and membrane fouling. Results from the CST test (Fig. 5.12a and Table 5.2) show that MCRT has a very large effect on the ability of the mixed liquor to hold water, with samples at shorter MCRT giving up their water much more readily than those at long MCRT.

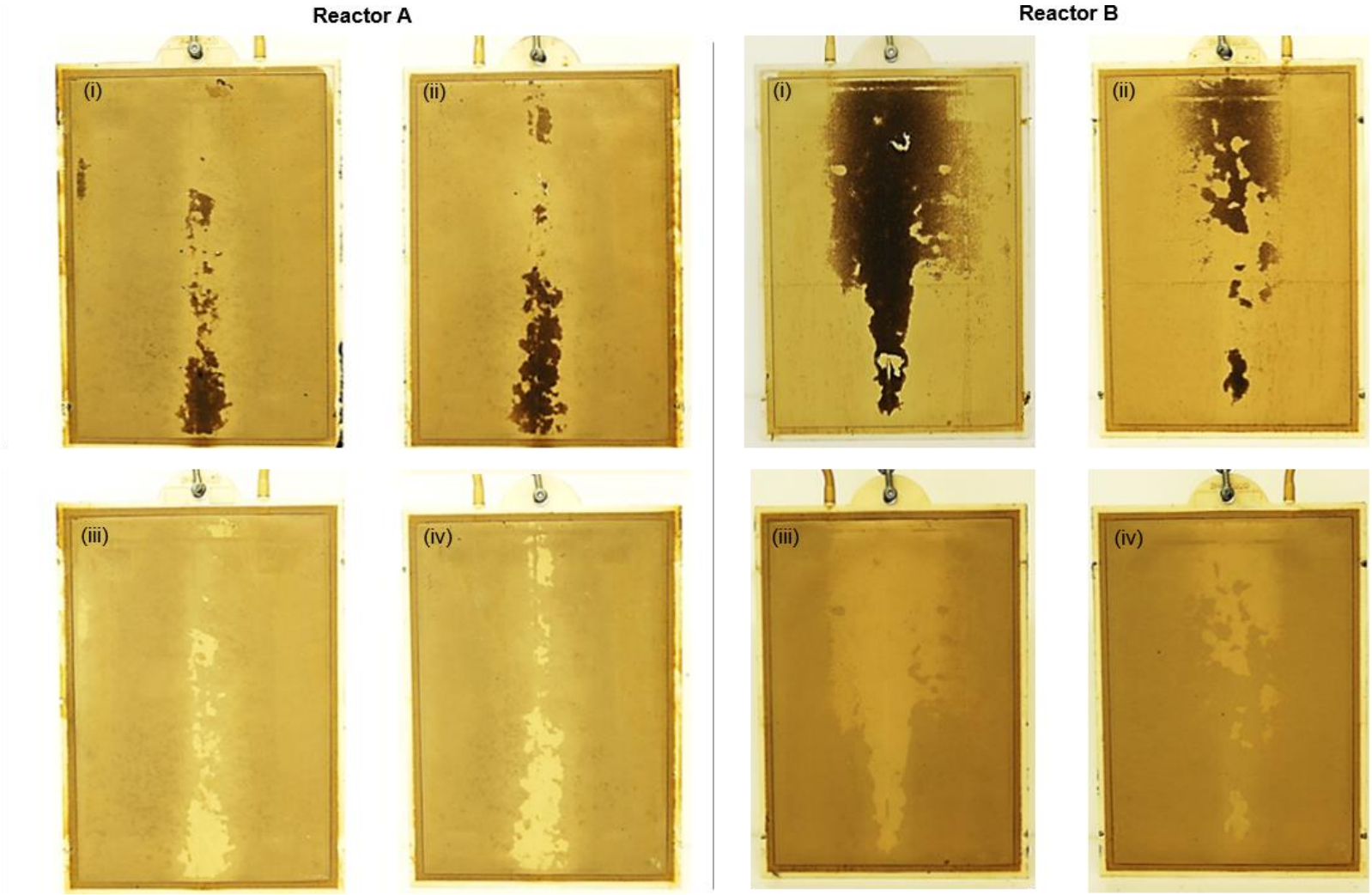

Fig. 5.11 Membrane fouling at the end of experimental run before and after rinsing with running tap water and gentle manual wiping – MCRT effect experiment at 36 ^{o}C: (i) membrane front – before rinse, (ii) membrane back – before rinse, (iii) membrane front – after rinse, (iv) membrane back – after rinse.

During start-up and EP-1 when Reactors A and B were operated as replicates, similar increases in CST time were seen in both reactors. When the MCRT in Reactor A was reduced in EP-2 the CST time also decreased, giving a more than 3-fold difference in CST by the end of this phase. This could not be attributed simply to a change in MLSS concentration as, when normalised against MLSS (CST_{MLSS},Fig. 5.12b), a significant change can be seen from day 100 onwards. This trend of reduction in both CST and CST_{MLSS} continued through EP-3 and EP-4 with CST times of < 25 seconds being achieved at MCRT of 25 and 15 days, compared to an average close to 800 seconds at 96 days MCRT. The CST_{MLSS} results confirm that the MCRT has a considerable effect on the mixed liquor filterability and therefore on membrane fouling, independently of the MLSS concentration.

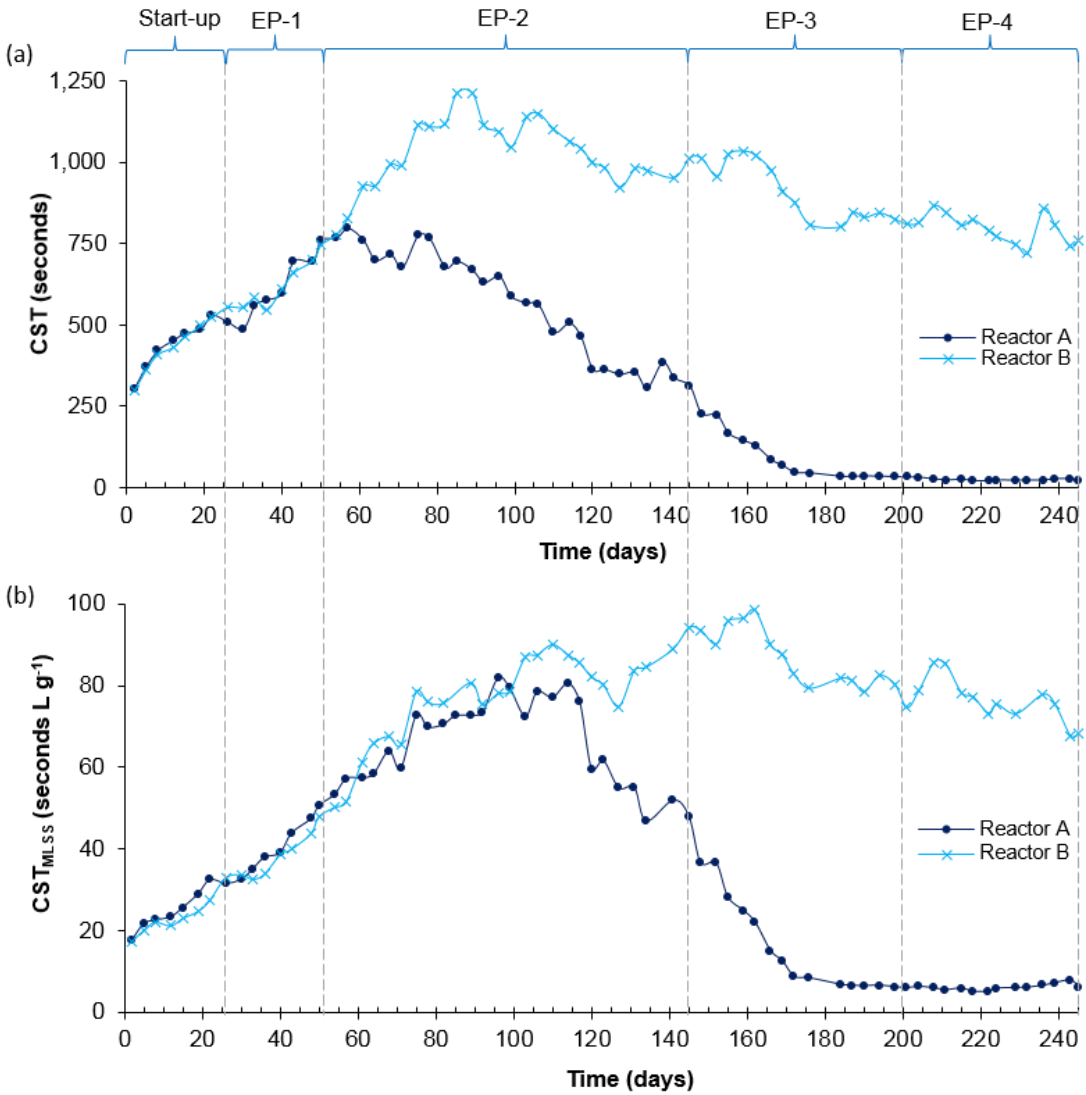

Fig. 5.12. Mixed liquor filterability during experimental period – MCRT effect experiment at 36 ^{o}C: (a) CST; (b) CST_{MLSS}

5.2.3.2. Microbial growth and kinetics

Besides having a major effect on mixed liquor characteristics, manipulation of MCRT controls the growth rate of a microbial population and hence its potential growth yield. This is shown in Fig. 5.13 where it can be seen that the amount of biomass produced during the start-up and EP-1 followed the same trend in both reactors. With each reduction in MCRT in phases EP-2, EP-3 and EP-4 there was a sharp increase in the observed biomass yield at the beginning of each stage, followed by a gradual decrease until a stable value for MLSS was reached: this reflected the adjustment to the new conditions, as changes in biomass stored in the reactor during unsteady state periods were not taken into account in the calculation.

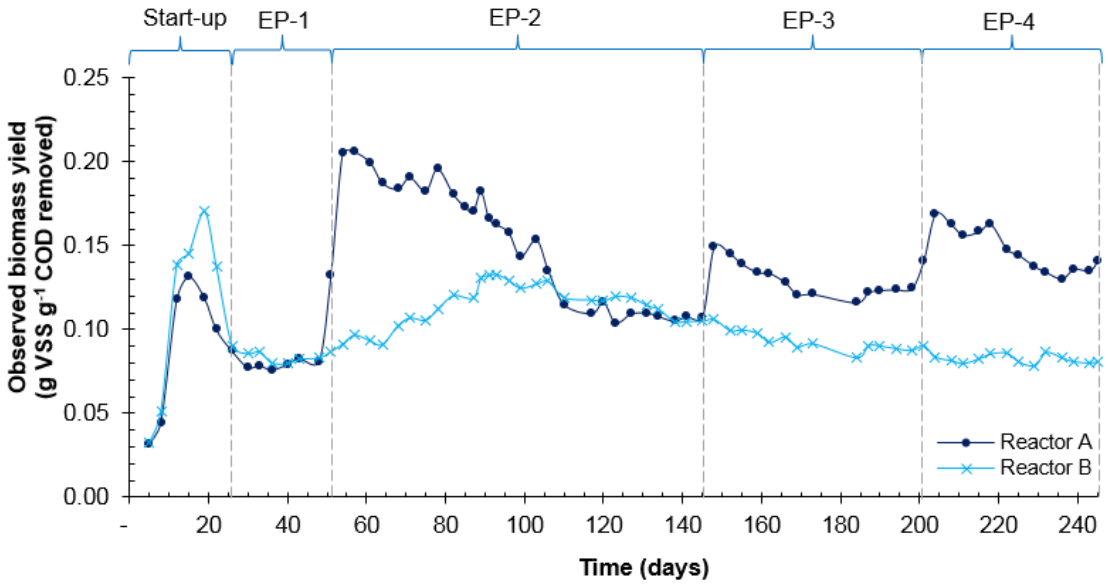

Fig. 5.13. Observed biomass yield during experimental period – MCRT effect experiment at 36 ^{o}C

This stable observed biomass yield at the end of each phase was considered to be the representative value for that MCRT and was equal to: 0.111 ± 0.004 g VSS g^{-1} $COD_{removed}$ for 40-day MCRT; 0.132 ± 0.008 g VSS g^{-1} $COD_{removed}$ for 25-day MCRT; and 0.143 ± 0.006 g VSS g^{-1} $COD_{removed}$ for 15-day MCRT. In contrast, the constant MCRT of 96 days showed a long-term observed biomass yield from day 180 onwards of 0.092 ± 0.009 g VSS g^{-1} $COD_{removed}$. The estimated COD used in observed biomass growth is shown in Fig. 5.14 where it can be seen that the fraction of the total COD input used for biomass production when stable performance is achieved is greater at shorter MCRTs.

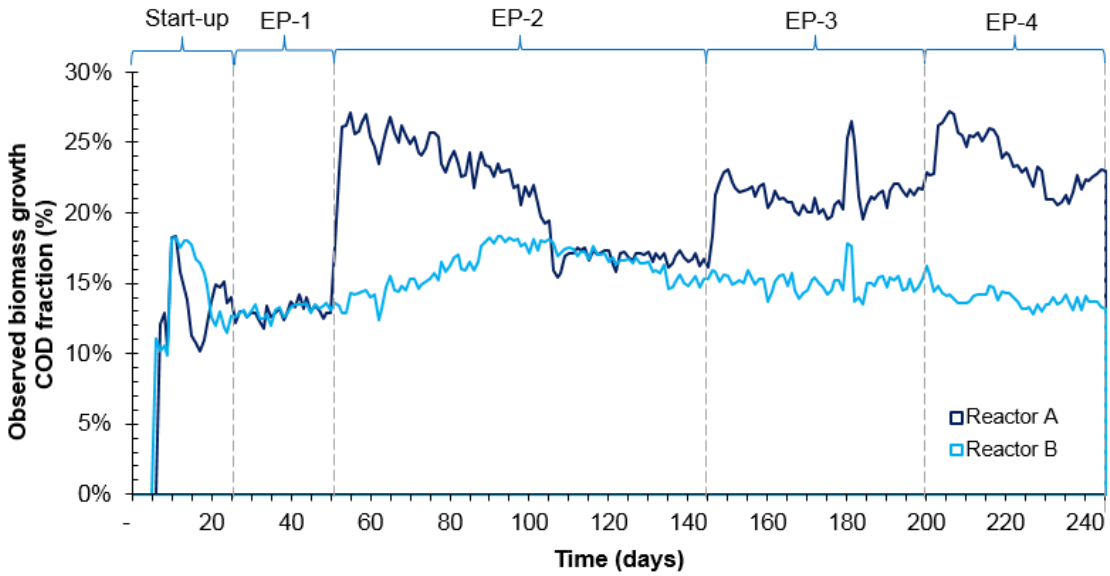

Fig. 5.14. Observed biomass growth COD fraction during experimental period – MCRT effect experiment at 36 ^{o}C

These results further reinforce the above argument that at the shorter MCRT a larger proportion of the available carbon is diverted away from methane production into cellular growth, thus reducing the SMP and increasing the sludge production.

5.3. Conclusions

Long-term operation of two SAnMBRs on a substrate of low to intermediate strength with a high suspended solids content was achieved without change in the TMP throughout four experimental phases, during which the MCRT in one reactor was progressively reduced. This allowed very accurate measurements to be made of the membrane flux rates associated with different MCRT, accompanied by determination of COD removal efficiencies and a COD mass balance, as well as estimation of observed biomass yield and physical characterisation of each mixed liquor using CST time. The results showed that membrane flux was affected by MCRT, with shorter MCRT giving the best performance. Operation at short MCRT, however, resulted in lower specific methane production, although overall COD removal was not affected. Short MCRT also led to greater waste sludge production, and no further improvement in membrane flux was seen at MCRT < 25 days. There is clearly a trade-off to be made between enhanced membrane performance, specific methane production and sludge yield when considering the most suitable operational MCRT.

The results of this experiment at 36 ^{o}C are of interest for the treatment of industrial effluents that are at a higher temperature such as brewery, chemical, dairy and paper industries (Shore *et al.*, 2012, Gutierrez *et al.*, 1991, Dereli *et al.*, 2012) and for applications where waste heat is available to raise the digester temperature. The next stage of this work looks at lower temperature ranges more typical of wastewater types such as municipal wastewater.

6. RESULTS – EFFECT OF MCRT ON SANMBR OPERATING AT 20 ^{O}C

Objective: To assess the long-term effect of MCRT on membrane flux, mixed liquor characteristics and overall performance of SAnMBRs treating low-to-intermediate synthetic wastewater at 20 ^{o}C.

6.1. Method summary

Four fully gravitational SAnMBRs designated A, B, C and D were operated for 245 days, including a start-up period and three experimental phases (EP). The TMP was varied from 1.8 kPa to the practical limit of 9.8 kPa, aiming to maintain the membrane flux and thus the organic loading rates constant. This was achieved by increasing or decreasing the differential head between the mixed liquor surface and the effluent outlet (Δh_{out}; Fig. 3.13). This approach, although slightly different from that adopted in the previous experiment, again allowed very accurate measurement of the sustainable membrane flux rates at different MCRT. Apart from during the start-up, the SAnMBRs were operated at different MCRTs as shown in Table 6.1. The experimental set up for this experiment is shown in Fig. 6.1 and Fig. 6.2.

The biochemical characteristics and stability of the reactors were assessed based on biogas production, biogas composition, COD conversion, specific methane production, pH, MLSS, and MLVSS. As in the previous experiment, reported SMP, SMP_{added} and SMP_{MLSS} values include methane dissolved in the effluent, which was estimated as in the previous experiment but with the saturation concentration at 20 ^{o}C resulting in an average value of 29.0 mL CH_4 L^{-1}. Also as in the previous experiment, COD removal efficiency was evaluated, a COD balance was constructed and measurements of the observed biomass growth yield at each MCRT were made along with physical characterisation of each mixed liquor using CST and FIC. Apart from this, the concentration of bound and soluble extracellular polymeric substances (EPS) was determined as described in Section 3.2.1.6, and a microscopic examination of the mixed liquor was carried out as described in Section 3.2.1.10.

Table 6.1. Start-up and experimental phases – MCRT effect experiment at 20°C

Phase	Duration (days)	Objectives and operation	Reactor	MCRT (days)
Start-up	60	Reactor stabilisation for sustainable operation at an operational temperature of 20 °C and performance coupling to establish a common baseline for the following experimental phases. Due to initial changes in membrane flux and HRT during stabilisation, OLR_v was maintained by adjusting feed concentration.	A	90
			B	90
			C	90
			D	90
EP-1	52	Evaluation of long-term effect of MCRT on membrane flux, mixed liquor characteristics and overall reactor performance, aiming to maintain target flux by varying TMP. Due to initial changes in membrane flux and HRT during stabilisation, OLR_v was maintained by adjusting feed concentration. At the end of the phase the feed concentration was stabilised.	A	30
			B	45
			C	60
			D	90
EP-2	48	As above - Feed concentration remained constant for the entire period, unless noted.	A	30
			B	45
			C	30
			D	90
EP-3	82	As above - Feed concentration remained constant for the entire period, unless noted.	A	20
			B	45
			C	30
			D	30

Before inoculation of the reactors, the inoculum (Millbrook WWTP mesophilic digestate; see Section 3.1.4) was pre-acclimated to the lower operating temperature for 48 days in a sealed and mechanically stirred container which was maintained at 20 °C in a water bath. During this period the inoculum was batch-fed with undiluted synthetic wastewater (Section 3.1.2) at an OLR_V of 0.5 g COD L^{-1} day^{-1}. After the pre-acclimation period the inoculum was diluted to 50% with tap water and then used to inoculate the four reactors, after which the reactor headspace was purged with nitrogen. Throughout the current experiment, during daily feeding the synthetic wastewater was maintained at 20 °C.

6.2. Results and discussion – MCRT effect experiment at 20 °C

6.2.1. Operational performance

The performance of the four reactors over the experimental period is shown in Fig. 6.3, and summary results are given in Table 6.2 and Table 6.3. Key parameters are discussed below in relation to operational changes in each of the three experimental phases.

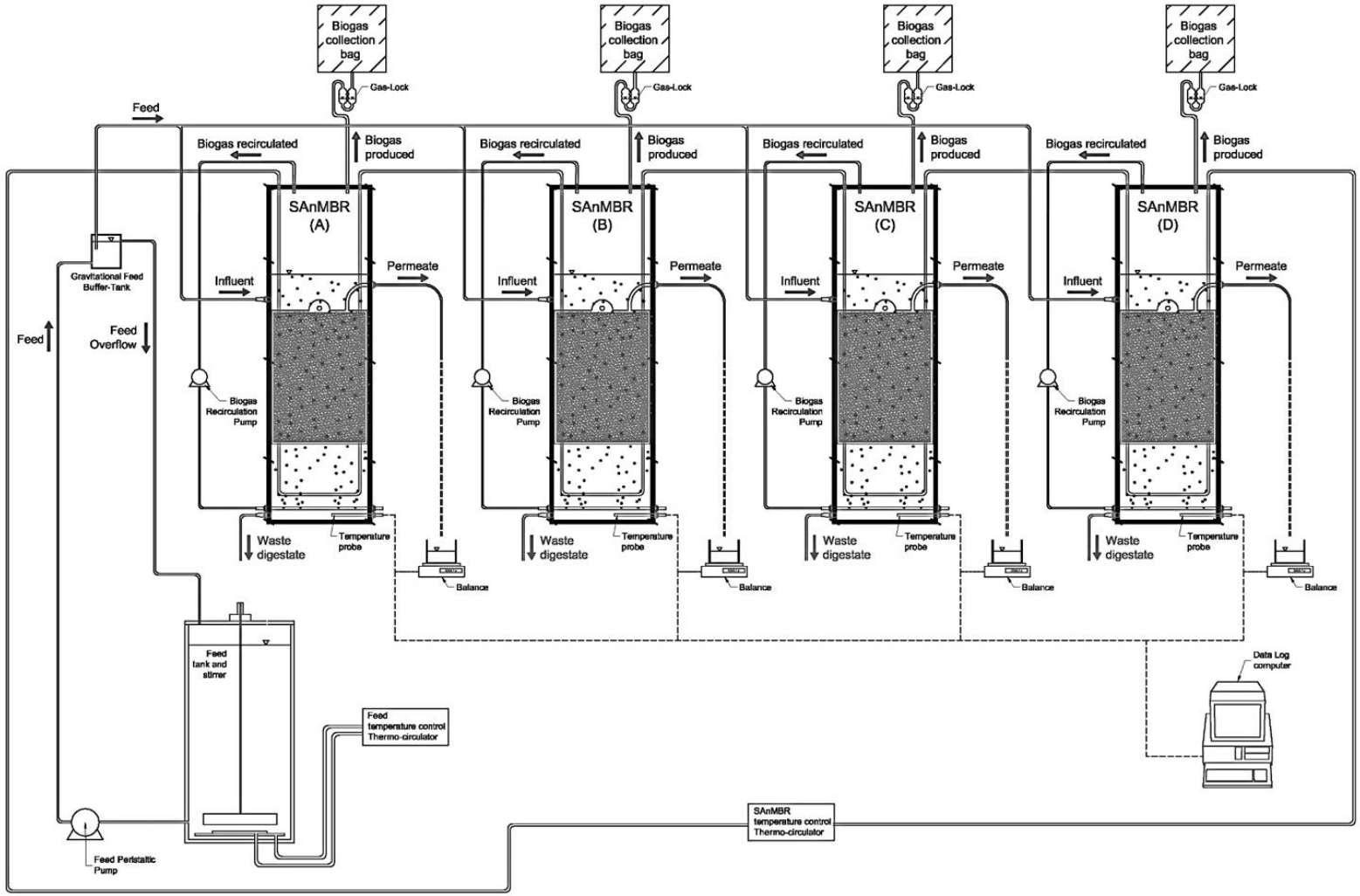

Fig. 6.1. Experimental set-up schematic diagram – MCRT effect experiment at 20 ^{o}C: biogas collection bags, biogas recirculation pumps, constant head device, effluent collection containers, effluent head-difference device, fermentation gas-lock, flux recording balance, SAnMBRs, stirred feed storage tank, and thermo-circulator

Fig. 6.2. Experimental set-up schematic picture – MCRT effect experiment at 20 ^{o}C: biogas collection bags, biogas recirculation pumps, constant head device, effluent collection containers, effluent head-difference device, fermentation gas-lock, flux recording balance, SAnMBRs, stirred feed storage tank, and thermo-circulator

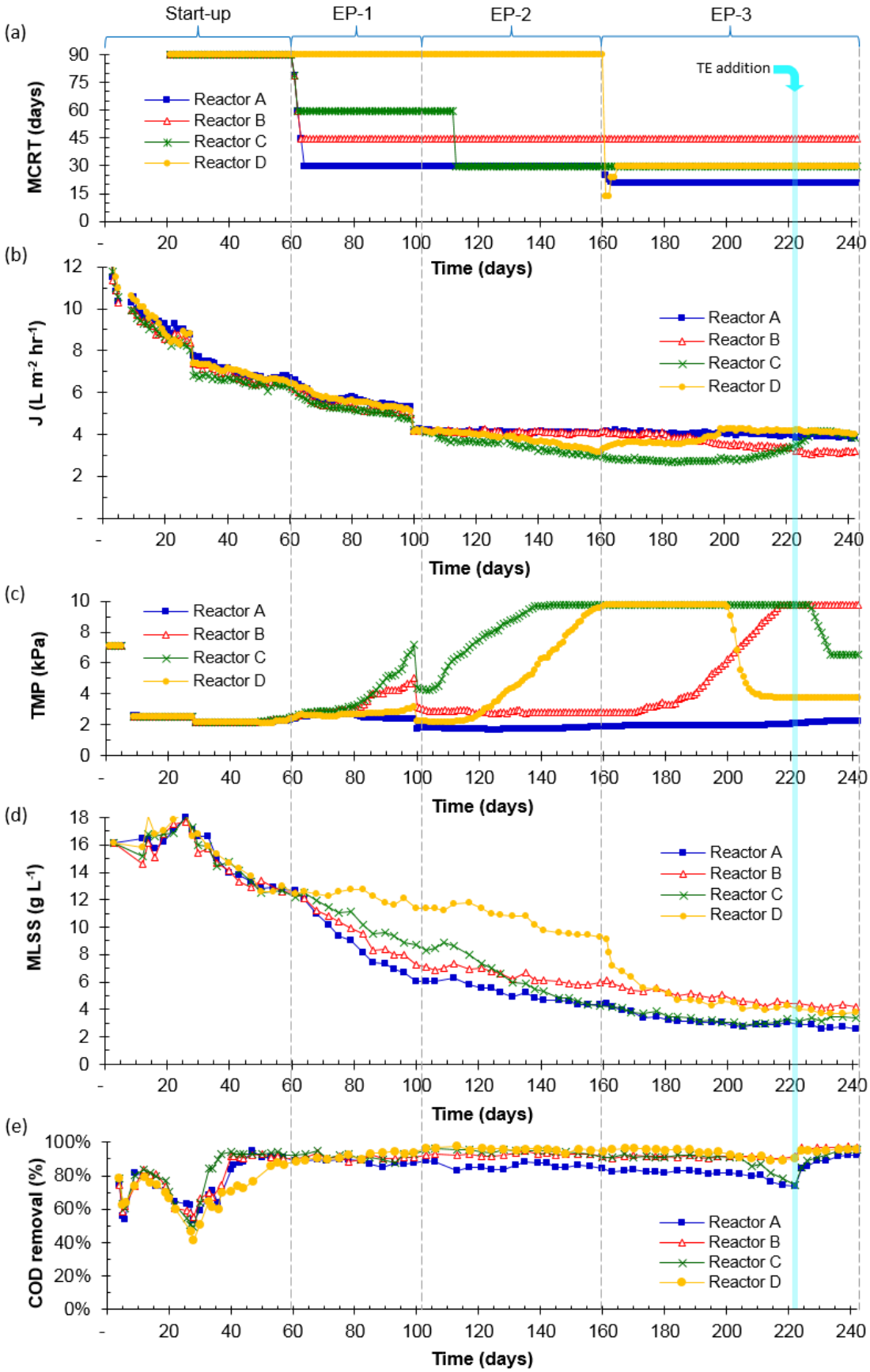

Fig. 6.3. Operational performance during experimental period – MCRT effect experiment at 20 ^{o}C: (a) MCRT, (b) Daily average membrane flux, (c) TMP (d) MLSS concentration, (e) COD removal rate

Table 6.2. Experimental results summary table – MCRT effect experiment at 20 ^{o}C: MCRT, TMP, daily average membrane flux, OLR_V, HRT, feed COD, effluent COD, COD removal rate

Parameter		MCRT	TMP	Membrane Flux (J)*	OLR_V	HRT	Feed COD	Effluent COD	COD removal rate
Phase	**Reactor**	(days)	(kPa)	(L m^{-2} $hour^{-1}$)	(g COD L^{-1} day^{-1})	(hours)	(mg L^{-1})	(mg L^{-1})	(%)
Start-up (60 days)	A	90	7.1 → 2.1 → 2.5	16.1 → 6.7	0.50 – 1.45	5.8 → 12.5	305 → 507	99 → 200 → 59	74% → 53% → 89%
	B	90	7.1 → 2.1 → 2.5	16.1 → 6.4	0.50 – 1.47	5.8 → 13.1	305 → 507	100 → 222 → 51	74% → 55% → 90%
	C	90	7.1 → 2.1 → 2.5	16.1 → 6.3	0.50 – 1.49	5.8 → 13.3	305 → 507	83 → 213 → 39	79% → 49% → 93%
	D	90	7.1 → 2.1 → 2.5	16.1 → 6.4	0.50 – 1.46	5.8 → 13.1	305 → 507	83 → 224 → 62	72% → 42% → 88%
EP-1 (52 days)	A	30	2.5 → 3.2 → 1.8	6.7 → 5.3 → 4.1	0.98 ± 0.03	12.5 → 15.8 → 20.2	567 → 860	59 → 144	88% ± 1%
	B	45	2.5 → 5.1 → 2.9	6.4 → 5.1 → 4.1	0.94 ± 0.04	13.1 → 16.5 → 20.3	567 → 860	51 → 65	91% ± 1%
	C	60	2.5 → 6.7 → 4.3 → 6.3	6.3 → 4.2 → 3.7	1.00 → 0.90	13.3 → 17.7 → 22.5	567 → 860	41 → 36	92% ± 2%
	D	90	2.5 → 3.2 → 2.2	6.4 → 5.3 → 4.1	0.97 ± 0.02	13.1 →16.2 → 20.4	567 → 860	61 → 21	88% → 97%
EP-2 (48 days)	A	30	1.8 ± 0.5	4.1 ± 0.0	0.98 ± 0.01	20.6 ± 0.2	843 ± 26	144 → 125	85% ± 2%
	B	45	2.8 ± 0.6	4.1 ± 0.0	0.99 ± 0.01	20.5 ± 0.2	843 ± 26	65 → 70	93% ± 1%
	C	30	6.3 → 9.8	3.7 → 3.0	0.90 → 0.72	22.5 → 28.5	843 ± 26	36 → 77	95% → 91%
	D	90	2.2 → 9.8	4.1 → 3.2	0.97 → 0.76	20.4 → 26.7	843 ± 26	21 → 44	96% ± 1%
EP-3 (82 days)	A	20	1.9 → 2.2	4.0 ± 0.1	0.98 ± 0.02	21.0 ± 0.4	853 ± 21	136 → 228 → 68	84% → 74% → 92%
	B	45	2.8 → 9.8	4.1 → 3.2	0.99 → 0.78	20.5 → 26.3	853 ± 21	70→ 84 → 22	92% → 92% → 97%
	C	30	9.8 → 3.8	3.0 → 2.7 → 4.0	0.72 → 1.02	28.5 → 31.5 → 21.9	853 ± 21	77 → 217 → 39	91% → 75% → 96%
	D	30	9.8 → 6.5	3.2 → 4.1	0.76 → 0.99	26.7 → 21.1	853 ± 21	44 → 91 → 34	95% → 89%→ 96%

(→) Variable trend: initial → middle → final; (±) Stable performance: One standard deviation to show the spread of the data from the average value under stable performance; (*) Daily average

Table 6.3. Experimental results summary table – MCRT effect experiment at 20 ^{o}C: MCRT, CH_4 in biogas, SMP, MLSS, MLVSS, CST and pH.

Parameter		MCRT	CH_4 in biogas**	SMP***	MLSS	MLVSS	CST	pH
Phase	**Reactor**	(days)	(%)	(L CH_4 g^{-1} COD removed)	(g L^{-1})	(g L^{-1})	(seconds)	
Start-up (60 days)	A	90	88% → 93%	0.00 → 0.35 → 0.21	16.2 → 12.7	12.5 →10.3	162 → 461 → 117	7.0 → 6.2 → 6.8
	B	90	81% → 92%	0.00 → 0.29 → 0.20	16.2 → 12.5	12.6 → 10.2	122 → 402 → 101	7.0 → 6.2 → 6.8
	C	90	76% → 93%	0.00 → 0.42 → 0.22	16.2 → 12.4	13.3 → 10.0	130 → 449 → 117	7.0 → 6.2 → 6.8
	D	90	87% → 93%	0.00 → 0.42 → 0.21	16.2 → 12.7	12.7 → 10.4	132 → 435 → 131	7.0 → 6.2 → 6.9
EP-1 (52 days)	A	30	92% ± 1%	0.21 ± 0.01	12.7 → 6.2	10.3 → 5.4	117 → 198	6.8 ± 0.0
	B	45	91% ± 1%	0.22 ± 0.02	12.5 → 7.3	10.2 → 6.2	101 → 252	6.8 ± 0.0
	C	60	92% ± 2%	0.23 ± 0.02	12.4 → 8.7	10.0 → 7.4	117 → 438	6.8 ± 0.0
	D	90	92% ± 2%	0.23 ± 0.02	12.7 → 11.7	10.4 → 9.8	131 → 430	6.8 ± 0.0
EP-2 (48 days)	A	30	90% ± 1%	0.22 ± 0.01	6.2 → 4.4	5.4 → 3.8	198 →215	6.7 ± 0.0
	B	45	90% ± 1%	0.24 ± 0.01	7.3 → 6.0	6.2 → 5.2	252 →291	6.7 ± 0.1
	C	30	90% ± 1%	0.23 ± 0.01	8.7 → 4.3	7.4 → 3.7	407 → 482 → 433	6.7 ± 0.0
	D	90	90% ± 1%	0.26 ± 0.02	11.7 → 9.3	9.8 → 8.1	430 → 569	6.8 ± 0.0
EP-3 (82 days)	A	20	90% ± 1%	0.23 ± 0.01	4.4 → 2.6	3.8 → 2.2	222→ 101	6.7 ± 0.0
	B	45	90% ± 1%	0.25 ± 0.01	6.0 → 4.2	5.2 → 3.7	291 → 488	6.8 ± 0.0
	C	30	90% ± 1%	0.23 ± 0.01	4.3 → 2.8 → 3.4	3.7 → 2.9	433 → 182	6.8 ± 0.0
	D	30	90% ± 1%	0.24 ± 0.01	9.3 → 6.4 → 3.8	8.1 → 3.3	569 → 240	6.8 ± 0.0

(→) Variable trend: initial → middle → final; (±) Stable performance: One standard deviation to show the spread of the data from the average value under stable performance; (**) Normalised to total biogas content in sample (i.e. neglecting air introduced dissolved through feed); (***) Takes into account the methane dissolved in the effluent

6.2.1.1. Start-up

The inoculation MLSS concentration in all reactors was 16.2 g L^{-1}. The four reactors were started at constant TMP of 7 kPa. No sludge was wasted during the first 10 days to aid acclimatisation, then daily biomass wastage was introduced aimed at giving an MCRT of 90 days.

The starting membrane flux in the four reactors was 16.1 L m^{-2} $hour^{-1}$, which decreased and converged throughout the first 5 days resulting in fluxes between 10.2-11.0 L m^{-2} $hour^{-1}$ (Fig. 6.3). As can be seen in Fig. 6.4, these high initial membrane fluxes and the associated low HRTs resulted in low COD removal rates (54-64 %) and no evident biogas production. The feed COD concentration was therefore adjusted during start-up depending on the membrane flux, with the aim of providing initial control of the OLR_V until a stable performance was achieved.

On day 6, because of the lack of biogas production, feeding and permeation were stopped in all the reactors and operation switched to a 'semi-continuous' mode in order to provide longer retention times for the biomass to deal with the organic load during the acclimatisation process. Feeding during this 'semi-continuous' period was achieved by adding a 0.1 L daily dosage of concentrated synthetic wastewater at approximately at 54 g COD L^{-1} (see Table 3.2), giving an OLR_v of 0.5 g COD L^{-1} day^{-1}. Although by the end of day 8 biogas production could be observed in the gas bags, the pH in all reactors had dropped from 7.0 to 6.2 since the start of the semi-continuous mode. It was hypothesised that this was caused by dissolved CO_2 accumulating in the digestate rather than leaving the system dissolved in the effluent. The continuous mode was re-established on day 9 by resuming gravitational feeding and permeation, but deliberately reducing the TMP from 7.0 to 2.5 kPa with the aim of achieving lower and more stable membrane fluxes as well as higher HRT to aid the start-up process. Despite the TMP reduction the membrane flux was similar to that observed before the semi-continuous period (9.9 – 10.6 L m^{-2} $hour^{-1}$), and this required a further reduction in the feed COD to around 160 mg L^{-1} in order keep the OLRv close to 0.5 g COD L^{-1} day^{-1} and avoid an organic loading shock (Fig 6.4g).

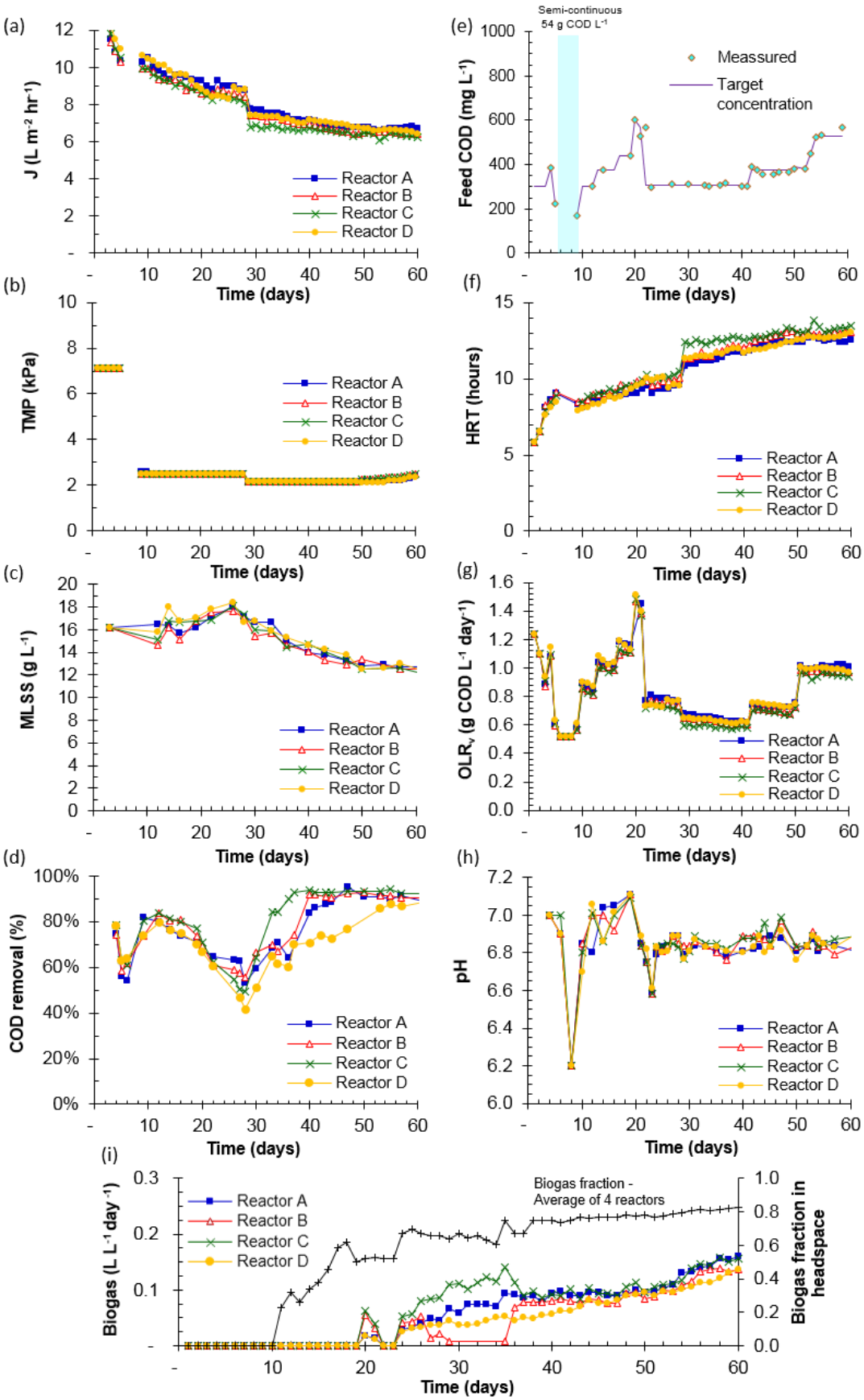

Fig. 6.4. Start-up performance from day 0 to 60 – MCRT effect experiment at 20 ^{o}C: (a) daily average membrane flux, (b) TMP, (c) MLSS, (d) COD removal, (e) feed COD, (f) HRT, (g) OLR_v, (h) pH, and (i) biogas production

Although by day 10 the membrane flux was relatively stable and the pH and COD removal rates had recovered to 6.9 -7.0 and 74-80%, respectively, there was still no observable biogas production. The OLR_v was then carefully increased by increasing the feed COD stepwise then holding it steady for three-day periods at around 0.9, 1.0, 1.1 and 1.5 g COD L^{-1} day^{-1} (Fig 6.4g). This was done with the aim of stimulating a response in the biogas production, in case the lack of production was also related to the low OLR_v. While this resulted in production of a perceptible volume of biogas and a considerable increase in the biogas fraction of the headspace gas composition, the COD removal rates started to decline and by the time the stepped increase in OLRv reached 1.5 g COD L^{-1} day^{-1} the pH showed a serious drop to 6.6.

At this point, it was clear that the lack of biogas production was not due to a low OLR_v but that in fact the system was overloaded. Consequently, on day 23 the OLR_V was reduced to 0.75 g COD L^{-1} day^{-1} and one tenth of the mixed liquor volume in all SAnMBRs was replaced with fresh diluted inoculum pre-conditioned at 20 ^{o}C for two days in order to aid the start-up of the reactors. This resulted in an immediate improvement in all the reactors with membrane fluxes stabilising at around 8.0-8.8 L m^{-2} $hour^{-1}$ and considerable increases in biogas production and headspace methane content by day 28.

Despite this, COD removal rates continued to decline and the OLR was therefore further reduced, but this time by reducing the TMP in all the reactors to 2.2 kPa, aiming for lower and steadier membrane fluxes and consequently longer HRTs. From this point onwards all operational parameters for the reactors, including the COD removal rates, started to improve considerably (Fig. 6.4). Between days 28-35 Reactor B did not show any biogas production due to a leak. Once this was detected and fixed, the performance of this started to match that of the other three reactors. After this continuing improvement in all reactors the OLR_V was again stepped increased from day 40, reaching 1.0 g COD L^{-1} day^{-1} by day 52. By the end of the start-up stability was achieved in all four SAnMBRs, with successful coupling of the membrane fluxes at around 6.3-6.7 L m^{-2} $hour^{-1}$, the COD removal rates at 88- 93%, the MLSS

concentrations at 12.4-12.7 g L^{-1}, and stable biogas composition and production. It was therefore decided to start the first experimental phase on day 60.

6.2.1.2. Membrane flux and TMP response to MCRT: observed changes in MLSS, HRT and OLR_V

EP-1. On day 60 MCRT was reduced in Reactor A to 30 days, in Reactor B to 45 days, in Reactor C to 60 days, while in Reactor D it remained at 90 days. At the beginning of this phase the TMP in all reactors was equal at 2.5 kPa, with corresponding membrane fluxes of 6.7, 6.4, 6.3 and 6.4 L m^{-2} $hour^{-1}$ for Reactors A, B, C and D, respectively (Fig. 6.3). As the membrane flux continued gradually to drop in all reactors, the TMP was individually adjusted aiming to stabilise the membrane flux at around 5 L m^{-2} $hour^{-1}$. The average COD concentration of the feed was also adjusted slightly in relation to the membrane flux, aiming for a constant OLR_V of 1 g COD L^{-1} day^{-1}; however the degree of adjustment in this phase was much less than during start-up (Fig. 6.5).

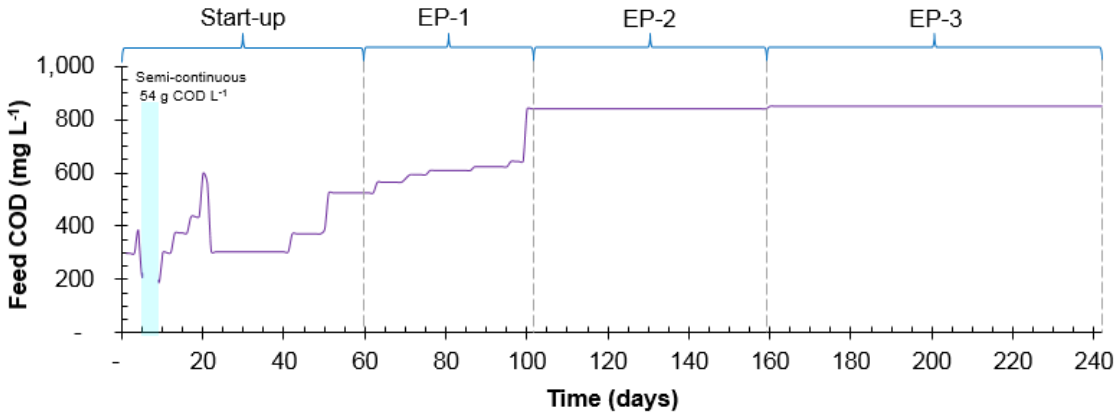

Fig. 6.5. Feed COD target COD concentration during experimental period– MCRT effect experiment at 20 °C

By day 67 the effect of changes in MCRT was already reflected in Reactor C, which showed signs of membrane fouling as substantial increases in TMP started to be necessary to maintain the membrane flux at around 5 L m^{-2} $hour^{-1}$. This was followed by Reactor B and Reactor D, which by day 80 also started to require increases in the TMP to meet the target flux, while in Reactor A it was necessary to decrease the TMP as the membrane flux was increasing. At this point, it was evident that the target membrane flux of 5 L m^{-2} $hour^{-1}$ was too high for the conditions of this experiment.

Consequently, on day 100 the target flux was reduced to 4 L m^{-2} $hour^{-1}$ by reducing the TMP to 1.8, 2.9, 4.3 and 2.2 kPa for Reactors A, B C and D, respectively. This resulted in an HRT around 20 hours and a constant OLR_V of 1.0 g COD L^{-1} day^{-1}, achieved with an average feed COD of 860 ± 23 mg COD L^{-1}. The slight variation in feed concentration here was due to minor day-to-day differences in batch make-up and measurement, with no further deliberate adjustment of influent strength. In Reactors A, B and D the membrane flux remained stable at 4 L m^{-2} $hour^{-1}$ with constant TMP until the end of the phase. In contrast, membrane flux in Reactor C continued to decrease despite increases in the TMP which reached 6.3 kPa by the end of the phase, resulting in a final HRT of 22.5 hours and OLR_V of 0.9 g COD L^{-1} day^{-1}. MLSS concentrations also reflected changes in MCRT, with all reactors starting the phase at similar concentrations between 12.4-12.7 g L^{-1} and ending at 6.2, 7.3, 8.7 and 11.7 g L^{-1} for Reactor A, B, C and D, respectively.

EP-2. At the start of this phase MCRT in Reactor C was reduced from 60 to 30 days, with an initial TMP of 6.3 kPa. MCRT in Reactor A, Reactor B, and Reactor D remained at 30, 45 days, and 90 days, with initial TMPs of 1.7, 2.9 and 2.2, respectively. While the membrane flux in Reactor A and Reactor B remained stable at 4 L m^{-2} $hour^{-1}$ without modifications to the TMP, the flux in Reactor C continued to decrease despite continuous increases in TMP (Fig. 6.3). As a result, on day 143 Reactor C reached the limit TMP of 9.8 kPa with a corresponding membrane flux of 3.6 L m^{-2} $hour^{-1}$. Membrane flux in Reactor D remained constant until day 115 when it started to fall leading to a requirement to increase the TMP in order to maintain the flux. By day 160, Reactor D reached the TMP limit of 9.8 kPa with a corresponding flux of 3.2 L m^{-2} $hour^{-1}$. The constant membrane flux in Reactor A and B resulted, in both reactors, in a stable HRT around 20.5 hours and an OLR_V of 1.0 g COD L^{-1} day^{-1}. Continuous decrease in membrane flux in Reactor C and D resulted in final HRTs of 28.5 and 26.6 hours and OLR_V of 0.7 and 0.8 g COD L^{-1} day^{-1}, respectively.

MLSS concentrations during this phase continue to reflect the changes in MCRT, with Reactor A and B stabilising around 4.4 and 5.8 g L^{-1}, respectively. The fall in MLSS in Reactor C reflected the reduction of the MCRT from 60 to 30 days as well as the

decrease in organic load applied due to the lower membrane flux, resulting in a final concentration of 4.3 g L^{-1}. MLSS concentration in Reactor D initially stabilised around 10.8 g L^{-1} but then decreased to 9.5 by the end of the phase, as a consequence of the decrease in membrane flux and thus in organic load applied.

EP-3. MCRT was reduced to 20 days in Reactor A, maintained at 45 days in Reactor B and at 30 days in Reactor C, and in Reactor D was reduced to 30 days. In Reactor D, however, the MLSS was abruptly reduced from 9.1 to 7.2 mg L^{-1}, aiming for a concentration near to the expected value at 30 days MCRT. This was done by removing a defined volume of mixed liquor which was then replaced with influent to give the same working volume in the reactor. This process was carried out in four daily iterations, until the mixed liquor reached the desired MLSS concentration. The volume removed was 700 ml of mixed liquor for days 160 and 161 and 400 ml of mixed liquor for days 162 and 163.

The membrane flux in Reactor A was maintained at 4 L m^{-2} $hour^{-1}$ throughout the phase, with only a small increase in TMP to 2.2 kPa (Fig. 6.3). In contrast, the membrane flux in Reactor B remained constant at 4 L m^{-2} $hour^{-1}$ until day 180 when it started dropping, requiring continuous increases in TMP. By day 216 Reactor B reached the maximum TMP of 9.8 kPa, and after this the membrane flux continued gradually to decrease, stabilising at around 3.2 L m^{-2} $hour^{-1}$ by the end of the phase. The membrane flux in Reactor C continued to fall reaching its lowest value on day 183 at 2.7 L m^{-2} $hour^{-1}$. After this, the membrane flux gradually increased reaching the target value of 4 L m^{-2} $hour^{-1}$ by day 228. Over the following five days the TMP was reduced to 6.5 kPa, while the membrane flux remained constant at 4.1 L m^{-2} $hour^{-1}$ until the end of the experiment. The abrupt MLSS reduction in Reactor D resulted in an instant increase in membrane flux, reaching the target of 4 L m^{-2} $hour^{-1}$ by day 200. In the following 10 days the TMP was reduced to 3.8 kPa, while the flux remained constant at 4.1 L m^{-2} $hour^{-1}$ until the end of the phase. HRT and OLR_V in Reactor A continued at 21.0 hours and 1.0 g COD L^{-1} day^{-1}, values later achieved by Reactors C and D once they reached the same sustainable membrane flux of 4 L m^{-2} $hour^{-1}$. The decrease in membrane flux in Reactor B led to an increase in HRT to 26.3 hours and a reduction in OLR_V to 0.8 g COD L^{-1} day^{-1}.

6.2.1.3. COD removal rates and COD balance

As reported above, several difficulties were experienced during start-up that resulted in high variability in the COD removal during this period (Fig. 6.4), which stabilised towards the end at around 88-93%. COD removal rates during the first 20 days of EP-1 remained similar in all the reactors at between 89-92% (Fig. 6.6). Differences in MCRT started to show an effect on COD removal rates through this phase, however, with Reactors A, B, C and D running at 30, 45 60 and 90 days MCRT ending the phase with COD removal rates of 88%, 92%, 96% and 98%, respectively. During EP-2, the COD removal rates in Reactors A, B and D stabilised at around 85 ± 2%, 93% ± 1% and 96% ± 1, respectively. In contrast COD removal rates in Reactor C, where MCRT was reduced from 60 to 30 days, showed a continuous reduction from 95% to 91%. COD removal rates in all reactors showed a slight decreasing trend during the first 30 days of EP-3, followed later by a significant decrease of 8% and 20% in Reactors A and C between days 197 and 222. This was hypothesised to be caused by a lack of trace elements in the mixed liquor, since these reactors had the highest overall turnaround of biomass due to the MCRTs evaluated, and therefore the highest probability of running out of essential nutrients. As a result, on day 223 trace element solutions as described in Section 4.1.2 were added to the feed for a period of three days at a rate 0.1 mL of each solution per liter of diluted synthetic wastewater. This resulted in an immediate increase in the COD removal rate in all the reactors, which by the end of EP-3 had stabilised at 92%, 97%, 95% and 96% for Reactors A, B, C and D, respectively. It thus appeared that some of the decline in COD removal was an effect of TE deficiency, but removal rates at shorter MCRTs were still slightly lower.

TE requirements and optimum dosing of these systems and its relationship with operational parameters may be an important topic for further work.

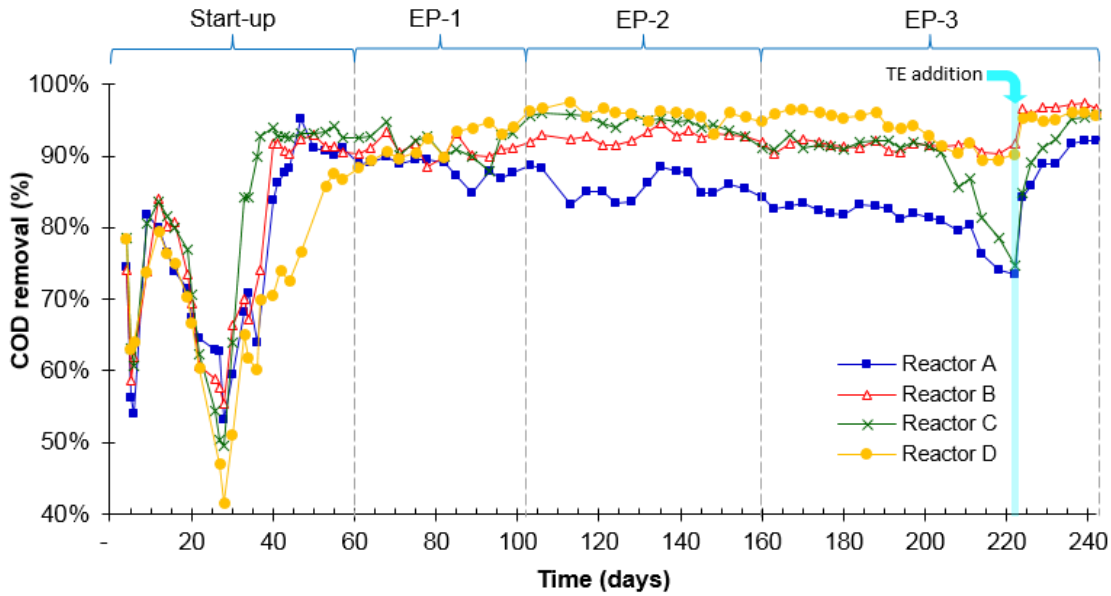

Fig. 6.6 COD removal rates during experimental period – MCRT effect experiment at 20 oC (expanded from Fig. 6.3)

COD balances (Fig. 6.7) showed a substantial proportion of this being converted to methane, from which a considerable fraction leaves the system dissolved in the effluent. The reaction to the addition of trace elements on day 223 can also be seen.

The COD balances in this experiment closed up to 92-96% during the steady state periods, where the missing fraction could be attributed to unaccounted-for biogas that leaves the reactors in gaseous form through the permeate line and as well as the H_2S fraction which was not considered. In addition, there could be an underestimation when calculating the volume of CH_4 in the effluent through Henry's law, since this is based on a saturation concentration, while the TMP could force additional methane in solution and therefore reach a point of supersaturation in the solution methane (Smith et al., 2012). As a result, the volume of methane dissolved in the effluent would be higher than calculated, particularly at low operational temperatures where the saturation concentration is increases.

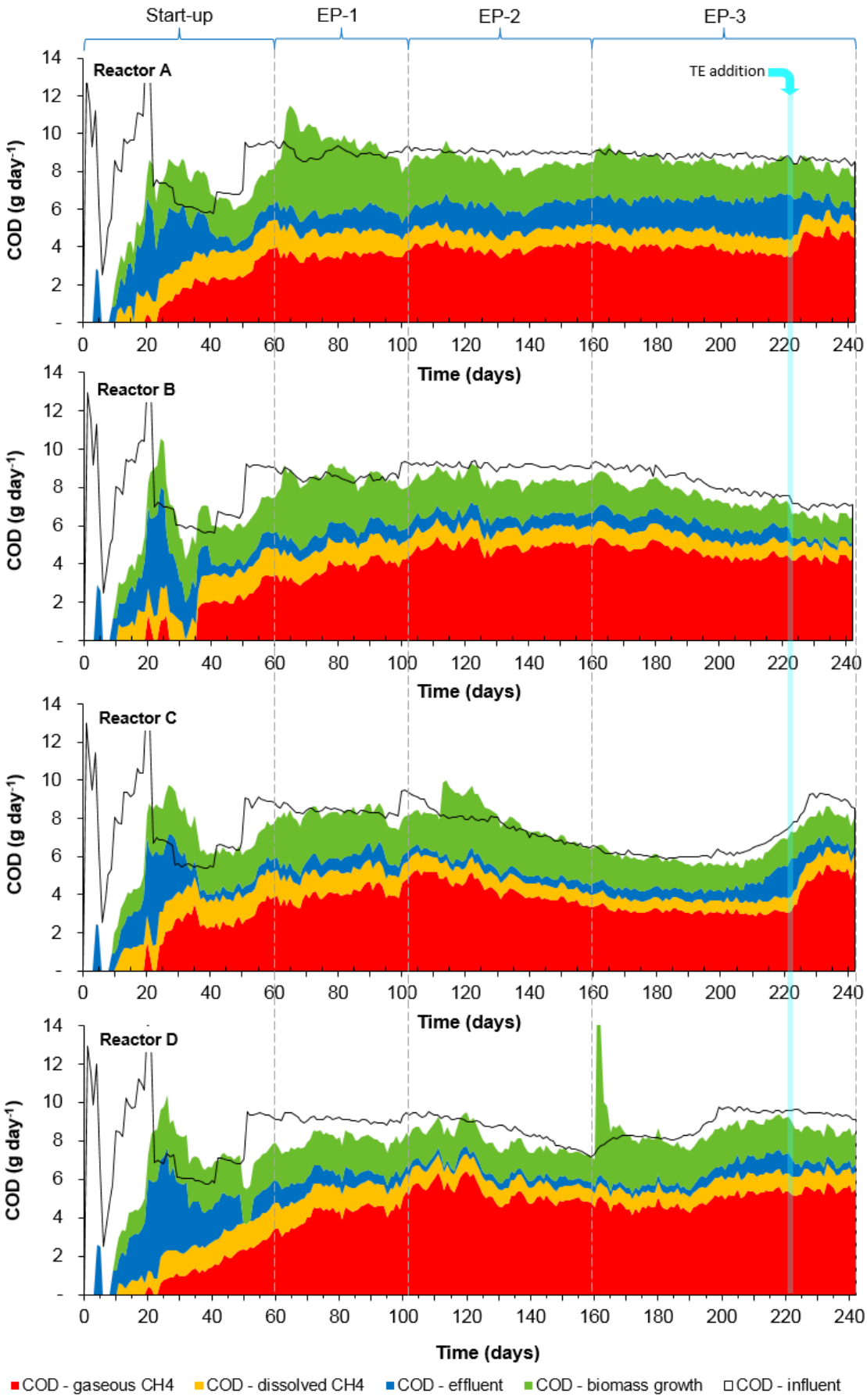

Fig. 6.7. COD balances during experimental period – MCRT effect experiment at 20 ^{o}C

6.2.1.4. Biogas composition

Biogas composition was stable in all reactors throughout the four experimental phases with 78% CH_4, 8% CO_2 and 14% atmospheric nitrogen (Fig. 6.8).

6.2.1.5. Specific methane production

SMP during the start-up showed the same trend in all reactors, starting from zero, sharply increasing between 0.29-0.42 L CH_4 g^{-1} COD and finally stabilising between 0.20 and 0.22 L CH_4 g^{-1} COD. As shown in Fig. 6.9b and summarised in Table 6.3, the SMP during the stable periods in the experimental phases was around: 0.23 ± 0.01 L CH_4 g^{-1} COD removed in Reactor A when running at 20 days MCRT; 0.22 ± 0.01, 0.23 ± 0.01 and 0.24 ± 0.01 L CH_4 g^{-1} COD removed in Reactors A, C and D when operating at 30 days MCRT; 0.25 ± 0.01 L CH_4 g^{-1} COD removed in Reactor B when operating at 45 days MCRT; and 0.26 ± 0.02 L CH_4 g^{-1} COD removed in Reactor D when operating at 90 days MCRT. The SMP in Reactor C at 60 days MCRT was 0.23 ± 0.02 L CH_4 g^{-1} COD removed, although fully stable conditions were not achieved. The results, however, again show lower SMP at shorter MCRT, most probably due to a higher fraction of carbon incorporated into biomass due to higher microbial growth rates.

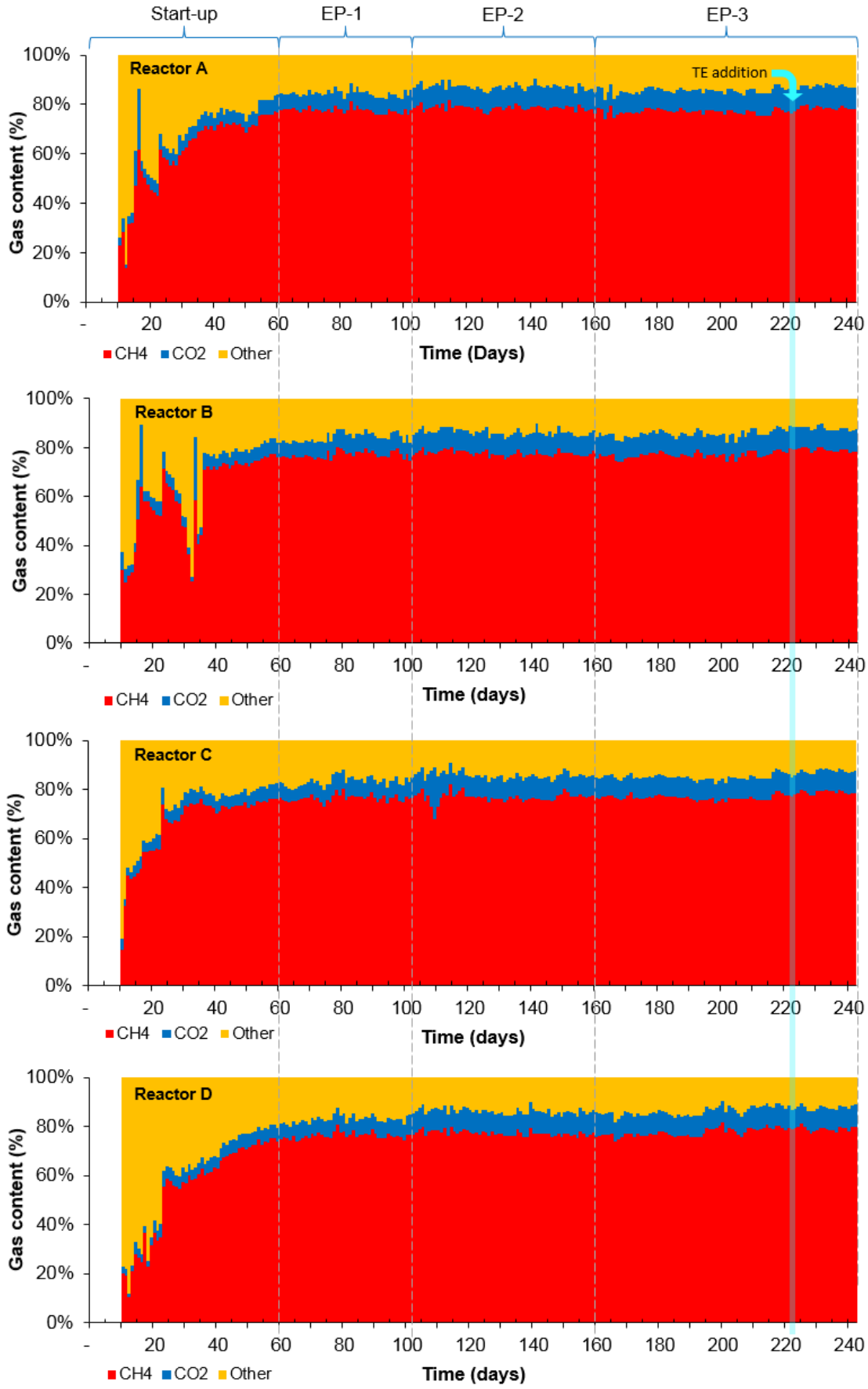

Fig. 6.8. Biogas composition during experimental period – MCRT effect experiment at 20 °C

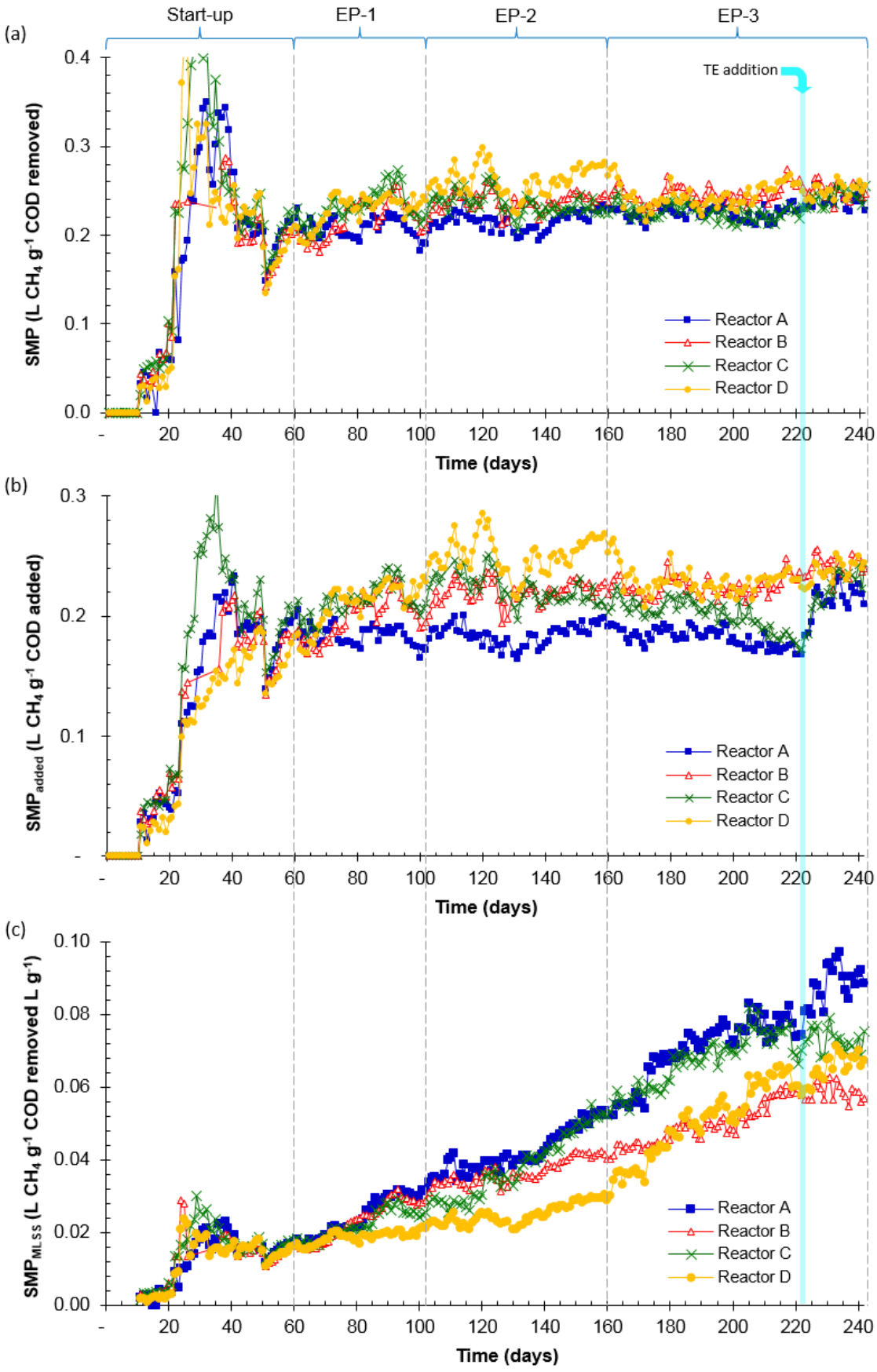

Fig. 6.9. Specific methane production during experimental period – MCRT effect experiment at 20 ^{o}C: (a) SMP, (b) SMP_{added} and (c) SMP_{MLSS}

This result was consistent with the outcome in the previous experiment at 36 ^{o}C but with lower overall SMP rates most probably caused by lower reaction rates at lower temperatures. As mentioned above, Huang et al. (2011) and Huang et al. (2013) also reported that SMP increased with increasing MCRT when treating low strength SWW in SAnMBRs at operating temperatures between 25-30 ^{o}C. They reported values of SMP of 0.13, 0.20 and 0.22 L CH_4 g^{-1} COD removed at 30, 60 and infinite days MCRT respectively when treating synthetic wastewater at OLR of between 1.1 and 1.67 g COD L^{-1} day^{-1}; and of 0.04, 0.09, 0.09 L CH_4 g^{-1} COD removed at 30, 60 and 90 days MCRT respectively when treating sewage at an OLR of 1.02 g COD L^{-1} day^{-1}. Their explanation for higher SMP was that longer MCRT would benefit methanogenesis and lead to more biogas generation. The SMP values reported in this experiment at 20 ^{o}C are generally higher than those reported by Huang et al. (2011) and Huang et al. (2013) at higher operational temperatures. This, however, could be due in part to inclusion of the estimated dissolved methane in the effluent for the SMP calculation in this experiment. Nonetheless, the trend of lower SMP at shorter MCRTs is still consistent between their studies and the outcome of this and the previous experiment at 36 ^{o}C.

As well as the SMP, the SMP_{added} in this experiment was also higher at longer MCRTs (Fig. 6.9b). The spread of values was much more marked than in the SMP, however, due to the differences in the COD removal rates, which were lower at shorter MCRTs. Even after the TE were supplemented the SMP_{added} was still higher at longer MCRTs. Regarding the SMP normalised with MLSS (SMP_{MLSS}), it again showed that the biomass was more efficient in terms of methane conversion at shorter MCRT Fig. 6.9c, as also observed in the previous experiment at 36 ^{o}C. Similar values to those in the previous experiment at 36 ^{o}C were observed, with the highest value around 0.090 L CH_4 g^{-1} COD removed L g^{-1} for Reactor A operating at 20 days MCRT, while Reactor D showed a value around 0.2 L CH_4 g^{-1} COD removed L g^{-1} during stable performance at 90 days MCRT between days 110 and 130. As mentioned above, the trends in SMP_{MLSS} calculated from the data reported by Huang et al. (2011) showed a higher methane productivity per unit of biomass at longer MCRTs (Table 5.3), contradicting the outcomes in this study at both 36 ^{o}C and 20 ^{o}C. Despite the fact that their result could be affected by unaccounted-for dissolved CH_4 in the effluent, the trend repeats in all

their trials at the same HRT, where the methane loss in the effluent should in theory be the same. The performance of this experiment at 20 oC can be again compared to the performance of laboratory-scale UASB reactors operated at 20 ^{o}C using the same synthetic wastewater and similar low COD concentrations in a recent study (Ali, 2014). The SMP reported for an OLR of 1 g COD L^{-1} day^{-1} and a HRT of 22 hours was 0.26 L CH_4 g^{-1} COD removed while the SMP_{added} for a similar COD removal rate of around 95% was 0.25 L CH_4 g^{-1} COD added, similar to the outcome of this experiment.

As shown in Fig. 6.10 the fraction of SMP dissolved in the effluent during the experimental phases ranged between 13-65%, depending on the membrane flux and COD removal rate. This was reduced to around 28-30% after the start-up when the COD removal rate was stabilised and to then between 13-20% after day 100 when the target membrane flux of 4 L m^{-2} $hour^{-1}$ was set; and was generally higher in the reactors with higher membrane flux and/or lower COD removal rates. It can be appreciated how the fraction of methane in dissolved in the effluent reduced in Reactors A and C, as a consequence of the COD removal rate recovery after the TE were added. After this, the fraction of SMP dissolved in the effluent remained higher in reactors with higher flux. Apart from the importance of quantifying the fraction of SMP dissolved in the effluent, this result shows that if the dissolved CH_4 is not taken into account, the apparent SMP for the reactor with the higher membrane flux would have been reduced by up to 7%.

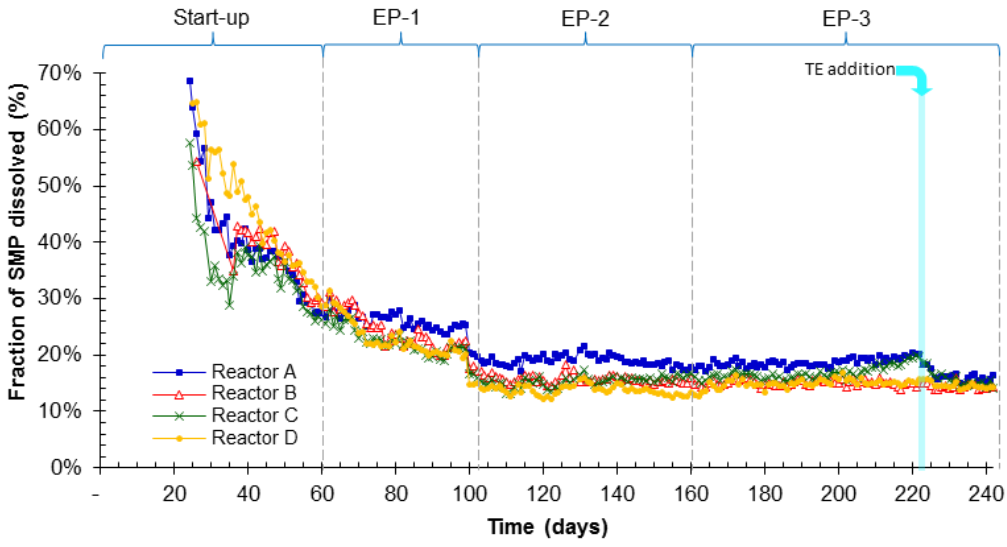

Fig. 6.10. Fraction of SMP corresponding to the CH4 dissolved in the effluent during experimental period – MCRT effect experiment at 20 ^{o}C

6.2.1.6. pH and operational temperature

Apart from the start-up, the pH remained relatively constant throughout the experimental phases (Fig. 6.11 and Table 6.3). As in the previous experiments addition of $NaHCO_3$ to prevent acidification was not required.

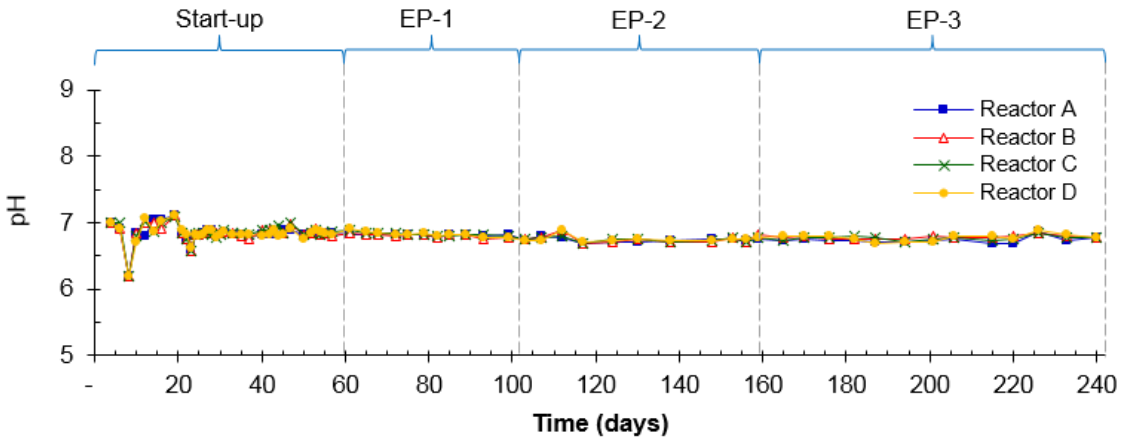

Fig. 6.11. pH during experimental period – MCRT effect experiment at 20 ^{o}C

The operational temperature of both reactors remained relatively constant throughout the experimental phases at 20.0 oC ± 0.5. (Fig. 6.12). The Operational temperature during the Start-up was slightly increased to 23 ^{o}C aiming to further acclimate the inoculum and help the start-up process due to the above discussed difficulties (Section 6.2.1.1). As the performance started to stabilise around day 30, the temperature was gradually reduced to 20 ^{o}C in order to start EP-1.

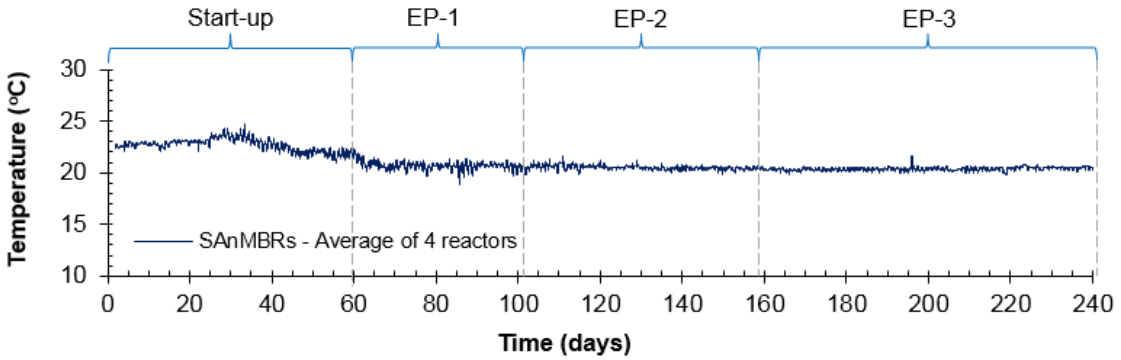

Fig. 6.12. Operational temperature of SAnMBRs during experimental period – MCRT effect experiment at 20 ^{o}C

6.2.2. Membrane performance and fouling phenomena

The results in this experiment at 20^{o}C showed that shorter MCRT result in better performance in terms of membrane flux, but with no clear benefit from operating at MCRTs lower than 30 days Fig. 6.3. in EP-1, however, Reactor B at 45 days MCRT and Reactor C at 60 days MCRT showed a faster increase in the TMP required to maintain the membrane flux (Fig 6.xc), compared to that in Reactor D at an MCRT of 90 days with a considerably higher MLSS concentration (Fig 6.x c and d). This suggested the onset of membrane fouling was earlier at an MCRT of 45 and 60 days than at 30 or 90 days. In EP-2 the required TMP in Reactor B at MCRT 45 days remained above that in Reactor D until day 120; while the TMP in Reactor C started to rise again sharply from day 106 despite the reduction in its MCRT to 30 days from day 100 on. TMP in Reactor D began to rise slightly from day 80, although it was until day 120 when it started to increase at a rate similar to that in Reactor C. Nonetheless, when the MCRT was reduced to 30 days in reactors C and D complete recovery of membrane flux to the target of 4 L m^{-2} hour^{-1} was achieved, along with significant corresponding reductions in TMP. Faster recovery of membrane flux was observed in Reactor D, most probably due to the abrupt reduction in MLSS compared to Reactor C. This behaviour not only shows that MCRT does have a considerable effect on membrane fouling, but also that membrane fouling could be reversed if the optimum MCRT is employed.

The above results show that MCRT can affect membrane fouling, and this is not necessarily just as a function of the MLSS concentration. As mentioned above, earlier research suggests that membrane fouling may result from constituents such as EPS and soluble microbial products, the production of which is related to growth and hence MCRT (Stuckey, 2012). Studies on the effect of MCRT on membrane fouling and overall performance in AnMBR are still scarce and thus the relationship between these factors is still unclear. Studies by Huang et al. (2011) in which performance decreased with increasing MCRT as well as the previous experiment at 36 ^{o}C, showed that fouling appears worse at longer MCRTs. Later work by Huang et al. (2013) treating sewage showed membrane fouling increased at both long and short MCRTs, with maximum flux rates being achieved at 60 days.

Physical examination of the membrane cassettes (Fig. 6.13) at the end of the experiment showed higher biocake formation in Reactor B (45 days MCRT) compared to Reactor A (20 days MCRT) and Reactors C and D (30 days MCRT). The possibility that this could be due to differences in the performance of the membrane gas scouring system was again discounted, as all reactors performed equally well when operated under the same conditions during the start-up. It is also interesting to highlight that membrane cassettes of Reactor C and D showed a similar biocake formation to that in Reactor A, despite the fact that these had the worse membrane performance when operating at 60 and 90 days MCRT. This supports the above suggestion of a potential reversal of membrane fouling as a result of MCRT change, as mentioned above in Section 6.2.2.

6.2.3. Mixed liquor characteristics

6.2.3.1. Capillarity suction time (CST)

Results from the CST tests (Fig. 6.14a and Table 6.3) again showed that MCRT has a large effect on the ability of the mixed liquor to hold water; with samples at shorter MCRT giving up their water much more readily than those at long MCRT. During start-up, when the four reactors were operated as replicates at 90 days MCRT, similar increases in CST time were seen in all of them. Differences in CST times between reactors started to be noticeable during EP-1 when the MCRT was changed to 30, 45, 60 days in Reactors A, B and C, and remained at 90 in Reactor D; being higher at longer MCRTs. By the end of EP-1, however, the CST time of Reactor C matched the CST time of Reactor D despite having a MLSS concentration 25% lower. This suggests that the MCRT of 60 days in Reactor C resulted in the worst condition for biomass filterability, which is also consistent with the reduction in membrane flux at that point despite the increase in TMP. When the MCRT in Reactor C was reduced from 60 to 30 days in EP-2, the CST time decreased and stabilised towards the end of this phase. Despite this, the CST time normalised against MLSS (CST_{MLSS}, Fig. 6.14b) continued to increase showing that the normalised mixed liquor filterability was actually still reducing. It is interesting to highlight that this parameter was nearly 2-fold higher than in Reactor D, operating at a MCRT three times longer.

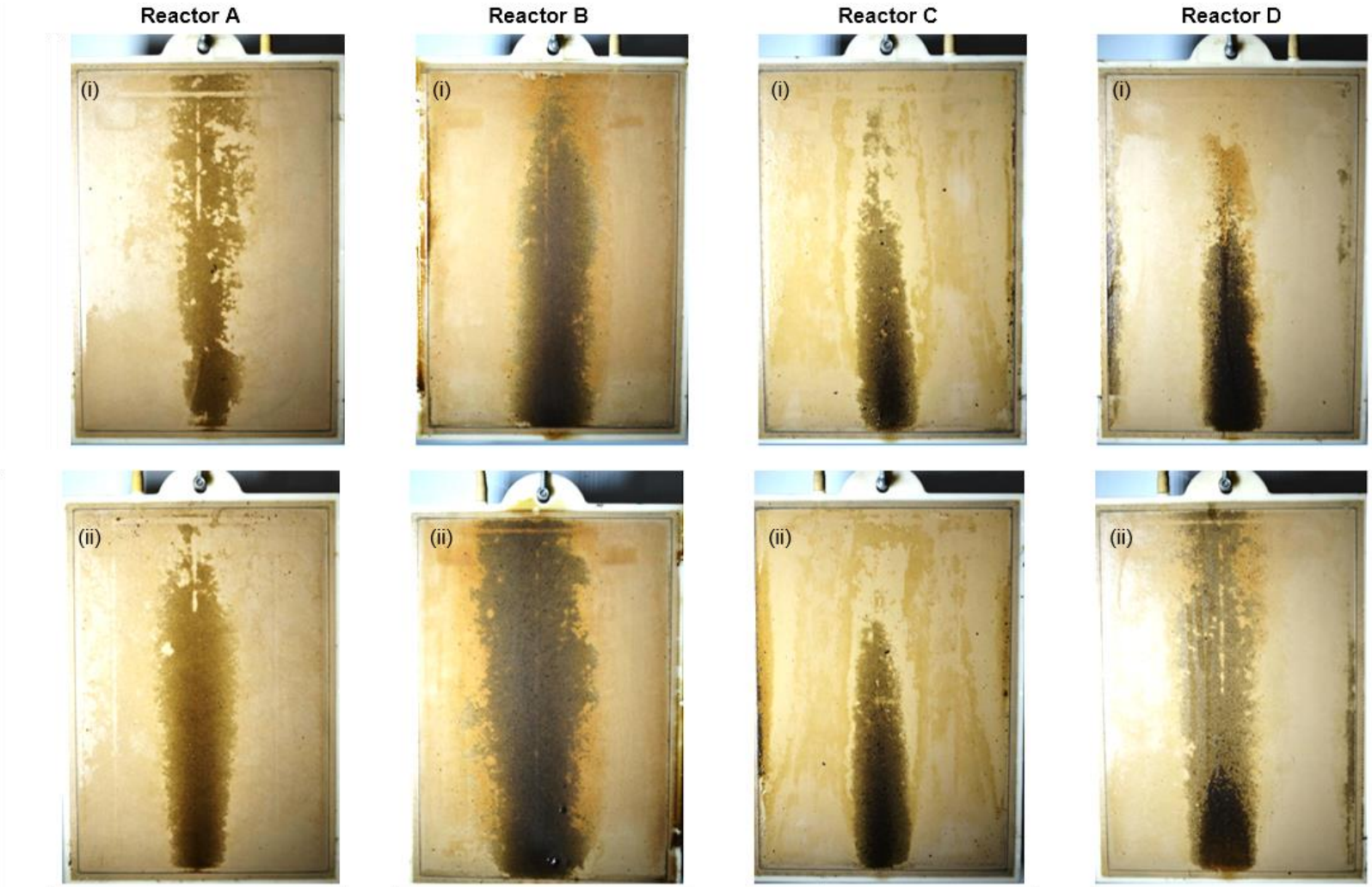

Fig. 6.13. Membrane fouling at the end of experimental run before and after rinsing with running tap water and gentle manual wiping – MCRT effect experiment at 20 ^{o}C: (i) membrane front – before rinse, (ii) membrane back – before rinse, (iii) membrane front – after rinse, (iv) membrane back – after rinse

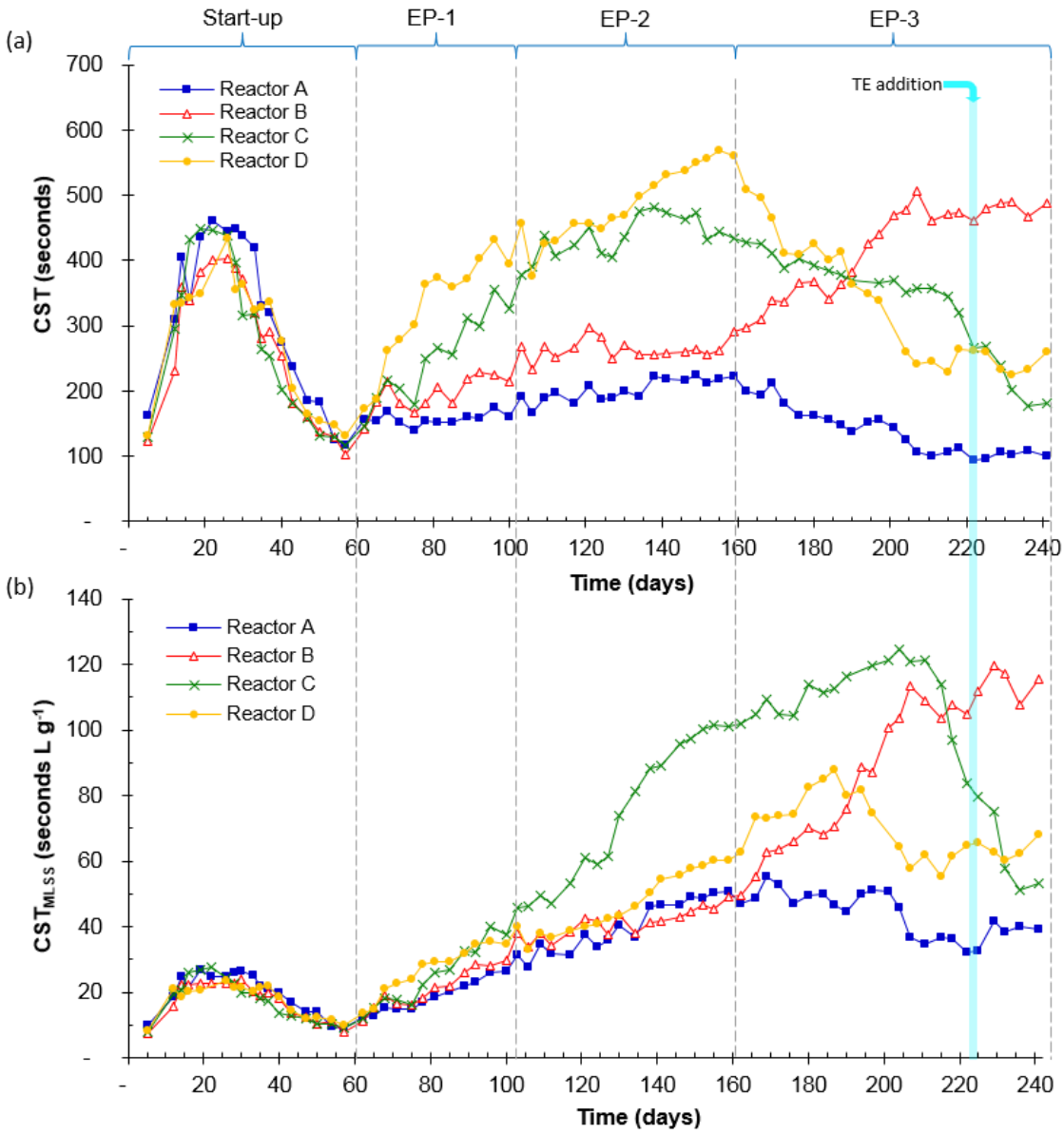

Fig. 6.14. Mixed liquor filterability during experimental period – MCRT effect experiment at 20 ^{o}C: (a) CST; (b) CST$_{MLSS}$

During EP-3 the MCRT in Reactor A was reduced from 30 to 20 days and in Reactor D from 90 to 30 days; the latter with an abrupt reduction in MLSS concentration. While CST times in Reactor A dropped even further, reaching values around 100 seconds, the abrupt reduction in MLSS in Reactor D resulted in a steep reduction from 500 to 250 seconds. CST times in Reactor C continued to decrease during this phase matching those in Reactor D. In contrast, CST times in Reactor B started to increase considerably along with a serious drop in membrane flux, stabilising close to 500 seconds. CST$_{MLSS}$ show how the abrupt MLSS reduction in Reactor D during EP-3 resulted in an immediate increase in mixed liquor filterability. This was consistent with the observed

recovery of the membrane flux which resulted in significant reductions in the TMP. Although the CST times stabilised and start dropping in Reactor C shortly after the MCRT was reduced from 60 to 30 days, it took around 100 days for the CST_{MLSS} to in this reactor start decreasing. This suggests that the increase in filterability by a reduction in the MCRT may be delayed if the MLSS is gradually changed, assuming that any 'fouling substances' present in the mixed liquor will take more time to be discarded from the system. On the other hand, if the MLSS is abruptly reduced when the MCRT is decreased (e.g. by removing a certain volume of mixed liquor and replacing it with a more dilute liquid), the biomass filterability will improve almost instantaneously and thus the membrane performance enhancement will occur much faster.

6.2.3.2. Frozen image centrifugation (FIC)

Results from the frozen image centrifugation (FIC) test also showed the large effect that MCRT has on the solid-liquid separation, with samples at shorter MCRT separating much more readily than those at long MCRT. As Shown in Fig. 6.15, the initial rate of separation during the first 1-3 minutes is much more rapid in reactors in reactors running at short MCRT. After day 154 three separation phases were observed during the test (Fig. 6.16), represented by the solid bars in the graph, which remained for a longer time during the test in reactors operated at longer MCRT. It is interesting to observe, however, how the duration of the three phase separation considerable reduced in Reactor C and D when the MCRT was reduced to 30 days, suggesting that the separation of the solid phase from the liquid phase improved, as the CST did too.

6.2.3.3. Extracellular Polymeric Substances (EPS)

As shown in Fig. 6.17a and Fig. 6.17b the protein and carbohydrate concentration in the bound EPS (lightly bound + tightly bound) was generally highest in Reactor A, operated at 30 and 20 days MCRT. These concentrations, however, showed an increase in Reactor C compared to the other reactors, when the MCRT was reduced from 60 to 30 days on day 112, with the increase in protein concentration being more delayed.

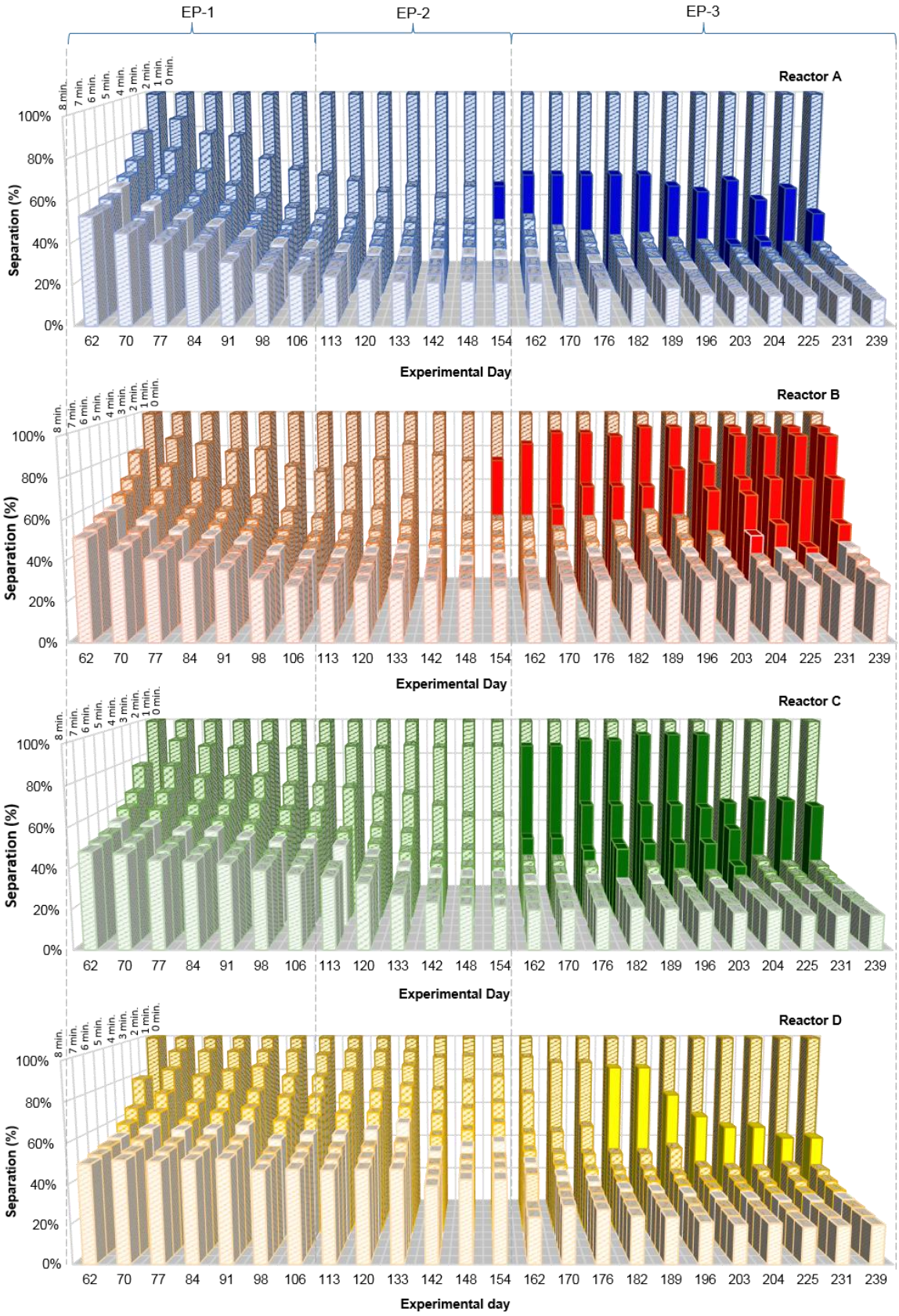

Note: Solid bars represent average value of three phase separation during test

Fig. 6.15. Mixed liquor centrifugation during experimental period – MCRT effect experiment at 20 ^{o}C: FIC test

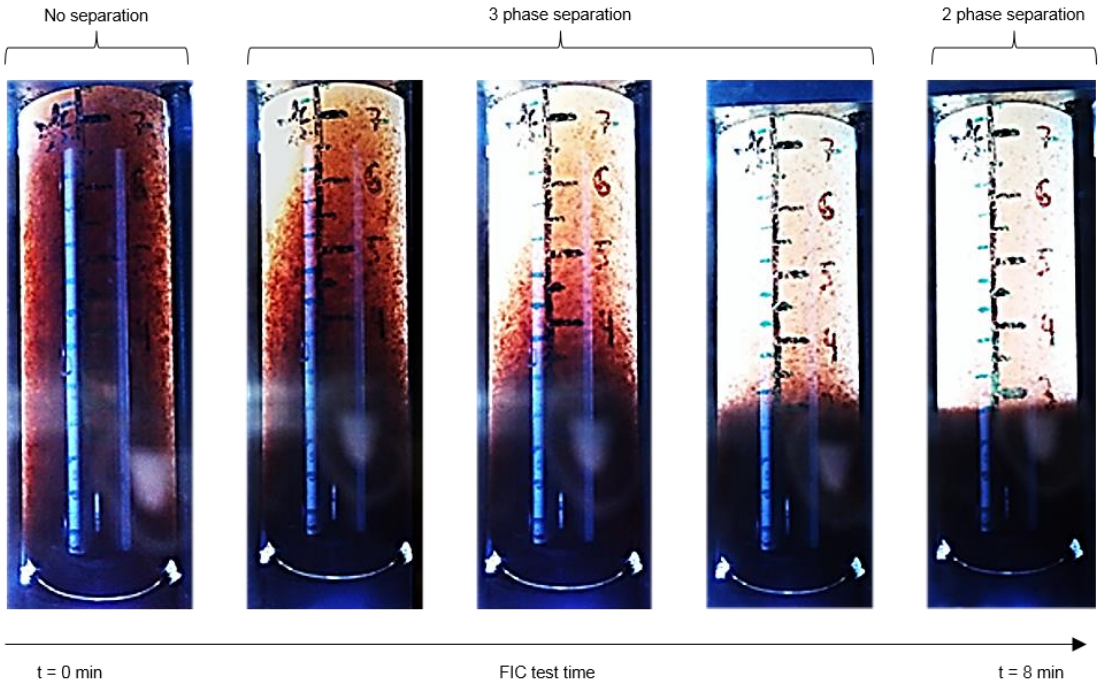

Fig. 6.16. Schematic picture of centrifuged mixed liquor (Reactor B, day 204) during FIC test; showing of no separation, 3 phase separation and 2 phase separation – MCRT effect experiment at 20 ^{o}C.

The carbohydrate and protein concentration also showed an increase in Reactor D compared to the other reactors when the MCRT was reduced to 30 days. Huang et al. (2013) and Huang et al. (2011) also observed higher protein concentrations in bound EPS at shorter MCRTs, and suggested that this may result in bigger flocs which in turn have a lower membrane fouling potential. On the other hand, they stated that longer MCRTs result in finer particles due to reduced flocculation in the presence of lesser amount of EPS, accelerating fouling development; consistent with the outcome of this experiment. The concentration of soluble EPS also showed some relationship with the membrane and reactor performances at longer MCRTs. As shown in Fig. 6.17c and Fig. 6.17d, the concentration of proteins and carbohydrates in the soluble EPS of Reactor C, which showed the fastest membrane fouling when operated at 60 days MCRT, was the highest compared to the other reactors for most of the time. Although the MCRT in Reactor C was changed to 30 days on day 112, the soluble EPS concentration did not respond to this change until day 200, at the same time that the CST times plummeted and the membrane flux started to recover.

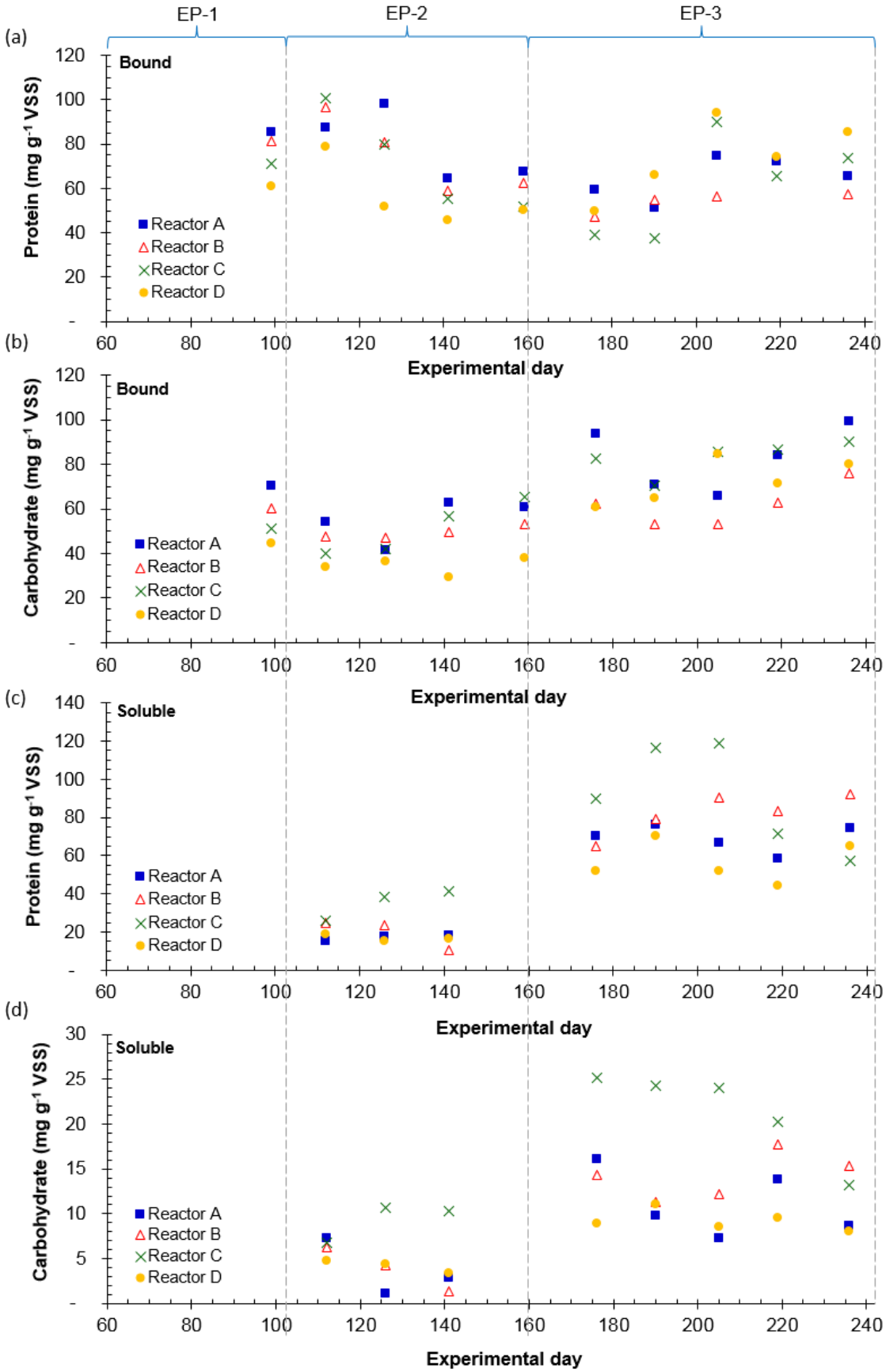

Fig. 6.17. EPS concentration during experimental period – MCRT effect experiment at 20 ^{o}C: (a) Bound EPS protein, (b) Bound EPS carbohydrates, (c) Soluble EPS protein, and (d) Soluble EPS carbohydrates.

Likewise, during EP-3 the concentration of carbohydrates and protein in the soluble EPS of Reactor B, operating at 45 days MCRT, started to become higher when compared to the other reactors which by then were all operating at lower MCRTs. This occurred at exactly the same time that the CST times in Reactor B started to increase and the membrane flux to reduce despite the TMP increase up to 9.8 kPa; finishing the experiment with the highest CST, highest TMP and lowest membrane flux. Huang et al. (2013) reported that at a short MCRT (30 days) the concentration of soluble microbial products was higher, which counteracts the effect of lower EPS and MLSS, resulting in rapid membrane fouling. This is in agreement with the results this experiment and the previous one at 36 ^{o}C where there was no further membrane performance enhancement at MCRT lower than 30 and 25 days, respectively.

In this study no soluble microbial products were measured. Laspidou and Rittmann (2002) suggested that soluble EPS could be similar to soluble microbial products in sludge liquor under some conditions, although Ramesh *et al.* (2006) were unable to prove this. The observed trends in soluble and bound EPS in this study are consistent with other reports, where the general understanding is that bound EPS concentrations tend to increase at shorter MCRT while soluble microbial products tend to decrease. Given the fact that the soluble EPS also decreased at shorter MCRTs, it could be said that if soluble EPS and soluble microbial products are not identical, at least their production could have a similar relationship with MCRT and its impact on membrane performance.

While some EPS differences were observed in this experiment when operating at different MCRT, these were not significant enough to support a strong correlation between the MCRT and the fouling phenomena. Nonetheless, the results are at least consistent with what has been reported in literature so far. On the other hand, although there could be a specific range of MCRT for each system where the concentrations of EPS and SMP could be optimised and thus enhance the membrane performance, the role of EPS quantity and characteristics in fouling as a function of MCRT as well as other operational variables is still not well understood in AnMBR. For

this reason, simpler methods are still necessary to assess the effect of operational parameters in mixed liquor characteristics and the effect on membrane fouling.

6.2.3.4. Microscopic examination

The mixed liquor microscopic examination carried out on day 112 (Fig. 6.18) appears to show bigger biomass floccules in Reactors A (30 days MCRT) and B (45 days (MCRT) when compared to those in Reactor C (60 days MCRT) and D (90 days MCRT). It is worth mentioning that the MLSS at that moment on Reactor A was about 50% of that in Reactor D and 70% of that in Reactor C. This confirms the above suggestion of bigger floc size due higher concentrations of bound EPS at shorter MCRTs.

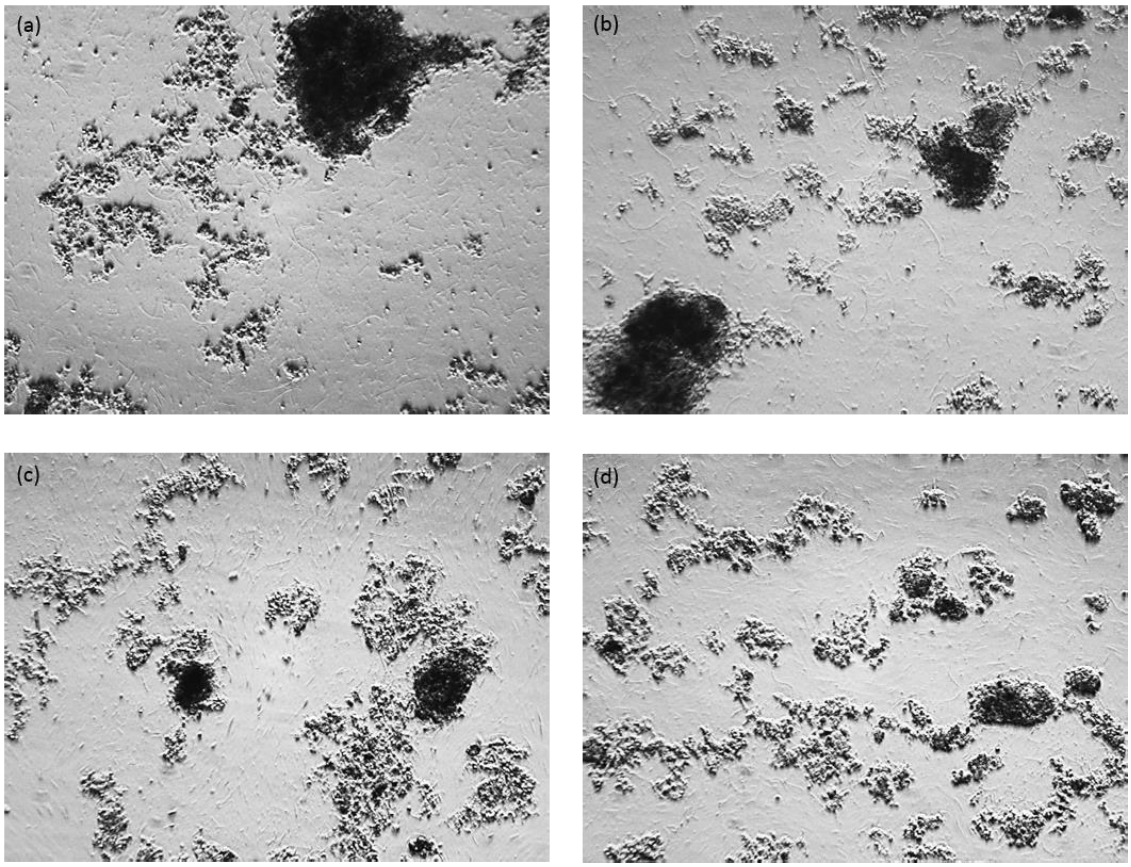

Fig. 6.18. Microscopic examination (10x) of mixed liquor on day 112: (a) Reactor A; (b) Reactor B; (c) Reactor C; (d) Reactor D.

6.2.3.5. Microbial growth and kinetics

In addition to having a major effect on mixed liquor characteristics, MCRT controls the microbial growth rate and hence the potential growth yield. As in the experiment at 36

oC, with each reduction in MCRT there was a sharp increase in the observed biomass yield, followed by a gradual decrease until the value stabilised (Fig. 6.19). This stable yield was taken as the representative for that MCRT and was equal to: 0.131 ± 0.008 g VSS g^{-1} $COD_{removed}$ for 20-day MCRT, 0.124 ± 0. 012 g VSS g^{-1} $COD_{removed}$ for 30-day MCRT, 0.114 ± 0.004 g VSS g^{-1} $COD_{removed}$ for 45-day MCRT. Observed biomass yields for 60 and 90 days MCRT are not reported as the reactors never achieved steady state at these retention times and thus values would not be representative.

The results of this experiment showed that shorter MCRT resulted in higher observed biomass yields, in agreement with the outcome of the previous experiment at 36 ^{o}C. As in the previous experiment, these results further support the argument that at the shorter MCRT a more available carbon is diverted away from methane production into cellular growth, thus reducing the SMP of the substrate. A higher biomass yield due to a shorter MCRT in a full scale system, however, could represent a larger volume of sludge for disposal and possibly a need to supplement with TE, of which both would represent further operational costs.

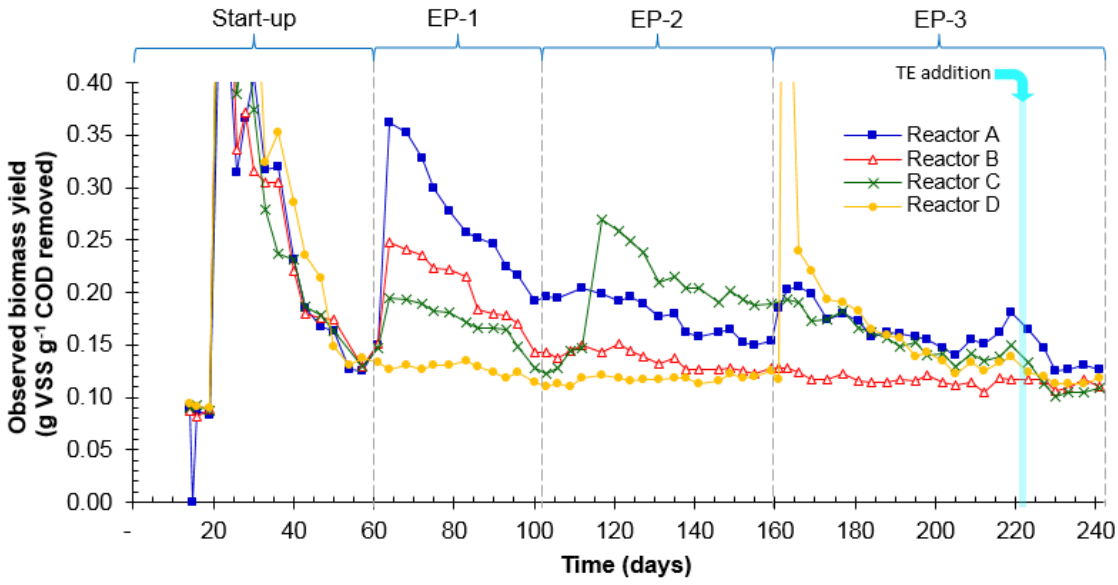

Fig. 6.19. Observed biomass yield

Fig. 6.20 shows the estimated COD used in the observed biomass growth, which resulted greater at shorter MCRTs a steady-state. This result is consistent with the

previous experiment and also supports the conclusion that the lower methane production is associated with high growth rate.

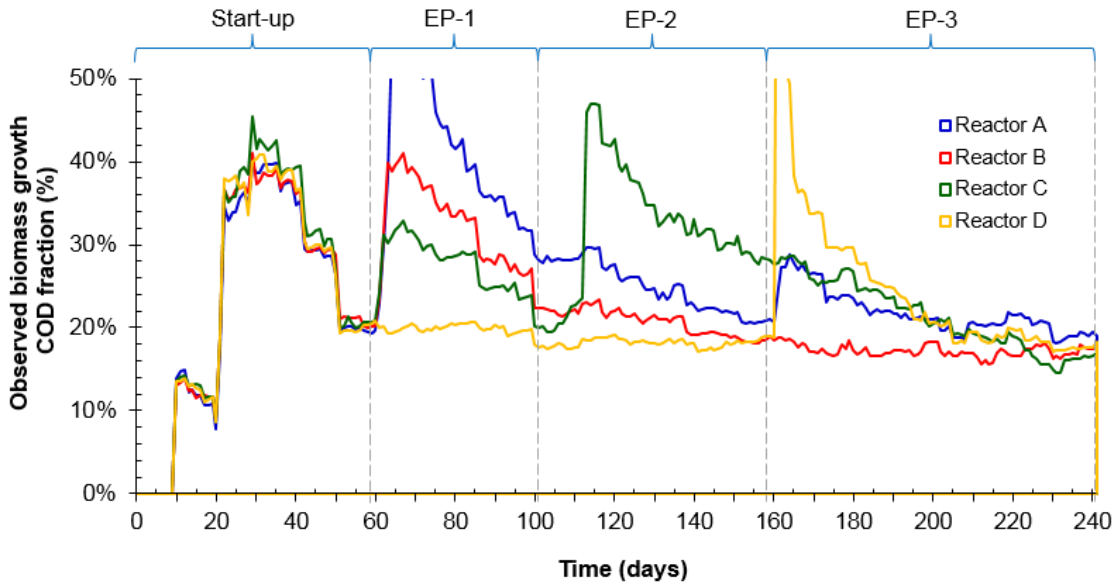

Fig. 6.20. Observed biomass growth COD fraction during experimental period – MCRT effect experiment at 20 ^{o}C.

6.3. Conclusions

Long-term operation of four SAnMBRs at 20 oC on a substrate of low to intermediate strength with a high-suspended solids content was achieved at different MCRTs. This again allowed accurate measurement of the membrane flux rates at different MCRT, as well as determination of COD removal efficiencies and a COD mass balance, estimation of observed biomass yield, and physical characterisation of each mixed liquor using CST tests, FIC tests and the determination of EPS concentration. The results showed a significant effect of MCRT on membrane flux, with shorter MCRT resulting in better membrane performance, better mixed liquor filterability and higher bound EPS concentrations but lower soluble EPS concentrations. Operation at shorter MCRT resulted in lower specific methane production and COD removal rates as well as higher observed biomass yields. Whilst no improvement in membrane performance was observed at MCRTs < 30 days, operation at 60 days MCRT resulted in an earlier onset of poor performance and membrane fouling than at 90 days MCRT. Lower COD removal rates at shorter MCRTs were probably caused by a faster washout of trace

elements due to higher biomass turnaround, confirm by a rapid recovery in the COD removal efficiencies when TE were added. These, however, still remained slightly lower at shorter MCRTs, suggesting that this effect could have also been caused by lower available biomass. Since the overall COD removal efficiencies achieved after the TE were added and the SAnMBRs performance recovered were very close to those observed in the experiment at 36 °C, the influence of the lower operational temperature on the COD removal efficiency was considered negligible. When taken with the results at 36 ^{o}C, this experiment confirmed that there is a potential trade-off to be made between enhanced membrane performance, specific methane production and sludge yield when considering the most suitable operational MCRT.

7. DISCUSSION

7.1. Comparative analysis of the effect of MCRT on SAnMBRs performance at 36 °C and 20 °C

This section presents an analytical comparison between the results from the experiments to evaluate the effect of MCRT on membrane flux, mixed liquor characteristics and overall reactor performance at 36 °C and 20 °C, reported in Chapter 5 and Chapter 6, respectively. Regardless of operational temperature, both experiments showed that shorter MCRTs resulted in better membrane fluxes due to a higher mixed liquor filterability, but lower SMP and higher observed biomass yields. There were, however, some differences between the two experiments due to the difference in operational temperature that are worth highlighting.

7.1.1. Membrane flux

Regardless of the MCRT employed, results also showed higher sustainable membrane fluxes at 36 °C (3.4 - 6.4 L m^{-2} h^{-1}), when compared to those achieved than at 20 °C (2.7 - 4.1 L m^{-2} h^{-1}). This was so even though the TMP during the experiment at 36 °C was generally lower and the overall range of OLR_V applied was higher (0.9 – 1.7 g COD L^{-1} day^{-1}) when compared with those applied in the experiment at 20 °C (0.7 – 1.0 g COD L^{-1} day^{-1}). It is worth mentioning that the narrower range of membrane fluxes and thus of OLR in the experiment at 20 °C, was due to the adjustment of the constant TMP. The higher overall membrane fluxes achieved at 36 °C compared to 20 °C could be related to a lower viscosity of the mixed liquor and thus higher mixed liquor filterability. This was supported by the CST_{MLSS}, which for the experiment at 36 °C resulted much higher than at 20 °C. For example, the average CST_{MLSS} time at 15 days MCRT operating at 36 °C was of 6 seconds L g^{-1}, compared to 44 seconds L g^{-1} obtained at an MCRT of 20 days when operating at 20 °C. In addition, as mentioned before, higher concentrations of soluble microbial products may be present in the mixed liquor when an AnMBR is operated at relatively low temperatures (Bérubé et al., 2006).

7.1.2. Capillary suction time

As mentioned in Section 2.3.4.2, EPS has for long been considered a main parameter to evaluate membrane fouling and the effect of operational parameters on it. Nonetheless, this parameter is far from been fully understood, while methods for analysis of EPS are laborious, complicated and still not standardised. This makes it difficult to compare EPS values from different studies or to find representative correlations with membrane fouling. On the other hand, CST is a simple, standardised and quick method that provides direct information on the dewaterability of the mixed liquor. So far, however, very few studies on AnMBR report this parameter, even though it appears to provide a clear and valuable insight on the effect of that operational parameters have on mixed liquor characteristics and consequently on membrane fouling. As shown in Fig. 7.1, the CST for both experiments at 36 ^{o}C and 20 ^{o}C was lower at shorter MCRTs thus indicating better mixed liquor filterability. It is interesting to note, however, that CST values at short MCRT were much lower at 36 ^{o}C than at 20 ^{o}C, while the CST values for long MCRT were much higher at 36 ^{o}C than at 20 ^{o}C. This suggests that mixed liquor has better filterability at higher temperatures when operating at a short MCRT and a better filterability at lower temperatures when operating at a long MCRT, an important difference between the two temperature ranges. It is interesting to note, however, that the slope of CST increase at longer MCRT is steeper at 36 ^{o}C than at 20 ^{o}C. In the current work the range of variation in CST values tended to be wider at longer MCRTs, most probably because the mixed liquor takes longer to achieve a 'stable state' at a longer MCRT and thus it goes through more changes resulting in greater variation of CST values.

7.1.3. Specific methane production

From Fig. 7.2 it can be seen that the SMP was generally higher at longer MCRTs at both operational temperatures. It can also be observed that overall SMP values were higher at 36 °C than at 20 °C, which could be explained by the influence of temperature on microbial growth. The majority of reactions in the biodegradation of organic matter proceed more slowly at low temperatures than at a mesophilic temperature optimum of 37°C (Lettinga et al., 2001). It is well documented that temperatures below the

optimum have a strong negative effect on the growth rate (see Fig. 2.7) and metabolic activity of anaerobic methanogens (Lettinga et al., 2001), resulting in lower rates of methane production.

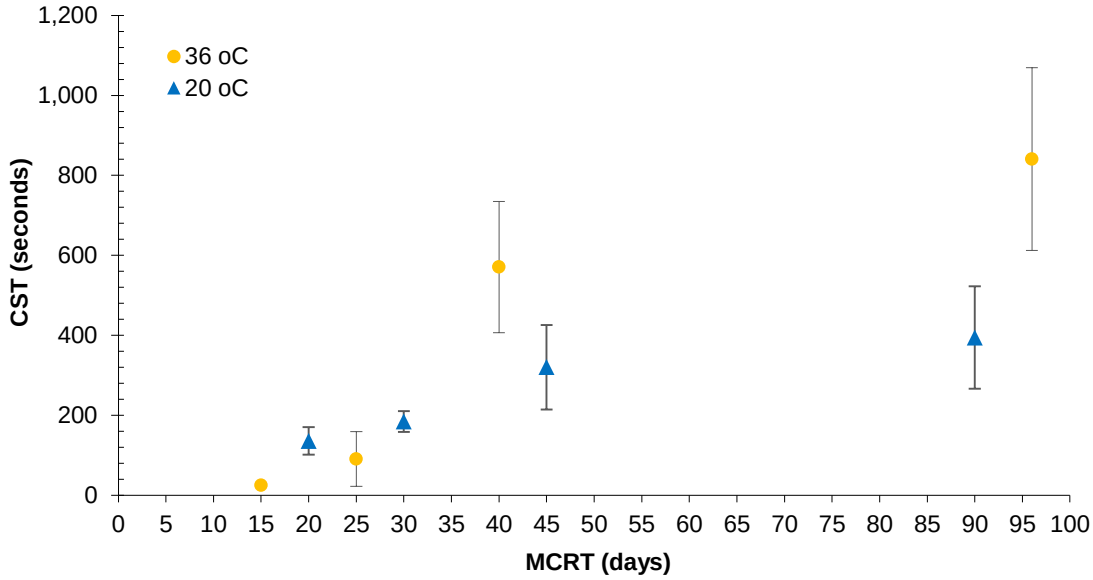

Fig. 7.1. Variation in CST with MCRT in experiments with AnMBR operating temperatures of 20 and 36 °C.

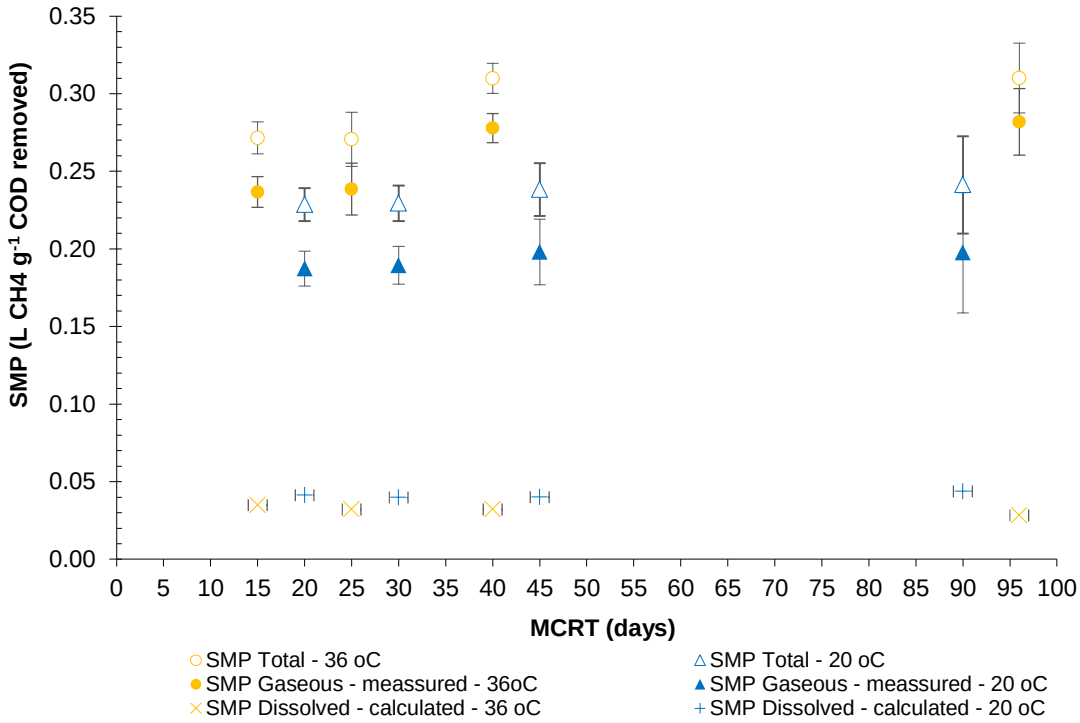

Fig. 7.2. Variation in SMP with MCRT in experiments with AnMBR operating temperatures of 20 and 36 °C[6].

[6] The SMP values shown correspond to the average during stable operation at each MCRT.

7.1.4. Gas composition

Dissolved CH_4 is an issue in all high rate anaerobic reactors for low strength wastewater treatment. As shown in Fig. 7.3, operation of AnMBRs at different temperatures also led to differences in the headspace gas composition; with 2% more CH_4, 6% less CO_2 and 4 % more "other" gases at 20 oC than at 36 ^{o}C. In summary 76% of the biogas produced at 36 ^{o}C was CH_4 (85% normalised to biogas content), compared to 78% at 20 ^{o}C (91% normalised to biogas content). These results suggest that higher solubility of CO_2 at lower temperatures concentrates the CH_4 content in the headspace even more than at 36 ^{o}C. High methane concentrations in the biogas produced are a consequence of the lower solubility of methane compared to CO_2, with a higher fraction of CO_2 leaving the system dissolved in the effluent. The increase in overall methane fraction in the headspace biogas when operating at 20 oC, is due to even lower solubility of methane compared to CO_2 at 20 ^{o}C, thus resulting in an even higher proportion of CO_2 in the liquid phase leaving the reactor. Similar results were reported in a recent review by Ozgun et al. (2013), where the methane content of the biogas was higher at low temperatures due to the difference in gas solubility difference.

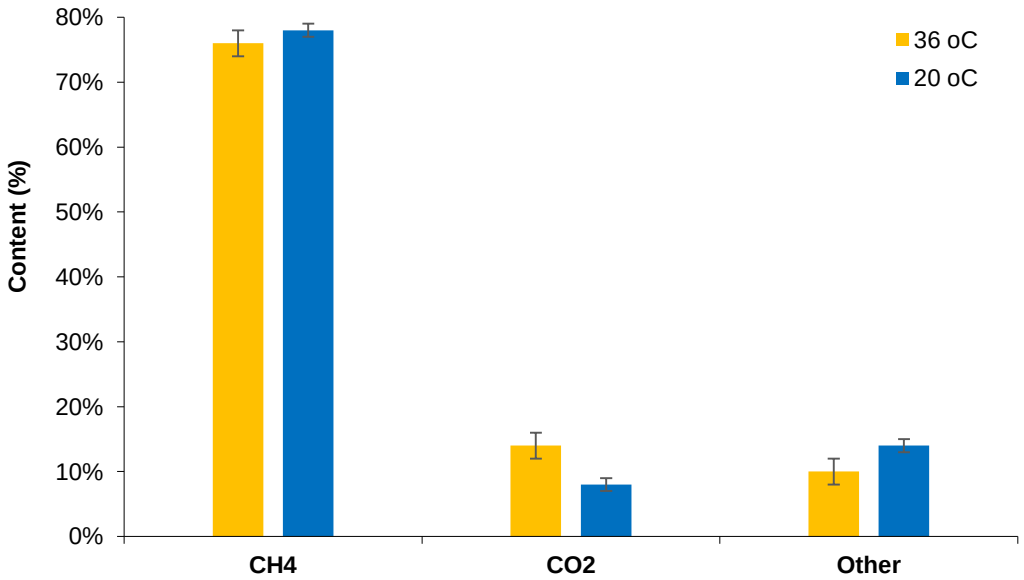

Fig. 7.3. Average gas composition during experiments with variable MCRT at at 36 ^{o}C and 20 ^{o}C.

7.1.5. MLSS

As shown in Fig. 7.4 the MLSS for similar MCRT and under comparable operational conditions was always lower at 20 ^{o}C than at 36 ^{o}C. One explanation for the observed differences could be related to lower overall OLR_v during the experimental phase at 20 ^{o}C (0.7-1.0 g COD L^{-1} day^{-1}) than at 36 ^{o}C (0.9-1.7 g COD L^{-1} day^{-1}). Another, however, could be the expected lower biomass growth rates expected at lower temperatures (Rittmann and McCarty, 2001), which will result in lower MLSS for a similar sludge removal rate.

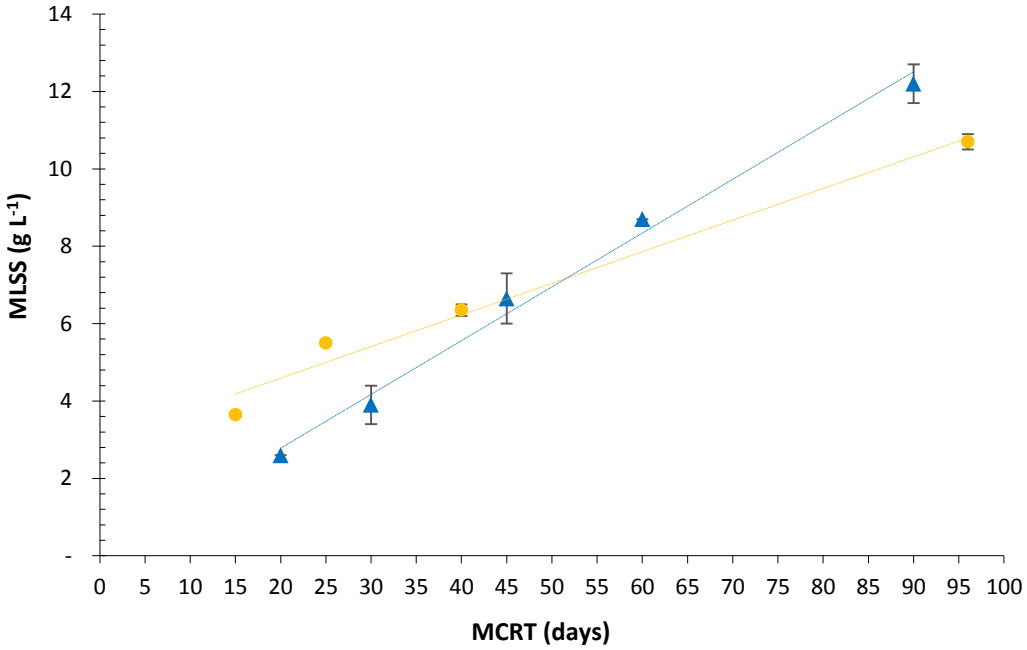

Fig. 7.4. Variation in MLSS with MCRT in experiments with AnMBR operating temperatures of 20 and 36 ^{o}C[7]

7.1.6. COD removal rates

The COD removal rates during the experiment at 36 ^{o}C were practically identical in both reactors irrespective of the MCRTs tested, at around 96%. In contrast, the experiment at 20 ^{o}C showed lower COD removal rates at shorter MCRTs. This was attributed to a more rapid washout of trace elements due to higher biomass turnaround, confirmed by a considerable improvement in the COD removal efficiencies after TE were added. These, however, still remained slightly lower at shorter MCRTs, suggesting that this could also have been caused by lower available biomass. The

[7]The MLSS values shown correspond to the average during stable operation at each MCRT.

influence of the lower operational temperature on the COD removal efficiency was considered negligible, however, as the overall COD removal efficiencies achieved after the TE were added and the SAnMBRs performance recovered were between 92-97%, close to those observed in the experiment at 36 °C under comparable operational conditions. It is clear that further work on the TE requirements and dosing of SAnMBR systems is essential to determine the range of operational parameters to achieve an optimum performance.

7.1.7. Observed biomass yield

Since the observed biomass yield parameter is based on the biomass removed at steady state divided by the COD removed (Section 3.3.8) it is difficult to make a representative comparison of this parameter between operational temperatures. Nonetheless, both experiments showed lower observed biomass yields at higher MCRT, while the overall values for the experiment at 20 ^{o}C were slightly lower than those at similar MCRT in the experiment at 36 ^{o}C. As above, the values for the observed biomass yield for reactors running at 60 and 90 days MCRT of the experiment at 20 ^{o}C were not included as steady-state was never achieved.

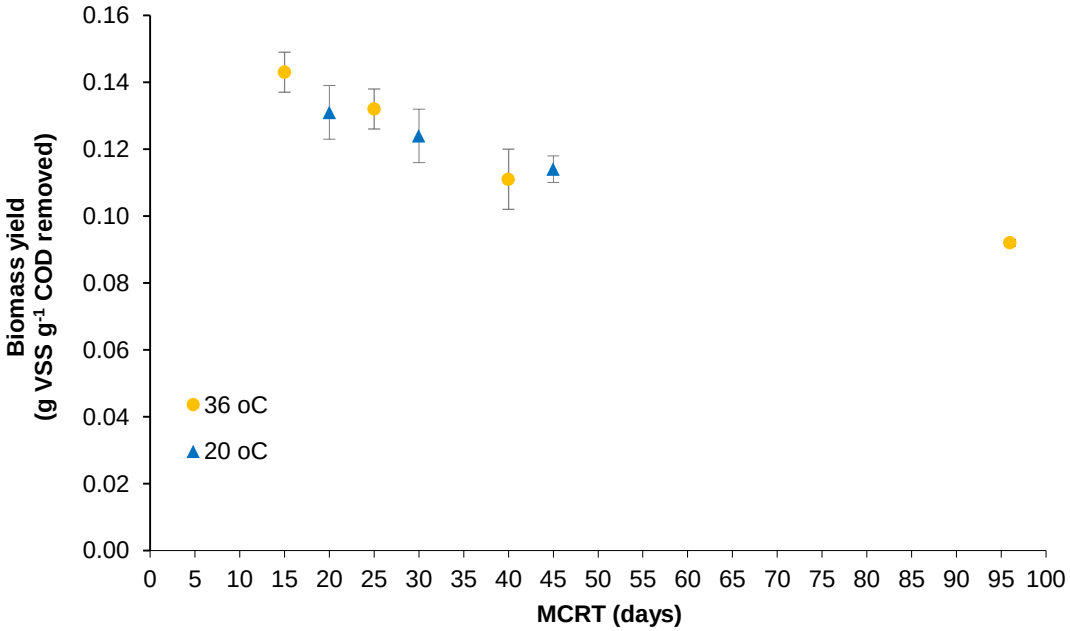

Fig. 7.5. Variation in average observed biomass yield with MCRT in experiments with AnMBR operating temperatures of 20 and 36 ^{o}C[8].

[8] The observed biomass yield shown correspond to the average during stable operation at each MCRT.

7.1.8. Mixed liquor characteristics

Mixed liquor characteristics such as settleability, flocculation ability, hydrophobicity, surface charge, and sludge viscosity play an important role in membrane performance and fouling (WEF, 2012). Samples of each reactor during the experiments in this work were taken to observe further differences in the mixed liquor characteristics due to MCRT, such as settleability. During operation at 36 ^{o}C the digestate of both reactors looked identical at the moment of extraction, with no immediate signs of settlement. By one hour after extraction, however, the biomass in the digestate of Reactor A (15 days MCRT) began to flocculate and float to the surface of the container (Fig. 7.6), while the digestate of Reactor B (96 days MCRT) remained without change or sign of settlement. After one day, most the biomass of Reactor A was flocculated and floating at the top of the container, while the biomass in Reactor B had settled to about two thirds of its initial volume. During operation at 20 ^{o}C the digestate of the reactors also looked identical at the moment of extraction with no immediate signs of settlement Fig. 7.7.

Fig. 7.6. Mixed liquor settleability through time – MCRT effect experiment at 36 ^{o}C: sample taken on day 245, where Reactor A was operated at 15 days MCRT, and Reactor B at 96 days MCRT.

As the time passed, however, initial settling of the biomass was observed in the mixed liquor from Reactor A, C and D. The biomass from Reactor A and D floated to the surface after 3 hours, followed by Reactor B after 4 hours. Biomass of the mixed liquor in Reactor C neither completely floated nor settled.

Fig. 7.7. Mixed liquor settleability through time – MCRT effect experiment at 36 ^{o}C: sample taken on day 209, where Reactor A was operated at 20 days MCRT, Reactor B at 45 days MCRT, Reactor C at 30 days MCRT, and Reactor D at 30 days MCRT.

This biomass flotation could be related to the dissolved biogas in the mixed liquor that lifts the biomass to the surface when desorbing after extracted from the reactor, as happens in a dissolved air flotation (DAF) systems; where the water oversaturated with dissolved air creates microscopic bubbles that adhere to the suspended solids causing them to float to the surface (Metcalf and Eddy, 2004, Féris and Rubio, 1999). This could also be due to residual biogas production in flocs which is more likely at 20 ^{o}C as the sample storage temperature was close to the operating temperature of the SAnMBRs. On the other hand, this effect could be accentuated by higher bound EPS concentrations that may cause higher flocculation of biomass (Huang et al., 2011), and thus increase its floatability. Longer MCRTs tend to lower bound EPS production as microbial growth is lower, resulting in finer particles and thus forming smaller flocs (Huang et al., 2013, Huang et al., 2011). This is consistent with the results in this work where longer MCRTs resulted in slower or no flotation of biomass, also suggested by lower bound EPS concentrations at shorter MCRT.

7.2. Advantages and disadvantages of the gravitational configuration for the study of SAnMBRs and its potential for scalability

The main aim of the gravitational configuration developed in this study was to provide an alternative method to evaluate the performance of the membrane and overall SAnMBR under different operational parameters. Although the main advantages and disadvantages of using the gravitational configuration for this purpose are summarised in Table 7.1, it is important to highlight that the developed configuration proved to be a useful system for the precise assessment of the membrane performance in SAnMBRs under different operational parameters. This also proved to be effective for the evaluation of particular effects such as temperature and substrate characteristics, local restrictions in the permeate line and effluent biogas dissolution.

The results of this study also showed that this configuration represents an alternative to reduce the inherent energy consumption as no pumps are required to feed or withdraw the permeate, which according to Martin et al. (2011) account up to 5% of the total energy consumption in SAnMBRs. In principle the flux induced by a gravitational system should be the same as that for a pumped system when the TMP

values are the same and all other conditions are equal. As mentioned above, a main limitation in a gravitational system is the maximum TMP value that can be induced, and this is dependent on the hydrostatic pressure head which is determined by the engineering design. For example some full-scale Kubota AeMBR use vertically-stacked membrane cassettes to create additional hydrostatic head; this of course is only energetically more favourable where additional head is available in the system upstream of the reactor. While absolute values of flux are dependent on the membrane cleaning system, the nature of the wastewater substrate, and the characteristics of the biomass, the results suggest that a gravitational system could be an alternative to pumped systems if additional head is available and measures are developed to incorporate this into the design, as they have been for AeMBRs. Until steady state conditions are established in the gravitational system, the influent flow and load will decline as these are regulated by the achievable membrane flux and thus the HRT and OLR will vary. Once a constant flux is achieved, however, the system becomes self-regulating, and thus could be simpler to operate and control than a pumped system.

Table 7.1. Advantages and disadvantages of the SAnMBRs in a gravitational configuration

Advantages
• Membrane performance can be critically analysed by direct change in flux rather than TMP • Robust, simple and reliable configuration • Low cost and maintenance configuration • Relatively low TMP required for permeation • Long term sustainable operation can be achieved with constant fluxes, potentially reducing membrane cleaning frequency • Direct inherent energy savings through reduction in pumping costs • Self-regulating influent and effluent • Constant positive pressure inside the reactor • Constant flux can be adjusted by simply varying the TMP via an increase or decrease in the head difference.
Disadvantages
• Variable flux when operated at constant TMP during start-up and membrane fouling stabilisation, resulting in fluctuating HRT and thus OLR • Long flux stabilisation period (although if required this could be reduced by deliberate pre-fouling if enough is known about preferred operating flux) • Operational TMP range limited by head difference available

Another potential benefit of the gravitational SAnMBR are relatively low TMPs required for operation. Although this results in lower membrane fluxes and thus a higher membrane area required, it also represents a less intensive system which could be attractive in some cases, especially if installed membrane costs continue to fall with respect to the energy and operation costs (Stuckey, 2012).

Operation of full-scale membrane bioreactors at constant flow is preferable to constant TMP: this research demonstrated that it is possible to obtain a sustainable flux under a constant TMP in a fully gravitational SAnMBR. It was also demonstrated that TMP can be easily adjusted by increasing or decreasing the head difference and maintain constant membrane fluxes if fouling conditions change. This results extend the full-scale applicability, as a sustainable flux provides an acceptable compromise between capital, operational and maintenance costs for membrane systems (WEF, 2012). The system tested was able to ensure a balance between the influent and effluent as well as a constant positive pressure, self-regulating the feed flux according to the membrane flux (permeate). One of the most complex issues in operation of closed systems with a restriction, such as a membrane, is the coupling of the input and output streams and this successful operation represent a significant achievement. It also increases the potential for scale-up, since regardless of the scale of the reactor the head differences required for gravitational feed and low TMP permeation were only 5 cm and around 20 cm of water head, respectively. Moreover, the MCRT control in a gravitational SAnMBRs could offer a route to achieve a long term sustainable operation and constant flux. This in turn, results in the reduction or omission of chemical membrane cleaning frequency and membrane replacement, which represents direct economic savings in potential full scale systems.

8. CONCLUSIONS AND FUTURE WORK

8.1. Conclusions

A fully gravitational SAnMBR was developed, successfully tested and used to evaluate the effect of MCRT on membrane flux, mixed liquor characteristics and overall reactor performance when treating low-to-intermediate strength wastewater operating at 36 ^{o}C and 20 ^{o}C. The fully gravitational SAnMBR proved to be a useful system for precise observation and assessment of the membrane performance under different operational parameters. It was also able to provide an insight into particular effects such as temperature and substrate characteristics, local restrictions in the permeate line and effluent biogas dissolution.

The work carried out in this research focused on relatively low-to intermediate strength municipal-type wastewaters, using a synthetic substrate composed of sterilised yeast (settleable cellular component), common dairy and meat products (colloidal organic components), sugar (readily utilisable soluble carbon source) and urea (final breakdown product present in urine). The applied OLR_V was achieved by adjusting the synthetic substrate COD by dilution and was limited by HRT, in turn defined by the membrane flux achieved at the constant TMP governed by the hydrostatic head applied across the membrane.

This developed fully gravitational SAnMBR was used in the two core experiments of this research to evaluate the long-term effect of MCRT on membrane flux, mixed liquor characteristics and overall reactor performance operating at 36 ^{o}C and 20 ^{o}C. The experiment at mesophilic temperatures (36 ^{o}C) aimed to elucidate the impacts of MCRT at the optimum temperature of anaerobic systems and thus establish a baseline for operational comparison. The experiment at 20 ^{o}C aimed to clarify the impact of MCRT at a more realistic and feasible operational temperature for low-to-intermediate strength wastewater treatment, and allow comparison with the outcome at mesophilic temperatures.

The biochemical characteristics and stability of the reactors during these two experiments were assessed based on COD conversion, COD removal efficiency, specific methane production (SMP, SMP_{added} and SMP_{MLSS}), pH, MLSS, and MLVSS. COD mass balances were also constructed taking into account carbon converted into new biomass and that as dissolved methane in the effluent. Measurements of observed biomass yield at each MCRT were made along with physical characterisation of each mixed liquor using CST and FIC. For the experiment at 20 ^{o}C the concentration of bound and soluble extracellular polymeric substances (EPS) was also determined.

The experiment at 36 ^{o}C was carried out at a fixed TMP of 2.3 kPa and COD concentration during the experimental phases of 890 g COD L^{-1} resulting in OLR_V between 0.9-1.7 g COD L^{-1} day^{-1}. During the experiment at 20 ^{o}C the TMP was modified within 1.8-9.8 kPa aiming to maintain the membrane flux in all the reactors as close as possible, and thus a narrow the range of operational OLR_V. As a result the OLR_V ranged between 0.7-1.0 g COD L^{-1} day^{-1} with a stable COD concentration during most of the experimental phases of 850 g COD L^{-1}.

The inoculum employed in all the experiments of this work proved to acclimate quite well to the synthetic substrate used, and allowed relatively fast start-up periods. The start-up at 20 ^{o}C, however, showed to be considerably more problematic than at 36 ^{o}C. This was in part due to the need for the biomass to acclimate to the lower temperature, but also possibly due to the effects of dissolved air addition to a diluted inoculum during feeding. Although some lessons were learnt a more detailed study would be valuable to allow development of a suitable protocol for the start-up of SAnMBRs particularly at low operational temperatures.

Although the start-up at 20 ^{o}C took longer to reach a stable performance when compared to operation at 36 ^{o}C, after 60 days the performance was satisfactory to start the experimental phases. Long term sustainable operation was achieved in both experiments, allowing a critical assessment of the membrane performance, and thus a successful evaluation of the effect of MCRT. At either 36 ^{o}C or 20 ^{o}C the results showed that short MCRT gave better performance in terms of membrane flux. There was no

performance enhancement at MCRTs below 25 days and 30 days for 36 ^{o}C and 20 ^{o}C, respectively. Operation at 60 days MCRT in the experiment at 20 ^{o}C showed a faster decrease in membrane flux than at 90 days MCRT at a higher MLSS concentration, despite considerable increases in TMP, suggesting a higher membrane fouling rate. This shows that there may be a particular range of MCRT which combines the worst features for fouling development, and which is not necessarily at the highest or the lowest end of the operational range of the parameter. The correct identification and explicit study of this 'adverse' range of MCRT could result in a breakthrough in the understanding of the effect that the MCRT has on mixed liquor characteristics and consequently in membrane performance. This outcome, however, will inevitably be affected by the nature of the substrate as well as other operational parameters such as the OLR. Therefore, it is crucial to expand this work towards different substrate types and concentrations in order to identify factors affecting them and help determine a generalised optimum MCRTs operational range.

No significant effect of MCRT was observed on COD removal rates when operating at 36 ^{o}C, with COD removal rates always above 96% in both reactors throughout the entire experimental period, despite the different MCRT used. The COD removal rates during the experiment at 20 oC were found to be lower in conditions of suspected TE deficiency. This was confirmed by a considerable recovery in COD removal rates after the addition of trace elements, which rose to 92-97%. Lower OLR_v in the experiment at 20 ^{o}C, compared to the experiment at 36 ^{o}C, could be the reason why this was manifested in this experiment. The observed recovery and high overall COD removal efficiencies achieved after adding TE during the experiment at 20 ^{o}C, helped eliminate the idea of a possible influence of the lower operational temperature on the COD removal efficiency.

The constructed COD mass balances allowed accurate analysis of the impact of MCRT on methane and biomass production. COD balances in both experiment suggested that higher SMP at longer MCRTs could be caused by supplemental methane generation due to endogenous decay; this as a result of lower biomass yields that result in more COD available to be converted to biogas rather than biomass, when compared to short

MCRTs. On the other hand, gaps on the COD balances could be explained by unaccountable biogas that leaves the reactors in gaseous form through the permeate and the COD fraction corresponding to gaseous and dissolved H_2S. Therefore, it is important to appreciate the utility of COD balances as a tool, not only to better understand the performance of a system, but to identify all the phenomena that are involved as well as all the possible mistakes in the calculation of separate elements.

SMP during both experiments was always lower at shorter MCRT, most probably due to a higher fraction of carbon incorporated into biomass due to higher microbial growth rates. Lower overall SMP rates were observed at 20 ^{o}C when compared to those observed at 36 ^{o}C, probably caused by less available biomass as the MLSS concentrations also showed to be generally lower. Yet, low MLSS concentrations could be consequence of a lower OLR_v at 20 ^{o}C but also due to lower biomass growth rates. The SMP_{added} in the experiment at 36 ^{o}C did not show any difference with the SMP values due to the identical COD removal rates during the entire experimental period. In the experiment at 20 ^{o}C, however, the SMP_{added} resulted considerably lower at shorter MCRTs due to the lower COD removal efficiencies COD removal rates probably caused by a faster deficiency of TE in at short retention times. Despite the difference reduced considerably after the TE were added, the SMP_{added} remained slightly higher at longer MCRTs, further supporting the idea of lower carbon availability for methane production at shorter MCRTs. SMP normalised with MLSS (SMP_{MLSS}) in both experiments showed an increase with reducing MCRT, clearly indicating a higher metabolic activity which is consistent with kinetic theory. This, however, contradict the values obtained from data reported by Huang et al. (2011) and Huang et al. (2013), which suggest the opposite tendency. SMP reported in both experiments considered the measured volume of methane produced in the headspace as well as the methane dissolved in the effluent; the latter to improve the comparability between the reactors.

Regarding the effect that MCRT has on mixed liquor characteristics, the outcome of this work showed that this parameter had a very large effect on the ability of the mixed liquor to hold water; with samples at shorter MCRT giving up their water much more readily than those at long MCRT. Consequently short MCRT resulted in in higher

mixed liquor filterability, lower membrane fouling and thus higher membrane fluxes. CST normalised with respect to MLSS confirmed that the MCRT has a direct effect on the biomass filterability, despite the MLSS concentration. The CST test also confirmed observations where too short MCRT did not represent any further improvement in membrane performance or biomass filterability. On the other hand, the CST test results when operating at 20 ^{o}C also showed, at some point, similar CST and even higher CST_{MLSS} at 60 days MCRT to those at 90 days MCRT, despite the fact that the reactor 60 days MCRT had a 25% lower concentration. This result supports the above suggestion of a particular MCRT range which combine the worst features for fouling development, which for the particular conditions of the experiment at 20 ^{o}C happened to be around 60 days MCRT. The outcome of this research clearly demonstrates that CST is a simple but yet reliable test to correlate the impact of operational parameters on mixed liquor characteristics and thus membrane flux and overall reactor performance.

Results from the frozen image centrifugation (FIC) test also showed the large effect that MCRT has on the solid-liquid interface, with samples at shorter MCRT separating the solid phase from the liquid phase much more readily than those at long MCRT. A three phase separation was observed which considerable reduced in Reactor C and D when the MCRT was reduced to 30 days, suggesting that the separation of the solid phase from the liquid phase improved, as the CST did too.

Regarding the EPS tests during the experiment at 20 ^{o}C, shorter MCRT resulted in higher concentrations of carbohydrates and proteins in the bound EPS. In contrast, shorter MCRT resulted in lower concentrations of carbohydrates and proteins in the soluble EPS. This is consistent with the results in this work where longer MCRTs resulted in a delayed or not present flotation of biomass; also supported by lower bound EPS concentrations at shorter MCRT. While the observed differences in EPS were not significant enough to support a strong correlation between the MCRT and the fouling phenomena, the results are at least consistent with what has been reported in literature so far. Moreover, the determination of EPS is very complex and there is no standard method so far.

Overall, the results of this research showed that the MCRT has a considerable effect on the mixed liquor characteristics and thus on the membrane flux and overall reactor performance. It therefore appears that there may be the potential for trade-offs between membrane flux, specific methane production and sludge yield when considering the most suitable operational MCRT.

8.2. Future Work

Further studies are required in order to fully understand the extent of the effect that MCRT has on membrane flux and the global reactor performance. Future research should aim to address the following points:

- Validate the results obtained so far with real sewage or low strength wastewater. Despite the clear advantages of synthetic wastewater for the investigation of processes wastewater treatment, the use of real wastewater is critical to understand the performance of SAnMBRs under real conditions. This however, would provide specific results for the wastewater analysed, and thus a wide range of wastewaters at different concentrations and OLR_v should be tested to broaden the knowledge of the effect of MCRT on SAnMBRs.
- The results obtained in this work could be used as a benchmark of the operational parameters for future work aiming to find the optimum MCRT for this configuration treating sewage at ambient temperature. This in order to find a balance between the membrane performance, methane production and sludge wastage. With this a net energy balance could be constructed and hence a strategy to optimise the energy usage and increase the applicability of this systems for low strength wastewaters.
- Methane loss, either dissolved in the effluent or as observed in this work in gaseous form through the permeate line, is probably the biggest barrier for the application of this systems for the treatment of low-to-intermediate strength wastewater, particularly if operating at ambient temperatures. It is therefore necessary to: (1) improve current methods for determination of dissolved methane in the effluent, in order to enhance the assessment of energy losses

of the system; and (2) investigate the most recent advances for the recovery of a methane loss either dissolved in the effluent and determine if there is any progress in the recovery of the gaseous form in the permeate line.

REFERENCES

Ahmed, Z., Cho, J., Lim, B.-R., Song, K.-G. & Ahn, K.-H. 2007. Effects of sludge retention time on membrane fouling and microbial community structure in a membrane bioreactor. *Journal of Membrane Science,* 287**,** 211-218.

Aiyuk, S., Forrez, I., Lieven, D. K., Haandel, A. v. & Verstraete, W. 2006. Anaerobic and complementary treatment of domestic sewage in regions with hot climates—A review. *Bioresource Technology,* 97**,** 2225–2241.

Akram, A. & Stuckey, D. C. 2008. Flux and performance improvement in a submerged anaerobic membrane bioreactor (SAMBR) using powdered activated carbon (PAC). *Process Biochemistry,* 43**,** 93-102.

Ali, M. A. G. 2014. *Energy recovery from treatment of a synthetic municipal-type wastewater in UASB reactors at ambient temperatures and elevated sulphate concentrations.* PhD thesis, University of Southampton.

APHA, AWWA & WEF 2012. *Standard Methods for the Examination of Water and Wastewater,* Washington, USA, American Public Health Association.

Appels, L., Lauwers, J., Degrève, J., Helsen, L., Lievens, B., Willems, K., Impe, J. V. & Dewil, R. 2011. Anaerobic digestion in global bio-energy production: Potential and research challenges. *Renewable and Sustainable Energy Reviews,* 15**,** 4295–4301.

Aquino, S. F., Hu, A. Y., Akram, A. & Stuckey, D. C. 2006. Characterization of dissolved compounds in submerged anaerobic membrane bioreactors (SAMBRs). *Journal of Chemical Technology & Biotechnology,* 81**,** 1894-1904.

Aslam, M., McCarty, P. L., Bae, J. & Kim, J. 2014. The effect of fluidized media characteristics on membrane fouling and energy consumption in anaerobic fluidized membrane bioreactors. *Separation and Purification Technology,* 132**,** 10-15.

Baek, S. H., Pagilla, K. R. & Kim, H.-J. 2010. Lab-scale study of an anaerobic membrane bioreactor (AnMBR) for dilute municipal wastewater treatment. *Biotechnology and Bioprocess Engineering,* 15**,** 704-708.

Bérubé, P. R., Hall, E. R. & Sutton, P. M. 2006. Parameters Governing Permeate Flux in an Anaerobic Membrane Bioreactor Treating Low-Strength Municipal Wastewaters: A Literature Review. *Water Environment Research,* 78**,** 887-896.

Chabaliná, L. D., Pastor, M. R. & Rico, D. P. 2013. Characterization of soluble and bound EPS obtained from 2 submerged membrane bioreactors by 3D-EEM and HPSEC. *Talanta,* 115**,** 706-712.

Chan, Y., Chong, M., Law, C. & Hassell, D. 2009. A review on anaerobic-aerobic treatment of industrial and municipal wastewater. *Chemical Engineering Journal,* 155**,** 1-18.

Chernicharo, C., van Lier, J., Noyola, A. & Ribeiro, T. 2015. Anaerobic sewage treatment: state of the art, constraints and challenges. *Reviews in Environmental Science and Bio/Technology,* 14**,** 649–679.

Collet, P., Helias, A., Lardon, L., Ras, M., Goy, R. A. & Steyer, J. P. 2011. Life-cycle assessment of microalgae culture coupled to biogas production. *Bioresource Technology,* 102**,** 207-214.

Dereli, R. K., Ersahin, M. E., Ozgun, H., Ozturk, I., Jeison, D., van der Zee, F. & van Lier, J. B. 2012. Potentials of anaerobic membrane bioreactors to overcome treatment limitations induced by industrial wastewaters. *Bioresource technology,* 122**,** 160-170.

Domínguez, L., Rodríguez, M. & Prats, D. 2010. Effect of different extraction methods on bound EPS from MBR sludges. Part I: Influence of extraction methods over three-dimensional EEM fluorescence spectroscopy fingerprint. *Desalination,* 261**,** 19-26.

Dubois, M., Gilles, K. A., Hamilton, J. K., Rebers, P. & Smith, F. 1956. Colorimetric method for determination of sugars and related substances. *Analytical chemistry,* 28**,** 350-356.

Environment-Agency 2007. The determination of chemical oxygen demand in waters and effluents (2007). Bristol, UK.

Féris, L. & Rubio, J. 1999. Dissolved air flotation (DAF) performance at low saturation pressures. *Filtration & separation,* 36**,** 61-65.

Foresti, E., Zaiat, M. & Vallero, M. 2006. Anaerobic processes as the core technology for sustainable domestic wastewater treatment: Consolidated applications, new trends, perspectives, and challenges. *Reviews in Environmental Science and Bio/Technology* 5**,** 3-19.

Frølund, B., Griebe, T. & Nielsen, P. 1995. Enzymatic activity in the activated-sludge floc matrix. *Applied Microbiology and Biotechnology,* 43**,** 755-761.

Gao, D.-W., Zhang, T., Tang, C.-Y. Y., Wu, W.-M., Wong, C.-Y., Lee, Y. H., Yeh, D. H. & Criddle, C. S. 2010. Membrane fouling in an anaerobic membrane bioreactor: Differences in relative abundance of bacterial species in the membrane foulant layer and in suspension. *Journal of Membrane Science,* 364**,** 331-338.

Gao, W. J., Leung, K. T., Qin, W. S. & Liao, B. Q. 2011. Effects of temperature and temperature shock on the performance and microbial community structure of a submerged anaerobic membrane bioreactor. *Bioresource Technology,* 102**,** 8733-8740.

Gimenez, J. B., Robles, A., Carretero, L., Duran, F., Ruano, M. V., Gatti, M. N., Ribes, J., Ferrer, J. & Seco, A. 2011. Experimental study of the anaerobic urban wastewater treatment in a submerged hollow-fibre membrane bioreactor at pilot scale. *Bioresour Technol,* 102**,** 8799-8806.

Gomec, C. Y. 2010. High-rate anaerobic treatment of domestic wastewater at ambient operating temperatures: A review on benefits and drawbacks. *Journal of Environmental Science and Health Part A* 45**,** 1169–1184.

Gutierrez, J. R., Encina, P. G. & Fdz-Polanco, F. 1991. Anaerobic treatment of cheese-production wastewater using a UASB reactor. *Bioresource technology,* 37**,** 271-276.

Henze, M. & Comeau, Y. 2011. Wastewater Characterization. *In:* HENZE, M., LOOSDRECHT, M. C. M. V., EKAMA, G. A. & BRDJANOVIC, D. (eds.) *Biological Wastewater Treatment: Principles, Modelling and Design.* London: IWA Publishing.

Ho, J. & Sung, S. 2009. Anaerobic membrane bioreactor treatment of synthetic municipal wastewater at ambient temperature. *Water Environment Research,* 91**,** 922-928.

Hong, Y., Bayly, R. A., Salasso, D., Cumin, J. R., Sproule, D. E. & Chang, S. 2012. *Method for utilizing internally generated biogas for closed membrane system operation*. USA patent application.

Hu, A. Y. & Stuckey, D. C. 2006. Treatment of Dilute Wastewaters Using a Novel Submerged Anaerobic Membrane Bioreactor. *Environmental Engineering,* 132**,** 190-198.

Hu, A. Y. & Stuckey, D. C. 2007. Activated Carbon Addition to a Submerged Anaerobic Membrane Bioreactor: Effect on Performance, Transmembrane Pressure, and Flux. *Journal of Environmental Engineering,* 133**,** 73-80.

Huang, Z., Ong, S. L. & Ng, H. Y. 2011. Submerged anaerobic membrane bioreactor for low-strength wastewater treatment: effect of HRT and SRT on treatment performance and membrane fouling. *Water Research,* 45**,** 705-713.

Huang, Z., Ong, S. L. & Ng, H. Y. 2013. Performance of submerged anaerobic membrane bioreactor at different SRTs for domestic wastewater treatment. *J Biotechnol,* 164**,** 82-90.

Idrus, S. 2013. *Washing of wheat straw to improve its combustion properties with energy recovery by anaerobic digestion of the washwate.* PhD, University of Southampton.

Janus, T. & Ulanicki, B. 2010. Modelling SMP and EPS formation and degradation kinetics with an extended ASM3 model. *Desalination,* 261**,** 117-125.

Jinsong, Z., Chuan, C. H., Jiti, Z. & Fane, A. G. 2006. Effect of Sludge Retention Time on Membrane Bio-Fouling Intensity in a Submerged Membrane Bioreactor. *Separation Science and Technology,* 41**,** 1313-1329.

Judd, S. 2008. The status of membrane bioreactor technology. *Trends Biotechnol,* 26**,** 109-116.

Judd, S. & Judd, C. 2011. *The MBR Book: Principles and Applications of Membrane Bioreactors for Water and Wastewater Treatment,* Oxford, Elsevier Science Ltd.

Judd, S., Kim, B.-g. & Amy, G. 2008. Membrane Bio-reactors. *In:* HENZE, M., LOOSDRECHT, M. C. M. V., EKAMA, G. A. & BRADJANOVIC, D. (eds.) *Biological Wastwater Treatment: Principle, Modeling and Design.* London: IWA Publishing.

Kunacheva, C. & Stuckey, D. C. 2014. Analytical methods for soluble microbial products (SMP) and extracellular polymers (ECP) in wastewater treatment systems: a review. *Water Res,* 61**,** 1-18.

Laspidou, C. S. & Rittmann, B. E. 2002. A unified theory for extracellular polymeric substances, soluble microbial products, and active and inert biomass. *Water Research,* 36**,** 2711-2720.

Le-Clech, P., Chen, V. & Fane, T. A. G. 2006. Fouling in membrane bioreactors used in wastewater treatment. *Journal of Membrane Science,* 284**,** 17-53.

Lettinga, G., Rebac, S. & Zeeman, G. 2001. Challenge of psychrophilic anaerobic wastewater treatment. *TRENDS in Biotechnology,* 19**,** 363-370.

Lew, B., Tarre, S., Belavski, M. & Green, M. 2004. UASB reactor for domestic wastewater treatment at low temperatures: a comparison between a classical UASB and hybrid UASB-filter reactor. *Water Science & Technology,* 49**,** 295-301.

Liang, Z., Li, W., Yang, S. & Du, P. 2010. Extraction and structural characteristics of extracellular polymeric substances (EPS), pellets in autotrophic nitrifying biofilm and activated sludge. *Chemosphere,* 81**,** 626-632.

Liao, B.-Q., Kraemer, J. T. & Bagley, D. M. 2006. Anaerobic Membrane Bioreactors: Applications and Research Directions. *Critical Reviews in Environmental Science and Technology,* 36**,** 489-530.

Lin, H., Chen, J., Wang, F., Ding, L. & Hong, H. 2011. Feasibility evaluation of submerged anaerobic membrane bioreactor for municipal secondary wastewater treatment. *Desalination,* 280**,** 120-126.

Lin, H., Peng, W., Zhang, M., Chen, J., Hong, H. & Zhang, Y. 2013. A review on anaerobic membrane bioreactors: Applications, membrane fouling and future perspectives. *Desalination,* 314**,** 169-188.

Liu, H. & Fang, H. H. 2002. Extraction of extracellular polymeric substances (EPS) of sludges. *Journal of Biotechnology,* 95**,** 249-256.

Lousada-Ferreira, M. 2011. *Filterability and sludge concentration in Membrane Bioreactors*, TU Delft, Delft University of Technology.

Lousada-Ferreira, M., Geilvoet, S., Moreau, A., Atasoy, E., Krzeminski, P., Van Nieuwenhuijzen, A. & van der Graaf, J. 2010. MLSS concentration: Still a poorly understood parameter in MBR filterability. *Desalination,* 250**,** 618-622.

Mahmoud, N., Zeeman, G., Gijzen, H. & Lettinga, G. 2004. Anaerobic sewage treatment in a one-stage UASB reactor and a combined UASB-Digester system. *Water Research,* 38**,** 2348–2358.

Mara, D. 2003. *Domestic Wastewater Treatment in Developing Countries*, Earthscan.

Mara, D. & Horan, N. 2008. Handbook of Water and Wastewater Microbiology. 1-621.

Martin, I., Pidou, M., Soares, A., Judd, S. & Jefferson, B. 2011. Modelling the energy demands of aerobic and anaerobic membrane bioreactors for wastewater treatment. *Environmental Technology,* 32**,** 921-932.

Martinez-Sosa, D., Helmreich, B., Netter, T., Paris, S., Bischof, F. & Horn, H. 2011. Anaerobic submerged membrane bioreactor (AnSMBR) for municipal wastewater treatment under mesophilic and psychrophilic temperature conditions. *Bioresour Technol,* 102**,** 10377-10385.

Meng, F., Yang, F., Shi, B. & Zhang, H. 2008. A comprehensive study on membrane fouling in submerged membrane bioreactors operated under different aeration intensities. *Separation and Purification Technology,* 59**,** 91-100.

Menniti, A. & Morgenroth, E. 2010. The influence of aeration intensity on predation and EPS production in membrane bioreactors. *Water Research,* 44**,** 2541-2553.

Metcalf & Eddy 2004. *Water Engineering Treatment and Reuse,* New York, McGraw Hill.

Muga, H. & Mihelcic, J. 2008. Sustainability of wastewater treatment technologies. *Journal of environmental management,* 88**,** 437-447.

Navaratna, D. & Jegatheesan, V. 2011. Implications of short and long term critical flux experiments for laboratory-scale MBR operations. *Bioresource Technology,* 102**,** 5361–5369.

Ng, H. Y., Tan, T. W. & Ong, S. L. 2006. Membrane Fouling of Submerged Membrane Bioreactors: Impact of Mean Cell Residence Time and the Contributing Factors. *Environmental Science & Technology,* 40**,** 2706-2713.

Ozgun, H., Dereli, R. K., Ersahin, M. E., Kinaci, C., Spanjers, H. & van Lier, J. B. 2013. A review of anaerobic membrane bioreactors for municipal wastewater

treatment: Integration options, limitations and expectations. *Separation and Purification Technology,* 118**,** 89-104.

Parker, W. J., Jones, R. M. & Murthy, S. Year. Characterization of the COD/VSS Ratio during Anaerobic Digestion of Waste Activated Sludge: Experimental and Modeling Studies. *In:* WEFTEC 2008. 524-533.

Peace-software. *Calculation of thermodynamic state variables* [Online]. Berlin, Germany.[Accessed 27/11/2014]Available http://www.peacesoftware.de/einigewerte/co2_e.html; http://www.peacesoftware.de/einigewerte/methan_e.html

Perry, R. H. & Green, D. W. 1999. *Chemical Engineer's Handbook*, McGraw Hill.

Purdue-University. Year. Proceedings of the 50th Industrial Waste Conference. *In:* Industrial Waste Conference, 1995 West Lafayette, Indiana. Ann Arbor Press.

Rajeshwari, K.V., Balakrishnan, M., Kansal, A., Lata, K. and Kishore, V.V.N., 2000. State-of-the-art of anaerobic digestion technology for industrial wastewater treatment. Renewable and Sustainable Energy Reviews, 4(2), pp.135-156.

Ramesh, A., Lee, D.-J. & Hong, S. 2006. Soluble microbial products (SMP) and soluble extracellular polymeric substances (EPS) from wastewater sludge. *Applied microbiology and biotechnology,* 73**,** 219-225.

Rittmann, B. E. & McCarty, P. L. 2001. *Environmental Biotechnology: Principles and Applications,* New York, USA, McGraw-Hill.

Rosenberger, S., Laabs, C., Lesjean, B., Gnirss, R., Amy, G., Jekel, M. & Schrotter, J. C. 2006. Impact of colloidal and soluble organic material on membrane performance in membrane bioreactors for municipal wastewater treatment. *Water Res,* 40**,** 710-720.

Sander, R. 1999. Compilation of Henry's Law Constants for Inorganic and Organic Species of Potential Importance in Environmental Chemistry. Germany: Air Chemistry Department, Max-Planck Institute of Chemistry.

Sawalha, O. & Scholz, M. 2007. Assessment of capillary suction time (CST) test methodologies. *Environ Technol,* 28**,** 1377-1386.

Scholz, M. 2005. Review of recent trends in Capillary Suction Time (CST) dewaterability testing research. *Ind. Eng. Chem. Res.,* 44**,** 8157 - 8163.

Seadi, T. A., Rutz, D., Prassl, H., Köttner, M., Finsterwalder, T., Volk, S. & Janssen, R. 2008. *Biogas Handbook,* Esbjerg, Denmark, University of Southern Denmark Esbjerg.

Seghezzo, L., Zeeman, G., Van Liel, J., Hamelers, H. & Lettinga, G. 1998. A Review: The anaerobic Treatment of Sewage in UASB and EGSB Reactors. *Bioresource Technology,* 65**,** 175-190.

Shore, J. L., M'Coy, W. S., Gunsch, C. K. & Deshusses, M. A. 2012. Application of a moving bed biofilm reactor for tertiary ammonia treatment in high temperature industrial wastewater. *Bioresource technology,* 112**,** 51-60.

Siembida, B., Cornel, P., Krause, S. & Zimmermann, B. 2010. Effect of mechanical cleaning with granular material on the permeability of submerged membranes in the MBR process. *Water Research,* 44**,** 4037-4046.

Skouteris, G., Hermosilla, D., López, P., Negro, C. & Blanco, Á. 2012. Anaerobic membrane bioreactors for wastewater treatment: A review. *Chemical Engineering Journal,* 198-199**,** 138-148.

Smith, A. L., Skerlos, S. J. & Raskin, L. 2013. Psychrophilic anaerobic membrane bioreactor treatment of domestic wastewater. *Water research,* 47**,** 1655-1665.

Smith, A. L., Stadler, L. B., Cao, L., Love, N. G., Raskin, L. & Skerlos, S. J. 2014. Navigating wastewater energy recovery strategies: a life cycle comparison of anaerobic membrane bioreactor and conventional treatment systems with anaerobic digestion. *Environ Sci Technol,* 48**,** 5972-5981.

Smith, A. L., Stadler, L. B., Love, N. G., Skerlos, S. J. & Raskin, L. 2012. Perspectives on anaerobic membrane bioreactor treatment of domestic wastewater: A critical review. *Bioresource Technology,* 122**,** 149-159.

Souza, C., Chernicharo, C. & Aquino, S. 2011. Quantification of dissolved methane in UASB reactors treating domestic wastewater under different operating conditions. *Water Science & Technology,* 64.

Spagni, A., Casu, S., Crispino, N. A., Farina, R. & Mattioli, D. 2010. Filterability in a submerged anaerobic membrane bioreactor. *Desalination,* 250**,** 787-792.

Speece, R. E. 1996. *Anaerobic Biotechnology for Industrial Wastewaters*, Archae Press.

Spellman, F. R. 2003. *Handbook of Water and Wastewater Treatment Plant Operations,* New York, USA, Lewis Publishers.

Stuckey, D. C. 2012. Recent developments in anaerobic membrane reactors. *Bioresource Technology,* 122**,** 137-148.

SWQB 2007. Wastewater systems operator certification study manual. New Mexiuco, USA: Surface Water Quality Bureau , Water Utilities Technical Assistance Program.

Tan, T. W., Ng, H. Y. & Ong, S. L. 2008. Effect of mean cell residence time on the performance and microbial diversity of pre-denitrification submerged membrane bioreactors. *Chemosphere,* 70**,** 387-396.

Ueda, T. & Hata, K. 1999. Domestic Wastewater treatment by a Submerged Membrane Bioreactor with Gravitational Filtration. *Water Research,* 33**,** 2888-2892.

Ueda, T. & Horan, N. 1999. Fate of indigenous bacteriophage in a membrane bioreactor. *Water Research,* 34**,** 2151-2159.

van Lier, J. B., Mahmoud, N. & Zeeman, G. 2008. Anaerobic Wastewater Treatment *In:* HENZE, M., LOOSDRECHT, M. C. M. V., EKAMA, G. A. & BRADJANOVIC, D. (eds.) *Biological Wastewater Treatment - Principles, Modelling and Desing.* IWA Publishing.

Visvanathan, C. & Abeynayaka, A. 2012. Developments and future potentials of anaerobic membrane bioreactors (AnMBRs). *Membrane Water Treatment,* 3**,** 1-23.

Vyrides, I. & Stuckey, D. C. 2009. Saline sewage treatment using a submerged anaerobic membrane reactor (SAMBR): effects of activated carbon addition and biogas-sparging time. *Water Res,* 43**,** 933-942.

Walker, M., Zhang, Y., Heaven, S. & Banks, C. 2009. Potential s in the quantitative evaluation of biogas production in anaerobic digestion processes. *Bioresource Technology,* 100**,** 6339-6346.

Walsh, K. & McaLaughlan, R. 1998. Bubble extraction of dissolved gases from groundwater samples. *Water, Air, and Soil Pollution,* 115**,** 525-534.

Water-UK 2011. Sustainability Indicators 2010/11. Water-UK.

WEF 2012. *Membrane bioreactors - WEF Manual of Practice no. 36,* Alexandria, Virginia, Water Environment Federation.

Whalley, C. P. 2008. *Performance of variable climate waste stabilisation ponds during the critical spring warm-up period.* PhD thesis, University of Southampton.

WTW 2000. Application report O2 500230. Germany.

Yeo, H., An, J., Reid, R., Rittmann, B. E. & Lee, H. S. 2015. Contribution of Liquid/Gas Mass-Transfer Limitations to Dissolved Methane Oversaturation in Anaerobic Treatment of Dilute Wastewater. *Environ Sci Technol,* 49**,** 10366-10372.

Yeo, H. & Lee, H.-S. 2013. The effect of solids retention time on dissolved methane concentration in anaerobic membrane bioreactors. *Environmental Technology,* 34**,** 2105-2112.

Zamalloa, C., Vrieze, J. D., Boon, N. & Verstraete, W. 2012. Anaerobic digestibility of marine microalgae Phaeodactylum tricornutum in a lab-scale anaerobic membrane bioreactor. *Applied Microbiology and Biotechnology,* 93**,** 859–869.

Zheng, X. & Liu, J. 2006. Dyeing and printing wastewater treatment using a membrane bioreactor with a gravity drain. *Desalination,* 190**,** 277-286.

Zheng, X. & Liu, J. X. 2005. Optimization of operational factors of a membrance bioreactor with gravity drain. *Water Science & Technology,* 52**,** 10-11.

APPENDIX A. – LITERATURE REVIEW ON RELEVANT SANMBRS TREATING LOW-TO-INTERMEDIATE STRENGTH WASTEWATER - EXPERIMENTAL SET-UP AND OPERATIONAL PARAMETERS

Appendix A - Table 1. Literature compilation of relevant SAnMBRs treating low-to-intermediate strength wastewater - experimental set-up and operational parameters

Reference	Experiment Length (days)	Substrate (mg COD L^{-1})	Inoculum	Stage / Permeate Mode	Module Type	Working volume (L)	Packing density (m^2 L^{-1})*	Flux (L m^{-2} $hour^{-1}$)	TMP (kPa)	OLRv (g COD L^{-1} day^{-1})	Temp (ºC)	HRT (hours)	MCRT (days)	MLSS (g L^{-1})	MLVSS (g L^{-1})	Sparging (L min^{-1})	COD removal (%)
Hu and Stuckey (2006)	105	Synthetic wastewater (460± 20 mg L^{-1})	Sieved seed sludge	Single stage / Pumped	HF	3	-	15.0 10.0 1.25	50 40 8	0.46 *	35	48-3	-	4.1 ± 0.5	3.0 ± 0.2	5.0	90 %
		Synthetic wastewater (460± 20 mg L^{-1})	Sieved seed sludge	Single stage / Pumped	FS	3	0.04	15.0 10.0 1.25	40 29 2.5	0.46 *	35	48-3	-	4.1 ± 0.5	3.0 ± 0.2	5.0	90 %
		Glucose (460± 20 mg L^{-1})	Sieved seed sludge	Single stage / Pumped	FS	3	0.04	15.0 10.0 1.25	38 27 2	0.46 *	35	48-3	-	4.1 ± 0.5	3.0 ± 0.2	5.0	90 %
Lin et al. (2011)	106	Municipal wastewater (342–527 mg L^{-1})	-	Single stage / Pumped	FS	60	0.01	12.0	-	1.00	30 ± 3	10	∞	6.4 – 9.3	-	5.0	88 %
Huang et al. (2011)	2-3 weeks start up + 5 months per HRT test*	Synthetic wastewater (550 mg L^{-1})	Seed biomass from anaerobic sludge digester	2 stage / Pumped	CSTR + FS	5+1	0.02	5.3	0 – 30	1.00	25 - 30	12	30 60 ∞	5.6 ± 0.6 5.7 ± 0.7 6.5 ± 1.1	5.1 ± 0.5 5.2 ± 0.7 5.4 ± 1.0	-	99 % 98 % 97 %
		Synthetic wastewater (550 mg L^{-1})	Seed biomass from anaerobic sludge digester	2 stage / Pumped	CSTR + FS	5+1	0.02	6.4	0 – 30	1.32	25 - 30	10	30 60 ∞	7.0 ± 0.6 8.9 ± 1.0 9.1 ± 0.9	6.4 ± 0.5 7.9 ± 0.8 7.9 ± 0.9	-	97 % 98 % 98 %
		Synthetic wastewater (550 mg L^{-1})	Seed biomass from anaerobic sludge digester	2 stage / Pumped	CSTR + FS	5+1	0.02	7.9	0 – 30	1.65	25 - 30	8	30 60 ∞	7.1 ± 0.8 8.7 ± 1.2 10.5 ± 0.8	6.5 ± 0.7 7.3 ± 1.1 9.4 ± 0.7	-	99 % 98 % 95 %
Huang et al. (2013)	50	Municipal wastewater (426.8 ± 60 mg L^{-1})	Seed biomass from anaerobic sludge digester	2 stage / Pumped	CSTR + FS	5+1	0.02	5*	0 – 30	1.02 ± 0.14	25 - 30	10	30	8.0	6.0	-	84 %
		Municipal wastewater (426.8 ± 60 mg L^{-1})	Seed biomass from anaerobic sludge digester	2 stage / Pumped	CSTR + FS	5+1	0.02	5*	0 – 30	1.02 ± 0.14	25 - 30	10	60	12.6	9.3	-	85 %
		Municipal wastewater (426.8 ± 60 mg L^{-1})	Seed biomass from anaerobic sludge digester	2 stage / Pumped	CSTR + FS	5+1	0.02	5*	0 – 30	1.02 ± 0.14	25 - 30	10	90	13.6	9.9	-	86 %

Appendix A – Table 1 (continued). Literature compilation of relevant SAnMBRs treating low-to-intermediate strength wastewater - experimental set-up and operational parameters

Reference	Experiment Length (days)	Substrate (mg COD L^{-1})	Inoculum	Permeate Mode	Module Type	Working volume (L)	Packing density (m^2 L^{-1})*	Flux (L m^{-2} $hour^{-1}$)	TMP (kPa)	OLRv (g COD L^{-1} day^{-1})	Temp (ºC)	HRT (hours)	MCRT (days)	MLSS (g L^{-1})	MLVSS (g L^{-1})	Sparging (L min^{-1})	COD removal (%)
Spagni et al. (2010)	250	Synthetic wastewater	Wet granular seed sludge from full scale UASB	Single stage / Pumped	FS	11	0.01	Start-up 6; 9; 11-12 Test 2	Start-up 30; 100; 500 Test < 500	13.00	35 ± 1	-	Start-up ∞	Start-up 5.5 - 20.4 Test: up to 53.0		20.0	-
Aquino et al. (2006)	100	Synthetic wastewater (450 ± 20 mg L^{-1})		Single stage / Pumped	FS	3	0.04	10.0 20.0	15 25 – 27		35 ± 1	6	150		2.6 ± 0.1	5.0	90 %
		Synthetic wastewater (450 ± 20 mg L^{-1})		Single stage / Pumped	FS + PAC	3	0.04	10.0 20.0	0 10.0		35 ± 1	6	150		3.7 ± 0.2	5.0	90 %
Akram and Stuckey (2008)	52	Synthetic wastewater (4000 mg L^{-1})	Digestate from previous SAnMBR work	Single stage / Pumped	FS	3	0.04				35 ± 1	15	250		12.4	5.0	96 %
	32	Synthetic wastewater (4000 mg L^{-1})	Digestate from previous SAnMBR work	Single stage / Pumped	FS + PAC	3	0.04				35 ± 1	6	250		11.4	5.0	98 % 88 %
	32	Synthetic wastewater (4000 mg L^{-1})	Digestate from previous SAnMBR work	Single stage / Pumped	FS + PAC	3	0.04				35 ± 1	6	250		16.1	5.0	98 %
Baek *et al.* (2010)	440	Municipal wastewater		Single stage / Pumped	CSTR + FS	10					?	24	19 - 217	-	-	-	
Yeo and Lee (2013)	60	Glucose (5000 mg L^{-1})	Digestate from glucose operated AD reactor	Single stage / Pumped	HF	5.72	0.01				23 ± 1	240*	20 40	1.25 ± 0.0 0.86 ± 0.1	0.93 ± 0.1 0.71 ± 0.0	0.8	
Hu and Stuckey (2007)	93	Synthetic wastewater (460 ± 20 mg L^{-1})		Single stage / Pumped	FS	3	0.04	10 – 20	13 – 26		35	24, 12, 6, 3	100	4.3 – 4.8	2.9 – 3.3	5.0	> 90%
		Synthetic wastewater (460 ± 20 mg L^{-1})		Single stage / Pumped	FS + PAC (1.7 g L-1)	3	0.04	10 – 20	0 – 12		35	24, 12, 6, 3	100	4.3 – 4.8	2.9 – 3.3	5.0	> 90%
		Synthetic wastewater (460 ± 20 mg L^{-1})		Single stage / Pumped	FS + GAC (1.7 g L-1)	3	0.04	10 – 20	10 – 16		35	24, 12, 6, 3	100	4.3 – 4.8	2.9 – 3.3	5.0	> 90%

Appendix A – Table 1 (continued). Literature compilation of relevant SAnMBRs treating low-to-intermediate strength wastewater - experimental set-up and operational parameters

Reference	Experiment Length (days)	Substrate (mg COD L^{-1})	Inoculum	Permeate Mode	Module Type	Working volume (L)	Packing density (m^2 L^{-1})*	Flux (L m^{-2} $hour^{-1}$)	TMP (kPa)	OLRv (g COD L^{-1} day^{-1})	Temp (ºC)	HRT (hours)	MCRT (days)	MLSS (g L^{-1})	MLVSS (g L^{-1})	Sparging (L min^{-1})	COD removal (%)
Vyrides and Stuckey (2009)	203	Synthetic wastewater (465 ± 20 mg L^{-1}) Salinity 10, 15, 20, 35 mg NaCl L^{-1}	Conventional sludge digester conditioned to salinity lower than 2 g NaCL L-1	Pump Single stage / Pumped	FS	3	0.04	5 – 8	27 – 47	2.0	35 ± 1	20, 8	250	-	2 – 3	5.0	40 – 99% (DOC removal)
Gimenez et al. (2011)	150	Municipal wastewater (445 ± 95 mg L^{-1})	Seed biomass from anaerobic sludge digester	2 stage / Pumped	CSTR + HF (2)	900 + 600 (2) 2100	0.03	8 - 20	8 (10 L M^{-2} hr^{-1})	-	33	6 – 21	70	19 (MLTS)	12.5 (MLVS)	66 (1.1 L m^{-2} min^{-1})	86.9%
Martinez-Sosa et al. (2011)	100	Municipal wastewater + glucose (630 ± 82 mg L^{-1})	Seed biomass from anaerobic sludge digester	Single stage / Pumped Cycles: feeding, filtration, relaxation & backwashing	FS	350	0.01	7	16 – 26	0.6 – 1.1	35, 28, 20	19.2	680	13 – 22	8 – 16	?	≈ 90%
Aslam *et al.* (2014)	-	Synthetic wastewater (513 mg COD L^{-1})		Single stage / Pumped	FS	1.0	0.04	50	0 – 55	-	Ambient	0.5	-	-	-	-	-
Smith et al. (2013)	350	Synthetic wastewater (440 mg COD L^{-1})	Seed sludge combined from UASB, anaerobic digester and anaerobic lagoon	Single stage / Pumped (Sparging + back flush)	FS	5	0.007	7 – 8	-10 (backwash)	0.5 – 0.7	16 – 24	16	300	-	6 – 10.6	4.7	92%
		Synthetic wastewater (440 mg COD L^{-1})	Seed sludge combined from UASB, anaerobic digester and anaerobic lagoon	Single stage / Pumped (Sparging)	FS	5	0.007	5 – 7	-10 – 50	0.5 – 0.7	16 – 24	16	300	-	6 – 10.6	4.7	92%

* Value calculated form data in reference

APPENDIX B. – CONSIDERATIONS FOR OPERATION AND PERFORMANCE EVALUATION

I. Measurement considerations for synthetic wastewater

a. Feed COD

The trend of COD reduction over time was tested with synthetic wastewater diluted to a concentration of 1 g COD L^{-1} at 20°C and continuously stirred, which showed an approximately linear trend, as shown in Appendix B - Fig. 1. This confirmed that considering only the initial COD of the feed would represent a big error in calculations, therefore using for all calculations the average value of the feed COD on preparation and at the end of the feeding period as stated in Section 3.2.1.1.

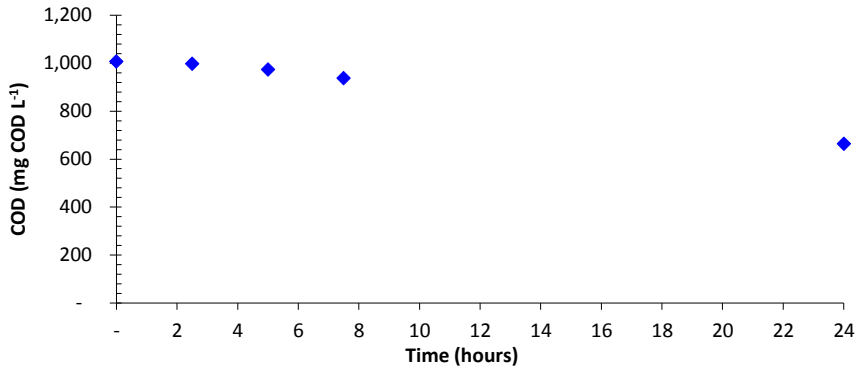

Appendix B - Fig. 1. COD reduction due to degradation and adherence on walls and lines at 20°C

b. Effluent COD

Dissolved methane contribution in permeate samples for the COD test depends on the sampling method, time between sampling and analysis, and sample storage (Purdue-University, 1995). It is commonly assumed dissolved gases does not contribute to COD, as it is readily released to the atmosphere (Yeo et al., 2015). This was confirmed by taking effluent samples by two different methods from the four AnMBR reported in Chapter 6 working at 20 °C under different conditions (day 211). In the first method, the effluent sample was allowed to drip from the permeate outlet into a container in contact with the atmosphere, and left to rest for at least 30-60 min to strip any dissolved gas left. In the second the sample was taken with a syringe, avoiding contact

with the atmosphere and desorption of methane. As shown in Appendix B - Fig. 2, the COD of the samples taken without contact with the atmosphere was on average 32% higher than those in contact with the atmosphere, suggesting a possible contribution from dissolved CH_4 and H_2S in the COD test. Therefore, in order to avoid the contribution of dissolved gases such as CH_4 and H_2S in the effluent COD measurements samples should be taken by direct dropping from the permeate outlet into a container and left to rest before testing for at least 30 minutes. Although all the effluent samples in this work were taken using the first method, this quick test was carried out to better understand the influence of dissolved gases in COD measurement and avoid mistakes in sampling methods in future research. It is worth mentioning that other methods are reported for removal of the hydrogen sulphide from solution by adding iron (II) sulphide or potassium sulphide and allowing the sample to stand for 24 hours (Environment-Agency, 2007).These methods, however, are mainly intended for the recovery of mercury in COD tests that employ this substance (not the case in this research) and will result very laborious to carry them out in every effluent sample.In the current work it was considered that the approach described above was enough to remove the dissolved gases such as CH_4 and H_2S from the samples and thus to avoid their interference with the COD values to a practical extent.

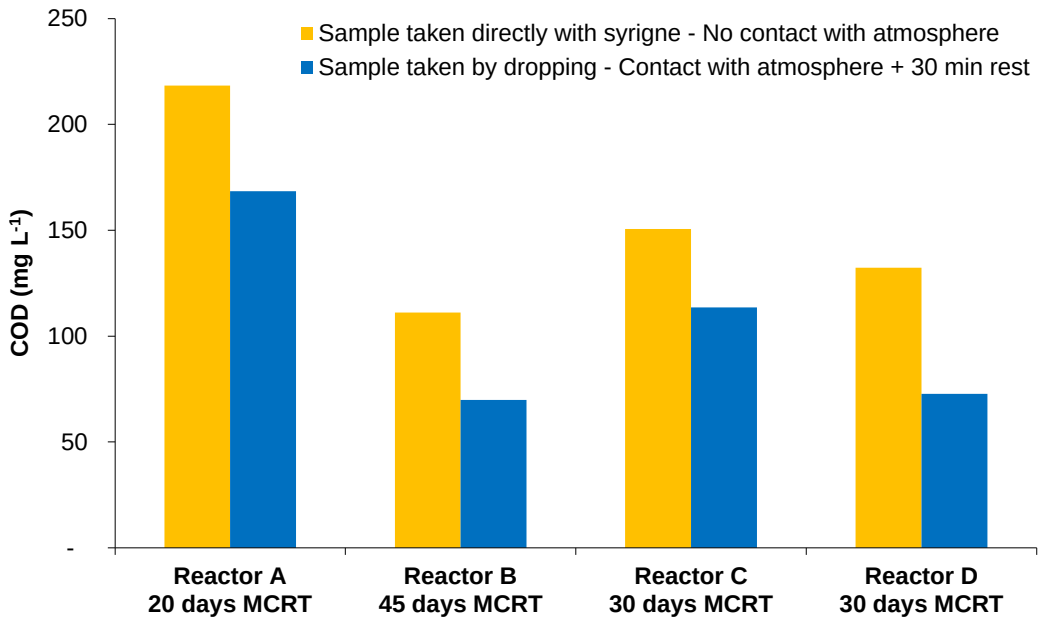

Appendix B - Fig. 2. Dissolved CH_4 contribution to COD in test: effluent samples from MCRT effect experiment at 20 ^{o}C (Chapter 6) of operational day 211.

II. Correction of the biogas quantification due to dissolved air in the inflow

As shown in Chapters 0 and 0, the added fraction of CH_4 and CO_2 in the gas produced in during the experiment at 36 ^{o}C resulted of 90% whilst of 86% when operated at 20 ^{o}C. The remainder was assumed to be mainly N_2 and CO_2 from atmospheric air dissolved in the feed. This was confirmed by checking retention time of peak in GC analysis of the unknown gas in the biogas produced (0.36 min) with that for an injection of standard nitrogen (0.38 min) and an injection of atmospheric air (0.38 min), as shown in Appendix B - Fig. 3.

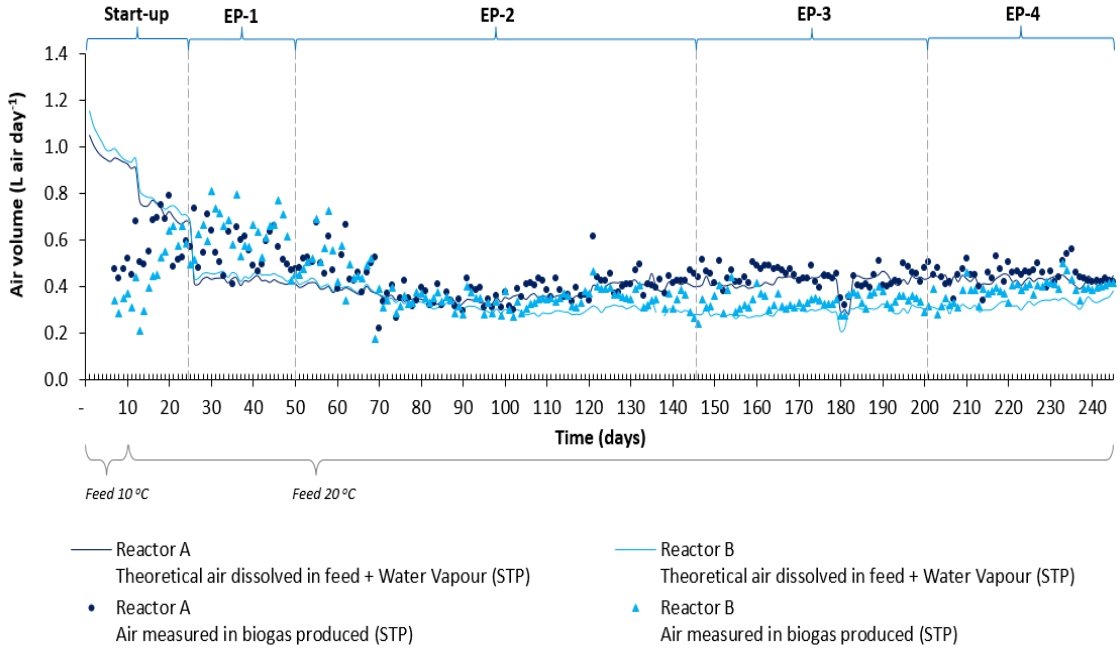

Appendix B - Fig. 3. Air measured in biogas produced compared to the theoretical air entering the system dissolved in the feed at the saturation concentration – MCRT effect experiment at 36 ^{o}C (Chapter 5).

This was then checked with data of the experiment in Chapter 5 by calculating the theoretical volume of air that could enter dissolved with the feed (Appendix B - Equation. 1) and comparing the resulting biogas concentrations with the measured values (Appendix B - Equation. 2). The results showed that the air measured in the daily biogas volume produced resulted quite near to the calculated volume of air that could have entered the system dissolved in the feed plus the water vapour. This outcome confirmed that the identified air fraction in the biogas produced was indeed air entering the system dissolved in the feed.

$$Dissolved\ air_{max\ theoretical} = (C_{air})(Q)\left(24\frac{hrs}{day}\right)$$ Appendix B - Equation. 1

Where:

Q = reactor flux (L hour^{-1})

C_{air}= saturation concentration of air dissolved in water @ 20 ^{o}C (mL air L^{-1})

$$Air\ in\ biogas\ produced = \left(Biogas\ V_{stp}\right)(air\ \%)$$ Appendix B - Equation. 2

Where:

$Biogas\ V_{stp}$= measured biogas volume (L d^{-1}) corrected with Equation 3.8

Air % = air fraction in the gas composition

III. Improvement of the method for the experimental determination of dissolved CH_4 in the effluent

As mentioned in Section 3.2.2.3, two different sampling procedures were used in this work for the experimental determination of CH_4 in the effluent. The first approach consisted in slowly filling a vial by effluent dropping, where part of the dissolved methane has time to equilibrate and disrobe from the effluent before the vial is filled and caped. The second procedure was improved by using a syringe instead to take the sample avoiding it to be in contact with the atmosphere and thus avoid any desorption of methane.

Appendix B - Fig. 4. shows the data obtained from the experimental determination of dissolved CH_4 in the effluent during the experiment reported in Chapter 5 operated at 36 ^{o}C, in which the first sampling method was employed. It can be observed that the CH_4 in the effluent of both reactors varied widely between 1-18 mL CH_4 L^{-1}, and was lower than the theoretical saturation concentration at 36 ^{o}C estimated at 22.9 mL CH_4 L^{-1}.

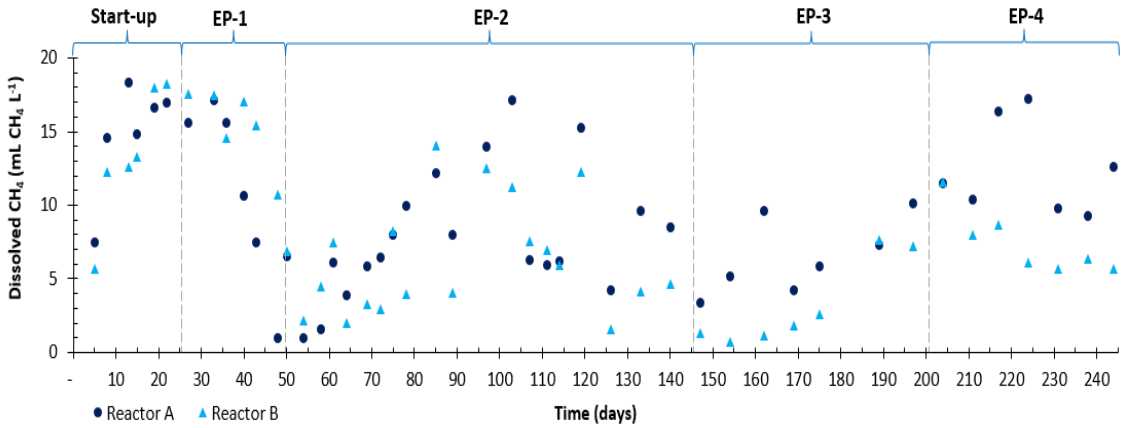

Appendix B - Fig. 4. Dissolved CH_4 in the effluent – MCRT effect experiment at 36 ^{o}C (Chapter 5).

On the other hand, Appendix B - Fig. 5 shows the data obtained from the experimental determination of dissolved CH_4 in the effluent during the experiment reported in Chapter 6 operated at 20 ^{o}C, in which the samples were taken with the second sampling procedure. It can be observed that the dissolved methane of the four reactors during this experiment varied between 15-29 mL CH_4 L^{-1} with an overall average of 21.5 mL CH_4 L^{-1}. Although this value is still under the saturation concentration at 20 ^{o}C estimated at 29.3 mL CH_4 L^{-1}, the method was considerably improved. It is clear, however, that the method for the experimental determination of methane in the effluent is still a long way from being precise and reliable and therefore future work in its development is essential.

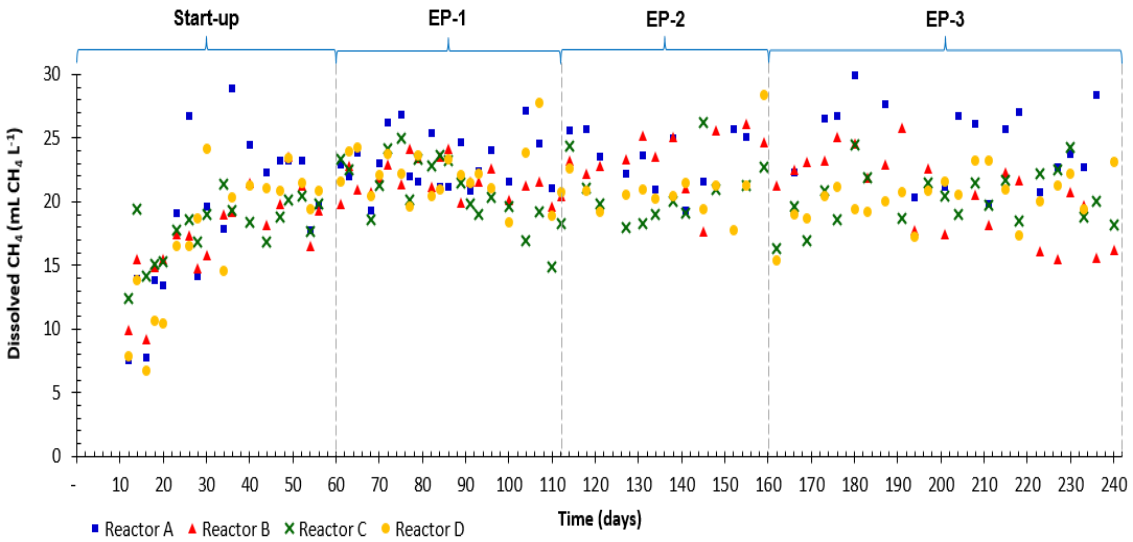

Appendix B - Fig. 5. Dissolved CH_4 in the effluent – MCRT effect experiment at 20 ^{o}C (Chapter 6).

APPENDIX C. – TMP EQUATION VALIDATION

Bernoulli equation states:

$$H = z + \frac{P}{\rho g} + \frac{V^2}{2g} + h$$

Appendix C - Equation. 1

Where:

H =Total head or energy head (m)

V = velocity (m s^{-1})

P = pressure (kPa)

h = head loss (m)

Given the representation of an MBR in a gravitational mode (Appendix C - Fig. 1)

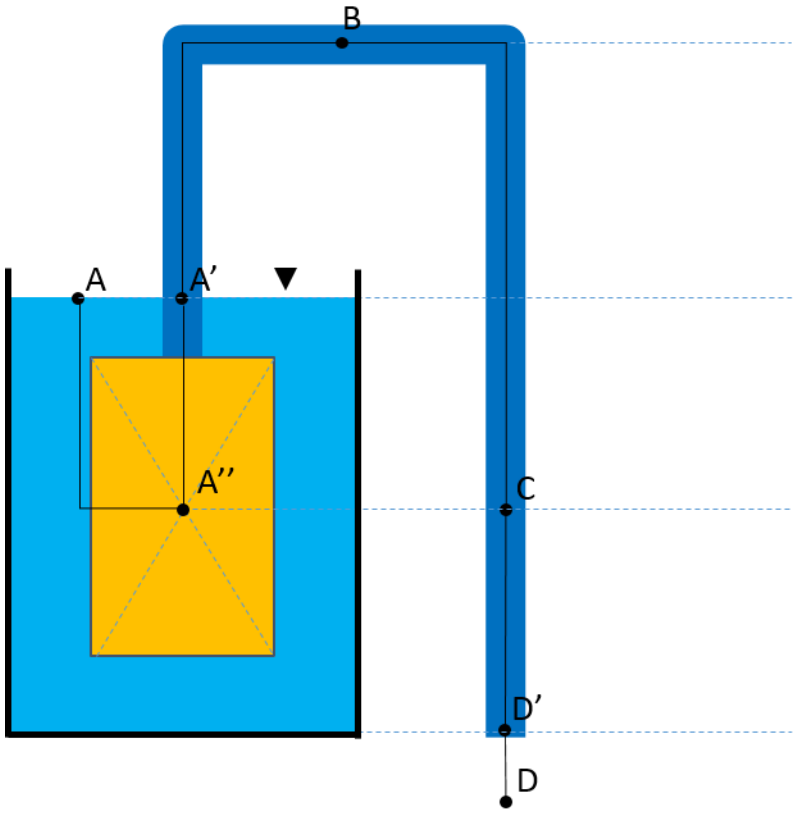

Appendix C - Fig. 1. MBR gravitational Bernoulli diagram

Solving from point *A* to point *D*

$$z_A + \frac{P_A}{\rho g} + \frac{{V_A}^2}{2g} = z_D + \frac{P_D}{\rho g} + \frac{{V_D}^2}{2g} + h$$

Since: A is in a big tank, we can assume that $V_A \approx 0$; and A and C are at atmospheric pressure, we can assume that $P_A = P_D = P_{atm}$. Therefore:

$$z_A = z_D + \frac{{V_D}^2}{2g} + h \quad \rightarrow \quad V_D = \sqrt{2g(z_A - z_D - h)}$$

It is therefore clear that $V_D \gg V_A$

Solving from point *A'* to point *D*

Although A should be quite similar to A', the velocity in A' is not negligible and the pressure is not atmospheric anymore and therefore should be calculated.

$$z_{A'} + \frac{P_{A'}}{\rho g} + \frac{{V_{A'}}^2}{2g} = z_D + \frac{P_D}{\rho g} + \frac{{V_D}^2}{2g} + h$$

Given the continuity principle of Bernoulli $V_{A'} = V_D$. Therefore:

$$z_{A'} + \frac{P_{A'}}{\rho g} = z_D + \frac{P_D}{\rho g} + h \quad \rightarrow \quad \frac{P_{A'}}{\rho g} - \frac{P_D}{\rho g} = -z_{A'} + z_D + h$$

If zero-referenced against ambient air pressure (gage pressure) $P_D = 0$ and the pressure at the point A' would be:

$$P_{A'} = (z_D - z_{A'} + h)\rho g \approx TMP$$

Given that the TMP is constant across the entire membrane surface, the TMP calculated at point A' would therefore be the same as at A'', assuming that there are no head losses. For the particular application of this calculation for the SAnMBRs of this study the backpressure of the biogas produced in the headspace was considered as an additional head difference as mentioned in Section 3.3.2.